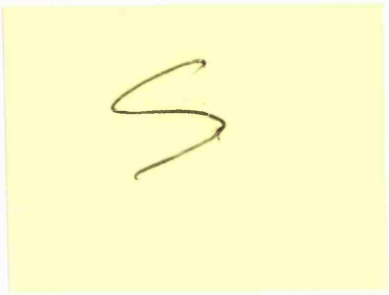

The Role Of Cellular Glutathione Concentration In Dictating Astrocytic And Neuronal Susceptibility To Oxidative Stress

By

Matthew Edward Gegg

A thesis submitted as partial fulfilment for the degree of Doctor of Philosophy in the Faculty of Science at the University of London

October 2002

Department of Molecular Pathogenesis
Division of Neurochemistry
Institute of Neurology
University College London
Queen Square
London WC1N 3BG
United Kingdom

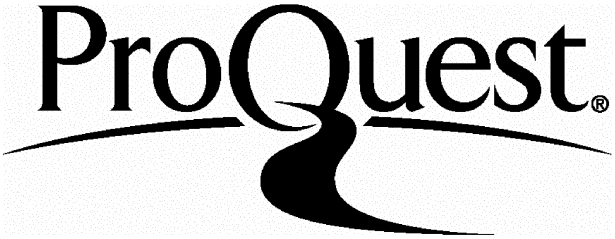

ABSTRACT

The availability of the antioxidant glutathione (GSH) within astrocytes and neurones has been suggested to protect the mitochondrial electron transport chain (ETC) from inactivation by reactive oxygen and nitrogen species. Since perturbed glutathione metabolism, increased production of reactive nitrogen species, and impaired mitochondrial function have been implicated in several neurological disorders, the effect of oxidative stress on GSH metabolism in astrocytes and neurones, and the consequences this has on ETC function and cell viability has been investigated. When cultured alone, neurones were more susceptible to ETC damage and cell death, compared to astrocytes, following exposure to the nitric oxide (NO) donor DETA-NO, or 3-hydroxy-4-pentenoic acid, a drug previously reported to specifically deplete mitochondrial GSH in liver. A reason for this maybe that the activity of glutamate-cysteine ligase, the rate-limiting enzyme in GSH synthesis, was increased in astrocytes but not neurones following treatment, and resulted in elevated GSH levels. The rate of GSH efflux and the activity of γ-glutamyltranspeptidase (γ-GT), an ectoenzyme that metabolises GSH to cysteinylglycine (CysGly), were also increased in astrocytes exposed to NO. The supply of CysGly from astrocytes has previously been shown to increase GSH levels in neurones when cocultured with astrocytes. This thesis has shown that the elevation of neuronal GSH levels relied on the release of GSH from astrocytes only, and does not appear to require a concomitant increase in neuronal GCL activity. Therefore, the increased release of GSH from astrocytes, and the activity of γ-GT upon NO exposure, may increase the supply of CysGly to neurones in coculture and *in vivo*, and therefore give them greater protection. Interestingly, neurones can increase GCL activity when cultured with astrocytes that did not release GSH. In summary, GSH metabolism in both astrocytes and neurones can be modulated upon oxidative stress as a possible protective mechanism.

ACKNOWLEDGEMENTS

I would like to thank Dr Simon Heales and Professor John Clark for their excellent supervision, advice, and support throughout this thesis.

I thank all the members of the Division of Neurochemistry for all their help over the past three years and for making it an enjoyable time.

I also thank Dr Juan Bolanos and Silvia Salas-Pino (Departmento de Bioquimica y Biologia Molecular, Universidad de Salamanca, Spain) for their assistance with the Northern Blot.

I am also grateful to Dr Ralf Dringen (University of Tubingen, Germany) and Dr David Selwood (The Wolfson Institute for Biomedical Research, University College London) for the cysteinylglycine standards and 3-hydroxy-4-pentenoic acid respectively.

Finally, I thank Wendy Morris for her constant encouragement and for putting up with a student for too long.

I am indebted to the Brain Research Trust for the generous funding of this thesis.

CONTENTS

LIST OF FIGURES AND TABLES

ABBREVIATIONS

AD	Alzheimer's disease
AIF	apoptosis initiating factor
ALS	amyotrophic lateral sclerosis
ANT	adenine nucleotide translocase
BH_4	tetrahydrobiopterin
BSA	bovine serum albumin
L-BSO	L-buthionine -(S,R)-sulfoximine
CN	cyanide
CS	citrate synthase
Cys-Cys	cystine
CysGly	cysteinylglycine
DETA-NO	(z)-1-[2-aminoethyl)-N-(2-ammonioethyl)amino]diazen-1-ium-1,2-diolate
DEPC	diethylpyrocarbonate
DTNB	5,5' dithio-bis-(nitrobenzoic acid)
DTT	dithiothreitol
EBSS	Earle's balanced salt solution
eNOS	endothelial nitric oxide synthase
EpRE	electrophile response element
ETC	electron transport chain
FAD	flavin adenine dinucleotide
FITC	fluorescein isothiocyanate
FMN	flavin mononucleotide
γ-GC	γ-glutamylcysteine
GCL	glutamate-cysteine ligase
GCL_h	glutamate-cysteine ligase catalytic subunit
GCL_l	glutamate-cysteine ligase regulatory subunit
γ-GCT	γ-glutamylcyclotransferase
GFAP	glial fibrillary acidic protein
$GS^{\bullet}$	thiyl radical
GS	glutathione synthetase

GSH	reduced glutathione
GSSG	oxidised glutathione
γ-GT	γ-glutamyltranspeptidase
H_2O_2	hydrogen peroxide
HBDH	3-hydroxybutyrate dehydrogenase
HBSS	Hank's balance salt solution
HPLC	high performance liquid chromatography
IFN-β	interferon-β
IFN-γ	interferon-γ
ILBD	incidental Lewy body disease
iNOS	inducible nitric oxide synthase
LDH	lactate dehydrogenase
LPS	lipopolysaccharide
MEM	minimal essential medium
MOPS	3-[N-morpholino]propanesulfonic acid
MPP^+	1-methyl-4-phenylpyridinium
MPT	mitochondrial permeability transition
MPTP	1-methyl-4-phenyl-1,2,3,6-tetrahydropyridine
MRP	multidrug resistance protein
MS	multiple sclerosis
mtDNA	mitochondrial DNA
NF	neurofilament
nNOS	neuronal nitric oxide synthase
NO	nitric oxide
$O_2^{\bullet-}$	superoxide
$OH^{\bullet}$	hydroxyl radical
$O_2H^{\bullet}$	hydroperoxyl radical
OHPA	(*S*)-3-hydroxy-4-pentenoic acid
$ONOO^-$	peroxynitrite
PA	4-pentenoic acid
PBS	phosphate buffered saline
PD	Parkinson's disease

RNS	reactive nitrogen species
$RO_2^{\bullet}$	lipid peroxyl radical
ROS	Reactive oxygen species
rpm	revolutions per minute
SDS	sodium dodecyl sulphate
SNAP	*S*-nitroso-N-acetylpenicillamine
SOD	superoxide dismutase
$T^{\bullet}$	α-tocopherol radical
$UQ^{\bullet-}$	ubisemiquinone
UQ	ubiquinone
UQH_2	ubiquinol

Chapter 1

Introduction

This thesis has investigated the role of cellular glutathione levels in dictating astrocytic and neuronal susceptibility to oxidative stress. Specifically, the modulation of glutathione metabolism in astrocytes and neurones upon oxidative stress, and the protection that this confers to the mitochondrial respiratory chain was investigated. This chapter will explain what oxidative stress means, and review the literature to date on glutathione metabolism, the effect of oxidative stress on the mitochondrial respiratory chain in the brain, and the implications this may have for neurological diseases such as Parkinson's disease. Finally, the rationale behind this thesis will be explained.

1.1.Free radicals and other oxidising species

Free radicals are molecules that contain one or more unpaired electrons and are able to exist independently (Halliwell & Gutteridge, 1989). Radicals can be formed by either the gain (reduction) or loss (oxidation) of a single electron. For example, oxygen is a good oxidising species, and the addition of a single electron to an atomic orbital will produce the superoxide radical ($O_2^{\cdot -}$). The unpaired electron of free radicals makes the species very reactive towards other molecules. Free radicals naturally occur *in vivo* and include superoxide, the hydroperoxyl radical ($O_2H^{\cdot}$), the hydroxyl radical ($OH^{\cdot}$), and nitric oxide (NO)(Boveris & Chance, 1973; Palmer *et al.*, 1987; Halliwell & Gutteridge, 1989). The reactive nature of free radicals can cause significant damage to DNA, protein, and lipids (Halliwell & Gutteridge, 1989; Cheng *et al.*, 1992; Griffiths *et al.*, 2002b).

The oxidation/reduction of free radicals, or reactions between free radical species, can also result in reactive species. Such species are often termed as reactive oxygen species (ROS) and reactive nitrogen species (RNS). Any biological system generating superoxide will produce hydrogen peroxide (H_2O_2) by dismutation (**reaction 1.1**; Halliwell & Gutteridge, 1989).

$$O_2^{\cdot -} + O_2^{\cdot -} + 2H^+ \rightarrow H_2O_2 + O_2 \qquad \textbf{(1.1)}$$

The rate of dismutation shown above is much greater when catalysed by the enzyme superoxide dismutase (SOD; Oury *et al.*, 1992; Yim *et al.*, 1996).

Hydrogen peroxide is a relatively weak oxidising agent, but can readily cross membranes, and is a source for the highly reactive hydroxyl radical (Halliwell & Gutteridge, 1989).

NO can be reduced by biological molecules such as cytochrome c or SOD to form the nitroxyl ion (NO^-; Sharpe & Cooper, 1998, Hughes, 1999), or oxidised by metals and other cellular oxidising species to form the nitrosyl cation (NO^+), under physiological conditions (Gaston, 1999; Hughes, 1999). The reaction of NO with superoxide can produce the highly reactive species peroxynitrite ($ONOO^-$; **reaction 1.2**; Beckman & Koppenol, 1996; Quijano *et al.*, 1997).

$$NO + O_2^{\cdot -} \rightarrow ONOO^- \qquad \textbf{(1.2)}$$

Superoxide reacts approximately six times faster with NO, compared to SOD, and therefore out competes SOD for superoxide (Beckman & Koppenol, 1996). Under physiological conditions, peroxynitrite can also decompose to form a species with the reactivity of the hydroxyl radical and nitrogen dioxide (Beckman & Crow, 1993; Beckman & Koppenol, 1996).

The metabolites of NO have distinctive chemical properties. Peroxynitrite is a stronger oxidising agent than both NO and superoxide, and readily oxidises thiols, ascorbate, lipids, and can cause nitration of tyrosine residues (Quijano *et al.*, 1997; Hughes, 1999; Patel *et al.*, 1999). NO^- can react with thiols and protein metal centres (Sharpe & Cooper, 1998; Hughes, 1999), while NO^+ is the key species involved in the nitrosation of thiol groups (*e.g.*, -SNO; Hughes, 1999, Patel *et al.*, 1999).

1.2. Generation of free radicals and ROS/RNS in eukaryotic cells

Free radicals and ROS are generated by a variety of chemical and biochemical reactions, many of which are a consequence of the aerobic conditions of the cell.

1.2.1. Generation of ROS by mitochondria

The mitochondrial electron transport chain (ETC) is recognised as a significant source of ROS within the cell (Boveris & Chance, 1973). The ETC is located on the inner membrane, and reduces oxygen to water using electrons transferred from reducing equivalents derived from molecules such as NADH and succinate (Mitchell, 1961; reviewed by Scheffler, 1999). The reduction of oxygen to water is not 100% efficient. Mammalian mitochondria have been shown to produce hydrogen peroxide (Boveris & Chance, 1973; Paradies *et al.*, 2000), and is estimated to account for1-2% of the total oxygen consumed by cells *in vitro* (Boveris & Chance, 1973). Superoxide is considered to be the first oxygen reduction product of mitochondria, which is then dismutated to hydrogen peroxide (Paradies *et al.*, 2000; Han *et al.*, 2001). Superoxide has been postulated to be formed by the autooxidation of ubisemiquinone at complex I (NADH:Ubiquinone oxidoreductase; EC 1.6.5.3) and complex III (cytochrome bc_1 complex; EC 1.10.2.2) of the ETC (**reaction 1.3**; Han *et al.*, 2001). Normally ubiquinone (UQ) is reduced by an electron from NADH at complex I (Tormo & Estornell, 2000), or ubiquinol (UQH_2) is oxidised by complex III (Crofts *et al.*, 1999), to form ubisemiquinone ($UQ^{\cdot-}$; **reaction 1.3**). Ubisemiquinone can then be reduced at complex I, or oxidised at complex III, to generate ubiquinol or ubiquinone respectively. However ubisemiquinone can also react with oxygen to form superoxide (Han *et al.*, 2001).

$$UQ + e^- \leftrightarrow UQ^{\cdot-} \leftrightarrow UQH_2 \qquad \textbf{(1.3)}$$

$$\downarrow O_2$$

$$UQ + O_2^{\cdot-}$$

Inhibition of complex I by rotenone or 1-methyl-4-phenylpyridinium (MPP^+) have been shown to increase hydrogen peroxide and superoxide production in cultured astrocytes and non-dopaminergic neurones (McNaught & Jenner, 2000; Nakamura *et al.*, 2000a). However isolated mitochondria brain mitochondria or dopaminergic neurones (under certain conditions; see below) treated with MPP^+ or rotenone

have been shown to reduce hydrogen peroxide and superoxide production (Bates *et al.*, 1994; Nakamura *et al.*, 2000a). The period for which complex I was inhibited for may explain the difference in results, with longer treatments resulting in increased production of oxidising species *e.g.*, the increased hydrogen peroxide production from astrocytes and dopaminergic neurones was observed following incubation for 24 hours, while the isolated mitochondria were only inhibited for 1 hour. The source of the mitochondria may also be important, as shown by the differential effect of dopaminergic and non-dopaminergic neurones to MPP^+ (Nakamura *et al.*, 2000a). Finally, since the increased production of hydrogen peroxide and superoxide was detected from cultured cells, it is not certain whether the effects of MPP^+ and rotenone were definitely due to inhibition of mitochondria.

Inhibition of complex III of the ETC antimycin A in isolated rat liver and pigeon heart mitochondria has been shown to increase the production of superoxide and hydrogen peroxide by mitochondria (Boveris & Chance, 1973; Paradies *et al.*, 2000; Han *et al.*, 2001).

1.2.2. NO synthases

The free radical NO is synthesised by the NO synthases in mammals (NOS; EC 1.14.13.39) (Kwon *et al.*, 1990; Leone *et al.*, 1991). Three isoforms of NOS have been characterised and cloned to date, and are termed neuronal NOS (nNOS), inducible NOS (iNOS), and endothelial NOS (eNOS)(reviewed by Knowles & Moncada, 1994; Stuehr, 1999; Alderton *et al.*, 2001). The presence of NOS in mitochondria has also been postulated, although this is controversial. NOS activity has been reported in isolated rat liver mitochondria (Tatoyan and Giulivi, 1998; Giulivi *et al.*, 1998), while an eNOS antibody was localised to the inner membrane of rat liver and brain mitochondria by immunohistochemistry (Bates *et al.*, 1995). However, cytosolic contamination of the mitochondrial preparations was not determined when NOS activity was measured (Tatoyan and Giulivi, 1998; Giulivi *et al.*, 1998). Furthermore, no gene has been cloned on either the

mitochondrial or nuclear genome, and no putative mitochondrial targeting sequences have been identified in the three other isoforms of NOS.

The nNOS isoform was the first to be identified, and is found predominantly in neuronal tissue (Bredt & Snyder, 1990), and together with eNOS, are calcium dependent and constitutively expressed (although expression can be increased under certain conditions *e.g.,* depletion of glutathione, oxidative stress (Baader & Schilling, 1996; Heales *et al.*, 1996a)). Expression of the iNOS isoform can be induced by a variety of stimuli such as lipopolysaccharide (LPS) and cytokines (Simmons & Murphy, 1992), and is less dependent on calcium (Alderton *et al.*, 2001). The iNOS isoform has been localised to a variety of cells including macrophages (Stuehr *et al.*, 1991) and astrocytes (Simmons & Murphy, 1992; Bolanos *et al.*, 1994).

All three NOS isoforms are coded for by three separate genes, with the human nNOS, iNOS and eNOS genes located on chromosomes 12q24.2, 17cen-q11.2, and 7q35 respectively (Alderton *et al.*, 2001). The NOS enzymes have very similar domain structures, with a N-terminal oxygenase domain, a C-terminal reductase domain, and a calmodulin recognition site (**Figure 1.1a;** Sheta *et al.*, 1994; Lowe *et al.*, 1996). The NOS isoforms are only active as homodimers (Stuehr *et al.*, 1991), with each monomer associated with one molecule of calmodulin, which binds calcium (Stuehr *et al.*, 1991; Mathews & van Holde, 1990). The reductase domain binds NADPH, and transfers electrons through the reductase domain via flavin adenine dinucleotide (FAD) and flavin mononucleotide (FMN), to the haem bound to the oxygenase domain. The oxygenase domain contains the active site, and binds oxygen (using the haem) and arginine, to produce citrulline and NO (**Figure 1.1b**; Knowles & Moncada, 1994; Alderton e*t al.*, 2001). The cofactor tetrahydrobiopterin (BH_4) is also required for NOS activity, however the functional role of BH_4 in NOS is not clear, with the molecule being implicated in several processes such as promoting dimer formation, and coupling of NADPH oxidation to NO synthesis (reviewed by Alderton *et al.*, 2001).

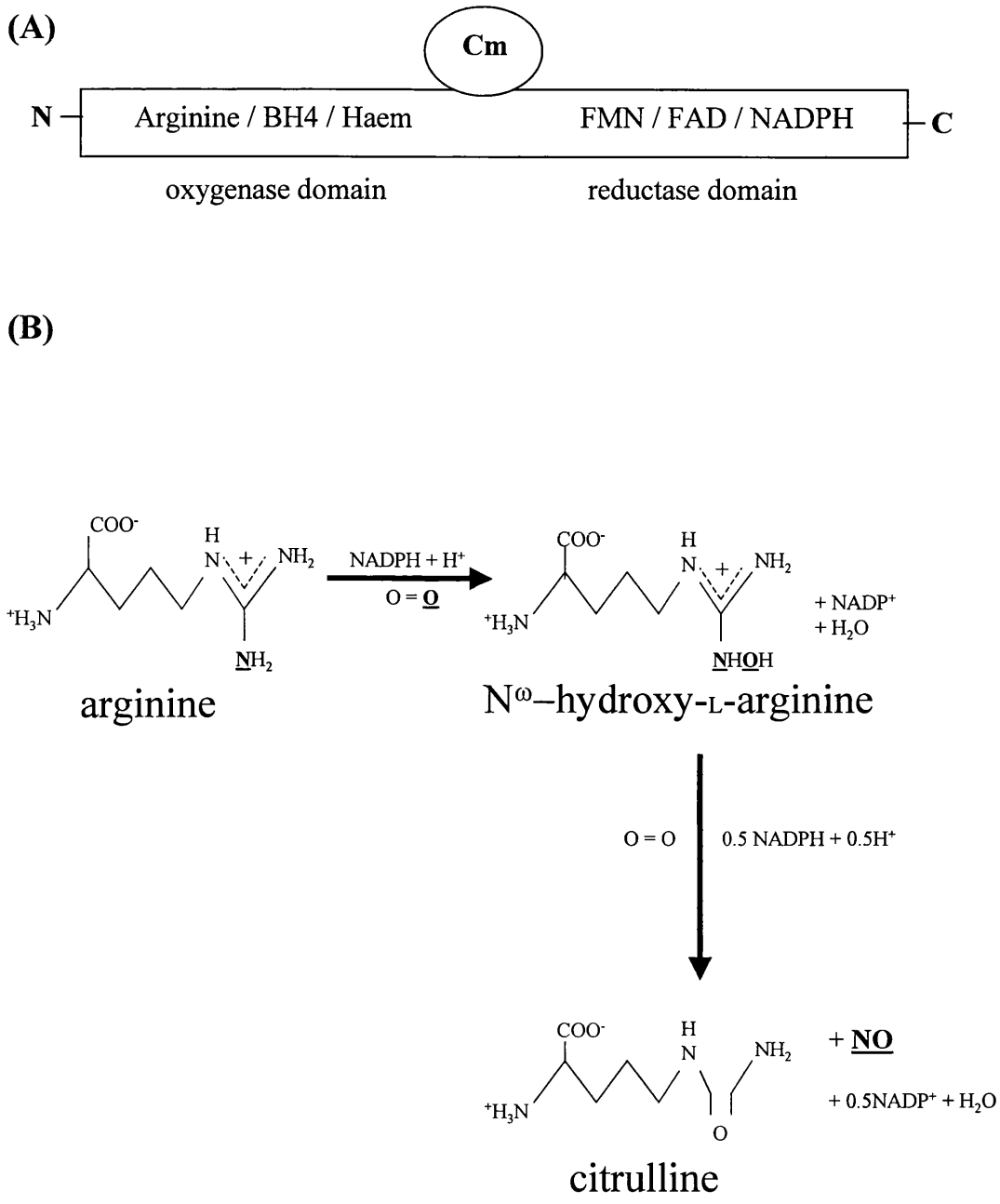

Figure 1.1. Domain structure and catalytic mechanism of NO synthase

The domain structure of NO synthase is shown in (A). The oxygenase domain is at the N-terminal, while the reductase domain is at the C terminal. Calmodulin (Cm) associates with both domains. The catalytic mechanism of NO synthase is shown in (B). The atoms from citrulline and oxygen that form NO are underlined and in bold.

1.2.3. Other enzymes as a source of ROS

The large number of oxidases located in the peroxisome, endoplasmic reticulum, mitochondrion, and cytosol, such as monoamine oxidase, NADPH oxidase, the cytochrome P450 oxidases, and xanthine oxidase are sources of ROS production within the cell (Mathews & van Holde, 1990; Maher & Schubert, 2000). As mentioned previously, the SODs also catalyse the conversion of superoxide to hydrogen peroxide (**reaction 1.1;** Yim *et al.*, 1996, Han *et al.*, 2001).

1.2.4. Non-enzymatic generation of hydroxyl radical

Hydroxyl radicals ($OH^{\cdot}$) can be generated by the Haber-Weiss reaction (**reaction 1.4**), or by the Fenton reaction in the presence of transition metals (**reaction 1.5**; Fe^{3+} and Fe^{2+} are ferric and ferrous iron respectively; Halliwell & Gutteridge, 1989). Note that the rate of the Haber-Weiss reaction is also significantly greater when catalysed by transition metals such as copper or iron.

$$O_2^{\cdot-} + H_2O_2 \rightarrow O_2 + OH^- + OH^{\cdot} \qquad \textbf{(1.4)}$$

$$Fe^{2+} + H_2O_2 \rightarrow Fe^{3+} + OH^- + OH^{\cdot} \qquad \textbf{(1.5)}$$

1.3. Oxidation of macromolecules

Free radicals and other oxidising species can attack proteins, lipids, and nucleic acids and alter their function. The most widely studied marker of protein oxidation is the formation of protein carbonyl groups, which are formed by the oxidation of amino acid side chains such as arginine and threonine (Hensley *et al.*, 1995; Mecocci *et al.*, 1999). Cysteine residues (RSH, where R is the protein backbone) can also be oxidised to sulfenic (RSOH), sulfinic (RSO_2H) or sulfonic (RSO_3H) acid. Protein sulfinates and sulfonates, unlike protein sulfenates, are relatively stable oxidation products, and cannot be reduced back to cysteine under biological conditions (Klatt & Lamas, 2000). Cysteine residues can also be nitrosated by

NO^+ or peroxynitrite to form RSNO (Patel *et al.*, 1999; Klatt & Lamas, 2000). Alternatively, formation of disulphide bridges between thiol groups under oxidising conditions may also alter protein activity (Huang *et al.*, 1993; Sriram *et al.*, 1998; Tu & Anders, 1998b). Hydroxyl groups (*e.g.*, tyrosine) and tryptophan can be nitrated (RONO) by peroxynitrite (Patel *et al.*, 1999), while NO can also react with the iron centres of proteins (e.g., cytochrome c oxidase (EC 1.9.3.1) and haemoglobin)(Wainio, 1955; Kharatinov *et al.*, 1996).

Free radicals can also initiate lipid peroxidation. Hydroxyl and peroxyl radicals can abstract hydrogen from a methylene ($-CH_2-$) group next to a double bond in membrane fatty acids (**Figure 1.2, reaction 1;** Halliwell & Gutteridge, 1989; Patel *et al.*, 1999; Griffiths *et al.*, 2002b). The carbon radical is stabilised by rearrangement of the double bond to form a conjugated diene (**Figure 1.2, reaction 2**). These lipid radicals can then either cross link with another fatty acid, or react with oxygen to yield a peroxyl radical (**Figure 1.2, reaction 3;** Halliwell & Gutteridge, 1989; Ham & Liebler, 1997). The fatty acid peroxyl radical can then abstract hydrogen from a neighbouring fatty acid to form another carbon radical, thus propagating lipid peroxidation (**Figure 1.2, reaction 4;** Halliwell & Gutteridge, 1989) or attack and damage membrane proteins. The end products of

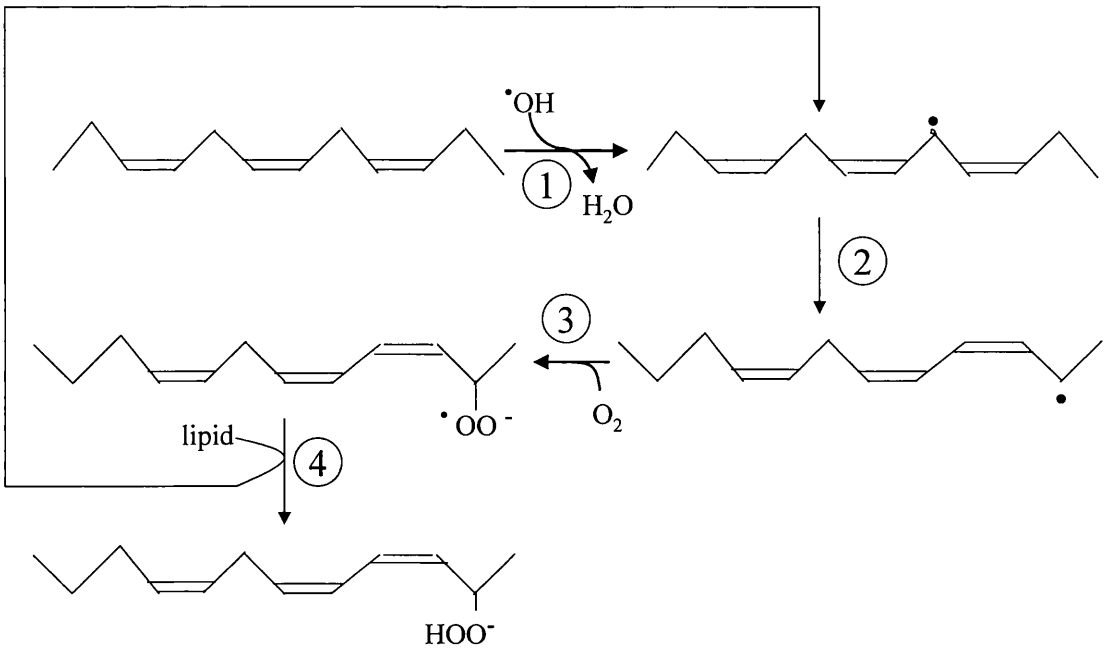

Figure 1.2. Lipid peroxidation pathway

lipid peroxidation include the aldehydes malodialdehyde and 4-hydroxy-2-nonenal (Halliwell & Gutteridge, 1989; Griffiths *et al.*, 2002b). These molecules can cross link with protein and DNA, and therefore alter their properties (Halliwell & Gutteridge, 1989, Beal, 2002).

The reaction of DNA with radicals can cause strand breaks and the modification of DNA bases (Halliwell & Gutteridge, 1989, Mecocci *et al.*, 1999). A common oxidised base is 8-hydroxy-2-deoxyguanosine, which can mispair with adenine leading to point mutations, and cause misreading of adjacent bases during replication or transcription (Cheng *et al.*, 1992; Mecocci *et al.*, 1999).

1.4. Cellular protection against free radicals and ROS/RNS by small molecules and enzymes

Mammalian cells contain several enzymes and small molecules that react with free radicals and other reactive species in order to prevent damage to cellular molecules.

Catalase (EC 1.11.1.6) and glutathione peroxidase (EC 1.11.1.9) are two enzymes that control the amount of hydrogen peroxide present in cells. Catalase, which contains a haem group bound to its active site, reacts with hydrogen peroxide as shown in **reaction 1.6** (Halliwell & Gutteridge, 1989; Voet & Voet, 1990).

$$2H_2O_2 \rightarrow 2H_2O + O_2 \qquad \textbf{(1.6)}$$

Catalase is primarily found in peroxisomes (subcellular organelles bound by a single membrane (Mathews & van Holde, 1990)), with little catalase activity located in mitochondria or the endoplasmic reticulum (Halliwell & Gutteridge, 1989; Brighelius-Flohe, 1999).

Hydrogen peroxide generated by mitochondria and cytosolic enzymes is largely disposed of by glutathione peroxidases (Flohe *et al.*, 1973; Halliwell & Gutteridge, 1989; Dringen & Hamprecht, 1997). The glutathione peroxidases catalyse the oxidation of glutathione (see section 1.12 for detailed discussion of

glutathione) at the expense of hydrogen peroxide (**reaction 1.7**; GSSG, oxidised glutathione).

$H_2O_2 + 2GSH \rightarrow GSSG + 2H_2O$ **(1.7)**

The superoxide dismutases (SODs; EC 1.15.1.1) remove superoxide intracellularly and extracellularly (Mathews & van Holde, 1990; Oury *et al.*, 1992; Yim *et al.*, 1996; Han *et al.*, 2001). The active site of cytosolic and extracellular SOD contains one copper and one zinc ion, greatly accelerating the dismutation of superoxide (**reaction 1.8**; Halliwell & Gutteridge, 1989; Oury *et al.*, 1992). Note that the zinc atom is not involved in the catalytic mechanism, but stabilises the enzyme (Halliwell & Gutteridge, 1989).

$Enzyme\text{-}Cu^{2+} + O_2^{\cdot-} \rightarrow Enzyme\text{-}Cu^{+} + O_2$ **(1.8)**

$Enzyme\text{-}Cu^{+} + O_2^{\cdot-} + 2H^{+} \rightarrow Enzyme\text{-}Cu^{2+} + H_2O_2$

Mitochondrial SOD contains manganese rather than copper and zinc (Han *et al.*, 2001), but catalyses exactly the same reaction (Halliwell & Gutteridge, 1989).

Three small molecules that are important antioxidants *in vivo* are ascorbic acid, glutathione, and α-tocopherol. Ascorbic acid (vitamin C) can act as a reducing agent, making it useful as an antioxidant (Halliwell & Gutteridge, 1989). Ascorbate reacts rapidly with superoxide, hydroxyl, and peroxyl radicals (Halliwell & Gutteridge, 1989; Rice, 2000). Donation of one electron produces semidehydroascorbate radical, which is further oxidised to dehydroascobate. Ascorbate can be regenerated from dehydroascorbate or semidehydroascorbate by glutathione either nonenzymatically, or by dehydroascorbate reductase (**reaction 1.9**; EC 1.8.5.1; Meister, 1994; Rice, 2000).

Dehydroascorbate + 2GSH → GSSG + ascorbate **(1.9)**

It should be noted that ascorbate can also act as a pro-oxidant. Ascorbate can reduce Fe^{3+} to Fe^{2+}, which can then generate hydroxyl radicals by the Fenton

reaction (**reaction 1.5**) and an ascorbyl radical (Cardoso *et al.*, 1999; Arroyo *et al.*, 2000). Furthermore, at higher concentrations (1 mM), ascorbate can generate hydrogen peroxide (Sakagami *et al.*, 1998)

Glutathione in addition to being a substrate for glutathione peroxidase is also a scavenger of superoxide, hydroxyl radicals, and reactive nitrogen species such as peroxynitrite (Halliwell & Gutteridge, 1989; Quijano *et al.*, 1997). The properties and functions of glutathione are discussed in much further detail in section 1.12.

α-tocopherol (vitamin E) is a hydrophobic molecule, and is concentrated in the interior of biological membranes (Mathews and van Holde, 1990). α-tocopherol can be oxidised by hydroxyl and peroxyl radicals (Halliwell & Gutteridge, 1989; Brigelius-Flohé & Traber, 1999). However α-tocopherols main function in biological membranes is probably to react with lipid peroxyl radicals, thus terminating the chain reaction of peroxidation (**reaction 1.10**; $RO_2^{\cdot}$, lipid peroxyl; TH, α-tocopherol; Halliwell & Gutteridge, 1989; Ham & Liebler, 1997)

$$RO_2^{\cdot} + TH \rightarrow RO_2H + T^{\cdot} \qquad \textbf{(1.10)}$$

The α-tocopherol radical ($T^{\cdot}$) is not reactive enough to abstract H from lipid membranes, and the unpaired electron is delocalised into the aromatic structure (Halliwell & Gutteridge, 1989). Ascorbic acid has been postulated to reduce $T^{\cdot}$ back to α-tocopherol (Rice, 2000).

Recently, ubiquinol has also been postulated to have antioxidant properties, and may be particularly important in protecting against lipid peroxidation. Ascorbyl and tocopheryl radicals have been shown to be scavenged by ubiquinol (Landi *et al.*, 1997; Arroyo *et al.*, 2000). Furthermore, a decrease in peroxynitrite-mediated nitration of proteins in mitochondrial membranes has been observed with increasing concentrations of ubiquinol (Schopfer *et al.*, 2000).

1.5. What is Oxidative stress?

Under physiological conditions, mammalian cells are able to counteract the potentially toxic effects of free radicals generated by a variety of biochemical processes by a host of enzymes and small molecules such as the SODs and glutathione. However, should the balance between production of free radicals and cellular defence mechanisms be disrupted, oxidative stress may occur. Oxidative stress could occur due to increased production of free radicals such as increased expression of iNOS (Simmons & Murphy, 1992; Bolanos *et al.*, 1994), or inhibition of the ETC (Boveris & Chance, 1973; Paradies *et al.*, 2000). Alternatively, perturbed cellular defences, such as modification of CuZnSOD function (Rosen *et al.*, 1993; Yim *et al.*, 1996), or depletion of glutathione (Riederer *et al.*, 1989; Sian *et al.*, 1994a), could cause oxidative stress.

1.6. Mitochondria

Mitochondria are double membrane bound organelles that are typically spherical or rod shaped (reviewed by Scheffler, 1999). The inner membrane of mitochondria is highly convoluted to form cristae, and encloses the soluble matrix. The inner membrane is separated from the outer membrane by the intermembrane space.

Every compartment of the mitochondria is associated with different biochemical processes. Metabolic pathways such as the tricarboxylic acid cycle and β-oxidation of fatty acids are located in the matrix of the mitochondria. Mitochondrial DNA (mtDNA), and the proteins required for transcription and repair of mtDNA are also located in the matrix (Anderson *et al.*, 1981; Croteau *et al.*, 1997). Human mtDNA is a circular, double stranded DNA molecule consisting of 16.6 kb (Anderson *et al.*, 1981). Each mitochondrion contains several copies of mtDNA. The DNA molecule has no introns and codes for 2 ribosomal RNA molecules, 22 transfer RNA molecules and 13 polypeptides, all of which code for constituents of the oxidative phosphorylation system (Anderson *et al.*, 1981; Taanman, 1999). The majority of mitochondrial proteins however are coded for by the nucleus, with the complexes of the mitochondrial electron

transport chain a hybrid of mitochondrial and nuclear encoded proteins (see below; Loeffen *et al.*, 1997; Hirawake *et al.*, 1999; Taanman, 1999).

The inner membrane is the site of the mitochondrial electron transport chain (ETC) and oxidative phosphorylation (Mitchell, 1961), in addition to a number of transport systems (*e.g.,* adenine nucleotide translocase; Klingenberg, 1992), while the outer membrane also has a number of transport systems (*e.g.,* voltage dependent anion channel; Crompton *et al.*, 1999), and several enzymes such as the monoamine oxidases (Ragan *et al.*, 1987; Mathews & van Holde, 1990).

In recent years, the role of mitochondria in neurodegeneration has come under intense scrutiny. Dysfunction of the mitochondrial ETC has been reported in several neurological disorders such as Parkinson's disease and Huntington's disease (Schapira *et al*, 1990; Gu *et al.*, 1996). Furthermore, the opening of the mitochondrial permeability transition pore under certain conditions (*e.g.,* oxidative stress, ischaemia) causes mitochondria to uncouple and ATP hydrolysis by reversal of ATP synthase (Nieminen *et al.*, 1995; Halestrap *et al.*, 1998; Crompton *et al.*, 1999). The release of cytochrome c and other apoptosis initiating factors from mitochondria have also been implicated in mechanisms leading to cell death (Yang *et al.*, 1997; Brookes *et al.*, 2000).

1.7. The electron transport chain

The electron transport chain (ETC) is located on the inner membrane of the mitochondria, and is comprised of more than 80 polypeptides grouped together into four enzyme complexes (**Figure 1.3;** Michel *et al.*, 1998**;** Zhang et al., 1998**;** Sazanov *et al.*, 2000). The ETC facilitates the transfer of electrons from NADH and $FADH_2$ (generated by carbohydrate and fatty acid metabolism), to oxygen, which is reduced to water at complex IV (Michel *et al.*, 1998). The reduction of oxygen is coupled to the synthesis of ATP (oxidative phosphorylation) by ATP synthase (EC 3.6.3.14; complex V; Mitchell, 1961). Complexes I–IV contain bound redox centres (*e.g.,* iron-sulphur complexes, FAD), which transfer electrons sequentially from one to another via increasing reduction potentials (Ohnishi,

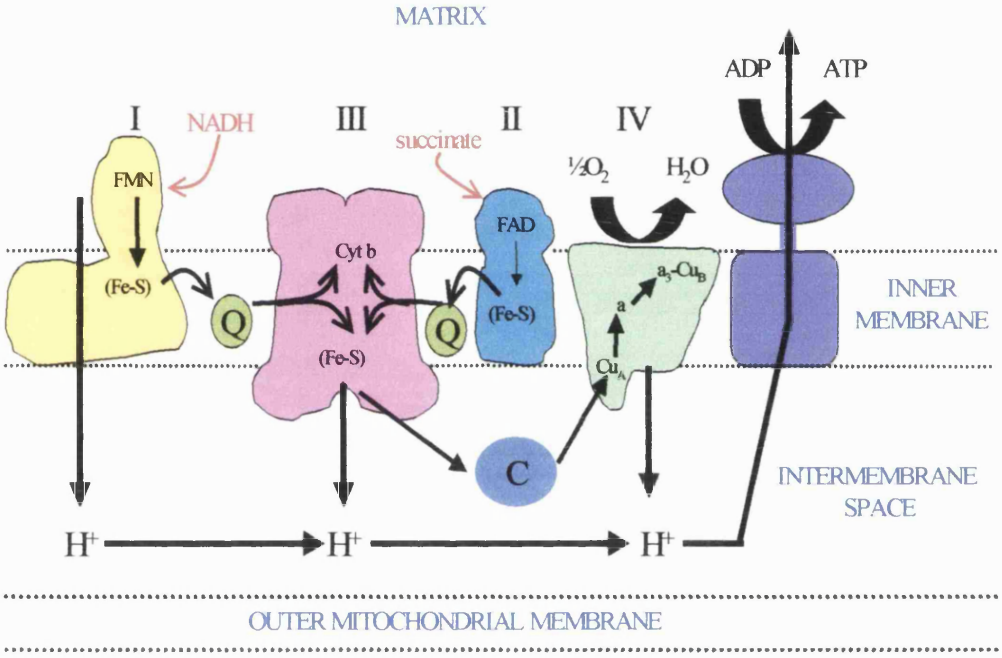

Figure 1.3. The mitochondrial electron transport chain

Complexes I-IV of the ETC and ATP synthase localised to the inner membrane of the mitochondria. C, cytochrome c; Q; ubiquinol. Thin arrows denote movement of electrons, while thick arrows signify movement of protons.

1998; Zhang *et al.*, 1998; Michel, 1998). Ubiquinol transfers two electrons from both complex I and complex II to complex III, while cytochrome c transfers one electron from complex III to complex IV (**Figure 1.3**; Crofts *et al.*, 1999; Tormo & Estornell, 2000).

The free energy generated by the transfer of electrons is conserved by the pumping of protons from the mitochondrial matrix into the intermembrane space by complexes I, III, and IV (Mitchell, 1961; Videira, 1998; Michel, 1998; Crofts *et al.*, 1999). This results in an electrochemical gradient across the inner membrane equivalent to a pH difference of 1.4, and a membrane potential (ψ) of 150 mV (reviewed by Scheffler, 1999). This proton motive force is dissipated through the membrane domain of ATP synthase leading to the phosphorylation of ADP (Mitchell, 1961).

1.7.1. Complex I

NADH:Ubiquinone oxidoreductase (complex I; EC 1.6.5.3) is the largest enzyme in the ETC, with 43 subunits and a molecular mass of approximately 900 kDa (Grigorieff, 1999; Sazanov *et al.*, 2000). Complex I catalyses the transfer of two electrons from NADH to ubiquinone by an unknown mechanism via several bound prosthetic groups (one non-covalently bound FMN, at least six iron-sulphur clusters and two ubiquinone binding sites; Ohnishi, 1998; Tormo & Estornell, 2000). This transfer is coupled to the translocation of four to five protons from the matrix to the intermembrane space to generate the proton gradient required for ATP synthesis.

Seven subunits of complex I are coded for by the mitochondria, with the remainder coded for by the nucleus (Ton *et al.*, 1997; Loeffen *et al.*, 1998; Sazanov *et al.*, 2000). These mitochondrial encoded subunits are located in the membrane domain, are similar to bacterial cation / H^+ antiporters, and therefore thought to be responsible for proton translocation across the membrane (Videira, 1998). The matrix domain contains all the prosthetic groups and biochemical activity of complex I (Videira, 1998). The polypeptides in the matrix domain that

are not involved in the biochemical activity of the enzyme have been termed 'accessory' proteins, although the majority of subunits have yet to be assigned a particular function (Sazanov *et al.*, 2000). Phosphorylation of the 18 kDa subunit by cAMP-dependent kinase activates complex I in human and mouse fibroblasts, and may be a mechanism by which overall ETC activity is regulated (Sardanelli *et al.*, 1995; Scacco *et al.*, 2000; Papa *et al.*, 2001).

1.7.2. Complex II

The flavoprotein succinate:ubiquinone oxidoreductase (complex II; EC 1.3.5.1) oxidises succinate to fumarate, transferring the electrons to ubiquinone. Complex II is the only enzyme that serves as a direct link between the citric acid cycle and the electron transport chain (Hagerhall, 1997; Ackrell, 2000). Unlike the other complexes in the electron transport chain, the four polypeptides of complex II are all coded for by nuclear genes (Hirawake *et al.*, 1999). A flavoprotein and iron-sulphur protein form a hydrophilic domain that projects in to the matrix, while two hydrophobic peptides anchor the matrix domain to the membrane (Lee *et al.*, 1995; Lancaster *et al.*, 1999; Ackrell, 2000).

The matrix domain contains the succinate dehydrogenase activity (Hagerhall, 1997; Lancaster *et al.*, 1999; Ackrell, 2000), while the anchor domain provides the binding sites for two ubiquinone molecules (one on each polypeptide) and cytochrome b, which is thought to play an important role in the assembly of the enzyme (Yu et al., 1992; Lee *et al.*, 1995; Hagerhall, 1997; Shenoy *et al.*, 1999).

1.7.3. Complex III

The cytochrome bc_1 complex (complex III; EC 1.10.2.2) transfers electrons from ubiquinol to cytochrome c. This electron transfer is coupled to proton pumping from the matrix to the inner membrane space contributing to the proton gradient required for ATP synthesis. The structure of complex III in a variety of mammalian species has been elucidated (Iwata *et al.*, 1998; Kim *et al.*, 1998;

Zhang *et al.*, 1998). The protein exists as a homodimer with each monomer consisting of 11 different subunits with a total molecular mass of approximately 240 kDa. Only one of these subunits (cytochrome b) is coded for by the mitochondria (Taanman, 1999). Complex III spans the membrane and projects into both the intermembrane space and matrix (Zhang *et al.*, 1998). The protein contains four redox centres: two b-type haem groups, one c-type haem of cytochrome c_1, and an iron-sulphur centre bound to the Rieske iron-sulphur protein (Iwata *et al.*, 1998; Kim *et al.*, 1998; Zhang *et al.*, 1998).

The mechanism by which electrons are transferred through complex III has been termed the Q cycle. One electron is sequentially transferred from ubiquinol to the Rieske iron-sulphur protein, which then transfers the electron to cytochrome c_1 located in the intermembrane space domain, and finally to soluble cytochrome c, which passes the electrons on to complex IV (Kim *et al.*, 1998; Zhang *et al.*, 1998). The transfer of an electron along this route results in bound semiubiquinone and the release of two protons into the intermembrane space. The electron from semiubiquinone is transferred consecutively via the two cytochrome b molecules, and finally to ubiquinone or semiubiquinone bound at another ubiquinone binding site on complex III. Fully reduced ubiquinol picks up two protons from the matrix and moves to the first ubiquinone binding site to provide more electrons to reduce cytochrome c (Crofts *et al.*, 1999; Snyder *et al.*, 2000).

1.7.4. Complex IV

Cytochrome c oxidase (complex IV; EC 1.9.3.1) is the terminus for electron transfer in the respiratory chain. The enzyme couples the reduction of oxygen to the pumping of protons from the matrix. The mechanism by which this is done is unknown.

Crystallisation of bovine heart complex IV by Tsukihara *et al* (1996) revealed that the mammalian enzyme has 13 different subunits, and several prosthetic groups including two haems (a and a_3) and two copper atoms. The protein exists in the inner membrane as a dimer with each monomer having a molecular mass of 211

kDa (Tsukihara *et al.,* 1996). Subunits I, II and III are mitochondrially encoded and form the core of the protein (Anderson *et al*, 1981; Michel *et al.*, 1998). Subunit II binds cytochrome c and transfers electrons to the haem a_3-Cu_B redox centre located in subunit I, which is involved in the reduction of oxygen to water (Tsukihara *et al.,* 1996; Michel *et al.*, 1998; Riistama *et al.*, 2000). Subunit III has been proposed to be the oxygen channel (Riistama *et al.*, 2000). The remaining ten subunits of mitochondrial cytochrome c oxidase are nuclear encoded. The function of these subunits is still largely unknown. They may play a role in insulation, regulation, stabilisation or assembly of complex IV (Grossman & Lomax, 1997; Huttemann *et al.*, 2001).

1.7.5. Complex V

ATP synthase (EC 3.6.3.14; F_1F_O-ATP synthase) uses the proton motive force generated across the inner mitochondrial membrane by electron transfer through the ETC to drive ATP synthesis. Bovine heart ATP synthase is comprised of 16 different subunits and is divided into three domains (Abrahams *et al.*, 1994). The matrix globular domain, F_1, containing the catalytic site is linked to the intrinsic membrane domain, F_O, by a central stalk (**Figure 1.4**; Abrahams *et al.*, 1994; Karrasch & Walker, 1999). Proton flux through F_O causes the subunit to rotate, which is transferred to the central stalk, and is utilised by F_1 domain to synthesise ATP (Noji *et al.*, 1997; Boyer, 1997; Tsunoda *et al.*, 1999).

The F_1 catalytic domain contains three α subunits and three β subunits with the nucleotide binding sites located at the interfaces between the α and β-subunits (Abrahams *et al.*, 1994; Boyer, 1997). Rotation of the stalk changes the conformation of the active sites making the synthesis of ATP more favourable (Boyer *et al.*, 1997). A stator prevents the F_1 domain following the rotation of the stalk and F_O domains (Karrasch & Walker, 1999).

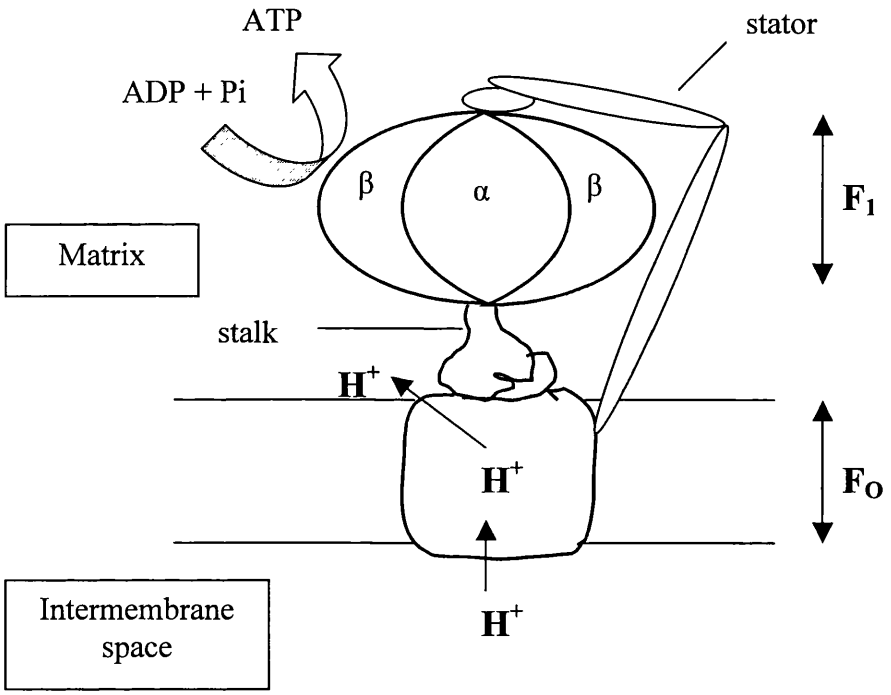

Figure 1.4. Structure of ATP synthase

1.8. Oxidative inactivation of the ETC in brain

The complexes of the ETC are susceptible to inactivation following exposure to both reactive oxygen and nitrogen species. Decades before the involvement of NO in biological processes was discovered, complex IV was known to bind NO (Wainio, 1955). NO competes with oxygen to bind to complex IV, and can rapidly and reversibly inhibit astrocyte respiration (Brown *et al.*, 1995). However, prolonged exposure (*e.g.,* 24 hours) of astrocytes and neurones to NO results in a persistent inhibition of complex IV (Bolanos *et al.*, 1994; Bolanos *et al.*, 1996; Stewart *et al.*, 1998a, 2000). Complexes II+III of the ETC are also inhibited following prolonged exposure to NO (Bolanos *et al.*, 1994, 1996; Stewart *et al.*, 1998a, 2000). The inhibition of complexes II+III, and IV of the ETC was also observed in astrocytes and neurones treated with peroxynitrite (Bolanos *et al.*, 1995). Inhibition of complex II following exposure to the NO donor S-nitroso-N-acetylpenicillamine (SNAP) has also been reported in astrocytes, microglia, and oligodendrocytes (Mitrovic *et al.*, 1994). The activity of complex I in astrocytes and neurones has been shown to be unaffected by both NO and peroxynitrite provided that cellular GSH levels were maintained (Bolanos *et al.*, 1996, Barker *et al.*, 1996). The loss of complex I activity and a concomitant depletion of GSH has also been reported in the J774 macrophage cell line following exposure to peroxynitrite (Clementi *et al.*, 1998).

Mitochondria are also susceptible to inhibition by reactive oxygen species. Complexes II and IV of the ETC were inhibited when heart sub-mitochondrial particles were exposed to hydrogen peroxide, hydroxyl radicals, or superoxide (Zhang *et al.*, 1990). Hydrogen peroxide generated from the oxidation of dopamine by monoamine oxidase also inhibited brain mitochondrial respiration (Berman & Hastings, 1999; Cohen & Kesler, 1999). The individual complexes of the ETC were not measured in either study. However, use of substrates that donate electrons at different points of the ETC implied that inhibition of complex III was the reason for impaired mitochondrial respiration (Berman & Hastings, 1999). Mitochondria exposed to exogenous hydrogen peroxide also results in reduced mitochondrial respiration (Sims *et al.*, 2000; Gluck *et al.*, 2002). Using a variety

of substrates, Gluck *et al* (2002) report that complex II is sensitive to hydrogen peroxide, but that the effects of hydrogen peroxide were not just confined to the ETC, but to other components of the mitochondria as well. Indeed, Sims *et al* (2000) concluded that hydrogen peroxide impaired the activity of mitochondrial enzymes involved in the generation of NADH rather than the ETC, since the complexes of the ETC appeared unaffected following exposure. Exposure of rat synaptosomes to ascorbate/iron (which will generate hydroxyl radicals) also results in the reduction of the activities of complexes II and III of the ETC, while complexes I and IV were unaffected (Cardoso *et al.*, 1998). All the studies reported above suggest that complexes II, III, and IV of the ETC are much more susceptible to reactive oxygen and nitrogen species, compared to complex I. However, the latter can become susceptible when glutathione availability is compromised (Barker *et al.*, 1996).

It should be noted that in addition to oxidative modification of proteins, prolonged exposure to oxidative species may also alter ETC activity by mutating DNA, and in particular mtDNA. mtDNA has been reported to be ten times more susceptible to oxidative stress than nuclear DNA due to less efficient repair systems, and a lack of histones (Mecocci *et al.*, 1993). Indeed, increased levels of 8-oxo-2'-deoxyguanosine and multiple deletions have been reported to in mtDNA following oxidative stress and ageing (Mecocci *et al.*, 1993; Nagley & Wei, 1998; Lu *et al.*, 2000). Since mitochondria have essentially no sequence redundancy, mutations and deletions could affect the functions of the thirteen polypeptides coding for components of complexes I, III, IV and V, or the ribosomal and transfer RNA molecules necessary for their translation.

1.9. Implications of ETC inhibition

Impairment of one or more of the ETC complexes could have important implications for the synthesis of ATP by the cell. Studies *in vitro* have suggested that each complex of the ETC has different inhibition thresholds before ATP synthesis is compromised, and that these thresholds vary from cell to cell (Davey & Clark, 1996; Davey *et al.*, 1998). For example, complex I in non-synaptic mitochondria needed to be inhibited by 72% before changes in mitochondrial

respiration and ATP synthesis were observed (Davey & Clark, 1996), while only a 25% inhibition of complex I was required in synaptic mitochondria (Davey *et al.*, 1998). Interestingly, depletion of glutathione in rat PC12 cells has been shown to lower the threshold at which inhibition of complex I affects respiration (Davey *et al.*, 1998). Complexes III and IV need to be inhibited by 70% and 60% in nonsynaptic mitochondria, and 80% and 70% in synaptic mitochondria (Davey & Clark, 1996; Davey *et al.*, 1998).

Inhibition of the complexes by oxidising species could also increase production of superoxide and hydrogen peroxide (Paradies *et al.*, 2000; Han *et al.*, 2001) and thereby further damage the complexes of the ETC, other cellular proteins, and mtDNA. The increased oxidising environment may also induce the opening of the mitochondrial permeability transition pore (Nieminen *et al.*, 1995; Costantini *et al.*, 1996), which could lead to necrosis and/or apoptosis of the cell.

1.10. The role of mitochondria in necrosis and apoptosis

Mitochondria are thought to play an important role in both apoptosis and necrosis. The opening of the mitochondrial permeability transition pore (MPT pore) has been implicated in necrosis (Lemasters *et al*, 1998; Halestrap *et al.*, 2000). The mitochondrial permeability transition (MPT) is the result of a sudden increase in permeability of the inner mitochondrial membrane to solutes with a molecular mass of less than 1500 kDa (Halestrap *et al.*, 1998; Crompton *et al.*, 1999). The increased permeability of the membrane causes membrane depolarisation, and therefore uncoupling of oxidative phosphorylation, resulting in a decrease in ATP synthesis (Halestrap *et al.*, 2000). MPT also causes the release of intramitochondrial ions and metabolites, and mitochondrial swelling (Halestrap *et al.*, 1998; Lemasters *et al.*, 1998; Crompton *et al.*, 1999). Swollen, uncoupled mitochondria have been observed in necrotic cells, and opening of the MPT pore has been observed following hypoxia and ischaemia (Halestarp *et al.*, 1998; Lemasters *et al.*, 1998).

Opening of the MPT pore is promoted by increased cellular calcium concentrations and increased inorganic phosphate (P_i) concentrations due to ATP

depletion within cells (Lemasters *et al.*, 1998 Halestrap *et al.*, 2000). Oxidative stress has also been implicated in the opening of the MPT pore. Exposure of liver mitochondria to oxidising species such as *tert*-butylhydroperoxide (Nieminen *et al.*, 1995; Costantini *et al.*, 1996), and oxidation of two thiols of the MPT pore induces MPT (Costantini *et al.*, 1996).

The components of the MPT pore are an area of controversy. Halestrap *et al* (2000) report that the MPT pore is composed of the inner mitochondrial membrane transporter adenine nucleotide translocase (ANT), and the mitochondrial matrix protein cyclophilin P. However, the voltage-dependent anion channel (VDAC; also known as porin), an outer membrane protein, has also been proposed to be a component of the MPT pore, in addition to ANT and cyclophilin P (Crompton *et al.*, 1998; Shimizu *et al.*, 1999).

The release of cytochrome c and apoptosis inducing factor (AIF) from mitochondria has been postulated to be an early event in apoptosis (Susin *et al.*, 1996; Yang *et al.*, 1997; Narita *et al.*, 1998). The MPT has been implicated in the release of these factors since inhibition of the MPT by cyclosporin A has been reported to prevent the release of cytochrome c (Lemasters *et al*, 1998; Narita *et al.*, 1998; Brookes *et al.*, 2000). It is unclear whether release is due to a non-specific rupture of the outer mitochondrial membrane following MPT or the formation of specific cytochrome c channel pores. The interaction of the Bcl-2 family of proteins (*e.g.,* Bax, Bak, Bad) with the MPT pore have also been reported to be necessary for cytochrome release to occur (Narita *et al.*, 1998; Shimizu *et al.*, 1999). Alternatively, the release of cytochrome c has been reported to be independent of the MPT since cytochrome c can be observed without a loss of membrane potential (Halestrap *et al.*, 2000). Furthermore, dimers of Bax can release cytochrome c without membrane swelling, loss of membrane potential, or inhibition by cyclosporin A (Eskes *et al.*, 1998; Halestrap *et al.*, 2000). Perhaps cytochrome c is released by a variety of methods, with the type of mitochondria (*e.g.,* brain versus heart), and/or the type of insult initiating release, determining which mechanism is used. The non-specificity of cyclosporin A (*e.g.,* it can also inhibit protein phophatase; Halestrap *et al.*, 2000) may have also lead to erroneous conclusions in some cases.

Once cytochrome c is released, it can bind with apoptotic protease-activating factor 1 (Apaf-1) in the presence of ATP or dATP. This complex can then activate caspase-9, which in turn can initiate the activation of other caspases and lead to apoptosis (reviewed by Desagher & Martinou, 2000; Jackson *et al.*, 2002). The release of AIF can also initiate apoptosis via a caspase-independent pathway (reviewed by Jackson *et al.*, 2002).

1.11. Glutathione

Glutathione (GSH) is a tripeptide (γ-glutamylcysteinylglycine; **Figure 1.5a**) with a molecular mass of 307, is ubiquitously found in both prokaryotes and eukaryotes, and is the most prevalent low molecular mass intracellular thiol in plants and animals (Meister & Anderson, 1983). Unusually, the peptide bond between the glutamate and cysteine residues is via the carboxyl group attached to the γ-carbon of glutamate, rather than the more orthodox α-carbon carboxyl group (**Figure 1.5a**). This has been postulated to protect the tripetide from degradation by aminopeptidases (Sies, 1999; Lu, 2000). Glutathione disulphide (GSSG; **Figure 1.5b**) is formed upon oxidation of GSH. The ratio of GSH to GSSG is approximately 100:1 in the cytosol (Meister & Anderson, 1983; Dringen & Hamprecht, 1997; Kirlin *et al.*, 1999), although intracellular GSSG levels can increase during oxidative stress (Meister & Anderson, 1983; Ben-Yoseph *et al.*, 1996; Dringen *et al.*, 1999b). The cellular GSH:GSSG ratio is in part determined by GSH reductase (EC 1.8.1.7) and the GSH peroxidases (EC 1.11.1.9; Meister & Anderson, 1983; Ben-Yoseph *et al.*, 1996).The millimolar concentrations of GSH within the cell and the high GSH:GSSG ratio maintains a reducing environment in the cell.

GSH has been implicated directly or indirectly in a variety of biological processes. The most important function of GSH is probably its role in protecting cells from free radicals and other oxidising species (Bolanos *et al.*, 1996; Barker *et al.*, 1996; Dringen *et al.*, 1999b; Iwata-Ichikawa *et al.*, 1999), and the maintenance of the redox potential of the cell (*e.g.*, maintaining protein thiols in a reduced state; Sriram *et al.*, 1998; Ehrhart & Zeevalk, 2001). GSH also acts as a carrier of cysteine around the body (Meister & Anderson, 1983; Dringen *et al.*, 1999a),

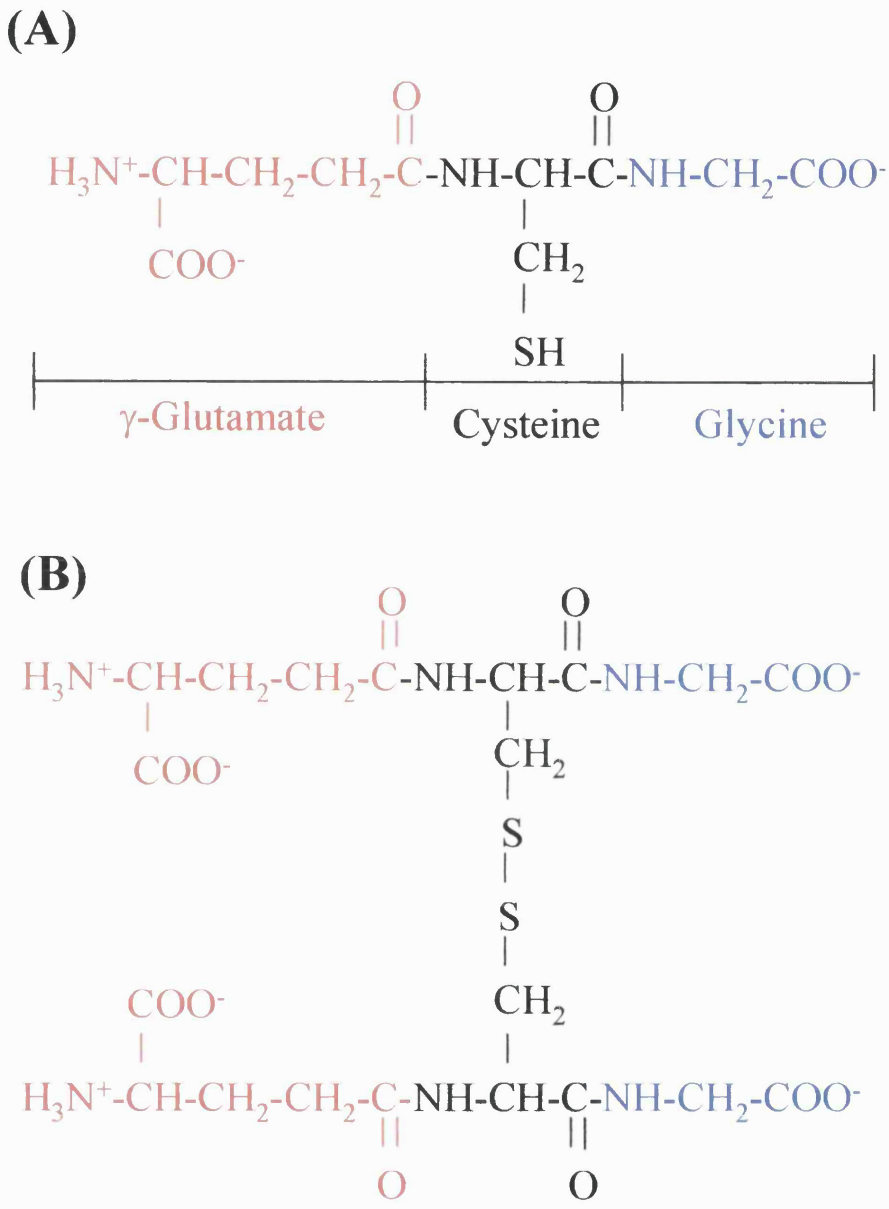

Figure 1.5. The structure of GSH

The structure of reduced GSH (A) and oxidised GSH (B).

detoxifies xenobiotica (Yamane *et al.*, 1998; Borst *et al.*, 1999), and has recently been implicated in the post-translational modification of proteins (Grant *et al.*, 1999; Klatt & Lamas, 2000; Pineda-Molina *et al.*, 2001).

1.12. Cellular Localisation of glutathione

Intracellular concentrations of GSH vary between species, organ, and cell type and have been reported to be as high as 20 mM (Meister & Anderson, 1983; Yudkoff *et al.*, 1990; Dringen *et al.*, 2000). In mammals the greatest amount of GSH has been reported in the liver, followed by the kidney, and the brain (Thompson *et al.*, 1999; Liu & Choi, 2000; Liu, 2002). Within the brain, GSH levels vary from region to region (*e.g.,* the cortex has more GSH than the cerebellum; Kang *et al.*, 1999; Liu, 2002), and between cell types (Sagara *et al.*, 1993; Maker *et al.*, 1994; Bolanos *et al.*, 1995). For example, cortical astrocytes cultured in isolation have higher GSH levels compared to neurones derived from the same region (Maker *et al.*, 1994; Bolanos *et al.*, 1995).

Glutathione is predominately located in the cytosol (80-90%), while 10-15% of GSH has been reported in mitochondria (Meredith & Reed, 1982; Jain *et al.*, 1991; Wullner *et al.*, 1999). Small pools of GSH have also been located in the endoplasmic reticulum and nucleus (Hwang *et al.*, 1992; Voehringer *et al.*, 1998).

Evidence suggests that the mitochondrial GSH pool is preferentially maintained over that of the cytosolic pool during conditions of GSH depletion (*e.g.,* inhibition of GSH synthesis). Cytoplasmic GSH in cerebellar neurones was depleted by 75% in cells treated with the GSH synthesis inhibitor L-buthionine-S,R-sulfoximine (L-BSO) before a loss of mitochondrial GSH was observed (Wullner *et al.*, 1999). Newborn rats treated with L-BSO for 9 days resulted in an 82% and 84% depletion of GSH in cerebral cortex cytosol and mitochondria respectively (Jain *et al.*, 1991). However, when these animals were treated with membrane permeable GSH monoethyl ester, the mitochondrial GSH pool was nearly restored to control values, while cytosolic GSH remained depleted by 66% (Jain *et al.*, 1991). The transport mechanism by which GSH is taken up into mitochondria is still unknown. Substrate competition studies with rat kidney mitochondria have

implicated a role for the mitochondrial dicarboxylate and 2-oxoglutarate carriers in GSH transport (Chen & Lash, 1998; Chen *et al.*, 2000).

Extracellular GSH concentrations have been reported in the micromolar range (Meister & Anderson, 1983; Han *et al.*, 1999). Extracellular GSH concentrations in whole rat brain, striatum, and substantia nigra have been reported to be between 1.6 and 2 μM (Han *et al.*, 1999), while 5.9 μM GSH has been detected in cerebral spinal fluid (Wang & Cynader, 2000). Blood plasma GSH levels from the carotid artery and jugular vein of adult rats have been reported as 18.9 and 12.3 μM respectively (Jain *et al.*, 1991).

1.13. Glutathione Metabolism

Glutathione (GSH) is synthesised by the consecutive action of the ATP-dependent cytosolic enzymes glutamate-cysteine ligase (GCL; also known as γ-glutamylcysteine synthetase; EC 6.3.2.2) and glutathione synthetase (GS; EC 6.3.2.3; **Figure 1.6, reactions 1 and 2**)(Yip & Rudolph, 1976; Schandle & Rudolph, 1981; Meister & Anderson, 1983). GSH can be degraded by γ-glutamyltranspeptidase (γ-GT; EC 2.3.2.2; **Figure 1.6, reaction 3**), which is predominantly located in the outer leaflet of plasma membranes (Meister & Anderson, 1983; Ikeda *et al.*, 1995; Dringen *et al.*, 1997a). The cysteinylglycine generated by γ-GT can be hydrolysed by dipeptidases (**Figure 1.6, reaction 4**) and the cysteine and glycine used for *de novo* GSH synthesis (Dringen *et al.*, 2001). γ-glutamylcysteine (γ-GC), the product of GCL, and substrate for GS, can also be utilised by γ-glutamylcyclotransferase (γ-GCT; EC 2.3.2.4; **Figure 1.6, reaction 5**) to generate cysteine and 5-oxoproline, which can be further metabolised to glutamate by 5-oxoprolinase (EC 3.5.2.9; **Figure 1.6, reaction 6**; Meister & Anderson, 1983; Griffith, 1999). The glutamate and cysteine generated by these two latter enzymes can then be recycled. It should be noted that the Km of γ-GCT for γ-GC is twelve fold higher than that of GS, and therefore the vast majority of γ-GC is converted to GSH, rather than 5-oxoproline (Griffith, 1999). GSH can also be utilised by glutathione peroxidase (EC 1.11.1.9; **Figure 1.6,**

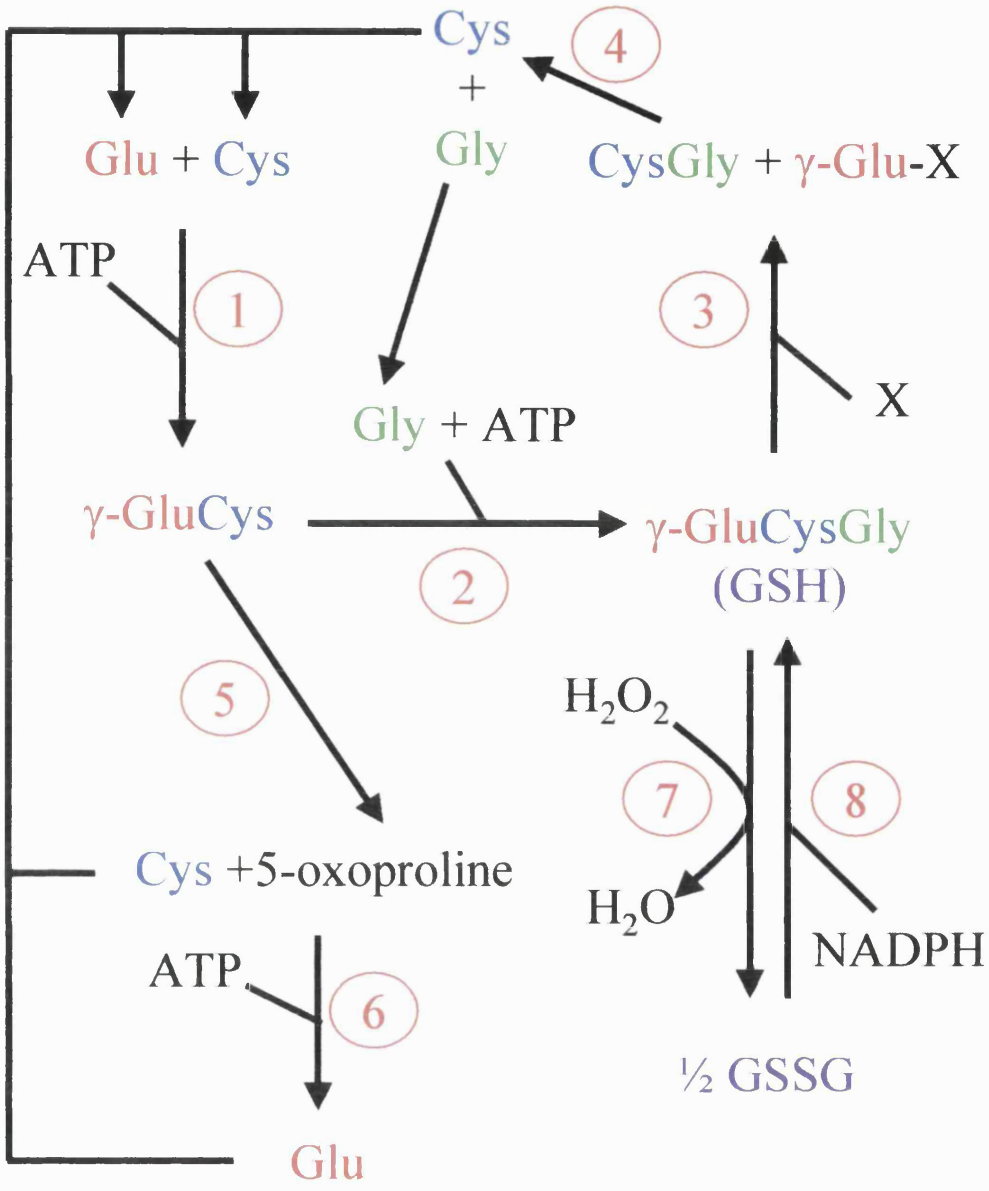

Figure 1.6. The γ-glutamyl cycle

1, glutamate cysteine ligase; 2, glutathione synthetase; 3, γ-glutamyltranspeptidase; 4, dipeptidase; 5, γ-glutamylcycoltransferase; 6, 5-oxoprolinase; 7, glutathione peroxidase; 8, glutathione reductase; Cys, cysteine; CysGly, cysteinylglycine; Gly, glycine; γ-GluCys, γ-glutamylcysteinylglycine Glu; glutamate; X, acceptor for γ-glutamyl moiety (see text for details).

reaction 7) to provide electrons to reduce hydrogen peroxide and other peroxides to water (Meister & Anderson, 1983; Ben- Yoseph *et al.*, 1996;Dringen *et al.*, 1999b). This results in the oxidation of GSSG, which can be reduced back to GSH by GSH reductase (EC 1.8.1.7; **Figure 1.6, reaction 8**) with the reducing equivalent NADPH (Meister & Anderson, 1983; Ben-Yoseph *et al.*, 1996).

1.13.1. Glutamate-cysteine ligase

GCL is the first enzyme in the GSH synthesis pathway, and is thought to be the rate-limiting step (Meister & Anderson, 1983; Grant *et al.*, 1997). GCL is a heterodimer, which can be dissociated into a large catalytic subunit (GCL_h) and a smaller regulatory/modifier subunit (GCL_l)(Huang *et al.*, 1993a; Tu & Anders 1998a). The catalytic domain of GCL in both rats and humans has been reported to have a relative molecular mass of approximately 73 kDa (Huang *et al.*, 1993a; Tu & Anders 1998a), while the regulatory subunit is approximately 30 kDa in these two species (Huang *et al.*, 1993b; Tu & Anders 1998a). The GCL_h and GCL_l subunits are encoded for by separate genes and have been mapped to chromosomes 6p12 and 1p21 respectively in humans (Gipp *et al.*, 1995; Tsuchiya *et al.*, 1995). Northern blotting of human GCL has indicated two ubiquitously expressed GCL_h transcripts (4.1 and 3.2 kb) and GCL_l transcripts (4.1 and 1.4 kb; Gipp *et al.*, 1995;). Rat GCL_l also has two transcripts (5.2 and 1.8 kb), while only one 4.1 kb transcript has been identified for GCL_h (Huang *et al.*, 1993b).

In rodents and chickens, GCL activity is greatest in the kidney (~10 nmol γ-GC synthesised/min/mg protein), with activity between 2 and 5-fold lower in the liver, and approximately 10 fold lower in brain (Maker *et al.*, 1994; Liu & Choi, 2000; Kang *et al.*, 1999; Liu, 2002).

GCL_h exhibits all the catalytic activity of the enzyme (Huang *et al.*, 1993a) and binds ATP, L-glutamate, and L-cysteine to form γ-glutamylcysteine (**Figure 1.6**; Yip & Rudolph, 1976; Schandle & Rudolph, 1981; Meister & Anderson, 1983). GCL_h is thought to bind ATP first, with L-glutamate and L-cysteine binding in a random order (Yip & Rudolph, 1976; Schandle & Rudolph, 1981). All substrates

must be bound before to the formation of products is observed (Schandle & Rudolph, 1981). The first step of the reaction is the attack of the γ-carboxyl group of glutamate attacking the γ-phosphoryl group of ATP to form γ-glutamylphosphate as an intermediate (**reaction 1.11**). The second step involves the amino group of cysteine reacting with γ-glutamylphosphate to form γ-glutamylcysteine and Pi (Orlowski & Meister, 1971; Griffith, 1982).

L-glutamate + ATP ➔ L-glutamylphosphate + ADP **(1.11)**

L-glutamylphosphate + L-cysteine ➔ L-glutamyl-L-cysteine + Pi

The availability of cysteine has been suggested to limit the rate of GCL activity (Meister & Anderson, 1983; Yudkoff *et al.*, 1990; Kranich *et al.*, 1998). The Km of rat kidney and recombinant human GCL for cysteine has been reported to be 0.2 mM and 0.8 mM respectively (Huang *et al.*, 1993a; Tu & Anders, 1998a). The Km of GCL for cysteine is very similar to the intracellular concentration of cysteine (*e.g.,* the intracellular GSH concentration in rat astrocytes has been reported to be approximately 1 mM; Meister & Anderson, 1983; Yudkoff *et al.*, 1990; Griffith, 1999). Therefore, the rate of GSH synthesis may be dependent on the intracellular cysteine concentration.

The GCL_l subunit does not have any catalytic activity, but does modify the affinity of GCL_h to substrates and inhibitors. The Km of rat kidney and recombinant human GCL_h for glutamate has been reported to be 18 and 3.5 mM respectively (Huang *et al.*, 1993a; Tu & Anders, 1998a). However when GCL_h is associated with GCL_l, the Km for glutamate is lowered to 1.4 and 0.7 mM in rat and human GCL respectively (Huang *et al.*, 1993a; Tu & Anders, 1998a). The Km of GCL_h for cysteine appears to be independent of GCL_l association (Huang *et al.*, 1993a; Tu & Anders, 1998a).

GCL activity is feedback-inhibited by GSH (Huang *et al.*, 1993a; Tu & Anders, 1993a). The association of rat GCL_l with GCL_h has been shown to increase the apparent Ki of GCL for GSH from 1.8 mM to 8.2 mM (Huang *et al.*, 1993a). The inhibition of GCL activity by GSH can be overcome in a competitive fashion by

increasing the concentration of glutamate (Huang *et al.*, 1993a). The reduction of disulphide bridges in GCL has been implicated in GSH-mediated inhibition. An unidentified intramolecular disulfide within GCL_h appears necessary for activity, since enzyme activity was inhibited when the enzyme was incubated with the reducing agent dithiothreitol (DTT; Tu & Anders, 1998b). However, this disulphide is unlikely to occur within the active site, since although there is a cysteine present, it must be in a reduced state for enzyme activity to occur (Seelig & Meister, 1982; Tu & Anders, 1998b). An intermolecular disulphide bridge between GCL_h and GCL_l has also been implicated in modulating enzyme activity. Mutation of cysteine-553 of human GCL_h to a glycine perturbed GCL holoenzyme activity and caused a greater dissociation of GCL_h from GCL_l (Tu & Anders, 1998b). Huang *et al* (1993a) have also reported that dissociation of GCL increased with greater GSH concentrations. Therefore, it appears that association of GCL_h and GCL_l induces some conformational change, which increases the affinity of the glutamate-binding site, while diminishing the competitive inhibition by GSH at the active site. However, reduction of possible intermolecular disulphide bridges between the two GCL subunits by GSH will favour GSH feedback inhibition.

1.13.2. Transcriptional regulation of GCL

A wide range of chemical, biological and physical agents in a variety of experimental paradigms have been shown to induce expression of GCL_h and/or GCL_l (reviewed in Soltaninassab *et al.*, 1999; Lu, 2000; Wild & Mulcahy, 2001). For example, induction of both GCL_h and GCL_l has been shown in cultured cells following exposure to oxidants such as hydrogen peroxide (astrocytes and epithelial cells), superoxide (epithelial cells), and NO (heart smooth muscle)(Tian *et al.*, 1997; Moellering *et al.*, 1998; Iwata-Ichikawa *et al.*, 1999), GSH depleting agents (hepatocytes)(Cai *et al.*, 1997; Huang *et al.*, 1999), and the lipid peroxidation product 4-hydroxy-2-nonenal (lung epithelia)(Liu *et al.*, 1998). Furthermore, exposure of hepatocytes to either insulin or alcohol increases expression of GCL_h only (Cai *et al.*, 1997; Huang *et al.*, 2000).

The promoters of mammalian GCL_l and GCL_h genes have been sequenced (Yang *et al.*, 2001a,b; reviewed in Wild & Mulcahy, 2001). Several putative regulatory sequences have been identified in both gene promoters including nuclear factor-$_\kappa$B (NF-$_\kappa$B), electrophile responsive element (EpRE; also known as antioxidant response elements) and AP-1 (Yang *et al.*, 2001a,b; reviewed in Wild & Mulcahy, 2001). However, there are conflicting reports as to which promoter elements are involved in both constitutive and inducible expression of the GCL genes (Reviewed in Wild & Mulcahy, 2001). It is probable that the inconsistencies so far observed may in part be due to the existence of agent-dependent alternative activation pathways and the multitude of cell culture systems investigated.

1.13.3. Post-translational modification of GCL

Apart from the possible reduction of disulphide bridges by GSH during feedback inhibition (see section 1.14.1), phosphorylation of GCL has been reported to modulate enzyme activity. Phosphorylation of GCL_h, but not GCL_l, has been observed in both purified rat kidney GCL and in cultured hepatocytes, by protein kinase A, protein kinase C, or Ca^{2+}/calmodulin-dependent kinase (Sun *et al.*, 1996). The phosphorylation of GCL resulted in a loss of enzyme activity, which was not due to dissociation of the subunits (Sun *et al.*, 1996). Given the role of these kinases in a variety of signalling pathways, this process maybe important in regulating cellular GSH concentration.

1.13.4. Glutathione synthetase

While GCL has been extensively studied, very little attention has been paid to the second enzyme of GSH synthesis Glutathione synthetase (GS). GS has been cloned from rat kidney and human (Gali & Board, 1995; Huang *et al.*, 1995). Rat kidney and human GS appear to be homodimers, with each subunit containing an active site and a molecular mass of approximately 53-59 kDa (Oppenheimer *et al.*, 1979; Gali & Board, 1995; Huang *et al.*, 1995). Gel filtration chromatography has

1.13.5. Inborn errors of GSH synthesis

Hereditary defects in both GCL and GS have been described (Dahl *et al.*, 1997; Ristoff & Larsson, 1998; Mayatepek, 1999). GCL deficiency is very rare with patients commonly exhibiting decreased GSH levels throughout the body and haemolytic anaemia (Ristoff & Larsson, 1998). In certain cases spinocerebellar and neuromuscular degeneration is also observed. Homozygous GCLh knockouts are embryonic lethal in mice (Dalton *et al.*, 2000) and may explain why this deficiency is rarely seen in humans. Hereditary GS deficiency is much more common and GSH depletion can either be localised to erythrocytes or be generalised (Ristoff & Larsson, 1998). Low GSH levels will result in a lack of feedback inhibition of GCL, and therefore over production of γ-GC. γ-GC is converted to 5-oxoproline by γ-GCT (**Figure 1.6, reaction 5**). Excessive production of 5-oxoproline exceeds the capacity of 5-oxoprolinase (**Figure 1.6, reaction 6**), and therefore 5-oxoproline accumulates causing metabolic acidosis and excretion of 5-oxoproline (~30%) (Meister & Anderson, 1983; Mayatepek, 1999). About half the patients have progressive CNS damage including mental retardation and ataxia (Dahl *et al.*, 1997; Ristoff & Larsson, 1998). It should be noted that γ-GC can act as an antioxidant and could alleviate some of the symptoms (Grant *et al.*, 1997).

1.13.6. γ-glutamyltranspeptidase

γ-glutamyltranspeptidase (γ-GT) catalyses the degradation of extracellular GSH (see section 1.15.1 for GSH release), and is primarily localised to the outer leaflet of the plasma membrane (Shine & Haber, 1981; Nash & Tate, 1984; Ikeda *et al.*, 1995). The mammalian enzyme is translated as a single polypeptide, and is then glycosylated and cleaved into a heavy and light subunit in the endoplasmic reticulum or golgi, prior to export to the plasma membrane (Nash & Tate, 1984; Ikeda *et al.*, 1995). The glycosylated human γ-GT heavy subunit (44 kDa) contains a small cytosolic domain (6 amino acids), a single transmembrane domain (20 amino acids), and a large carboxy terminal ectodomain (Ikeda *et al.*, 1995; Hanigan, 1998). The heavy subunit is thought to anchor the enzyme to the

membrane (Meister & Anderson, 1983; Ikeda *et al.*, 1995). The human light subunit (24 kDa) is an ectodomain associated with the heavy subunit, and contains the active site residues responsible for binding GSH (Meister & Anderson, 1983; Stole et al., 1990; Ikeda *et al.*, 1995). Several genes encoding for γ-GT have been identified in humans and are located on chromosomes 18, 19, 20 and 22 (3 genes)(Figlewicz *et al.*, 1993). A single gene locus encodes for γ-GT in rat. However, tissue-specific expression of several mRNA species has been identified due to multiple promoter start sites (Darbouy *et al.*, 1991). Indeed, the γ-GT propeptide in rat brain has been reported to be 74 kDa, while the rat kidney isoform has been estimated to have a molecular mass of 78kDa (Reyes & Barela, 1980; Nash & Tate, 1984). γ-GT activity in rat is greatest in kidney, brain and testis (Hemmings and Storey, 1999).

Within the brain, most γ-GT activity appears to be localised to the endothelial cells lining blood vessels (Hemmings and Storey, 1999). γ-GT activity has also been associated with glia, but probably not neurones (Shine & Haber 1981; Dringen *et al.*, 1997a; Hemmings and Storey, 1999).

γ-GT degrades GSH into a γ-glutamyl moiety and cysteinylglycine (**reaction 1.13**; Meister & Anderson, 1983; Dringen *et al.*, 1997a). The enzyme catalyses the transfer of the γ-glutamyl moiety to an acceptor (X), which could be an amino acid, a dipeptide, water, GSSG, or another molecule of GSH (Meister & Anderson, 1983; Stole *et al.*, 1994).

γ-glutamylcysteinylglycine + X ➔ γ-glutamyl-X + cysteinylglycine **(1.13)**
(GSH)

1.14. GSH metabolism in astrocytes and neurones

1.14.1. Astrocytic GSH release

Extracellular GSH has been reported in the micromolar range in the brains of rats (Han *et al.*, 1999). Several studies have reported that cultured rat astrocytes

release GSH into extracellular media (Yudkoff *et al.*, 1990; Sagara *et al.*, 1996; Stone *et al.*, 1999), with approximately 10% of intracellular GSH estimated to be released per hour (Sagara *et al.*, 1996; Dringen *et al.*, 1997a). Despite this release, intracellular astrocytic GSH levels remain unchanged. Neurones either release no GSH or very little (Wang & Cynader, 2000). Inhibition of γ-GT with acivicin (Stole *et al.*, 1994) increased the extracellular concentration of GSH detected, indicating that released GSH is a substrate for the enzyme (Dringen *et al.*, 1997a). Furthermore, prolonged incubation (10 hours) with acivicin caused a depletion of intracellular GSH levels, suggesting that the metabolism of GSH by γ-GT is required to provide precursors (*e.g.*, cysteine, glycine, and glutamate) for *de novo* GSH synthesis (Dringen *et al.*, 1997a). Indeed, when uptake of CysGly (a product of GSH degradation by γ-GT; **reaction 1.13**) in astrocytes was inhibited by blocking the peptide transporter PepT2, astrocytes were unable to maintain intracellular GSH levels (Dringen *et al.*, 1998).

The mechanism by which GSH is released by astrocytes is unknown. Sagara *et al* (1996) found that the rate of GSH release was dependent on temperature, and was susceptible to partial inhibition when thiols on the outer leaflet of the plasma membrane were oxidised. These results suggest that a protein transporter mediates GSH efflux from astrocytes. The multidrug resistance protein (MRP) family of transporters have been postulated to release GSH (Yamane *et al.*, 1998; Paulusma *et al.*, 1999). The MRP family were originally identified as playing a role in the drug resistance of cancer cells (Borst *et al.*, 1999). Over expression of MRP1 and MRP2 in cultured kidney cells have been shown to increase GSH efflux, while homozygous MRP2 knock-out rats did not release GSH into the bile duct and was concomitant with increased intracellular GSH levels (Paulusma *et al.*, 1999). MRP1, but not MRP2, has been shown to be expressed in rat astrocytes and to facilitate GSSG release (Hirrlinger *et al.*, 2001). No studies on MRP1-mediated GSH release from astrocytes have been reported to date.

1.14.2 Cultured astrocytes and neurones differ in their preference of amino acids for GSH synthesis.

Neurones cultured in isolation are considered to contain less GSH compared to astrocytes cultured in isolation (Sagara *et al.*, 1993; Makar *et al.*, 1994; Bolanos *et al.*, 1995; Dringen *et al.*, 1999b). It has been postulated that the availability of cysteine in culture media may limit the GSH content in neurones (Sagara *et al.*, 1993; Kranich *et al.*, 1996; Dringen *et al.*, 1999a). GSH levels in cultured neurones can be elevated when incubated with cysteine, but not cystine (Sagara *et al.*, 1993; Kranich *et al.*, 1996). Neurones have been shown to be capable of taking up cystine via both sodium-independent (*e.g.*, X_C- transporter) and sodium-dependent (*e.g.*, X_{AG}- transporter) transport systems (Allen *et al.*, 2001; McBean & Flynn, 2001). This would suggest that the reason why neurones cannot utilise cystine for GSH synthesis is not due to a lack of uptake. Incubation of neurones with glycine or glutamine (as a source for glutamate) had no effect on neuronal GSH levels, indicating that these two precursors of GSH are not limiting (Dringen *et al.*, 1999a). Astrocytes can utilise either cysteine or cystine as precursors for GSH synthesis (Cho & Bannai, 1990; Sagara *et al.*, 1993; Kranich *et al.*, 1996, 1998), with cystine suggested to be the preferred substrate (Kranich *et al.*, 1996, 1998). Once again, neither glutamate nor glycine appears to limit GSH synthesis in astrocytes (Dringen *et al.*, 1997b).

When neurones are cocultured with astrocytes, neuronal GSH levels are approximately doubled, compared to neurones cultured alone (Sagara *et al.*, 1993; Bolanos *et al.*, 1996; Dringen *et al.*, 1999a). The release of GSH by astrocytes has been postulated to provide precursors for *de novo* neuronal GSH synthesis (Dringen *et al.*, 1999a; Wang & Cynader, 2000). Wang and Cynader (2000) have proposed that the GSH released by astrocytes reduces the cystine present in the culture media to cysteine, which can then be taken up by neurones and utilised for GSH synthesis (**Figure 1.7, route 1**). Alternatively, Dringen *et al* (1999a) have suggested that the GSH released by astrocytes is metabolised to CysGly by γ-GT, with the CysGly then being used by neurones as a precursor for GSH synthesis (**Figure 1.7, route 2**). In support of this, neurones that are incubated with CysGly

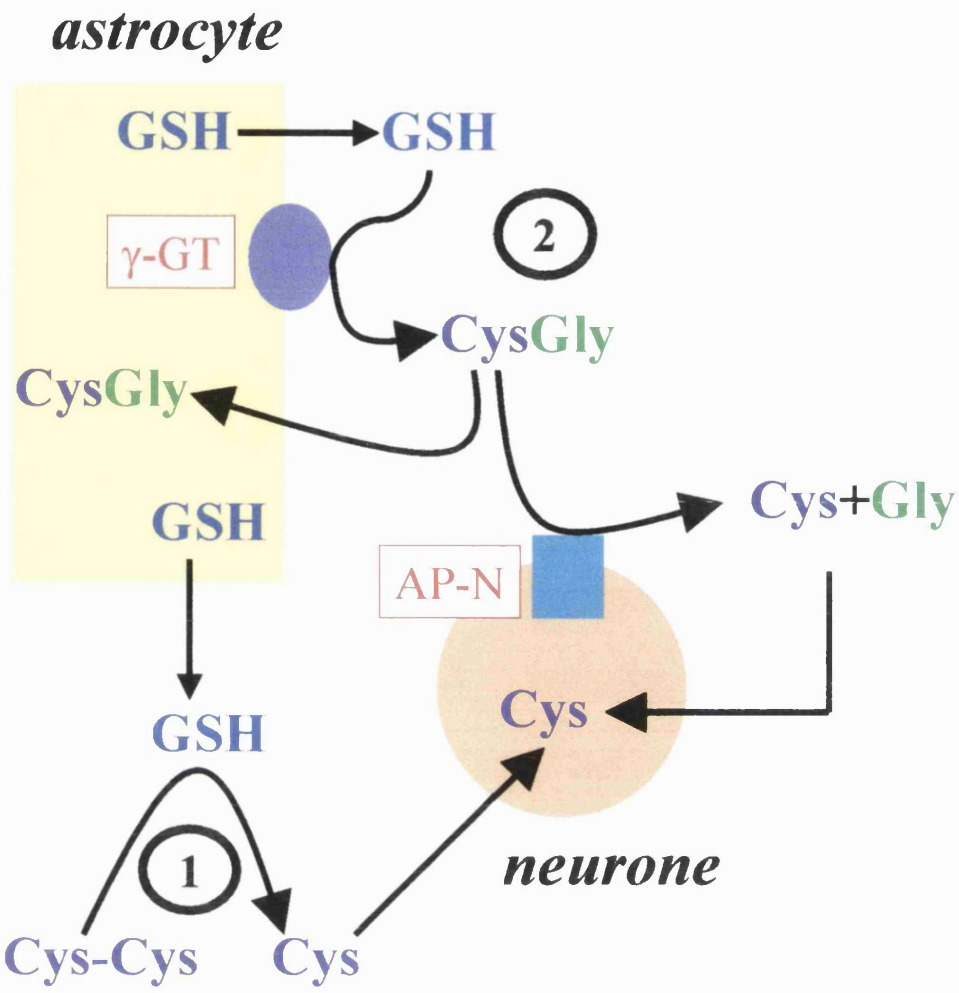

Figure 1.7. The supply of neuronal GSH precursors by astrocytes

Astrocytes release GSH which can either (1) reduce cystine (Cys-Cys) to cysteine (Cys), or (2) be metabolised by γ-glutamyltranspeptidase (γ-GT) to cysteinylglycine (CysGly), which can then be taken up by astrocytes to be recycled into GSH, or hydrolysed by aminopeptidase N (AP-N) on neurones, to generate cysteine and glycine (Gly). The cysteine generated by routes 1 and 2 can then be taken up by neurones for *de novo* GSH synthesis.

elevate their GSH levels (Dringen *et al.*, 1999a). Furthermore, inhibition of astrocytic γ-GT by acivicin prevented the elevation of neuronal GSH levels when they were cocultured with astrocytes (Dringen *et al.*, 1999a). Note that CysGly has also been shown to increase GSH levels in astrocytes (Dringen *et al.*, 1997b), and is thought to be taken up by the PepT2 dipeptide transporter (Dringen *et al.*, 1998). Indeed inhibition of this transporter causes depletion of GSH in astrocytes (Dringen *et al.*, 1998). Neurones have been shown not to express PepT2 (Dringen *et al.*, 2001). Instead CysGly has been reported to be hydrolysed by the dipeptidase aminopeptidase N (EC 3.4.11.2), which has been localised to the outer leaflet of the neuronal plasma membrane (Dringen *et al.*, 2001). The cysteine and glycine generated by this enzyme is then taken up by the neurones. Indeed, treatment of neurones with either CysGly or cysteine + glycine elevated GSH levels to a similar extent (Dringen *et al.*, 1999a, 2001). Furthermore, extracellular cysteine levels are elevated 7-fold when neurones are cocultured with astrocytes (Sagara *et al.*, 1993).

1.15. Antioxidant properties of glutathione

The thiol group of GSH makes the tripeptide an important scavenger of oxidising species such as hydrogen peroxide, hydroxyl radical, and reactive nitrogen species GSH is the substrate for the hydrogen peroxide removing enzyme GSH peroxidase (**Figure 1.6, reaction 7**; Flohe *et al.*, 1973; Meister & Anderson, 1983; Dringen & Hamprecht 1997; reviewed by Brigelius-Flohe, 1999). The four known GSH peroxidases contain selenocysteine at the active site, and can metabolise hydrogen peroxide and lipid peroxides (Flohe *et al.*, 1973; Dringen *et al.*, 1999b; reviewed by Brigelius-Flohe, 1999). GSH peroxidase 1 is located in the cytosol and mitochondria, and is a homotetramer, with each subunit containing one selenium atom (Flohe *et al.*, 1973; Meister & Anderson, 1983). The enzyme is ubiquitously expressed, however upon selenium deficiency, GSH peroxidase 1 is preferentially maintained in the brain, suggesting that the enzyme is an important defence against oxidants within the brain (Brigelius-Flohe, 1999). The activity of catalase has been reported to be considerably lower in the brain compared to the rest of the body (Halliwell & Gutteridge, 1989). Indeed, inhibition of catalase activity in cultured rat astrocytes had no effect on the

clearance of hydrogen peroxide (Dringen & Hamprecht, 1997), while cell viability in striatal and cerebral cortical neurones exposed to hydrogen peroxide was similar in the absence or presence of a catalase inhibitor (Ben-Yoseph *et al.*, 1996; Desagher *et al.*, 1996). However, it should be noted that the rate of hydrogen peroxide clearance from media by neurones isolated from whole rat brain was shown to be three-fold lower when incubated with a catalase inhibitor (Dringen *et al.*, 1999b).

Glutathione peroxidase catalyses the reduction of hydrogen peroxide to water, and the oxidation of GSH to GSSG (**reaction 1.14**). The GSH apparently reduces the bound selenium, which then reacts with the hydrogen peroxide (Meister & Anderson, 1983; Halliwell & Gutteridge, 1989).

$$H_2O_2 + 2GSH \rightarrow GSSG + 2H_2O \qquad \textbf{(1.14)}$$

Accumulation of GSSG will lower the GSH/GSSG ratio, which has been implicated in increased cytotoxicity (Dringen & Hamprecht, 1997; Cotgreave & Gerdes, 1998). Therefore GSSG is either released from cells (Hirrlinger *et al.*, 2001) or reduced back to GSH by the flavoprotein GSH reductase (**Figure 1.6, reaction 8**). Mammalian GSH reductase is a homodimer, with each active site binding GSSG, FAD, and NADPH (Meister & Anderson, 1983; Pai & Schulz, 1983; Voet & Voet, 1990).The enzyme is located in both the mitochondria and cytosol (Tamura *et al.*, 1996). NADPH has been reported to reduce FAD, which then passes on electrons to the disulphide bridge between GSSG (**Figure 1.5b**), thus generating two GSH (**reaction 1.15**; Meister & Anderson, 1983; Pai & Schulz, 1983).

$$GSSG + NADPH + H^+ \rightarrow 2GSH + NADP^+ \qquad \textbf{(1.15)}$$

The pentose phosphate pathway generates the reducing equivalent NADPH, which is necessary for GSSG to be reduced back to GSH by GSH reductase (Ben-Yoseph *et al.*, 1996; Salvemini *et al.*, 1999). The activity of the pentose phosphate pathway has been shown to be increased in astrocytes, and to a lesser extent in

neurones, upon exposure to hydrogen peroxide or NO (Ben-Yoseph *et al.*, 1996; Garcia-Nogales *et al.*, 1999).

As well as GSH being involved in the enzymatic-reduction of hydrogen peroxide and organic peroxides, GSH can also react non-enzymatically with reactive oxygen species such as the hydroxyl radical and superoxide to form a thiyl radical ($GS^{\cdot}$; **reaction 1.16-17**; Halliwell & Gutteridge, 1989; Quijano *et al.*, 1997).

$$GSH + OH^{\cdot} \rightarrow GS^{\cdot} + H_2O \qquad \textbf{(1.16)}$$

$$GSH + O_2^{\cdot} + H^+ \rightarrow GS^{\cdot} + H_2O_2 \qquad \textbf{(1.17)}$$

The thiyl radical can then react with other thiyl radicals to form GSSG.

Glutathione is also an important cellular defence against the oxidation and reduction products of the free radical NO. NO itself reacts relatively slowly with GSH (Gaston, 1999; Hughes, 1999). However, the oxidation of NO to NO^+ (*e.g.*, by metals or other oxidants) confers high reactivity with GSH to form S-nitrosoglutathione (GSNO; **reaction 1.18**; Gaston, 1999; Hughes, 1999).

$$GSH + NO^+ \rightarrow GSNO + H^+ \qquad \textbf{(1.18)}$$

GSNO can then react further with GSH via a complicated set of reactions to form GSSG, nitrite (NO_2^-), and NH_3 (Singh *et al.*, 1996).

NO^- (formed by the reduction of NO by superoxide dismutase or ferrocytochrome c) also reacts readily with GSH to form GSSG and hydroxylamine (**reaction 1.19**; Hughes, 1999).

$$GSH + NO^- + H^+ \rightarrow GSNHOH \qquad \textbf{(1.19)}$$

$$GSNHOH + GSH \rightarrow GSSG + NH_2OH$$

Peroxynitrite (formed by the reaction of NO with superoxide) will also react with GSH via several different reactions depending on various factors such as pH and GSH concentration (Quijano *et al.*, 1997). Under physiological conditions (*e.g.*, pH 7.4, 37°C, 5-10 mM GSH) the vast majority of peroxynitrite (>90%) reacts with GSH to form an unstable sulphenic acid (GSOH), which can then rapidly react with another GSH molecule to form GSSG (**reaction 1.20**; Quijano *et al.*, 1997).

$$GSH + ONOO^- \rightarrow GSOH + NO_2^- \qquad \textbf{(1.20)}$$

$$GSOH + GSH \rightarrow GSSG + H_2O$$

Recently the reversible covalent addition of GSH to cysteine residues on target proteins (*e.g.*, protein-SSG) during oxidative stress has been postulated to be a protective mechanism (reviewed by Klatt & Thomas, 2000). Increased protein-GSH mixed disulphides have been reported in mammalian brain, endothelial, and hepatocytes cells upon oxidative stress (*e.g.*, exposure to hydrogen peroxide or NO; Schuppe-Koistinen *et al.*, 1994; Jung & Thomas, 1996; Ehrhart & Zeevalk, 2001). It is postulated that GSH reacts with protein cysteine residues that have been reversibly oxidised to sulfenic acid (-SOH) by for example hydrogen peroxide or peroxynitrite (**reaction 1.20**), to prevent further oxidation of the residue to sulfinic ($-SO_2H$) or sulfonic ($-SO_3H$) acid, which will essentially irreversibly oxidise the protein (Klatt & Thomas, 1999). For example, in yeast three isoforms of the glycolytic enzyme glyceraldehyde-3-phosphate dehydrogenase (GAPDH) are expressed (TdH1-3; Grant *et al.*, 1999). Following exposure to hydrogen peroxide, Tdh2 is irreversible inactivated, while Tdh3 is restored following removal of the hydrogen peroxide (Grant *et al.*, 1999). Tdh3 was shown to form a protein-GSH mixed disulphide upon exposure to hydrogen peroxide, whereas Tdh2 did not (Grant *et al.*, 1999). Protein-GSH mixed disulphides could also protect critical cysteine residues from nitrosation (see **reaction 1.18**; Klatt & Lamas, 2000). Rabbit muscle GAPDH has been shown to bind GSH upon exposure to NO leading to inactivation of the enzyme (Mohr *et al.*, 1999). GAPDH activity was restored following incubation with the reducing agent dithiothreitol (Mohr *et al.*, 1999). Furthermore, the formation of protein-

GSH mixed disulphides in muscle results in the peroxynitrite dependent inhibition of Ca^{2+}-ATPase being a reversible process, rather than irreversible (Viner *et al.*, 1999).

1.16. The importance of GSH as an antioxidant within the brain

The role of GSH as an important cellular defence against reactive oxygen/nitrogen species in the brain has been demonstrated by a variety of experimental paradigms. Depletion of GSH levels in cultured rodent mesencephalic or cortical neurones by L-BSO has been shown to result in increased neuronal death (Bolanos *et al.*, 1996; Ibi *et al.*, 1999; Wullner *et al.*, 1999; Nakamura *et al.*, 2000b), with depletion of the mitochondrial GSH pool greatly increasing neuronal cell loss (Wullner *et al.*, 1999). Cellular GSH levels within the brain have also been widely reported to dictate susceptibility to reactive oxygen and nitrogen species. The amount of cell death in cultured neurones depleted of GSH is greater when exposed to nitric oxide, hydrogen peroxide, or organic peroxides (Ben-Yoseph *et al.*, 1996; Desagher *et al.*, 1996; Ibi *et al.*, 1999; Nakamura *et al*, 2000b). Furthermore, the lower GSH levels found in cultured neurones compared to astrocytes have been postulated to be a reason why neurones appear to be more susceptible to oxidative stress than astrocytes (Bolanos *et al.*, 1995,1996). A much greater amount of cell death has been observed in neurones exposed to the same amount of NO, peroxynitrite, or hydrogen peroxide compared to astrocytes (Bolanos *et al.*, 1995; Ben-Yoseph *et al.*, 1996; Iwata-Ichikawa *et al.*, 1999; Almeida *et al.*, 2001). Indeed, when GSH levels are elevated in either the neuroblastoma cell line SK-N-MC by expression of Bcl-2, or cultured rat neurones by induction of GCL expression, the cells are much less susceptible to hydrogen peroxide mediated cell death (Iwata-Ichikawa *et al.*, 1999; Lee *et al.*, 2001). The amount of lipid peroxidation and oxidised protein has also been reported to be less in cultured neurones, neuroblastoma cell lines, and rat synaptosomes in the presence of greater GSH levels (Anderson *et al.*, 1996; Cardoso *et al.*, 1999; Lee *et al.*, 2001).

The function of brain mitochondria appear to be particularly vulnerable to GSH depletion. GSH-depleted mitochondria from both the cerebral cortex of rats and

cultured rat neurones have been shown to be swollen and exhibit signs of degeneration (Jain *et al.*, 1991, Wullner *et al.,* 1999). Furthermore, cellular GSH status has been postulated to dictate susceptibility of the mitochondrial respiratory chain to oxidative stress in the brain (see below).

1.16.1. GSH and the mitochondrial electron transport chain

The availability of GSH within the brain has been postulated to play a role in protecting the ETC from oxidative stress (Barker *et al.*, 1996; Bolanos *et al.*, 1996), and may explain the differential susceptibility of the ETC to oxidative stress between cell types (*e.g.,* astrocytes and neurones; Bolanos *et al.*, 1995).

Depletion of brain GSH levels by L-BSO in both rats and mice has previously resulted in loss of ETC complex activity (Heales *et al.*, 1995; Merad-Saidoune *et al.*, 1999). A loss of complex I and IV activity was observed in rat brain homogenates depleted of GSH (Heales *et al.*, 1995), with the loss of complex IV activity apparently proportional to the depletion of GSH in the mitochondria (Heales *et al.*, 1996). Meanwhile in mice, the activities of complexes I, II, and IV were inhibited in brain homogenates depleted of GSH by 95% (Merad-Saidoune *et al.*, 1999).

Experiments with cultured astrocytes and neurones, rather than the brain as a whole, has provided further information on the relationship between GSH and the ETC in the brain. When GSH was depleted by 93% in rat cortical neurones by L-BSO, a concomitant loss in the activities of complexes I, II+III and IV of the ETC was observed (Bolanos *et al.*, 1996). An increase in lactate dehydrogenase (LDH) release, which was used as a measure of cell viability, was also observed in these neurones.

The complexes of the electron transport chain ETC have been reported to be inhibited by reactive oxygen and nitrogen species (see section 1.8; Bolanos *et al.*, 1995; Cardoso *et al.*, 1999; Berman & Hastings, 1999). When cultured neurones were exposed to peroxynitrite, a loss in the activities of complexes II+III and IV of the ETC and an increase in LDH release was observed (Bolanos *et al.*, 1995).

Conversely, the same concentrations of peroxynitrite had no affect on the complexes of the ETC or LDH release in astrocytes (Bolanos *et al.*, 1995). The GSH levels in neurones was estimated to be approximately half that of astrocytes, and it was postulated that this could be a reason for the differential susceptibility observed between the two cell types (Bolanos *et al.*, 1995). Further evidence for the role of cellular GSH levels determining the susceptibility of the ETC to oxidative stress was gained from neurone-astrocyte coculture experiments. Neuronal GSH levels are approximately doubled when neurones are cocultured with astrocytes, compared to when they are cultured alone (section 1.15.2; Sagara *et al.*, 1993; Bolanos *et al.,* 1996; Dringen *et al.,* 1999a). When neurones were cocultured with activated astrocytes (*i.e.,* generating NO; Simmons & Murphy, 1992; Bolanos *et al.*, 1994), neuronal GSH levels were still approximately double that of neurones cultured alone, while the complexes of the ETC were unaffected by exposure to NO (Bolanos *et al.*, 1996). However, neurones cultured alone and exposed to the NO donor S-nitroso-N-acetylpenicillamine (SNAP) were unable to maintain their GSH levels and showed extensive damage to complexes I, II+III, and IV of the ETC (Bolanos *et al.*, 1996). These results imply that the greater GSH concentration in cocultured neurones confers greater resistance to NO-mediated ETC damage, compared to those cultured alone. In support of this, the inhibition of complexes II and III in synaptosomal mitochondria by either ascorbate and iron or hydrogen peroxide was reversed when incubated with 250 μM GSH (Berman & Hastings, 1999; Cardoso *et al.*, 1999).

In the studies described above, loss of complex I activity was associated with a depletion in cellular GSH levels. Further studies using both cultured cells and whole brain have suggested that cellular GSH levels seem to be particularly important in protecting the activity of complex I. Mouse brain slices or isolated brain mitochondria exposed to diethylmaleate, a GSH conjugator, resulted in a significant loss of complex I activity (Balijepalli *et al.*, 1999). Furthermore, mice injected with the amino acid L-β-N-oxalylamino-L-alanine, an excitatory amino acid known to cause neurodegeneration in humans (Sriram *et al.*, 1998), exhibited a loss of complex I activity concomitant with a loss of GSH (Sriram *et al.*, 1998). In the rat dopaminergic PC12 cell line, inhibition of GCL expression by an

antisense polynucleotide resulted in GSH depletion and a loss of complex I activity (Jha *et al.*, 2000). Complex I activity was restored to control levels if the brain slices/PC12 cells were incubated with either exogenous GSH or DTT following treatment (Sriram *et al.*, 1998; Balijepalli *et al.*, 1999; Jha *et al.*, 2000). This suggests that GSH protects thiols on complex I that are necessary for enzyme activity. Indeed, treatment of complex I with iodoacetic acid, a thiol modifier, inhibited complex I activity, and was reversed by incubation with GSH (Balijepalli *et al.*, 1999).

In contrast to the results shown above, the relationship between complex I and GSH in astrocytes is quite different. L-BSO can deplete GSH by 95% in astrocytes without any affect on complex I activity (Barker *et al.*, 1996). Indeed, loss of complex I activity was only observed when GSH depleted astrocytes were exposed to peroxynitrite (Barker *et al.*, 1996). Recently, relatively mild depletion of GSH in cultured rat astrocytes (~ 50%) has been reported to increase the expression and activity of complex I by two-fold (Vasquez *et al.*, 2001). These two studies suggest that other mechanisms in addition to the availability of GSH may dictate complex I activity in astrocytes, and perhaps the rest of the ETC, following oxidative stress. Indeed, the differential distribution and activity of the ETC complexes reported to occur in astrocytes and neurones under basal conditions suggest that regulation of the ETC varies between cell types. For example, complex I activity is greater in cultured rat astrocytes isolated from Wistar rats compared to neurones (Bolanos *et al.*, 1995; Stewart *et al.*, 1998b), while cerebellar purkinje cells display much greater expression of the ND1 subunit of complex I, compared to the adjacent granule cells, in rat brain slices (Pettus *et al.*, 2000).

1.17. Oxidative stress, mitochondrial dysfunction and neurological disease

1.17.1. Parkinson's disease

Perturbed GSH metabolism, increased production of reactive oxygen and nitrogen species, and loss of complex I activity has been strongly implicated in the

pathogenesis of Parkinson's disease (PD). GSH levels have been reported to be specifically depleted by 40% in the substantia nigra (the area of the brain most affected by the disease) of PD brains at post mortem (Sian *et al.*, 1994a). A similar depletion of GSH has been reported in the substantia nigra of patients diagnosed with Incidental Lewy Body disease (ILBD), which is thought to be presymptomatic PD (Dexter *et al.*, 1994), suggesting that GSH depletion is an early event in the development of PD. Riederer *et al.* (1989) have also implied that GSH depletion is important in the progression of PD by reporting that the amount of neurodegeneration observed in PD brains correlates with the degree of GSH depletion. The reason for the depletion of GSH is unclear. GSSG levels are similar in both control and PD brains ruling out the possibility that the depletion of GSH maybe due to the oxidation of GSH to GSSG (Sian *et al.*, 1994a). The activities of GCL and GSH peroxidase have also been reported to be unaffected in PD (Sian *et al.*, 1994b). The only enzyme involved in GSH metabolism that has been reported to have altered activity in PD is γ-GT. The activity of γ-GT has been estimated to be increased by 76% (Sian *et al.*, 1994b). The increase in γ-GT may be a protective mechanism by the surviving cells in the substantia nigra to increase the amount of GSH precursors available for GSH synthesis, and/or to remove potentially toxic GSSG.

The increased production of free radicals and other oxidising species in PD brains may account for the depletion of GSH. Evidence of increased NOS activity has been observed in the substantia nigra at post-mortem (Hunot *et al.*, 1996; Gerlach *et al.*, 1999). The use of animal models has also implicated the involvement of NO in the pathogenesis of PD. Administration of the dopaminergic neurotoxin *N*-methyl-4-phenyl-1,2,3,6-tetrahydropyridine (MPTP) to rodents and primates mimics the biochemical characteristics of PD (*e.g.*, Lewy body formation, inhibition of complex I; Cassarino *et al.*, 1997; Zhang *et al.*, 2000). Increased iNOS expression and activity has been detected in both astrocytes and micoglia in the substantia nigra of mice injected with MPTP (Liberatore *et al.*, 1999). Furthermore, mice lacking the iNOS gene were more resistant to the effects of MPTP (Liberatore *et al.*, 1999).

The increased turnover of dopamine by monoamine oxidase in PD has also been postulated to increase production of hydrogen peroxide (Berman & Hastings, 1999; Cohen & Kesler, 1999). Monoamine oxidase catalyses the metabolism of dopamine to dihydroxyphenylacetic acid and hydrogen peroxide (Berman & Hastings, 1999). The increased levels of iron throughout the PD brain may also contribute towards free radical production by Haber-Weiss and Fenton reactions (Riederer *et al.*, 1989; Jenner & Olanow, 1998). However, it should be noted that the depletion of GSH observed in ILBD precedes the accumulation of iron (Dexter *et al.*, 1994).

An approximate 40% loss in complex I activity has also been reported specifically in the substantia nigra at post mortem in PD brains (Schapira *et al.*, 1990). The depletion of GSH and increased production of oxidising species may well contribute to the loss of enzyme activity. Indeed, complex I activity was reported to be unchanged in the substantia nigra of ILBD brains at post mortem, indicating that depletion of GSH precedes loss of complex I activity (Dexter et al., 1994).

The importance of complex I deficiency in the pathogenesis PD has been illustrated by the dopaminergic neurotoxin MPTP. MPTP is metabolised to 1-methyl-4-phenylpyridinium (MPP^+) by monoamine oxidase and taken up into mitochondria (Ramsay & Singer, 1986). MPP^+ can then inhibit complex I activity by binding to the ubiquinone binding site (Ramsay *et al.*, 1991). The inhibition of complex I by MPP^+ in rodents and primates has been shown to mimic the biochemical characteristics of PD such as degeneration of dopaminergic neurones and Lewy body formation (Cassarino *et al.*, 1997; Liberatore *et al.*, 1999; Zhang *et al.*, 2000). Rats that have been treated with the complex I inhibitor rotenone have also been shown to develop clinical features of PD (*e.g.,* rest tremor), loss of dopaminergic neurones, and Lewy Bodies (Betarbet *et al.*, 2000).

Alternatively, the complex I deficiency in PD could be caused by environmental toxins such as MPTP and rotenone (see above). The increased metabolism of dopamine to 7-(2-aminoethyl)-3,4-dihydro-5-hydroxy-2H-1,4-benzothiazine-3-carboxylic acid in PD has also been postulated to inhibit complex I (Li & Dryhurst, 1997). Oxidative stress and ageing have been postulated to increase the

accumulation of mutations in nuclear, and in particular, mitochondrial DNA (Mecocci *et al.*, 1993; Lu *et al.*, 2000; Chen *et al.*, 2002). Therefore the loss of complex I activity could be due to the mutation of either the mitochondrial or nuclear genes encoding the enzyme. However, no mutations have been described to date (Schapira, 1999).

The inhibition of complex I may also contribute towards the oxidative stress implicated in PD. Increased levels of the hydroxyl radical have been reported in the brains of MPTP injected mice (Cassarino *et al.*, 1997), while dopaminergic neurones exposed to MPTP significantly increase the production of superoxide (Nakamura *et al.*, 2000a).

1.17.2. Multiple Sclerosis

Considerable evidence supports the suggestion that increased NO and peroxynitrite production occurs in multiple sclerosis (MS). NO-inducing cytokines such as interferon-γ (IFN-γ) and interleukin-1β have been detected in MS lesions (Cannella & Raine, 1995), while cerebrospinal fluid from MS patients have indicated that nitrite + nitrate levels (stable degradation products of NO and peroxynitrite) are increased by 70% (Johnson *et al.*, 1995). Furthermore, elevated levels of iNOS mRNA and nitrotyrosine residues have been detected at post mortem (Bo *et al.*, 1994; Bagasra *et al.*, 1995).

While no direct evidence has shown impairment of mitochondrial function in MS, studies have suggested this may be the case. As described previously, inhibition of complexes II+III and IV of the ETC was observed in neurones cocultured with astrocytes that have been activated by lipopolysaccharide (LPS) and the cytokine IFN-γ to generate NO (Stewart *et al.*, 1998a, 2000). However, pre-treatment of astrocytes with IFN-β, which is used in the treatment of MS, prior to activation by LPS and IFN-γ prevented the inhibition of the ETC (Stewart *et al.*, 1998a). Therefore, the beneficial effects of IFN-β in treating MS may in part be mediated by the prevention of cytokine mediated activation of astrocytes, which will

therefore limit damage to the astrocytic and neuronal ETC. Mitochondrial damage has also been reported in MS lesions. Increased oxidative damage to mtDNA has been reported in active lesions (Lu *et al.*, 2000), which may affect the functions of the ETC polypeptides encoded for by mtDNA. Furthermore, a loss of NADH dehydrogenase activity, which may reflect a decrease in complex I activity, was also reported in MS lesions (Lu *et al.*, 2000).

1.17.3. Alzheimer's disease

Oxidative stress has also been reported in Alzheimer's disease (AD). Increased levels of protein 3-nitrotyrosine levels, a marker for peroxynitrite mediated damage, protein carbonyls and lipid peroxidation, have been reported in AD brains (Hensley *et al.*, 1995; Smith *et al.*, 1997; Montine *et al.*, 2002). However, there are no convincing reports implicating perturbed GSH metabolism as a factor in the pathogenesis AD. GSH levels have been reported to be unchanged in the hippocampus and other regions of AD brains at post-mortem (Perry *et al*, 1987). However, total GSH levels were measured (*i.e.*, GSH + GSSG) and therefore it is unknown whether the GSH:GSSG ratio is altered in AD. Glutathione peroxidase activity has been reported to be unchanged in the several brain regions including the cerebral hemisphere and cerebellum (Lovell *et al.*, 1995; Marcus *et al.*, 1998), while an increase in enzyme activity was observed in the hippocampus (Marcus *et al.*, 1998). An increase in glutathione reductase was also observed in the hippocampus and amygdala (Marcus *et al.*, 1998).

In addition to increased oxidative stress, the activity of complex IV has been reported to be lower in the cerebral cortex of AD brains (Kish *et al.*, 1992; Mutisya *et al.*, 1994). The activity of complex IV in isolated brain mitochondria has also been shown to be inhibited following exposure to β-amyloid, the peptide implicated in the pathogenesis of Alzheimer's disease (Canevari *et al.*, 1999; Casley *et al.*, 2002).

1.17.4. Amyotrophic lateral sclerosis

The discovery that some autosomal-dominant hereditary forms of amyotrophic lateral sclerosis (ALS) were linked to mutations in the CuZnSOD gene (Rosen *et al.*, 1993) meant that oxidative stress was implicated in the progression of this disease. Mutated CuZnSOD enzyme dismutates superoxide at a rate similar to that of the wild type enzyme (Przedborski et al., 1996), and it has been proposed that the mutation results in a gain of function for the enzyme (Yim *et al.*, 1996). In addition to the usual dismutation of superoxide, CuZnSOD has a peroxidative function that utilises hydrogen peroxide (the normal product of enzyme activity) to produce hydroxyl radicals (Yim *et al.*, 1996). Hydroxyl radical formation is increased in mutant CuZnSOD and is thought to be due to the lower Km of the enzyme for hydrogen peroxide (Yim *et al.*, 1996). Increased levels of 3-nitrotyrosine have also been measured at post mortem in both familial and sporadic ALS (Beal *et al.*, 1997) suggesting that peroxynitrite may also play a role in the disease. Indeed, Beckman *et al* (1993) have suggested that peroxynitrite may react with the Cu atom in both normal and mutant SOD active site, resulting in the formation of a nitronium-like (NO_2^+) intermediate that can nitrosylate proteins, and a decrease in the scavenging of superoxide by the enzyme.

There are conflicting reports as to whether GSH metabolism is affected in ALS. Glutathione peroxidase activity has also either been reported to be lower (Przedborski et al., 1996), or unchanged (Fujita *et al.*, 1996) in the precentral gyrus at post mortem.

Two reports have shown that complex IV activity is reduced in sporadic ALS in the spinal cord (Fujita *et al.*, 1996; Borthwick *et al.*, 1999). A complex I deficiency has also been reported in the platelets of ALS patients (Swerdlow *et al.*, 1998). However it is uncertain whether this has any bearing on the progression of the disease in the central nervous system.

1.17.5. Ischaemia/Reperfusion

Ischaemia and reperfusion have been shown to alter GSH levels, increase free radical production, and impair mitochondrial function. Increased expression of iNOS has been reported in activated astrocytes following global ischaemia in the rat hippocampus (Endoh *et al.*, 1994), while increased levels of 3-nitrotyrosine have been reported in brains at post mortem (Beal et al., 1997). Increased NOS activity has also been reported in astrocyte and neuronal cell culture systems following conditions mimicking ischaemia (Almeida *et al.*, 1998; Griffiths *et al.*, 2002a).

Mitochondrial GSH levels have also been reported to be altered following ischaemia. A transient increase in mitochondrial GSH levels in the striatum and cortex has been observed after thirty minutes of forebrain ischaemia in rats and 1 hour of reperfusion (Zaidan *et al.*, 1999). The increase in GSH levels was partially prevented when the MPT pore was inhibited by cyclosporin A. However, ischaemia in rats for 2 or 3 hours followed by reperfusion for either 1 or 3 hours significantly depleted mitochondrial GSH levels (Anderson & Sims, 2002). The loss of GSH was closely associated with the development of brain damage.

Evidence for impaired mitochondrial function following ischaemia and reperfusion has also been reported in animal models. A reduction in mitochondrial oxygen consumption and the loss in activity of complexes I, II+III, and V was observed following ischaemia in gerbil brain (Allen *et al.*, 1995; Almeida *et al.*, 1995). Reperfusion for 2 hours resulted in the restoration of complex I and V activities (Almeida *et al.*, 1998). However, complex II+III activity remained affected, while a dramatic loss of complex IV activity was observed after 2 hours of reperfusion.

1.18. Aims of thesis

Since the availability of GSH within the cell has been shown to be important in protecting the ETC from oxidative stress, and that perturbed GSH metabolism,

increased free radical production, and impaired mitochondrial function have been implicated in the pathogenesis of PD and possibly other neurological diseases, this thesis has set out to investigate:

(1) **The importance of the mitochondrial GSH pool, compared to the cytosolic pool, in protecting the ETC from oxidative stress in astrocytes and neurones.**

(2) **The effect of NO on GSH metabolism (*e.g.*, rate of GSH synthesis) in astrocytes and neurones, and the consequences this has for ETC dysfunction and cell viability**

(3) **The mechanisms by which neurones modulate GSH metabolism when cocultured with astrocytes, and whether this has any effect on the protection of the ETC from exposure to NO.**

Chapter 2

General Materials and Methods

2.1. Chemicals and Materials

All chemicals, enzymes and coenzymes were of analytical grade, and unless stated otherwise, were purchased from BDH Laboratory Supplies Ltd. (Poole, U.K.) or Sigma-Aldrich Company Ltd. (Poole, U.K.). In particular:

Deoxyribonuclease 1 (from bovine pancreas, EC 3.1.21.1), Earle's Balanced Salt Solution, Hank's Balanced Salt Solution, bovine serum albumin, L-glutamine, antibiotic antimycotic solution (100X), trypsin-EDTA solution (10X, porcine trypsin), rabbit fluorescein isothiocyanate-conjugated anti-mouse immunoglobulin-G antibody, reduced glutathione, oxidised glutathione, L-buthionine-[S,R,]-sulfoximine, acivicin, N-nitro-L-arginine methyl ester, rotenone, coenzyme Q1, antimycin A, the γ-glutamyltranspeptidase diagnostic kit (EC 2.3.2.2) and the 3-hydroxybutyrate diagnostic kit were all purchased from Sigma-Aldrich Company Ltd. (Poole, UK).

Trypsin (from bovine pancreas, EC 3.4.21.4) and oxidised cytochrome c (from horse heart) were purchased from Boehringer Mannheim (Lewes, UK)

Minimal essential medium, foetal bovine serum, and tissue culture plastics were purchased from Life Technologies (Renfrewshire, UK).

The nitric oxide donor (z)-1-[2-aminoethyl)-N-(2-ammonioethyl)amino]diazen-1-ium-1,2-diolate (DETA-NO) was purchased from Alexis Biochemicals (Nottingham, UK).

(*S*)-3-hydroxy-4-pentenoic acid was synthesised by Dr. David Selwood (The Wolfson Institute, UCL, London, UK).

The sephadex G-25M (PD-10 columns; 3.5 ml elution volume) used to remove ascorbate from reduced cytochrome c were bought from Amersham Biosciences (Little Chalfont, UK).

High performance liquid chromatography grade orthophosphoric acid was purchased from Fischer Scientific (Loughbrough, UK).

Techsphere octodecasilyl 5μm HPLC columns and guard columns were purchased from HPLC technologies (Macclesfield, UK).

Graphite in-line filters to protect the electrochemical detector were purchased from ESA (Aylesbury, UK).

Chromacol HPLC vials and caps were purchased from VWR International (Poole, UK).

γ-glutamylcysteine and cysteinylglycine standards were supplied by Bachem Feinchemikalien AG (Bubendorf, Switzerland) and were a gift from Dr. Ralf Dringen (University of Tubingen, Germany).

The Microcon 12 kDa molecular mass cut-off centrifugal filter devices were purchased from Millipore (Watford, UK).

The Bio-Rad protein assay kit was purchased from Bio-Rad Laboratories (Hercules, California, USA).

The mouse monoclonal anti-glial fibrillary acidic protein and anti-neurofilament antibodies were purchased from Sternberger Monoclonals Inc. (Lutherville, Maryland, USA).

Cytofluor was purchased from Cytofluor Ltd. (London, UK).

2.2. Tissue culture

2.2.1. Cell Culture Media Composition

Solution A was composed of Earle's balanced salt solution (EBSS) containing 75 Kunitz units/ml of Deoxyribonuclease 1, 1% (vol/vol) antibiotic antimycotic solution (10 units/ml penicillin, 1μg/ml streptomycin, 2.5 ng/ml amphotericin) and 3 mg/ml bovine serum albumin (BSA).

Solution B was composed of 20 ml solution A supplemented with 562.5 Kunitz units/ml Deoxyribonuclease 1 and 27.5 units/ml trypsin.

Astrocyte medium: D-valine or L-valine based minimal essential medium (MEM) was supplemented with 2 mM L-glutamine, 10% (vol/vol) foetal bovine serum and 1% (vol/vol) antibiotic antimycotic solution.

Neurone medium: D-valine based MEM was supplemented with 25 mM KCl, 2 mM L-glutamine, 10% (vol/vol) foetal bovine serum and 1% (vol/vol) antibiotic antimycotic solution.

2.2.2. Primary astrocyte culture

Astrocytes were isolated from neonatal (0-2 days) Wistar rats by a method adapted from Tabernero *et al* (1993). Neonates were decapitated, and the cortex removed from the brain and triturated in solution A (section 2.2.1). The triturated brain solution was then centrifuged at 500 x g for 5 minutes at 4 °C. The supernatant was discarded and the pellet digested by solution B (section 2.2.1) for 10-15 minutes at 37 °C. Digestion was terminated by adding 1 ml foetal bovine serum, and the astrocytes pelleted by centrifugation at 500 x g for 5 minutes at 4 °C. The pellet was resuspended in solution A and passed through nylon gauze (40 μM pore size) to remove cell debris. Astrocytes were plated in 80-cm^2 flasks (1 head per flask) and cultured in D-valine based astrocyte medium (section 2.2.1) in an incubator (95% air/5% CO_2) at 37 °C for 7 days (media changed every 3 days).

Astrocytes were grown in D-valine based media because D-valine inhibits the growth of fibroblasts, while allowing astrocytes to proliferate (Cholewinski *et al.*, 1989).

2.2.2.1 Passage of astrocytes

Astrocytes were passaged on day 7 when they reached confluence. Cell media was removed, the cells washed with Hank's Balanced Salt Solution (HBSS), and incubated with 5 ml trypsin/EDTA solution (0.5% (wt/vol) trypsin, 0.2% (wt/vol) EDTA) for 5 minutes. Trypsinisation was terminated by the addition of 10% (vol/vol) foetal bovine serum, and the astrocytes pelleted by centrifugation at 500 x g for 5 minutes at 4 °C. Astrocytes were resuspended in L-valine based astrocyte medium (section 2.2.1) and cultured for a further 6 days (media changed every 3 days) in the conditions described above.

2.2.2.2 Plating of Astrocytes

On day 13, astrocytes were removed from the flasks with trypsin as described above (section 2.2.2.1.) and resuspended in fresh L-valine based astrocyte media. The cells were counted and seeded onto poly-lysine coated (10 μg/ml) 6-well plates ($1x10^6$ cells/well in 1 ml astrocyte medium). The cells were incubated for 18-24 hours whereupon they were ready for experimental procedures.

2.2.2.3. Immunostaining of astrocytes

The purity of the astrocytic cultures was determined using an antibody against glial fibrillary acidic protein (GFAP). Astrocytes on day 13 in culture were removed from flasks with trypsin as above, and $50x10^5$ cells in 1 ml of astrocyte medium were seeded onto poly-lysine (10 μg/ml) coated glass coverslips (5.3 cm^2) placed in 6-well plates. The cells were than incubated for approximately 24 hours. The medium was removed and the cells washed three times with 1ml of phosphate buffered saline (PBS; 0.14M NaCl, 2mM KH_2PO_4, pH 7.4). Astrocytes were fixed by adding 2 ml pre-chilled methanol (-20 °C) per well and incubating on ice for 5 minutes. The methanol was then removed and washed three times

with 1 ml PBS. Each coverslip was then blocked by addition of 1 ml 1% (vol/vol) horse serum in PBS for 30 minutes at room temperature. Coverslips were then washed three times with 1 ml PBS. The GFAP antibody (1 ml; 1:2000 (vol/vol) in PBS) was then incubated with the each coverslip for 18 hours in the dark at 4 °C. then diluted. One coverslip was incubated with 1 ml PBS as a blank control. Following the overnight incubation, all coverslips were then washed three times with PBS, and then incubated with 1 ml of fluorescein isothiocyanate (FITC)-conjugated secondary anti-mouse immunoglobulin-G antibody (1:500 (vol/vol) in PBS) in the dark for 1 hour at room temperature. The coverlips were then washed three times with PBS. Cells were then incubated with 1 ml 0.5% (vol/vol in PBS) 4'-6-diamidino-2-phenyllindole (DAPI) in the dark for 10 minutes at room temperature to stain cell nuclei. Finally, the coverslips were washed three times with PBS and mounted on glass microscope slides (BDH Ltd; 76 x 26 mm) with 10 µl Cytofluor. Digital imaging of cells was performed using a Zeiss 510 CLSM laser scanning confocal microscope (Solent Scientific, Portsmouth, UK) equipped with a 40X oil immersion quartz objective lens and a 20X quartz objective lens. The fluorescence of the FITC-conjugated antibodies was imaged by illuminating cells using the 488 nm emission line of a helium-neon laser, and the fluorescence was collected at wavelengths longer than 505 nm. In order to image DAPI fluorescence, cells were illuminated using the 351nm laser line of an argon laser and the fluorescence signal was collected at 435 and 485nm. The microscope pinhole was maintained at a confocal thickness of about 5 mm.

The purity of the cultures was calculated by determining the proportion of DAPI fluorescence containing cells that were also positive for GFAP fluorescence. Astrocyte cultures showed a 95 ± 1% immunopositivity against GFAP (n=3; **Figure 2.1**). No GFAP fluorescence was detected in the blank control incubated with just the secondary antibody.

2.2.3 Primary neurone culture

Neurones were isolated from Wistar rat foetuses (embryonic day 17) as described above (section 2.2.2). Neurones were plated onto poly-ornithine (10 µg/ml) coated

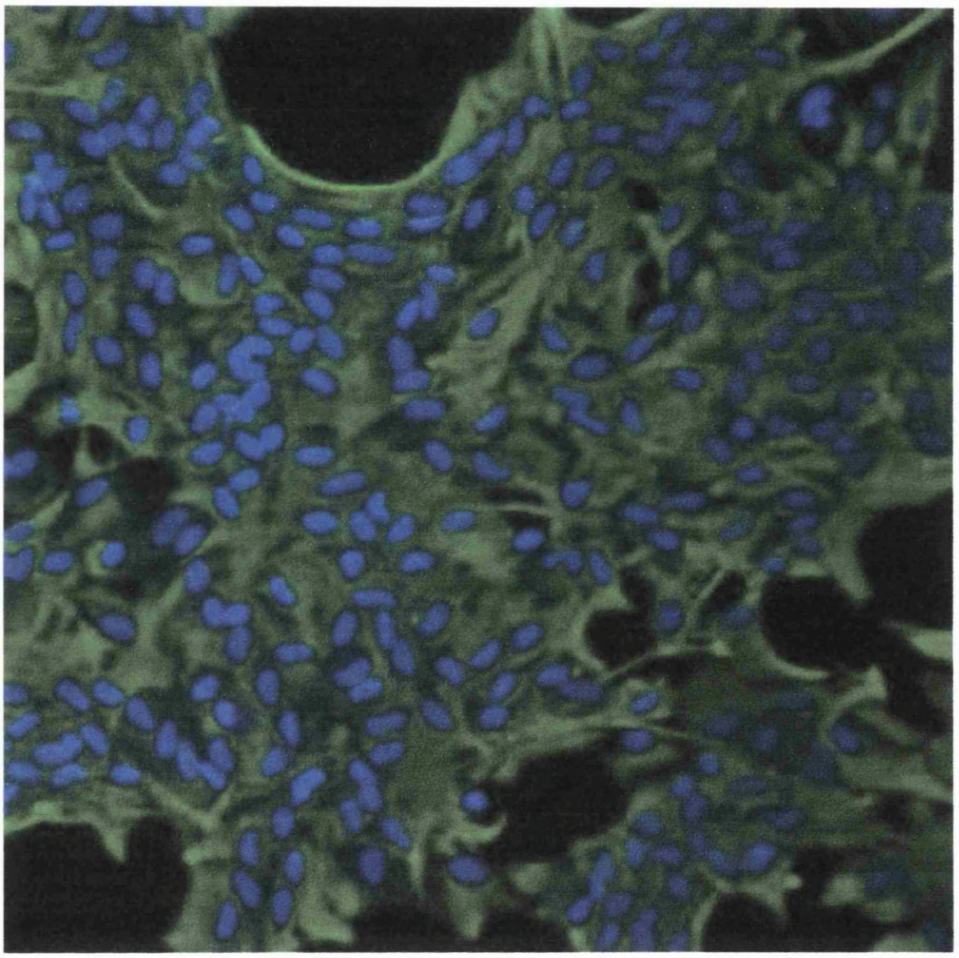

Figure 2.1. GFAP stained astrocytes

Astrocytes (~ $50x10^5$ cells/coverslip) were incubated with a GFAP antibody and a secondary antibody conjugated to FITC. Cell nuclei were also detected using the fluorescent dye DAPI. Cells were imaged using confocal microscopy. Cell nuclei are blue, while astrocyte associated GFAP fluorescence is green. Astrocytes were magnified 20X.

6-well plates ($2.5x10^6$ cells/well in 1.5 ml neuronal media) and cultured in an incubator (95% air/5% CO_2) at 37 °C for 3 days. On day 3, neurones were fed with fresh neuronal media supplemented with 1 mM cytosine β-D-arabino-furanoside, and cultured in the incubator for a further 3 days. Experimental procedures were performed on neurones on day 6 in culture.

2.2.3.1. Immunostaining of neurones

Neurones were isolated from Wistar rats as above, and $50x10^5$ cells seeded on to poly-lysine (100 μg/ml) coated coverslips in 1.5 ml neuronal medium. The neurones were then cultured for 6 days as above (section 2.2.3). The purity of neuronal cultures was then determined using a mouse antibody against neurofilament (NF) protein. Neurones were stained as above (section 2.2.2.3) with 1 ml NF primary antibody (1:200 (vol/vol) in PBS) and a FITC-conjugated secondary antibody. Neuronal cultures showed a 90 ± 4 % immunopositivity against NF (n=4; **Figure 2.2**). No NF fluorescence was detected in the blank control incubated with just the secondary antibody.

2.2.4. Treatment and Harvest of Astrocytes/Neurones

Astrocytes and neurones plated in 6-well plates were incubated with 1 ml fresh astrocyte/neuronal media respectively containing the appropriate treatments for a defined period of time. Upon completion of the experiment, the cells were washed in HBSS, removed from the wells with 1 ml trypsin, and centrifuged as above (2.2.2.1). Pelleted cells were resuspended in 300 μl isolation medium (320 mM sucrose, 10 mM Tris, 1 mM EDTA, pH 7.4), frozen in liquid nitrogen, and stored at –70°C except where stated.

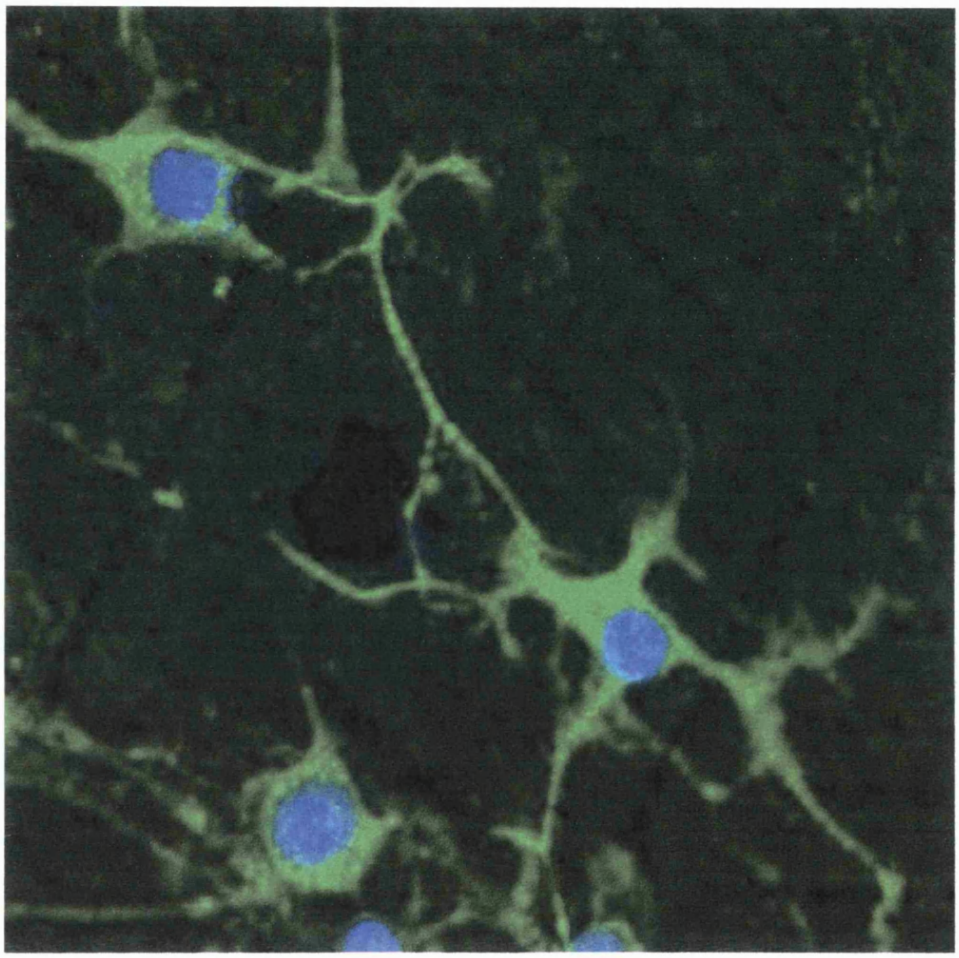

Figure 2.2. Neurones immunopositive for neurofilament

Neurones (~ $50x10^5$ cells/coverslip) were incubated with NF antibody and a secondary antibody conjugated to FITC. Cell nuclei were also detected using the fluorescent dye DAPI. The neurones were imaged using confocal microscopy. Cell nuclei are blue, while neurone associated NF fluorescence is green. Neurones were magnified 40X.

.

2.3. Isolation of Mitochondria

2.3.1. Isolation of mitochondria from astrocytes and neurones

Mitochondria were isolated from neurones (day 6 in culture) and astrocytes (day 14 in culture) as previously described by Almeida & Medina (1997). Neurones (~$20x10^6$) and astrocytes (~$15x10^6$) were removed from 6-well plates and flasks respectively by incubating the cells with 0.07% (wt/vol) trypsin resuspended in isolation medium (section 2.2.4) for 5 minutes. Trypsinisation was stopped by addition of an equal volume of isolation medium supplemented with 10% foetal bovine serum. The cells were pelleted by centrifugation at 500 x g for 5 minutes at 4 °C and resuspended in 4 ml isolation medium. Cells were optimally homogenised on ice by 35 strokes of a tight fitting glass-teflon homogeniser revolving at 550 rpm. Cell homogenates were centrifuged at 1500 x g for 10 minutes at 4 °C, the supernatant placed on ice, and the pellet resuspended in 3 ml isolation medium, homogenised and centrifuged as above. The supernatants were then combined and centrifuged once more at 1500 x g (10 minutes, 4 °C). The pellet was discarded, and the supernatant centrifuged at 17000 x g for 11 minutes at 4 °C. The mitochondrial pellet was resuspended in 280 µl isolation medium (protein concentration ~ 0.5 mg/ml), frozen in liquid nitrogen, and stored at –70 °C until required. The activity of the mitochondrial marker enzyme citrate synthase (section 2.4.4) was enriched approximately 3-fold between the initial cell homogenate and the final mitochondrial pellet in both astrocytes and neurones when cells were homogenised with 35 strokes (**Table 2.1.**). This is comparable to the 3 to 4 fold mitochondrial enrichment reported by Almeida & Medina (1997).

2.3.2. Liver mitochondria preparation

Liver mitochondria were isolated from adult Wistar rats using the method described by Hayes *et al* (1985). The liver was chopped up in 'high' EDTA isolation medium (210 mM mannitol, 70 mM sucrose, 50 mM Tris, 10 mM EDTA (K^+ salt), pH 7.4) manually and with a blender. The liver was then homogenised in a tight fitting glass-glass homogeniser. The homogenate was then centrifuged at

Fraction	Citrate Synthase Activity (nmol/min/mg protein)	
	astrocyte	neurone
homogenate	102.7 ± 4.3	163.0 ± 24.5
mitochondria	330.0 ± 25.8	457.4 ± 19.3
cytosol	5.9 ± 1.5	30.7 ± 10.3

Table 2.1. Enrichment of citrate synthase activity during isolation of mitochondria from astrocytes and neurones.

Mitochondria were isolated from astrocytes and neurones and citrate synthase activity assayed in each fraction. Data are mean ± SEM of 5-7 independent mitochondrial isolations.

1500 x g for 3 minutes at 4 °C, the supernatant stored on ice, and the pellet homogenised and centrifuged as above. The supernatants were combined and centrifuged at 17000 x g for 11.1 minutes (4 °C). Red blood cells were removed and the mitochondrial pellet was resuspended in 'low' EDTA isolation medium (225 mM mannitol, 75 mM sucrose, 10 mM Tris, 100 μM EDTA (K^+ salt), pH 7.4) in a loose fitting glass-teflon homogeniser. The homogenate was spun once more at 17000 x g as above. Finally, the mitochondrial pellet was homogenised with a loose fitting glass-teflon homogeniser in 'low' EDTA isolation medium. Citrate synthase activity was enriched approximately 3 fold between initial homogenate and the final mitochondrial pellet.

2.4. Enzyme Assays

2.4.1. Complex I Assay (NADH:ubiquinone reductase; EC 1.6.5.3)

Complex I activity was determined spectrophotometrically using an Uvikon 941 spectrophotometer as described by Ragan et al (1987). Sample (10-20 μg protein; freeze-thawed three times in liquid nitrogen) was mixed with 20 mM phosphate buffer (20 mM KH_2PO_4, 20 mM K_2HPO_4, 8 mM $MgCl_2$, pH 7.2), 2.5 mg/ml BSA, 0.15 mM NADH, and 1 mM KCN in a cuvette. The reaction was started by the

addition of 50 μM coenzyme Q1. Enzyme activity was measured at 30 °C by following the oxidation of NADH to NAD^+ at 340 nm for 5 minutes (NADH extinction coefficient 6.81 x 10^3 $M^{-1}cm^{-1}$; total volume 1 ml; path length 1 cm). After 5 minutes, 20 μM rotenone was added, and rotenone insensitive NADH oxidation was measured for 5 minutes. Complex I activity was calculated by subtracting the rotenone insensitive NADH oxidation rate from total NADH oxidation rate (units = nmol/min/mg protein). Note that all cuvettes were run against a reference cuvette that contained sample and all the substrates except coenzyme Q1. Complex I activity was proportional to protein between 5 and 25 μg protein (R^2 0.9886).

2.4.2. Complex II+III assay (succinate cytochrome c reductase; EC 1.8.1.3)

Complex II+III activity was determined spectrophotometrically using an Uvikon 941 spectrophotometer as described by King (1967). Sample (10-20 μg protein; freeze-thawed three times in liquid nitrogen) was mixed with 100 mM phosphate buffer (100 mM KH_2PO_4, 100 mM K_2HPO_4, pH 7.4), 0.3 mM EDTA, 1 mM KCN, and 100 μM oxidised cytochrome c (from horse heart) in a cuvette. The reaction was started by addition of 20 mM succinate and enzyme activity measured at 30 °C by following the reduction of cytochrome c at 550 nM for 5 minutes (cytochrome c extinction coefficient 19.2x10^3 $M^{-1}cm^{-1}$; total volume 1 ml; path length 1 cm). After 5 minutes, 10 μM antimycin A was added, and the antimycin A insensitive rate of cytochrome c reduction was followed for a further 5 minutes. Complex II+III activity was calculated by subtracting the antimycin A insensitive cytochrome c reduction rate from total cytochrome c reduction rate (units = nmol/min/mg protein). Note that all cuvettes were run against a reference cuvette that contained sample and all the substrates except succinate. Complex II+III activity was proportional to protein between 5 and 35 μg protein (R^2 0.9776).

2.4.3. Complex IV assay (cytochrome c oxidase; EC 1.9.3.1)

2.4.3.1. Reduction of oxidised cytochrome c

Ascorbate crystals were added to oxidised cytochrome c (0.8mM, horse heart) until a colour change was observed from dark to light red. The reduced cytochrome c was then passed through a PD_{10} gel filtration column (column equilibrated by washing column with 30 ml of 10 mM phosphate buffer, pH 7.0) to remove the ascorbate from the reduced cytochrome c. The concentration of reduced cytochrome c was determined by mixing 50 µl reduced cytochrome c with 950 µl H_2O in both a sample and reference cuvette. The sample cuvette was 'zeroed' against the reference cuvette at an absorbance of 550 nm. 1 mM ferricyanide was then added to the reference cuvette to oxidise the reduced cytochrome c, and the absorbance of the sample cuvette noted (cytochrome c extinction coefficient 19.2×10^3 $M^{-1}cm^{-1}$; total volume 1 ml; path length 1 cm).

2.4.3.2. Measurement of complex IV activity

Complex IV activity was determined spectrophotometrically using an Uvikon 941 spectrophotometer as described by Wharton & Tzagoloff (1967). In a sample and reference cuvette, 10 mM phosphate buffer (10 mM KH_2PO_4, 10 mM K_2HPO_4, pH 7.0) and 50 µM reduced cytochrome c was mixed, and the sample cuvette zeroed against the reference. To the reference cuvette, 1mM ferricyanide was added to oxidise the cytochrome c, yielding an absorbance of approximately 1.0 at 550 nm in the sample cuvette prior to addition of sample. Sample (10-20 µg protein; freeze-thawed three times in liquid nitrogen) was then added to the sample cuvette and the oxidation of cytochrome c at 550 nm was measured for 5 minutes at 30 °C against the reference cuvette (cytochrome c extinction coefficient 19.2×10^3 $M^{-1}cm^{-1}$; total volume 1 ml; path length 1 cm). Since complex IV activity is dependent on the concentration of cytochrome c, complex IV activity is expressed as the first order rate constant k per minute per mg protein. Activity was determined by noting the highest positive absorbance following sample addition (t = 0 minutes), and the absorbance every minute after that for 3 minutes. k was

calculated by: ((ln ($A_{550\ t=0}$ / $A_{550\ t=n}$) / number of minutes)/protein concentration. The rate constant for each sample was taken as the mean of k at 1, 2 and 3 minutes. Complex IV activity was proportional to protein between 2 and 20 μg protein (R^2 0.9802).

2.4.4. Citrate Synthase Assay (EC 4.1.3.7)

Citrate synthase (CS) activity was determined spectrophotometrically using an Uvikon 941 spectrophotometer as described by Shepherd & Garland (1969). Sample (10-20 μg protein; freeze-thawed three times in liquid nitrogen) was mixed with buffer (100 mM Tris, 0.1% (v/v) Triton X-100, pH 8.0), 0.1 mM acetyl coenzyme A, and 0.2 mM 5,5' dithio-bis-(nitrobenzoic acid)(DTNB) in a cuvette (total volume 1 ml, path length 1 cm). The reaction was started by the addition of 0.2 mM oxaloacetate, and activity measured at 412 nm for 5 minutes at 30 °C (DTNB extinction coefficient 13.6×10^3 $M^{-1}cm^{-1}$). Samples were run against a reference cuvette that contained sample and all substrates except oxaloacetate. Citrate synthase activity was linear between 5 and 25 μg protein (R^2 0.999).

2.4.5. 3-hydroxybutyrate dehydrogenase assay (EC 1.1.1.30)

This spectrophotometric assay is based on the method described by Zhang *et al* (1989) with minor modifications. Sample (5-25 μg protein freeze thawed three times) was mixed with assay buffer (10 mM KH_2PO_4, 10 mM K_2HPO_4, pH 7.35), 0.5 mM EDTA, 0.3 mM DTT, 0.4 mg/ml BSA, 2 mM NAD^+ and 15 μM rotenone), and incubated at 37 °C for 10 minutes. The reaction was then initiated by the addition of 20 mM 3-hydroxybutyrate to the sample cuvette (reference cuvette contained all components except 3-hydroxybutyrate) and enzyme activity measured by following the reduction of NAD^+ at 340 nm for 5 minutes (NADH extinction coefficient 6.81×10^3 $M^{-1}cm^{-1}$; total volume 1 ml; path length 1 cm). Enzyme activity (nmol/min/mg protein) was linear with respect to protein between 5 and 300 μg (R^2 0.9943).

2.4.6. Lactate Dehydrogenase Assay (EC 1.1.1.27)

Lactate dehydrogenase (LDH) activity was determined spectrophotometrically as described by Vassault (1983). LDH released into 1 ml cell culture media by $1x10^6$ astrocytes or $2.5x10^6$ neurones was used as an index of cell viability. Assay buffer (100 mM KH_2PO_4, 100 mM K_2HPO_4, 170 mM sodium pyruvate, pH 7.5) was mixed with 0.16 mM NADH in the sample and reference cuvettes. Absorbance was then monitored at 340 nm for 2 minutes. Sample (20 µl cell homogenate solubilised in 0.1% (v/v) Triton X-100 and freeze thawed once; 33 µl cell culture media freeze thawed once) was added to the sample cuvette and the oxidation of NADH measured at 340 nm for 5 minutes at 30 °C (NADH extinction coefficient $6.81x10^3$ $M^{-1}cm^{-1}$; total volume 1 ml; path length 1 cm). The % release of LDH into culture medium was calculated as: LDH activity in media / LDH activity in media + cells (Bolanos *et al.*, 1995). LDH activity was linear with respect to protein (5-20 µg, R^2 0.9999).

2.4.7. γ-glutamyltranspeptidase assay (EC 2.3.2.2)

γ-glutamyltranspeptidase (γ-GT) activity was measured using the Sigma Diagnostics kit. γ-GT catalyses the following reaction:

L-γ-glutamyl-3-carboxy-4-nitroanilide + glycylglycine

↓ γ-GT

5-amino-2-nitrobenzoate + L-γ-glutamylglycylglycine

Enzyme activity was measured by following the formation of 5-amino-2-nitrobenzoate at an absorbance of 405 nm (extinction coefficient 9.5 x 10^3 $M^{-1}cm^{-1}$). Following experimental procedures, astrocytes/neurones were scraped into 300 µl HBSS and kept on ice. A 25 µl aliquot of sample (~ 20 µg) was added to 1 ml γ-GT reagent (containing 4.36 mM L-γ-glutamyl-3-carboxy-4-nitroanilide, 60 mM glycylglycine) and activity measured for 5 minutes at 37 °C. Activity was

completely inhibited following addition of the γ-GT inhibitor acivicin (220 μM). Activity was proportional to protein between 5 and 25 μg protein (R^2 0.9773).

2.5. Protein Determination

Sample protein concentration was determined by the Lowry method (Lowry *et al.*, 1951). To 200 μl of sample (freeze thawed twice; typically diluted 1/10 or 1/20 (vol/vol) in water) or BSA standards, 100 μl of alkaline copper tartate and 800 μl of Folin-Ciocalteu phenol reagent was added. Samples were vortexed and incubated at room temperature in the dark for 20 minutes. Absorbance was measured on an Uvikon 941 spectrophotometer at 750 nm. Sample protein concentration was calculated from the BSA standard calibration curve (0-200 μg/ml).

2.6. GSH Quantitation

Cellular GSH concentration was determined by reverse-phase HPLC coupled to a dual-electrode electrochemical detector as previously described by Riederer *et al.* (1989).

2.6.1. Reverse-phase HPLC

A scheme of the reverse-phase HPLC system is shown in **Figure 2.3.** Sample (20 μl) was injected by a Kontron HPLC 360 autosampler (Watford, U.K.) through a guard column (octadecasilyl; 3mm x 10 mm) to remove debris, and resolved using a reverse-phase Techsphere octadecasilyl column (particle size 5 μm, 4.6 mm x 250 mm) maintained at 30°C by a column heater (Jones Chromatography; Glamorgan, U.K.). The mobile phase was 15 mM orthophosphoric prepared in 18.2 MΩ H_2O (pH 2.5) and degassed by a DEG-1033 degasser (Kontron Instruments). The flow rate was maintained at 0.5 ml/min by a Jasco PU-1580 pump (Great Dunmow, UK). Following separation by the column, GSH was electrochemically detected by an ESA 5010 analytical cell containing an upstream

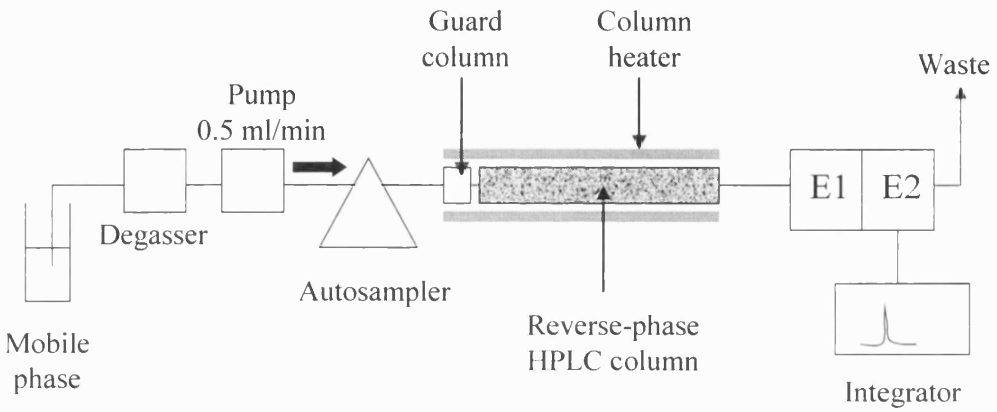

Figure 2.3. Scheme to illustrate the apparatus used to determine GSH by reverse-phase HPLC and electrochemical detection.

E1, upstream electrode; E2, downstream electrode.

and downstream electrode (ESA Analytical; Aylesbury, UK). The upstream electrode screens out molecules with a lower oxidation potential than GSH, while the downstream electrode oxidises GSH (see section 2.6.2). The magnitude of current generated by the oxidation of GSH at the downstream electrode was proportional to the amount of GSH and was recorded as a chromatogram on a Thermoseparation Products Chromejet integrator (Anachem; Luton, UK) at a chart speed of 0.25 cm/minute. Note that prior to detection of samples, mobile phase was circulated through the column and electrode for 18 hours. This allows the electrochemical detector to settle and yield a low baseline current (0.02-0.1 μA).

2.6.2. Electrochemical Properties of GSH

GSH standards (5 μM) were injected and measured at various downstream electrode potentials to determine the optimal potential for GSH detection (**Figure 2.4**; upstream electrode set at +100 mV). GSH detection by the downstream electrode reached a plateau between +575 to +600 mV. Electrochemical detection of GSH standards was linear between 1 and 10 μM (R^2 0.991).

2.6.3. Sample Preparation

GSH standards (1-10μM) were prepared in 15 mM orthophosphoric acid and stored at –70°C. GSH from cell homogenates/mitochondria were diluted in phosphate buffered saline (137 mM NaCl, 2.7 mM KCl, 10 mM Na_2HPO_4, 1.8 mM KH_2PO_4, pH 7.2) if required, and mixed 1:1 (vol/vol) with 15 mM orthophosphoric acid to extract GSH. Samples were then centrifuged at room temperature for 5 minutes at 14000 x g to pellet protein. The supernatant was then sealed in Chromacol HPLC vials ready for injection onto the HPLC column (see section 2.6.1.). A typical GSH chromatogram is shown in **Figure 2.5**. The current generated by samples was converted into sample concentration using a GSH standard calibration graph (1-10 μM). GSH concentration was expressed as nmoles GSH/mg protein. When astrocyte samples were spiked with GSH standard

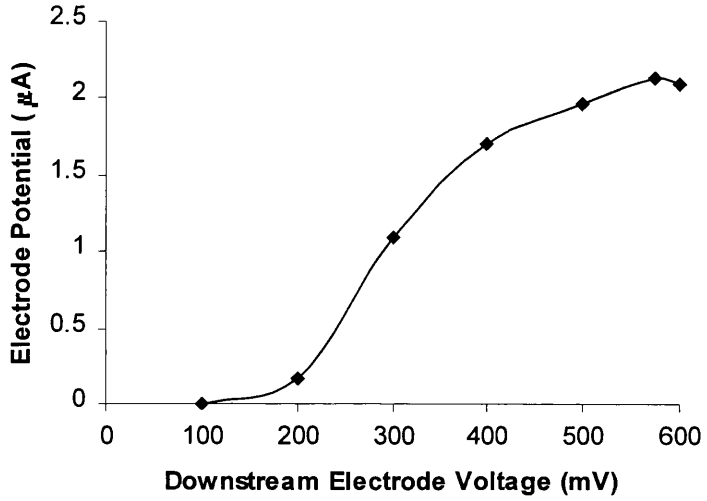

Figure. 2.4. Voltamogram of GSH

GSH standards (5μM) were separated by reverse-phase HPLC and detected by electrochemical detection. The upstream electrode was set at +100 mV while the downstream electrode was set at potentials between +100 and +600 mV. Optimal GSH detection occurs when the voltage of the downstream electrode is between +575 and +600 mV.

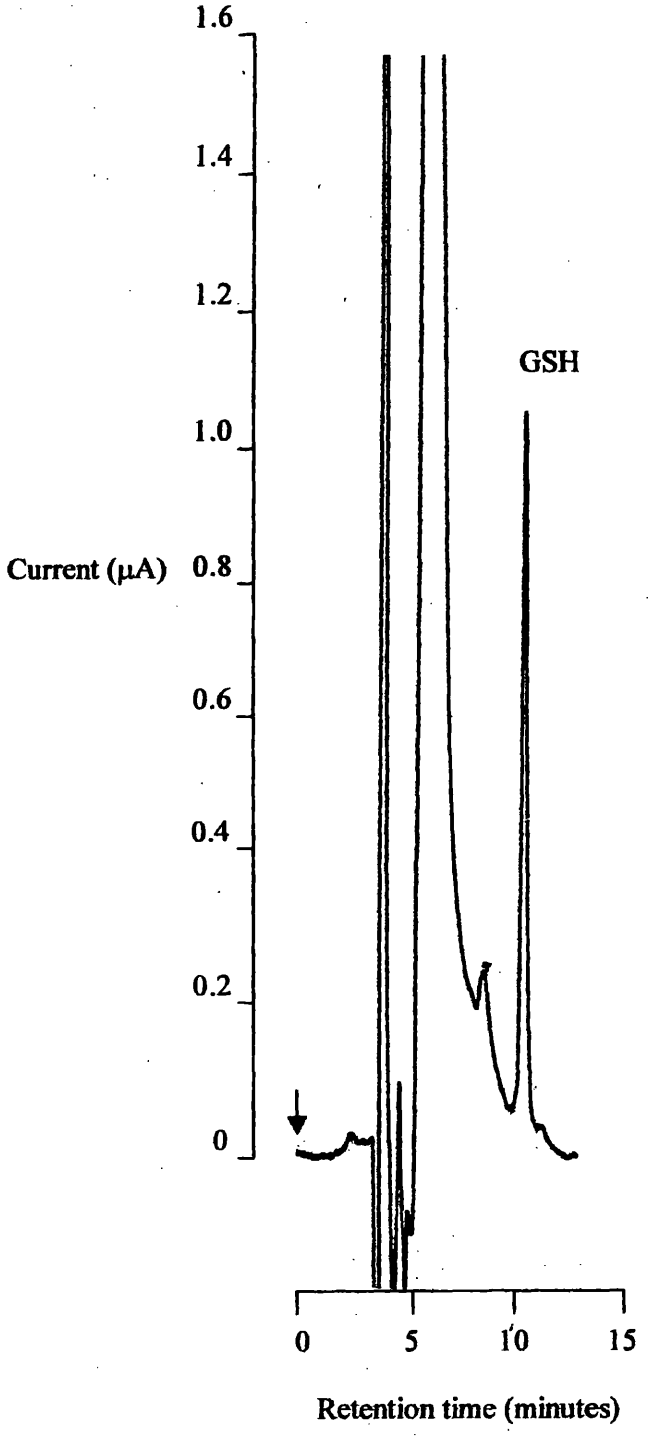

Figure 2.5. Chromatogram of an astrocyte sample

GSH from an astrocyte homogenate was extracted in to 15 mM OPA and quantitated by electrochemical detection following separation by reverse-phase HPLC. GSH has a retention time of 10.5 minutes. The arrow denotes point of injection.

(2.5μM), and extracted into orthophosphoric acid as above, a 98 ± 2% (n=6) recovery of GSH was obtained. The stability of GSH extracted into 15 mM orthophosphoric acid was unaffected at room temperature for at least 24 hours, or by freezing and storage at –70°C for at least a year.

2.7. Statistical Analysis

The linear regression of graphs was calculated using Microsoft Excel.

All results are expressed as mean ± SEM for the number of independent cell culture/mitochondria preparations stated. The statistical significance of data sets was assessed using either Student's t-test or one-way ANOVA followed by the least significant difference test where stated. $p < 0.05$ was considered significantly different compared to control. Complex activities expressed as a ratio against citrate synthase activity were transformed to yield data with a normal distribution before statistical evaluation (Personal communication from Professor Richard Lowry, Professor of Psychology, Vassar College, New York, USA).

Transformation = arcsin $\sqrt{}$(complex activity/citrate synthase activity)

Chapter 3

Development of a glutamate-cysteine ligase assay based on reverse-phase HPLC and electrochemical detection

3.1. Introduction

The biological functions of GSH are of considerable interest, with the tripeptide implicated in protecting cells from oxidative stress (Bolanos *et al.*, 1995, 1996; Barker *et al.*, 1996; Iwata-Ichikawa *et al.*, 1999; Jha *et al.*, 2001), acting as a storage and transport form of cysteine (Dringen *et al.*, 1999a; Lu, 2000), and detoxifying xenobiotica (Anderson & Meister, 1983).

GSH is synthesised by the consecutive action of the ATP dependent cytosolic enzymes glutamate-cysteine ligase (GCL; also known as γ-glutamylcysteinyl synthetase; EC 6.3.2.2; **reaction 3.1**) and glutathione synthetase (GS; EC 6.3.2.3; **reaction 3.2**;Yip & Rudolph, 1976; Anderson & Meister, 1983; Luo *et al.*, 2000).

L-glutamate + L-cysteine + ATP → γ-glutamylcysteine + ADP + P_i **(3.1)**

γ-glutamylcysteine + glycine + ATP → γ-glutamylcysteinylglycine + ADP+ P_i **(3.2)**

GCL is postulated to be the rate-limiting enzyme in GSH synthesis (Anderson & Meister, 1983; Grant *et al.*, 1997). Kinetic studies have indicated that the reaction catalysed by GCL requires all substrates to be bound before the products are formed (Orlowski & Meister, 1971; Yip & Rudolph, 1976). L-glutamate and ATP are thought to react first to form a tightly bound γ-glutamylphosphate group, which subsequently reacts with L-cysteine (Orlowski & Meister, 1971). The Km of purified rat kidney GCL for L-glutamate and L-cysteine are calculated to be 1.4 mM and 0.2 mM respectively (Huang *et al.*, 1993a). The specific GCL inhibitor L-buthionine-(S,R)-sulfoximine (L-BSO) binds to the enzyme at the site usually reserved for glutamate and cysteine (Griffith & Meister, 1979; Griffith, 1982). In the presence of ATP, GCL phosphorylates L-(S)-BSO resulting in the inhibitor being tightly, but noncovalently, bound to the GCL active site (Griffith & Meister, 1979; Campbell *et al.*, 1991). Since cells contain MgATP, L-(S)-BSO is considered to be an irreversible inhibitor when used *in vivo* or *in vitro*. Only L-(S)-BSO can be phosphorylated by GCL (Campbell *et al.*, 1991). L-(R)-BSO is a reversible inhibitor of GCL and binds competitively with glutamate (Ki 0.11 mM; Campbell *et al.*, 1991).

The availability of GSH has been implicated in dictating cellular susceptibility of astrocytes and neurones to oxidative stress (Bolanos *et al.*, 1995,1996; Iwata-Ichikawa *et al.*, 1999). Furthermore, alterations in GSH metabolism have been implicated in the pathogenesis of several neurological diseases such as Parkinson's disease (PD; Dexter *et al.*, 1994; Sian *et al.*, 1994a; Schulz *et al.*, 2000). Therefore, given the importance of GCL in determining cellular GSH concentration, and the aim of this thesis to investigate the effects of NO on GSH metabolism in astrocytes and neurones, it is imperative that the activity of this enzyme can be measured in biological samples following various experimental paradigms.

Existing GCL assays rely on either the derivitisation of γ-glutamylcysteine (γ-GC) or linked assays to measure enzyme activity. The widely used spectrophotometric method of Seelig and Meister (1984) measures the rate of ADP formation by GCL, in the presence of phosphoenolpyruvate, pyruvate kinase and lactate dehydrogenase, by following the oxidation of NADH by the latter enzyme at 340 nm. However, linking NADH oxidation to ADP production by GCL, via two exogenously added enzymes, inevitably leads to a loss of specificity as well as complicating the assay. Several HPLC methods for measuring γ-GC following defined incubations have also been reported in recent years. These assays depend on the derivitisation of γ-glutamylcysteine by *ortho*-phthalaldehyde, monobromobimane or *N*-(1-pyrenyl) maleimide prior to resolution by reverse-phase HPLC (Winters *et al.*, 1995; Noctor & Foyer, 1998; Liu *et al.*, 1998; Birago *et al.*, 2001). The modified γ-GC is measured either fluorometrically (Winters *et al.*, 1995; Noctor & Foyer, 1998; Liu *et al.*, 1998) or electrochemically (Birago *et al.*, 2001).

This chapter describes the development of a reverse-phase HPLC method that can directly measure the amount of γ-GC synthesised by GCL without the need for extensive preparation or derivitisation. Since this thesis will investigate the effects of NO on GSH metabolism in astrocytes and neurones, the assay has been validated for use with these cell types.

3.2. Methods

3.2.1. Cell culture

Primary astrocytes and were cultured as described in section 2.2. Astrocytes were harvested on day 14 from flasks 24 hours after change of media.

3.2.2. Reverse-phase chromatography and electrochemical detection

GSH and γ-GC concentration was determined by reverse-phase HPLC coupled to a dual-electrode electrochemical detector as previously described in section 2.6.1.

3.2.3. Preparation of sample standards

Stock γ-GC and GSH standards (5 μM) were prepared in 15 mM orthophosphoric acid and stored at –70°C until required. The stability of the standards was unaffected by freezing and storage. γ-GC or GSH prepared in 15 mM orthophosphoric acid was also stable at room temperature for at least 24 hours. To determine the percentage of the standards in the reduced form, 2.5 μM γ-GC and GSH standards were mixed with 20 μM DTNB and 100 mM Tris and the absorbance measured at 412 nm (DTNB extinction coefficient $13.6x10^3$ $M^{-1}cm^{-1}$; Ellman, 1959). The amount of reduced γ-GC and GSH was 99% and 98% respectively.

3.2.4. Determination of GCL activity in astrocytes and neurones

Astrocytes or neurones were harvested (as described in section 2.2.4.) and resuspended in 300 μl isolation medium (320 mM sucrose, 10 mM Tris, 1 mM EDTA (K^+ salt), pH 7.4). Samples were freeze/thawed in liquid nitrogen three times and centrifuged at 3000 x g for 5 minutes at 4 °C to pellet cell debris. The supernatant was then centrifuged through a microcon centrifugal filter device with

a 10 kDa molecular mass cut off filter at 12000 x g for 15 minutes at 4 °C. Approximately 70% of the liquid was forced through the columns. This step removes glycine, other amino acids, cofactors and small molecules (*e.g.* GSH) from the cell extracts to deter (i) the conversion of γ-GC to GSH during the course of the assay (equation 2, section 3.1) and (ii) GSH and other molecules interfering with the assay. An aliquot of retained protein (*i.e.* the 30% of sample not forced through the column) was mixed with assay buffer (0.1 M Tris-HCl, 0.15 M KCl, 20 mM $MgCl_2$, 2 mM EDTA (K^+ salt), pH 8.2), 10 mM ATP, 10 mM L-cysteine, 40 mM L-glutamate and 220 μM of acivicin (to inhibit the degradation of γ-GC by γ-glutamyltranspeptidase (γ-GT); Stole *et al.,* 1990) for 15 minutes at 37 °C (final reaction volume 100 μl). The reaction was stopped by the addition of 1 volume of 15 mM orthophosphoric acid and centrifugation at 14000 x g for 5 minutes. The γ-GC in the supernatant was then resolved by reverse-phase HPLC and detected by an electrochemical detector as described in section 2.6.

3.2.5. Other biochemical analyses

γ-GT activity and the protein concentration of the astrocyte samples retained by the centrifugal filter device were determined as described in sections 2.4.7. and 2.5. respectively.

3.3. Experimental protocols

Chromatography and electrochemical properties of γ-GC:

γ-GC standards (5 μM) were resolved by reverse-phase HPLC and measured at various downstream electrode potentials (between +100 and +650 mV) to ascertain (i) the optimal parameters for electrochemical detection and (ii) the retention time of γ-GC.

L-BSO inhibition curve of GCL activity:

GCL activity was determined in astrocyte cell extracts in the presence of the GCL inhibitor L-BSO to determine the specificity of the assay. Astrocyte samples (15 μg protein) were preincunated with 5 nM - 5 mM L-BSO and 10 mM ATP for 5

minutes at room temperature. GCL activity was then assayed as above (section 3.2.4) in the presence of the respective L-BSO concentration to determine the Ki of the enzyme for L-BSO.

Validation of GCL assay:

The GCL assay was validated in astrocytes to check (a) activity was linear with respect to protein (10-40 μg) and time (0-20 minutes), and (b) the assay was reproducible.

3.4. Results

3.4.1. Chromatography and electrochemical detection of γ-GC

The thiol group of GSH can be detected electrochemically following HPLC separation using orthophosphoric acid as the mobile phase (section 2.6; Riederer *et al.*, 1989). Therefore, the thiol group of γ-GC should also be electrochemically active under the same HPLC conditions. γ-GC standards (5 μM) were separated by reverse phase HPLC and measured at various downstream electrode potentials to ascertain the optimal parameters for γ-GC detection (**Figure 3.1**). The voltamogram revealed that γ-GC was electrochemically active, with a plateau of detection attained between +600 and +650 mV. However, when astrocyte samples were analysed (section 3.4.2.), several extra peaks were detected at +650 mV compared to +600 mV, which obscured detection of γ-GC. Consequently a downstream electrode potential of +600 mV was chosen for optimal γ-GC detection. Detection of γ-GC was linear between 1 and 10 μM (R^2 0.9984).

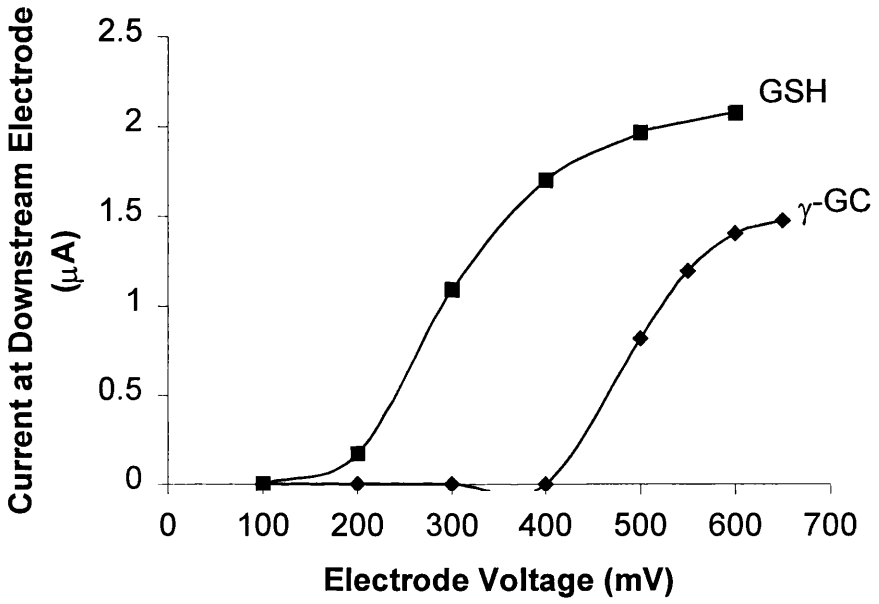

Figure 3.1. A voltamogram of γ-GC and GSH standards

γ-GC and GSH standards (5 μM) were resolved by reverse-phase HPLC and detected by an electrochemical detector. The upstream electrode was set at +100 mV, while the downstream electrode sequentially set at a potential between +100 and +650 mV to determine optimal conditions for detection. Optimal γ-GC and GSH detection was observed at a potential between +600 and +650 mV.

Although optimal electrochemical detection of both γ-GC and GSH occurred at a potential of +600 mV (**Figure 3.1**), the voltamagram of γ-GC was distinct to that of GSH, with the signal generated by equimolar γ-GC less than that for GSH. Since the GSH and γ-GC standards were between 98 and 99% in the reduced form, the difference in signal is likely to relate to the difference in the electrochemical properties of the two molecules. The separation of γ-GC and GSH standards by reverse-phase HPLC is shown in **Figure 3.2**. Under the chromatographic conditions employed γ-GC and GSH are distinguishable from each other, with the retention time of γ-GC approximately 30 seconds longer than that of GSH. The retention times of the GCL assay substrate cysteine, and cysteinylglycine, which may also occur in the reaction mixture, were approximately 5 minutes, and do not interfere with the γ-GC peak.

3.4.2. GCL activity in cultured astrocytes

Following incubation of astrocyte cell extracts with the assay reaction mixture, γ-GC could clearly be detected **(Figure 3.3).** GCL activity was calculated by measuring the amount of γ-GC synthesised over a defined period and related to the protein content of the sample assayed. The activity of GCL in astrocytes was estimated to be 9.7 ± 1.7 nmol γ-GC synthesised/min/mg protein (n = 9 independent cell culture preparations). The method was reproducible, with approximately 6 % variability observed when an astrocyte homogenate was assayed three times in separate reaction mixtures (*e.g.* different assay buffer, ATP *etc.*). The GCL assay was linear with respect to both protein (10 μg to 40 μg of protein (**Figure 3.4A**)) and time (0 to 20 minutes (**Figure 3.4B**)). A small γ-GC peak (≤ 0.2 μA) could be detected using 5 μg of protein, however this was found to be at the limit of detection and not advisable.

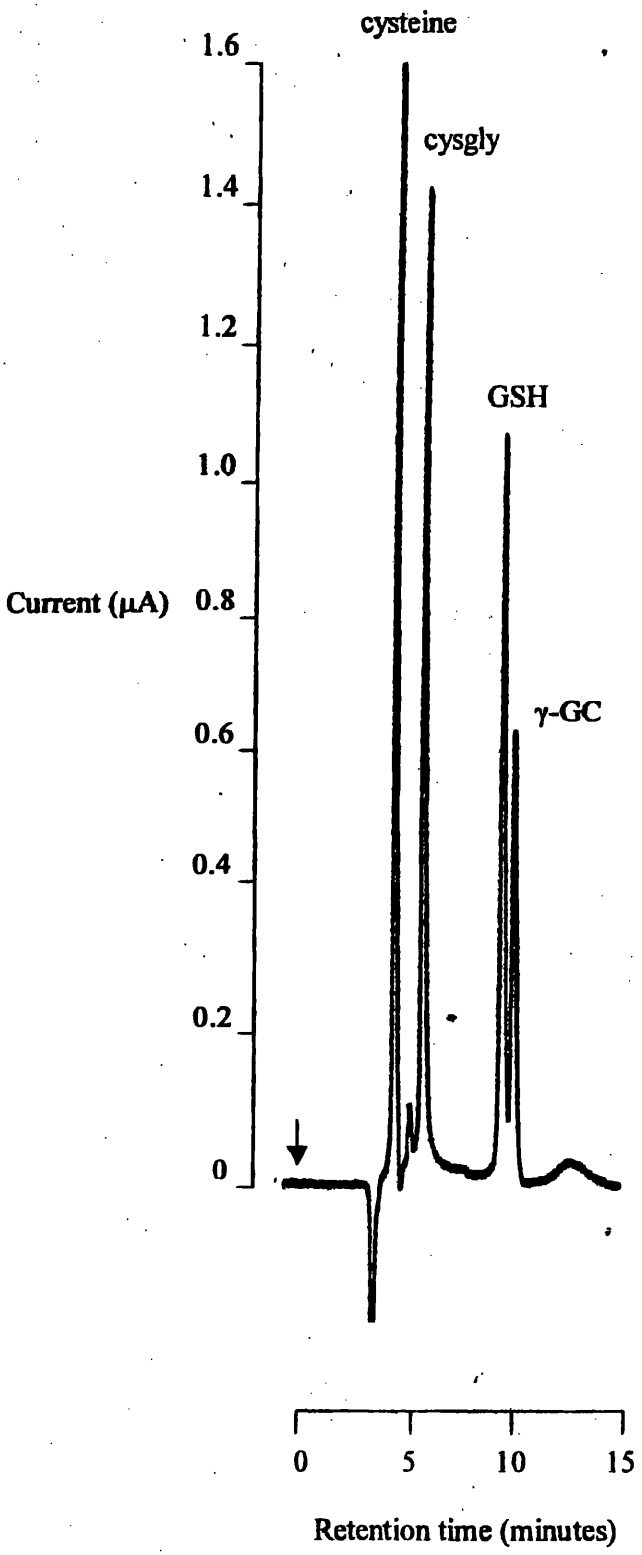

Figure 3.2. Chromatogram of γ-GC, GSH, cysteine and cysteinylglycine standards (2.5 μM).

Standards were separated by reverse-phase HPLC and detected electrochemically. Arrow denotes injection of standards

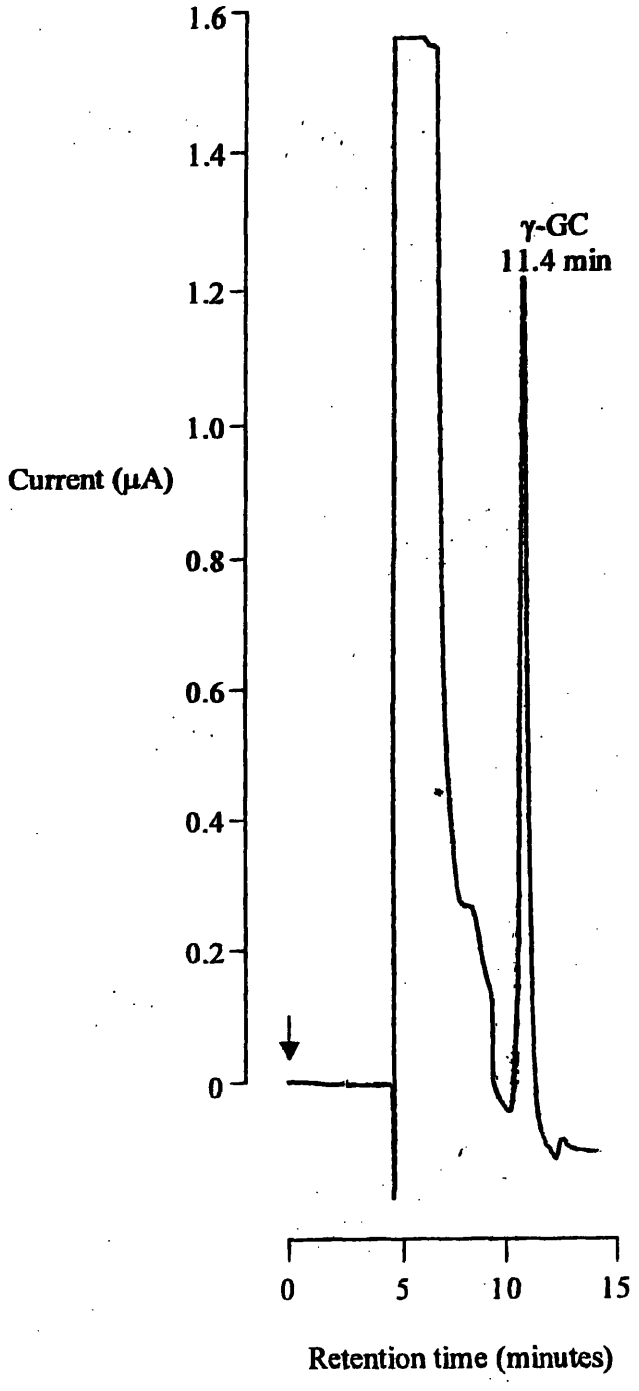

Figure 3.3. A typical GCL assay chromatogram

Astrocyte sample was assayed as described in section 3.2.4 and detected electrochemically following reverse-phase HPLC. Arrow denotes injection of sample.

(A)

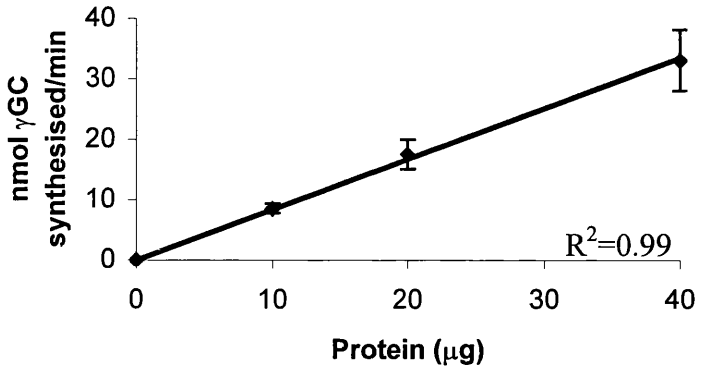

(B)

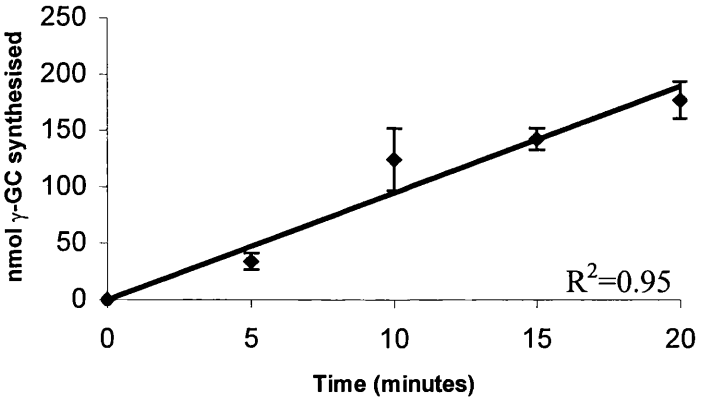

Figure 3.4. GCL activity against protein and time

Astrocyte samples were assayed for 15 minutes when determining whether GCL activity was linear with protein (a), while 15 μg protein was assayed for each time point in (b). Each point was assayed in triplicate.

To assess the specificity of the GCL assay, enzyme activity was determined in the absence or presence of the GCL inhibitor L-BSO. Astrocytic GCL activity was totally abolished when the assay was performed in the presence of 5 mM L-BSO. Astrocyte samples were also incubated with a range of L-BSO concentrations (5 nM - 500 μM) to obtain an inhibition curve (**Figure 3.5**). The Ki for L-BSO was estimated to be approximately 100 μM.

No γ-GC peak was observed following incubation of sample with just ATP alone (no cysteine or glutamate). Cysteine and cysteinylglycine (derived from the enzymatic degradation of GSH by γ-GT) were found to have a shorter retention time than γ-GC (Figure 3.2). Furthermore, cystine and GSSG, formation of which could also occur during the course of the assay, were undetectable at the electrode potentials used in this assay. Given the absence of a γ-GC peak in samples incubated with L-BSO or ATP alone, and the different retention times of other metabolites, the results suggest this assay is specifically measuring GCL activity.

It should be noted that a residual GSH peak was occasionally observed following sample preparation. The amount of residual GSH was estimated to be 0.91 ± 0.1 μM (n = 7). The peak was not due to *de novo* GSH synthesis since the GSH peak could also be seen when sample was incubated with just ATP alone or assayed in the presence of 5 mM L-BSO. The contaminating GSH should not affect the assay, as the Ki of GCL for GSH is 8.2 mM (Huang *et al.*, 1993a).

A 97-100% (n = 3) recovery of γ-GC standard was obtained when samples were spiked, indicating that there was little loss of product following acid extraction and precipitation of protein prior to loading on to the HPLC column. Spiking also indicated that there was no metabolism of γ-GC by enzymes in the cell extract such as γ-GT and γ-glutamylcyclotransferase (γ-GCT) of the γ-glutamyl cycle (Lu, 2000). Indeed, γ-GT activity in astrocyte samples (measured spectrophotometrically; section 2.4.7) was found to be completely abolished within 1 minute when treated with the acivicin concentration used in the GCL assay.

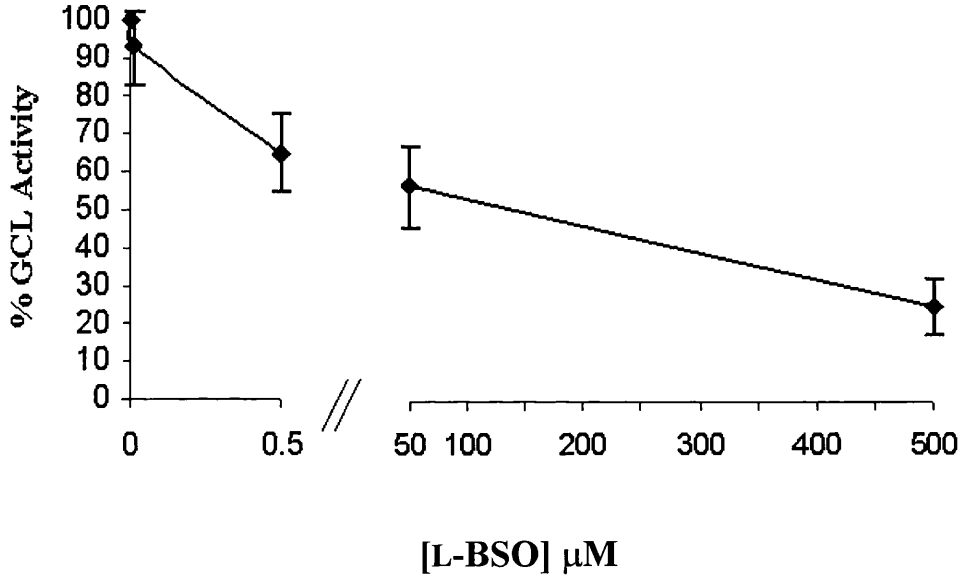

Figure 3.5. L-BSO inhibition curve of astrocyte GCL activity

Astrocyte sample (15 μg) was preincubated with 0-500 μM L-BSO and 10 mM ATP for 5 minutes. GCL activity was then assayed in the presence of L-BSO. Three independent cell culture preparations were assayed. Values are mean ± SEM.

3.5. Discussion

This chapter has established that γ-GC is electrochemically active when extracted into orthophosphoric acid. This observation led to the development of a GCL assay based on the electrochemical detection of γ-GC synthesised by GCL following separation by reverse-phase HPLC. The assay is rapid, convenient and appears to be specific since γ-GC synthesis was abolished in the presence of L-BSO.

The assay estimated that GCL activity in astrocytes was 9.7 ± 1.7 nmol γ-GC synthesised/min/mg protein. The activity of GCL in chick astrocytes has previously been reported as 2.8 ± 0.5 γ-GC synthesised/min/mg protein (Makar *et al.*, 1994). In the latter study, chick GCL activity was estimated by measuring the activity of the coupled enzyme γ-glutamylcyclotransferase (γ-GCT; **reaction 3.3**; Seelig & Meister, 1985).

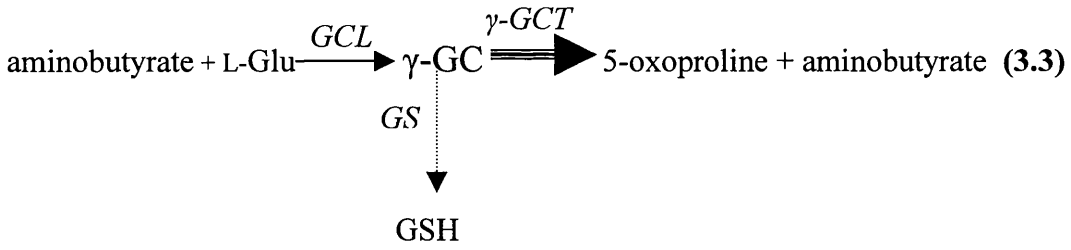

Makar *et al* measured the production of [^{14}C]-labelled 5-oxo-proline by astrocyte homogenate in the presence of labelled glutamate, aminobutyrate (instead of cysteine), and an excess of γ-GCT. However, GSH was not removed from the cellular homogenates. Since GSH inhibits GCL by negative feedback (Huang *et al.*, 1993a), this may explain why GCL activity is lower than reported here. Alternatively, the variation in GCL activity may reflect differences between species, brain regions, or culture techniques. Indeed a wide range of GSH levels in astrocytes and neurones have been reported (Makar *et al.*, 1994; Bolanos *et al*; 1995; Iwata-Ichikawa *et al.*, 1999; Dringen *et al.*, 1999b). Variation in cellular GSH concentration has also been observed between batches of primary astrocytes (Bolanos *et al.*, 1994, 1995). In view of the potential variability between cultures

every culture preparation used in this study was validated against protein, time and L-BSO sensitivity when assaying GCL activity.

The L-BSO inhibition curve estimated the Ki of GCL to be approximately 100 μM. This compares favourably with previous inhibition studies of mammalian GCL. A 44-68% depletion of intracellular GSH has been observed in cultured astrocytes incubated with 100 μM L-BSO for 24 hours (Vasquez *et al.*, 2001). Cloned Human GCL also shows a 50% loss of activity when preincubated with 50 μM L-BSO for 5 minutes (Kelley et al., 2002). GCL activity in this case was measured by the widely used spectrophotometric method described by Seelig & Meister (1984).

3.6. Conclusions

The method described here will be used to determine GCL activity in astrocytes and neurones following oxidative stress (see chapters 4 & 5). Increased transcription of GCL has been reported following a variety of stimuli (*e.g.* oxidative stress, GSH depleting agents, transition metals (Cai *et al.*, 1997; Moellering *et al.*, 1998; Iwata-Ichikawa *et al.*, 1999; Lu, 2000). This assay will complement such expression studies by determining whether changes in transcription results in altered enzyme activity in the cytosol. Furthermore, loss of GSH has also been reported in ageing and several neurological diseases such as Parkinson's disease (Sian *et al.*, 1994a; Schulz *et al.*, 2000). This method will be useful in ascertaining whether alterations in GCL activity are associated with such disorders.

Chapter 4

The effect of *(S)*-3-hydroxy-4-pentenoic acid on glutathione metabolism in astrocytes and neurones

4.1. Introduction

In mammalian cells intracellular GSH concentration has been reported in the millimolar range (1-12 mM) and is mainly compartmentalised into a cytosolic and mitochondrial GSH pool (approximately 90% and 5-10% respectively; Meredith & Reid; Meister & Anderson, 1983; Wullner *et al*., 1999). Small GSH pools have also been reported in the endoplasmic reticulum and nucleus (Hwang *et al*., 1992; Voehringer *et al*., 1998).

GSH is synthesised in the cytosol and is transported in to the mitochondria by an unknown mechanism. In rat kidney, the mitochondrial dicarboxylate and 2-oxoglutarate carriers have been implicated in the uptake of GSH (Chen & Lash, 1998; Chen *et al*., 2000). Studies in which cellular GSH has been depleted by chemical agents have implied that the mitochondrial GSH pool is preferentially maintained over that of the cytosol. Cytoplasmic GSH in cerebellar granule neurones and hepatocytes was depleted by approximately 75% (using the GSH synthesis inhibitor L-buthionine-(S,R,)-sulfoximine (L-BSO) and GSH conjugator diethylmaleate respectively) before a loss of mitochondrial GSH was observed (Garcia-Ruiz et al., 1995; Wullner *et al*., 1999). Jain *et al* (1991) have reported that cytosolic and mitochondrial GSH was depleted by 85% in the cerebral cortex of newborn rats treated with L-BSO for 9 days. However, if monoethyl ester GSH was also administered to L-BSO treated rats, mitochondrial GSH concentration returned to control levels, while cytosolic GSH concentration was depleted by approximately 65% (Jain *et al*., 1991).

Cellular GSH concentration has been implicated in protecting the enzymes of the electron transport chain (ETC) from oxidative stress (Bolanos *et al*., 1995, 1996; Barker *et al*., 1996). Loss of complex II+III and IV activity was greater in neurones treated with peroxynitrite compared to astrocytes (Bolanos *et al*., 1995). The lower GSH levels in neurones were postulated to be a reason why neurones were more susceptible to peroxynitrite. In support of this, NO-mediated inhibition of complex II+III and IV activity was suggested to be diminished in neurones cocultured with astrocytes, which contain twice the GSH concentration, compared to neurones cultured alone (Bolanos *et al*., 1996). Furthermore, inhibition of

complex I of the ETC in astrocytes by peroxynitrite only occurs when cellular GSH had been depleted 95% by L-BSO prior to treatment (Barker *et al.*, 1996). The preferential maintenance of the mitochondrial GSH pool during GSH depletion has led to the hypothesis that the mitochondrial GSH pool is important in protecting brain mitochondrial function, such as the ETC, from oxidative stress. Indeed, in L-BSO treated rats, loss of complex I and IV activity was observed in brain mitochondria depleted of GSH (Heales *et al.*, 1995), with loss of complex IV activity proportional to mitochondrial GSH concentration (Heales *et al.*, 1996b). Furthermore, loss of mitochondrial dehydrogenase activity and membrane potential has been observed to be greater in neurones in which both cytosolic and mitochondrial GSH was depleted, compared to cells where just cytosolic GSH was depleted (Wullner *et al.*, 1999). Electron micrographs have also shown mitochondria depleted of GSH to be structurally damaged and swollen (Jain *et al.*, 1991).

Since drugs such as L-BSO and diethylmaleate deplete both cytosolic and mitochondrial GSH, it has proven difficult to dissect out the importance of the mitochondrial GSH pool, compared to the cytosolic pool, in protecting the enzymes of ETC from insults such as peroxynitrite.

(*S*)-3-hydroxy-4-pentenoic acid (OHPA) has recently been reported to specifically deplete the mitochondrial GSH pool in liver (Shan *et al.*, 1993; Hashmi *et al.*, 1996). OHPA can deplete liver mitochondrial GSH by exploiting the mitochondrial localisation of the enzyme 3-hydroxybutyrate dehydrogenase (HBDH; EC 1.1.1.30; Shan *et al.*, 1993; Hashmi *et al.*, 1996). HBDH is an amphipathic enzyme located on the inner membrane of the mitochondria that normally catalyses the metabolism of ketone bodies (**reaction 4.1**; Zhang *et al.*, 1989; Marks *et al.*, 1992).

$$(R)\text{-3-hydroxybutyrate} + \text{NAD} \xleftrightarrow{\textbf{HBDH}} \text{acetoacetate} + \text{NADH} + \text{H}^+ \qquad \textbf{(4.1)}$$

OHPA can be taken up by mitochondria and is metabolised to 3-oxo-4-pentenoate by HBDH (Shan *et al.*, 1993). 3-oxo-4-pentenoate can then react nonenzymatically with GSH, thereby depleting the mitochondrial GSH pool

(**Figure 4.1.**; Shan *et al.*, 1993). Approximately 60% of mitochondrial GSH was depleted in hepatocytes treated with 0.5 mM OHPA for 30 minutes, with only a 20% depletion of cytosolic GSH observed Hashmi *et al.*, 1996). OHPA was reported not to have any effect on mitochondrial or cytosolic protein thiol concentrations (Shan *et al.*, 1993).

Consequently, in this chapter the effect of OHPA on mitochondrial GSH levels has been characterised in cultured astrocytes and neurones, with the aim of investigating whether the mitochondrial GSH pool plays a critical role in protecting the ETC.

4.2. Methods

4.2.1. Cell culture

Primary astrocytes and neurones were cultured as described in section 2.2 and treated with 0.5 mM OHPA (synthesised by Dr David Selwood, The Wolfson Institute for Biomedical Research, UCL, UK) in astrocyte or neurone medium (section 2.2.1) on day 14 and day 6 in culture respectively for the period indicated.

4.2.2. Isolation of mitochondria

Mitochondria were isolated from ~$15x10^6$ astrocytes and ~$20x10^6$ neurones following treatment with 0.5 mM OHPA as described in section 2.3.1. Liver mitochondria were isolated from adult Wistar rats as described in section 2.3.2.

4.2.3. GSH quantitation

GSH content in isolated liver mitochondria, and cultured astrocyte and neurone homogenates, cytosols and mitochondria were analysed by reverse-phase HPLC as described in section 2.6.

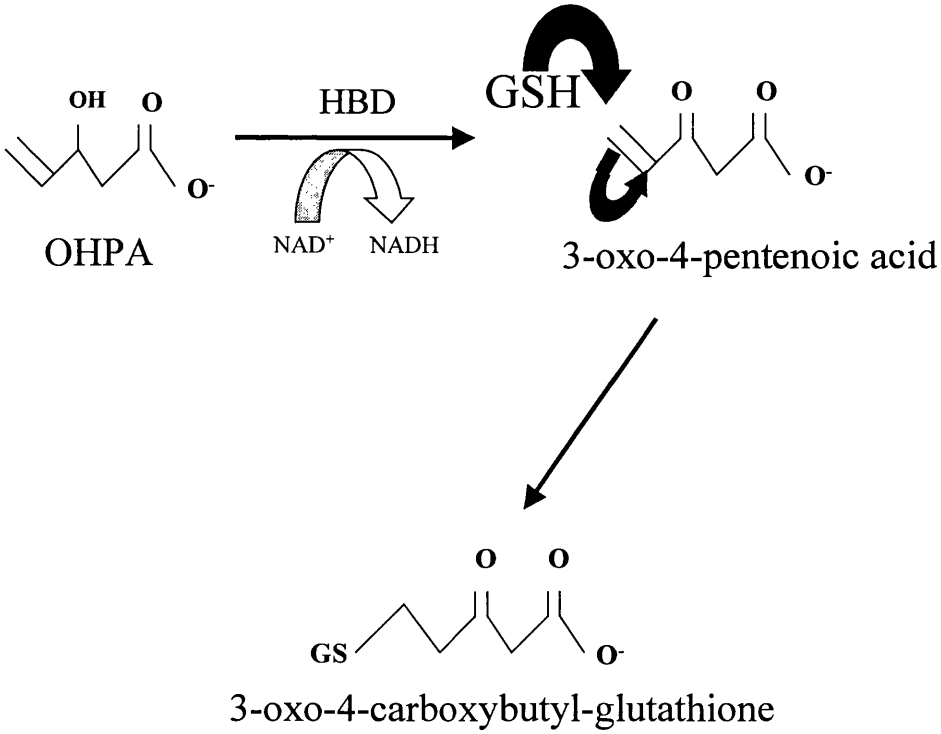

Figure 4.1. The proposed mechanism by which OHPA specifically depletes the mitochondrial GSH pool

4.2.4. Determination of GSSG content in liver mitochondria

GSSG levels in liver mitochondria were determined using the method of Hargreaves *et al* (2002). Firstly, GSH concentration in the sample (A) was determined as described in section 2.6. An aliquot of the same sample (B) was then treated with DTT to convert GSSG → 2 GSH. Total GSH concentration was determined in B, and GSSG concentration calculated by: (B-A)/2.

Briefly, liver mitochondria (5 mg/ml; 100 µl) were mixed with 100 µl 25 mM dithiothreitol (DTT) and 50 µl 100 mM Tris, and incubated on ice for 10 minutes. The reaction was stopped by the addition of 350 µl 15 mM orthophosphoric acid and the sample centrifuged at 14000 x g for 5 minutes. The supernatant was placed in chromacol HPLC vials and GSH concentration determined. As a positive control, 125 µM GSSG standard (20 µl) was mixed with 25 mM DTT (20 µl) and 100 mM Tris (10 µl), and incubated on ice for 10 minutes. 950µl of 15 mM orthophosphoric acid was then added and GSH concentration determined. Allowing for dilutions, if GSSG were fully converted to GSH, a peak approximating to 5 µM GSH was detected following separation by HPLC and detection by electrochemical detection.

4.2.5. Determination of glutamate-cysteine ligase activity

Glutamate-cysteine ligase activity was measured in OHPA treated astrocyte and neurone homogenates as described in section 3.2.

4.2.6. Spectrophotometric enzyme assays

Complexes I, II+III and IV of the ETC, and citrate synthase (CS) were assayed in cultured astrocyte and neurone homogenates, and isolated liver and astrocyte mitochondria as described in section 2.4.

Lactate dehydrogenase release from cultured astrocytes and neurones was measured as described in section 2.4.6.

HBDH activity in isolated liver, astrocyte and neurone mitochondria was determined by the method described in section 2.4.5. Purified microbial HBDH from the β-hydroxybutyrate diagnostic kit (Sigma Diagnostics) was used to determine the Km and Vmax of HBDH for OHPA. HBDH assay buffer (4.6 mM NAD^+, buffer, pH 7.6; 3 ml) was mixed with 2.5 units of microbial HBDH and the reaction started by addition of OHPA (0.3-1.5 mM). The formation of NADH was followed at an absorbance of 340 nm at 37°C using an Uvikon 941 spectrophotometer.

4.2.7. Protein determination

Sample protein concentration was determined using the Lowry method as described in section 2.5.

4.3. Experimental protocols

Validation of synthesised OHPA:

To ascertain whether the OHPA synthesised had similar properties to those previously reported (Shan *et al.*, 1993; Hashmi *et al.*, 1996), liver mitochondria (5 mg/ml) were incubated with OHPA (0-1 mM) for 15 minutes at 37 °C and mitochondrial GSH concentration determined. The Km and Vmax of HBDH for OHPA was also determined by measuring the initial rate of microbial HBDH when incubated with 0.15 to 1.5 mM OHPA at 37 °C.

Effect of OHPA on mitochondrial and cytosolic GSH metabolism in astrocytes and neurones:

Neurones ($20x10^6$) and astrocytes ($15x10^6$) were treated with media containing 0.5 mM OHPA for 4 or 18 hours respectively. Mitochondria were isolated from the cells and the GSH concentrations in the mitochondria and cytosol were determined. The activity of GCL, the rate-limiting enzyme in GSH synthesis

(Anderson & Meister, 1983; Huang *et al.*, 1993a), was also measured in astrocytes and neurones treated with OHPA for 18 hours.

Effect of OHPA on ETC:

Astrocytes were treated with astrocyte media containing 0.5 mM OHPA for 30 minutes and 4, 8, and 18 hours. The activities of the ETC complexes were then assayed in astrocytes homogenates or isolated astrocyte mitochondria. Neurones were treated with 0.5 mM OHPA for 4 or 18 hours and ETC activity determined in neuronal homogenates. ETC complex activities were also measured in isolated liver mitochondria following treatment with 0-1 mM OHPA for 15 minutes at 37 °C.

4.4. Results

4.4.1. Effect of OHPA on liver mitochondria

Mitochondria isolated from liver were incubated with OHPA to verify that the drug yielded similar results to that of Hashmi *et al* (1996). Mitochondria (5mg/ml) incubated with 0.125 and 0.25 mM OHPA for 15 minutes at 37°C showed a 44% and 69% depletion of mitochondrial GSH respectively (**Figure 4.2**), and were comparable to the findings of Hashmi *et al* (1996). At concentrations greater than 0.25 mM OHPA, GSH depletion attained a plateau.

The GSSG content in OHPA treated mitochondria was similar to that in control mitochondria (control, 0.5 ± 0.1; 0.5 mM OHPA, 0.3 ± 0.2 nmol GSSG/mg protein (n=3)) suggesting that GSH depletion was due to conjugation with 3-oxo-4-pentenoate rather than oxidation of GSH to GSSG (the conversion of GSSG standard to GSH during the course of these experiments was always > 95%).

The Km and Vmax of microbial HBDH for OHPA was estimated to be 0.5 mM and 23.2 μmol/min/ml respectively (**Figure 4.3**). The Km of HBDH for (*R,S*)-OHPA has previously been reported to be 1.5 mM in *Pseudomonas lemoignei* (Shan *et al.*, 1993).

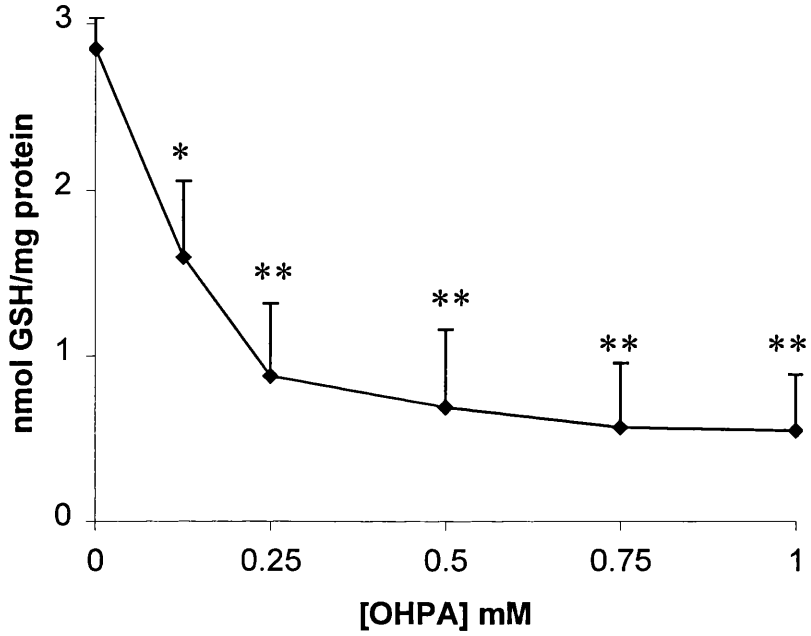

Figure 4.2. The effect of OHPA on liver mitochondria GSH

Liver mitochondria (5 mg/ml) were incubated with 0-1 mM OHPA for 15 minutes at 37°C and mitochondrial GSH content measured. OHPA depleted liver mitochondria GSH. Data are mean ± SEM of 3 or 4 independent mitochondrial isolations. Statistical significance was determined by one-way ANOVA followed by least significant difference test. * $p < 0.05$ and ** $p < 0.01$.

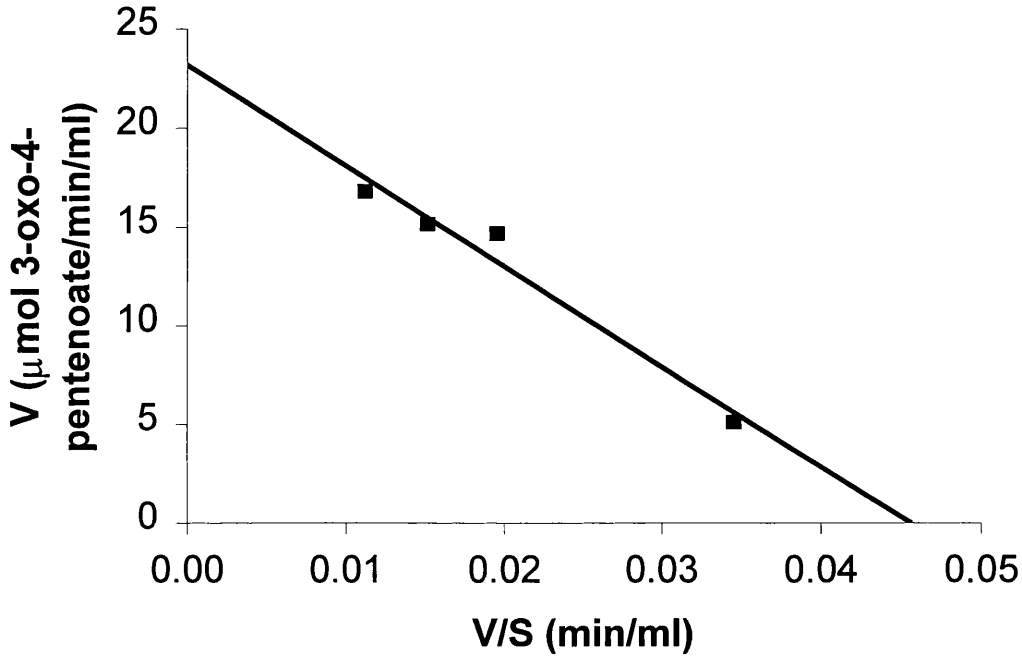

Figure 4.3. Eadie-Hofstee plot of HBDH for OHPA

Microbial HBDH (2.5 units) was incubated with 150 – 1500 μM OHPA (S) and the initial rate (V; μmol 3-oxo-4-pentenoate/min/ml) measured. The gradient of the graph and the intercept on the y-axis was used to calculate the Km and Vmax of HBDH respectively. All points were measured in duplicate.

The activities of complexes I to IV of the ETC were also measured in liver mitochondria treated with 0-1 mM OHPA (**Table 4.1**). No effect on complex I activity was observed in OHPA treated mitochondria. However, a significant dose dependent loss of complex II + III activity was observed in OHPA treated mitochondria. Inhibition of complex IV activity was also observed at 1 mM OHPA. OHPA treatment (0-1 mM) had no effect on the activity of the mitochondrial marker enzyme CS.

4.4.2. HBDH activity in cultured astrocytes and neurones

The specific activity of HBDH was assayed in mitochondria isolated from liver, astrocytes, and neurones to see if astrocytes and neurones express the enzyme (**Table 4.2**). The specific activity of HBDH in astrocytic and neuronal mitochondria was determined to be approximately 40-fold lower than in liver mitochondria.

4.4.3. The effect of OHPA on cultured astrocytes

4.4.3.1. The effect of OHPA on mitochondrial and cytosolic GSH concentration

Astrocytes were treated with 0.5 mM OHPA for 30 minutes, and the GSH levels in astrocyte homogenates, mitochondria and cytosol measured (**Figure 4.4**). No change in homogenate, mitochondrial or cytosolic GSH levels was observed. Previously in hepatocytes, mitochondrial GSH was depleted by 60% following exposure to OHPA for just 15 minutes (Hashmi *et al.*, 1996). However, since HBDH activity in astrocytes is 40-fold lower compared to liver, this may explain the lack of GSH depletion following 30 minutes of OHPA exposure.

Consequently, astrocytes were incubated with OHPA for 18 hours to see if this resulted in mitochondrial GSH depletion. No effect on mitochondrial GSH concentration was observed following incubation with 0.5 mM OHPA for 18

[OHPA] mM	Complex I nmol/min/mg protein	Complex II+III nmol/min/mg protein	Complex IV k/min/mg protein
0	52.9 ± 11.0	134.5 ± 15.6	14.6 ± 0.7
0.125	48.0 ± 8.9	113.0 ± 12.2	15.1 ± 1.7
0.25	47.4 ± 10.0	95.7 ± 12.2*	13.1 ± 1.7
0.50	52.9 ± 12.5	74.6 ± 9.2 **	11.2 ± 0.6
0.75	47.7 ± 8.0	66.7 ± 11.9 **	10.3 ± 1.0
1.0	55.4 ± 11.5	56.6 ± 7.7 **	8.6 ± 1.6*

Table 4.1. The effect of OHPA on the ETC

Liver mitochondria (5mg/ml) were incubated with 0-1 mM OHPA for 15 minutes at 37°C. Significant inhibition of complex II+III and complex IV was observed. Values are mean ± SEM (n=3-4 independent mitochondrial isolations). Statistical significance was determined by one-way ANOVA followed by least significant difference test. * $p < 0.05$ and ** $p < 0.01$.

	HBDH Activity (nmol/min/mg protein)
Liver	225.8 ± 13.7
Astrocyte	5.2 ± 2.4
Neurone	6.8 ± 1.5

Table 4.2. HBDH specific activity in liver, astrocyte and neurone mitochondria

Mitochondria were isolated from liver, astrocytes and neurones, and HBDH activity measured. Values are mean ± SEM (n=3-4 independent mitochondrial preparations).

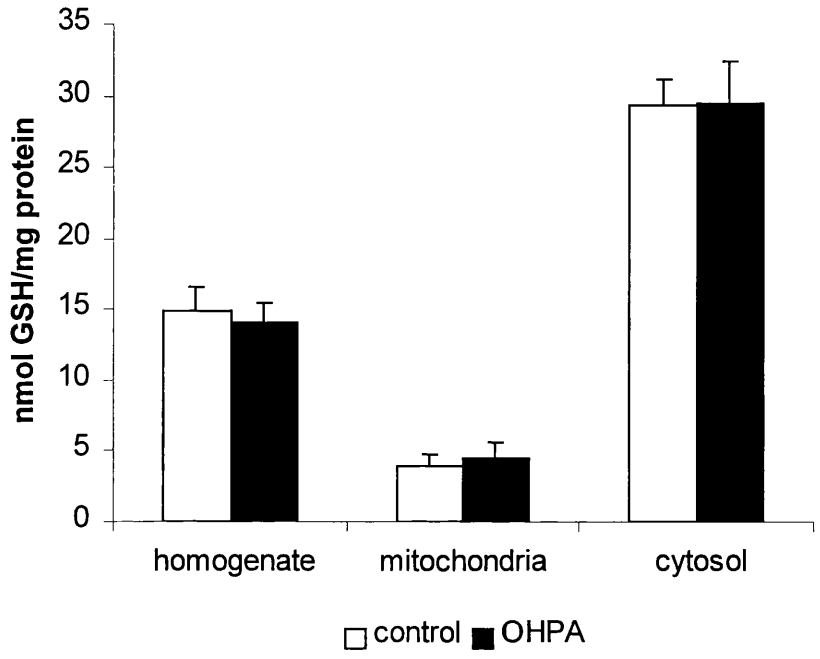

Figure 4.4. Cellular GSH levels in astrocytes treated with OHPA for 30 minutes

Astrocytes were treated with 0.5 mM OHPA for 30 minutes. Following treatment, mitochondria were isolated, and GSH concentration determined in the homogenate, mitochondria, and cytosol. OHPA had no affect on GSH levels Values are mean ± SEM (n=3 independent cell cultures). Statistical significance was determined by the Student's t-test.

hours. However, homogenate and cytosolic GSH levels were significantly increased by 41% and 88% respectively (**Figure 4.5**). Astrocytes treated with 0.5 mM pentenoic acid (PA) for 18 hours did not increase the GSH concentration in the cytosol (**Figure 4.5**), suggesting that the increase in GSH concentration was specific to OHPA, rather than a general property of carboxylic acids. Astrocytes were incubated with 0.5 mM OHPA for shorter periods to see if any change in GSH levels were seen at earlier time points. No change in GSH levels was observed in astrocyte homogenates incubated with 0.5 mM OHPA for either 4 or 8 hours (control 4hr, 20.2 ± 1.5; OHPA 4hr, 20.2 ± 2.5; control 8 hr, 25.1 ±1.0; OHPA 8 hr, 28.0 ± 1.6 nmol GSH / mg protein (n=5 independent cell preparations)).

4.4.3.2. The effect of OHPA on ETC complex activities in astrocytes

The activities of complexes I to IV of the ETC were measured in mitochondria isolated from astrocytes treated with 0.5 mM OHPA for 30 minutes and 18 hours (**Figure 4.6**). Complex activity was expressed against citrate synthase activity to account for differences in mitochondrial enrichment between isolations. Astrocyte ETC complex activity was unaffected following OHPA treatment for 30 minutes (**Figure 4.6A**). However, treatment for 18 hours resulted in a 21% loss of complex II+III activity (**Figure 4.6B**). Note that the loss of complex II+III activity was comparable if expressed against protein, rather than CS activity (control, 51.4 ± 4.7; OHPA, 36.7 ± 3.9 nmol/min/mg protein (n=5 independent cell preparations) $p < 0.05$). The loss of complex II+III activity was not due to OHPA or 3-oxo-4-pentenoic acid interfering with the enzyme assay. Incubation of astrocyte mitochondria in the presence of 0.5 mM OHPA or 3-oxo-4-pentenoic acid (generated by incubation of OHPA with microbial HBDH until substrates exhausted) during the complex II+III assay had no effect on activity (control, 0.37 ± 0.03; OHPA, 0.37 ± 0.02 (n=3); control, 0.34 ± 0.03, 3-oxo-4-pentenoic acid, 0.31 ± 0.03 (n=3)). Furthermore, complex II+III was unaffected in astrocytes treated with 0.5 mM OHPA for either 4 or 8 hours (measured in homogenates; control 4hr, 7.9 ± 0.7; OHPA 4hr, 7.3 ± 0.7; control 8 hr, 6.9 ± 0.7; OHPA 8 hr, 7.1 ± 0.5 nmol nmol/min/ mg protein (n=5 independent cell preparations)).

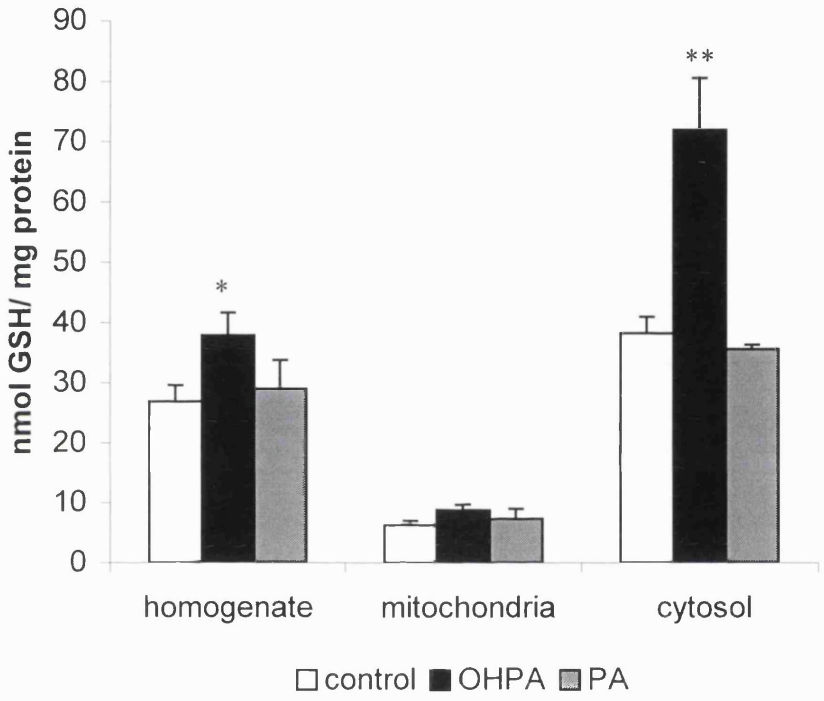

Figure 4.5. Cellular GSH levels in astrocytes treated with OHPA for 18 hours
Astrocytes were treated with 0.5 mM OHPA or 0.5 mM pentenoic acid (PA) for 18 hours. Following treatment, mitochondria were isolated, and GSH levels determined in the homogenate, mitochondria, and cytosol. Homogenate and cytosolic GSH levels were significantly increased in astrocytes treated with OHPA for 18 hours. Values are mean ± SEM (n=3-9 independent cell cultures). Statistical significance was determined by one-way ANOVA followed by least significant difference test. * $p < 0.05$, ** $p < 0.01$.

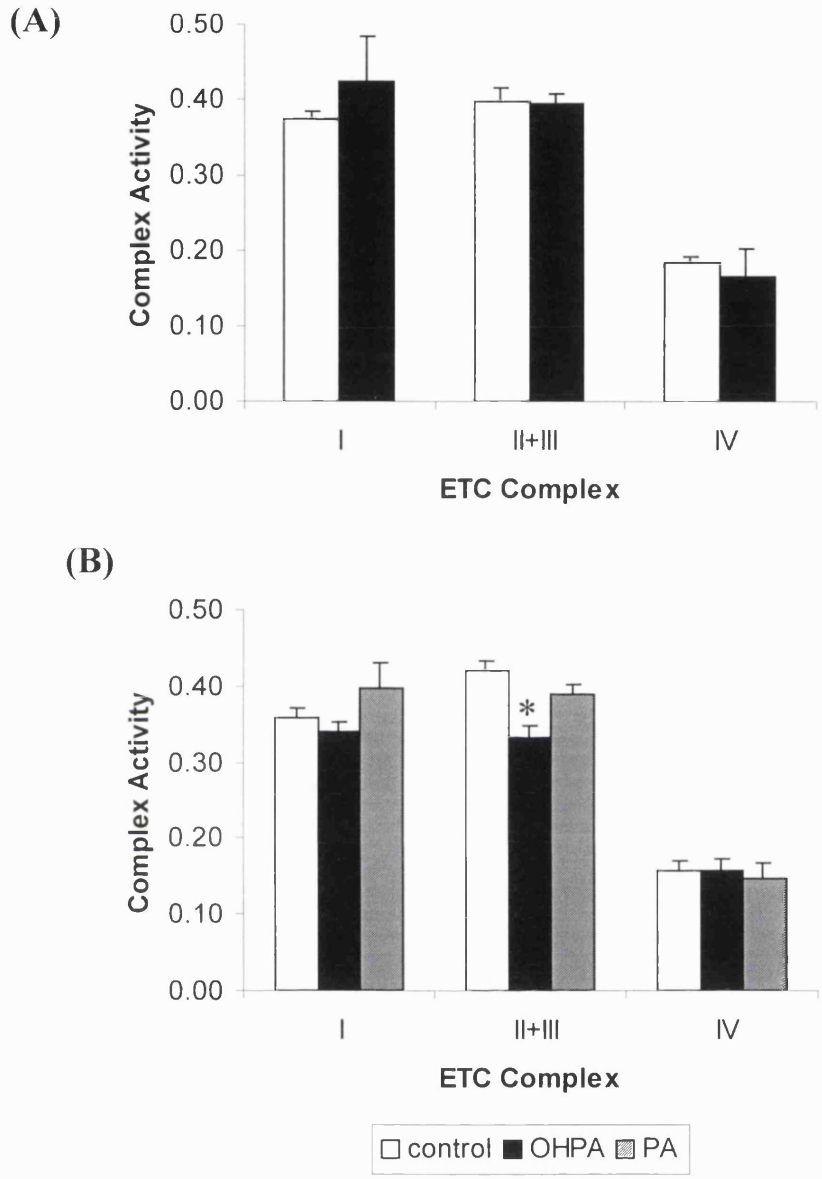

Figure 4.6. The effect of OHPA on the ETC

Astrocytes were treated with 0.5 mM OHPA for 30 minutes (A) or 18 hours (B), mitochondria isolated from the astrocytes, and complexes I to IV of the ETC assayed. Complex specific activities were expressed against CS activity and therefore have no units except complex IV activity (expressed as k/nmol). A significant loss of complex II+III activity was observed following OHPA treatment for 18 hours. Values are mean ± SEM (n=3-9 independent mitochondrial isolations). Statistical significance was determined by one-way ANOVA followed by least significant difference test. ** $p < 0.01$.

PA has previously been shown to inhibit mitochondrial fatty acid metabolism (Fukami & Williamson, 1971; Schulz, 1987). Therefore, astrocytes were incubated with 0.5 mM PA for 18 hours to see whether carboxylic acids could inhibit complex II+III activity. PA had no effect on the activity of complex II+III (**Figure 4.6B**).The activities of complexes I and IV of the ETC (**Figure 4.6B**), and CS (measured in astrocyte homogenates; control, 120.8 ± 12.0; OHPA, 116.7 ± 17.5 nmol/min/mg protein (n=5-6 independent mitochondrial isolations)) were unaffected by treatment with 0.5 mM OHPA for 18 hours. Treatment with 0.5 mM OHPA for 18 hours appeared to have no effect on astrocyte viability (control, 3.4 ± 0.9; OHPA, 3.6 ± 0.6 % LDH release (n=3)).

4.4.4. The effect of OHPA on cultured neurones

4.4.4.1. Neuronal viability following exposure to OHPA for 18 hours

Since the specific activity of neuronal HBDH is similar to that of astrocytes (**Table 4.2**), neurones were also incubated with 0.5 mM OHPA for 18 hours. Following OHPA treatment, an increased amount of cell debris was observed when neurones were viewed under a microscope (**Figure 4.7**). Furthermore, the amount of LDH released from OHPA treated neurones was significantly increased (control, 14.4 ± 4.6; OHPA, 32.7 ± 10.4 %LDH release (n = 4 independent cell preparations) $p < 0.05$). These two observations suggest that treatment of neurones with 0.5 mM OHPA for 18 hours results in cell death.

4.4.4.2. Neuronal GSH levels following 18 hours of OHPA exposure

GSH levels were measured in neurones surviving treatment with 0.5 mM OHPA for 18 hours. GSH levels in neuronal homogenates were significantly depleted by 42% in neurones following OHPA treatment for 18 hours (**Figure 4.8**). Due to the significant damage observed in neuronal mitochondria following OHPA treatment for 18 hours (see below), mitochondria were not isolated from neurones in order to determine mitochondrial GSH concentration.

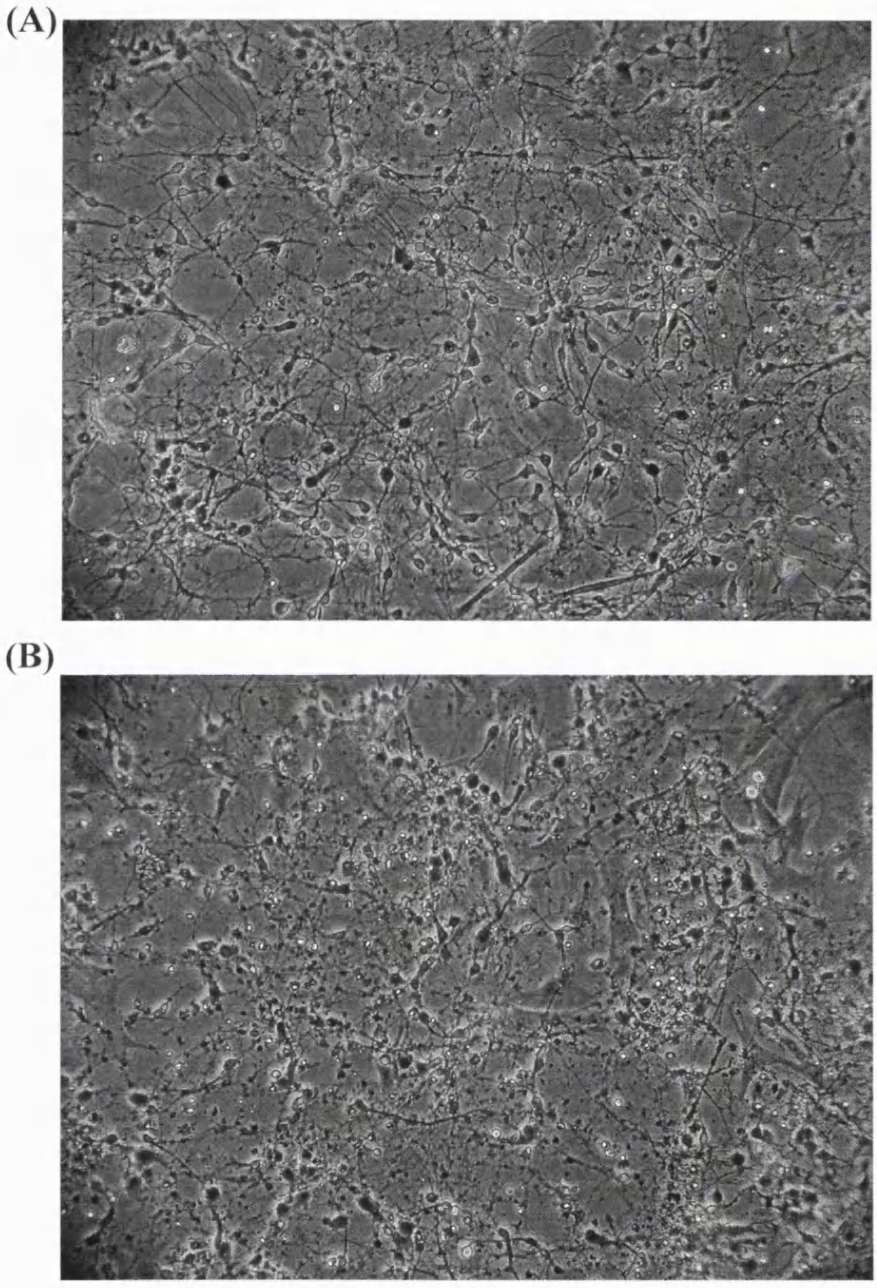

Figure 4.7. Morphology of neurones following OHPA exposure

Neurones ($2.5x10^6$ cells) were incubated in the absence (A) or presence (B) of 0.5 mM OHPA for 18 hours. Increased cell debris is observed in the wells containing neurones treated with OHPA. Neurones were viewed under 10X magnification.

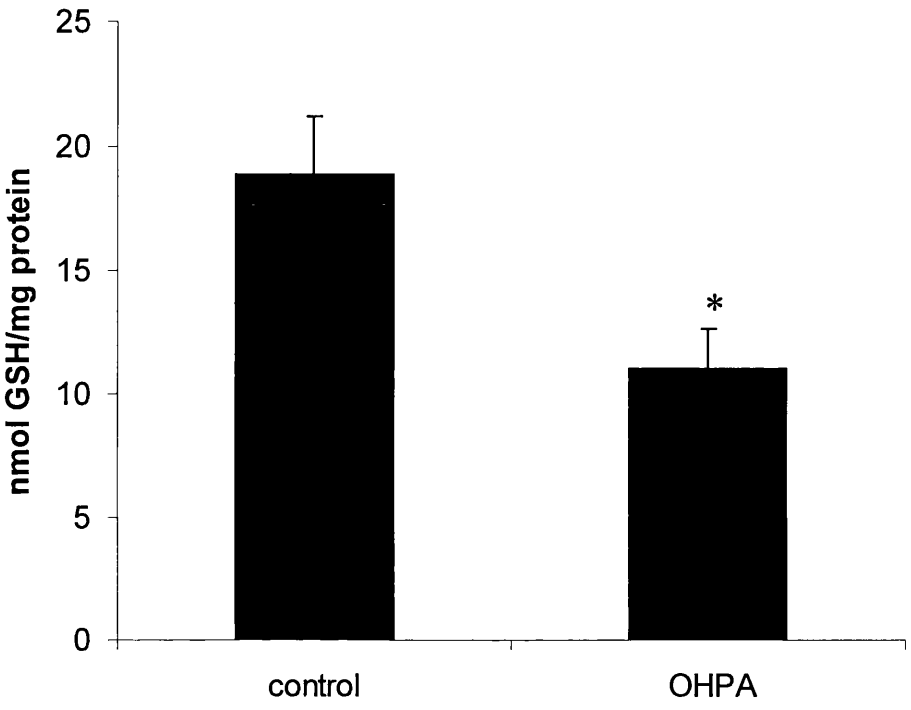

Figure 4.8. Cellular GSH levels in neurones treated with OHPA for 18 hours

Neurones were treated with 0.5 mM OHPA for 18 hours and cellular GSH levels determined in neuronal homogenates. GSH was significantly depleted in neurones treated with OHPA. Values are mean ± SEM (n=6 independent cell preparations). Statistical significance was determined by Student's t-test. * $p < 0.05$.

4.4.4.3. Neuronal ETC activity following 18 hours of OHPA exposure

The activities of the complexes of the ETC and CS were measured in neuronal homogenates following treatment with 0.5 mM OHPA for 18 hours. CS activity was decreased by 37% in neurones treated with OHPA for 18 hours. Furthermore, a 36%, 68%, and 33% loss of complex I, II+III, and IV activity respectively was also observed in neurones treated with OHPA for 18 hours when expressed against protein **(Table 4.3)**. When complex activity was expressed against CS activity rather than protein, the activities of complexes I and IV were unaffected by OHPA treatment, while, complex II+III activity was decreased by 38% (control, 0.29 ± 0.02; OHPA, 0.18 ± 0.03 (n=4-5 independent cell preparations) $p < 0.05$).

4.4.4.4 Mitochondrial and cytosolic GSH concentration in neurones following 4 hours of OHPA treatment

Neurones were treated with 0.5 mM OHPA for 1, 2, 3, and 4 hours. Depletion of GSH first occurred following treatment with 0.5 mM OHPA for 4 hours, with a significant 28% depletion observed in neuronal homogenates (**Table 4.4**).

When mitochondria were isolated from neurones treated with OHPA for 4 hours, a significant 52% depletion in mitochondrial GSH was observed (**Table 4.4**). The mean cytosolic GSH levels were also decreased by 31% in OHPA treated neurones, although not significantly.

4.4.4.5 Mitochondrial enzyme activity in neurones treated with OHPA for 4 hours

When the activities of the ETC complexes and CS were measured in neurones treated with 0.5 mM OHPA for 4 hours, a 41% loss of complex II+III activity, and a 25% loss of CS activity, was observed when expressed against protein (**Table 4.5**). No loss in complex I or IV activity was observed at this time point. When ETC complex activity was expressed against CS activity, complex II+III activity was inhibited by 23% (control, 0.27 ± 0.01, OHPA, 0.21 ± 0.03 (n=5 - 8 cell

Enzyme	Control	OHPA
I (nmol/min/mg protein)	17.4 ± 0.7	11.2 ± 1.9*
II+III (nmol/min/mg protein)	17.8 ± 1.0	5.7 ± 1.2**
IV (k/min/mg protein)	2.4 ± 0.3	1.6 ± 0.2*
CS (nmol/min/mg protein)	213.5 ± 14.0	135.2 ± 18.4*

Table 4.3. Mitochondrial enzyme activity in OHPA treated neurones

Neurones ($2.5x10^6$ cells/well) were treated with 0.5 mM OHPA for 18 hours and enzyme activity determined in neuronal homogenates. A significant loss of activity in complexes I, II+III, IV and CS was observed in OHPA treated neurones. Values are mean ± SEM (n=4-8 independent cell preparations). Statistical significance was determined by Student's t-test. * $p < 0.05$; ** $p < 0.01$.

Cellular Fraction	GSH Concentration (nmol GSH/mg protein)	
	Control	OHPA
Homogenate	14.5 ± 1.1	10.5 ± 1.2*
Mitochondria	3.3 ± 0.6	1.6 ± 0.4*
Cytosol	5.9 ± 1.0	4.1 ± 1.1

Table 4.4. Neuronal GSH levels following 4 hours of exposure to OHPA Mitochondria were isolated from neurones ($20x10^6$ cells) treated with 0.5 mM OHPA for 4 hours. GSH was significantly depleted in the mitochondria. Values are mean ± SEM (n=6-7 independent cell preparations). Statistical significance was determined by Student's t-test. * $p < 0.05$.

Enzyme	Control	OHPA
I (nmol/min/mg protein)	15.6 ± 0.8	13.5 ± 0.7
II+III (nmol/min/mg protein)	11.8 ± 0.7	7.0 ± 1.4*
IV (k/min/mg protein)	1.8 ± 0.2	2.1 ± 0.3
CS (nmol/min/mg protein)	167.4 ± 12.8	125.4 ± 7.9*

Table 4.5. Mitochondrial enzyme activity in neurones treated with OHPA for four hours

Neurones ($2.5x10^6$ cells/well) were treated with 0.5 mM OHPA for 4 hours and enzyme activity determined in neuronal homogenates. A significant loss in complex II+III and CS activity was observed. Values are mean ± SEM (n=7-10 independent cell preparations). Statistical significance was determined by Student's t-test. * $p < 0.05$.

preparations) $p < 0.05$). There was also no increase in LDH release from neurones treated with OHPA for 4 hours (control, 13.3 ± 4.4; OHPA, 18.7 ± 6.7 % LDH released (n=5 independent cell preparations)). No loss of complex II+III or CS activity was observed following 1, 2 or 3 hours of OHPA treatment.Note that the activities of the ETC complexes and CS appear to be greater in control neurones assayed at 18 hours (**Table 4.3**), compared to control neurones assayed at 4 hours (**Table 4.5**). In particular, both complex II+III and CS activities were significantly greater in control neurones at 18 hours, compared to 4 hours ($p< 0.05$). It is therefore important to always assay enzyme activity against time-matched controls.

4.4.5. The effect of OHPA on GCL activity in astrocytes and neurones

Since cytosolic GSH levels were approximately doubled in astrocytes treated with 0.5 mM OHPA for 18 hours (**Figure 4.5**), while neuronal GSH levels were depleted by 42% following the same treatment (**Figure 4.8**), the activity of GCL, the rate limiting enzyme in GSH synthesis (Anderson & Meister, 1983; Huang *et al.*, 1993a), was determined in these cells. Following exposure to 0.5 mM OHPA for 18 hours, GCL activity in astrocytes was increased by 30%, while GCL activity was unaffected in neurones (**Table 4.6**).

4.5. Discussion

The depletion of mitochondrial GSH in isolated liver mitochondria by OHPA in this study was comparable to that reported by Hashmi *et al* (1996), indicating that the OHPA synthesised had properties similar to those previously reported (Shan *et al.*, 1993; Hashmi *et al.*, 1996).

	GCL activity (nmol γ-GC synthesised/min/mg protein)	
	control	**OHPA**
astrocytes	**14.5 ± 0.8**	**18.9 ± 1.3***
neurones	**2.3 ± 0.6**	**2.5 ± 0.9**

Table 4.6. The effect of OHPA on GCL activity in astrocytes and neurones
Astrocytes and neurones were incubated with 0.5 mM OHPA for 18 hours, and GCL activity measured. GCL activity was significantly increased in astrocytes following OHPA treatment. Values are mean ± SEM (n=4-5 independent cell preparations). Statistical significance was determined using the Student's t-test

4.5.1. The differential effect of OHPA on GSH metabolism in astrocytes and neurones

The results in this chapter (summarised in **Table 4.7)** indicate that OHPA preferentially depletes mitochondrial GSH in neurones but not astrocytes. Indeed, rather than depleting GSH in the mitochondria, OHPA treatment approximately doubles cytosolic GSH in astrocytes. The preferential depletion of mitochondrial GSH in neurones occurs despite HBDH activity being similar in both astrocytes and neurones. The differing rate of GSH synthesis between astrocytes and neurones could explain this phenomenon. GCL activity in both control and OHPA treated neurones was estimated to be 2.5 nmol γ-GC synthesised/min/mg protein. Theoretically, as HBDH activity was observed to be 6.8 ± 1.5 nmol/min/mg protein in neurones, the rate of OHPA-mediated GSH depletion should be greater than the rate of *de novo* neuronal GSH synthesis, thus resulting in a net loss of GSH. Conversely, GCL activity in OHPA-treated astrocytes was estimated to be 8- fold higher than in neurones. Therefore, the rate of astrocytic GSH synthesis should be greater than the GSH depletion caused by OHPA treatment. GCL activity was estimated to be 6-fold higher in control astrocytes compared to control neurones. Previously, Makar *et al* (1994) reported that GCL activity was 8-fold lower in chick forebrain neurones compared to astrocytes.

As GCL is the rate-limiting enzyme in GSH synthesis, the estimated 30% increase in astrocytic GCL activity upon OHPA treatment probably contributes towards the 88% increase in cytosolic GSH concentration. Neurones were unable to increase GCL activity upon exposure to OHPA. Increased cellular GSH concentration has previously been observed in astrocytes and epithelial cells following exposure to reactive oxygen and nitrogen species (Iwata-Ichikawa *et al*, 1999; Moellering *et al.*, 1999; Buckley & Whorton, 2000). The induction of GCL transcription has been postulated to cause the increase in GSH concentration, with increased GCL mRNA levels reported in astrocytes exposed to hydrogen peroxide (Iwata-Ichikawa *et al*, 1999). Exposure of epithelial cells to 2,3-dimethoxy-1,4-naphthoquinone, a compound that generates superoxide and hydrogen peroxide, also increased the transcription of the regulatory subunit of GCL (Tian *et al.*,

Incubation time (hours)	Astrocytes			Neurones	
	0.5	4	18	4	18
GSH Concentration					
Homogenate	NC	NC	**↑41%**	**↓ 28%**	**↓ 42%**
Mitochondria	NC	-	NC	**↓ 52%**	-
Cytosol	NC	-	**↑ 88%**	NC	-
GCL Activity	-	-	**↑ 30%**	-	NC
LDH Release	-	-	NC	NC	**↑ 227%**
Mitochondrial Enzyme activity					
Complex I	NC	-	NC	NC	**↓36%**
Complex II+III	NC	NC	**↓ 21%**	**↓41%**	**↓68%**
Complex IV	NC	-	NC	NC	**↓33%**
CS	NC	NC	NC	**↓25%**	**↓37%**

Table 4.7. Summary of the effects of 0.5 mM OHPA on astrocytes and neurones

Values are % increase or decrease compared to time matched control. NC indicates no change; dash indicates that parameter was not measured.

1997), while nitric oxide was shown to increase transcription of both GCL genes in smooth muscle (Moellering *et al.*, 1998).

The mechanism by which GCL activity is increased by OHPA treatment is unknown. The inhibition of complex II+III by OHPA could increase the production of superoxide and hydrogen peroxide (Boveris & Chance, 1973; Paradies *et al.*, 1999; Han *et al.*, 2001). Unfortunately it is unclear whether inhibition of complex II+III activity precedes an increase in cellular GSH concentration, since both complex II+III and GSH concentration were unaffected at the two earlier time points assayed. Astrocytes could be incubated with antimycin A, an inhibitor of complex III (Paradies *et al.*, 1999), to see if GSH levels are increased. Alternatively, the increase in GCL activity may be due to a post-translational modification. Dephosphorylated purified rat kidney GCL has been reported to have greater enzyme activity than phosphorylated enzyme (Sun *et al.*, 1996).

4.5.2. OHPA and mitochondrial function

4.5.2.1. Complex II+III

Loss of complex II+III activity was observed in liver, astrocytes and neurones following OHPA treatment. In isolated liver mitochondria, loss of complex II+III was dose dependent, and was observed within 15 minutes of being incubated with OHPA, suggesting that inhibition is a result of either OHPA or 3-oxo-4-pentenoate directly interacting with the enzyme. Loss of complex II+III activity was shown not to be due to either OHPA or 3-oxo-4-pentenoate interfering with the assay. Despite HBDH activity being similar in astrocytes and neurones, loss of complex II+III activity was greater in neurones, compared to astrocytes. In astrocytes, a 21% loss in complex II+III activity was observed after 18 hours, while activity was unaffected after 4 or 8 hours of treatment. Complex II+III activity was inhibited by 41% in neurones treated with OHPA for 4 hours, with a 68% loss of activity observed after 18 hours. Loss of complex II+III was still observed when expressed against CS activity suggesting that the loss of activity

was not due to just a possible decrease in mitochondrial number (see below; section 4.5.2.2).

The greater susceptibility of neuronal complex II+III may in part be due to the depletion of mitochondrial GSH. However cellular GSH status cannot fully explain the differential effect of OHPA on complex II+III in astrocytes and neurones, as inhibition is still observed in astrocytes despite mitochondrial GSH being maintained, and cytosolic GSH concentration increased. It is not known whether the loss of activity is due to inhibition of either complex II and III, or both of them. Alternatively, co-enzyme Q_{10} may be affected by OHPA treatment, as the complex II+III assay requires endogenous Q_{10} (King, 1967). The complexes need to be assayed separately to see if either is affected by OHPA. Cellular levels of Q_{10} also need to be determined.

The inhibition of complex II+III by OHPA or 3-oxo-4-pentenoate in liver, astrocytes, and neurones limits its use for investigating the function of mitochondrial GSH. OHPA would be unsuitable for investigating the role of mitochondrial GSH in protecting the ETC, as it will be difficult to distinguish whether any effects that are observed are due to depletion of mitochondrial GSH, or the direct interaction of the drug with the ETC. However, the drug may be useful in liver and neurones for investigating GSH transport in to mitochondria.

4.5.2.2. Citrate synthase

Loss of CS was observed in neurones treated with OHPA for both 4 and 18 hours, while no loss in activity was observed in either astrocytes or liver. The 25% loss of CS activity after 4 hours is probably due to inhibition of the enzyme rather than a decrease in neuronal mitochondrial number, as the activities of both complexes I and IV were unaffected by OHPA treatment. Incubation of neuronal homogenates with OHPA during the CS assay had no effect on activity, indicating that loss in activity was not due to OHPA interfering with the assay. This is endorsed by the observation that neither liver nor astrocyte CS activity was affected by OHPA exposure. A 37% loss of CS activity was observed following OHPA treatment for 18 hours. It is difficult to ascertain whether this loss in activity is due to a decrease

in mitochondrial number, or inhibition of the enzyme, since complexes I to IV were all inhibited at this time point. Neuronal homogenates were assayed for monoamine oxidase, an enzyme located on the outer mitochondrial membrane (Ragan *et al.*, 1987), following OHPA treatment in order to determine whether a decrease in mitochondrial number occurs. However, enzyme activity could not be accurately determined due to the poor sensitivity of the assay. Monoamine oxidase activity in purified rat brain mitochondria has been reported to be 2.0 ± 0.2 nmol/min/mg protein (Heales *et al.*, 1995). Monoamine oxidase activity is likely to be considerably lower in neuronal homogenates, with detection of the oxidation of the substrate (benzylamine) below the sensitivity of the spectrophotometer. Unfortunately, other mitochondrial enzymes that could be measured, such as aconitase and α-ketoglutarate dehydrogenase, are also susceptible to oxidative stress (Gardner *et al.*, 1994; Chinopoulos *et al.*, 1999; Park *et al.*, 1999). Measurement of the amount of mitochondrial DNA present in OHPA treated neurones may be a method to determine if mitochondria are indeed lost following OHPA treatment.

4.5.2.3. Complex I

A 36% loss of complex I activity was observed in neurones treated with OHPA for 18 hours. The 36% loss of complex I activity was concomitant with a 42% depletion in cellular GSH concentration. The depletion of GSH could result in complex I becoming more susceptible to the effects of OHPA treatment. However, if OHPA treatment does result in loss of mitochondrial number (see above; 4.5.2.2), no inhibition of complex I was observed when expressed against CS activity, suggesting that the loss of activity maybe due to loss of mitochondria. No loss of complex I activity was observed in liver mitochondria depleted of GSH by OHPA. This could support the hypothesis that loss of complex I activity in neurones is due to a reduction in the number of mitochondria. Alternatively, complex I may have been unaffected in liver mitochondria because of the short incubation period (15 minutes).

4.5.2.4. Complex IV

Treatment of neurones with 0.5 mM OHPA for 18 hours resulted in a 37% loss of enzyme activity, while liver incubated with 1 mM OHPA for 15 minutes resulted in a 40% loss of activity. The depletion of mitochondrial GSH may leave complex IV more susceptible to inhibition by free radicals generated by mitochondria (Wullner *et al.*, 1999; Paradies *et al.*, 1999), or the direct action of OHPA or 3-oxo-4-pentenoate.

In the original paper that reported the depletion of isolated liver mitochondrial GSH by OHPA, Shan *et al* (1993) showed that 0.75 mM OHPA resulted in a 30% decrease in mitochondrial oxygen consumption. However they did not indicate whether this was significant or not. The inhibition of complexes II+III and IV shown here could be contributing towards the possible decrease in oxygen consumption.

4.6. Conclusion

Mitochondrial GSH is preferentially depleted by OHPA in neurones compared to astrocytes. This is possibly due to the observation that, unlike astrocytes, the rate of *de novo* neuronal GSH synthesis is less than the rate of OHPA-mediated GSH depletion. Cytosolic GSH levels were actually doubled in astrocytes upon exposure to OHPA. This elevation in cytosolic GSH was probably due to the 30% increase in GCL activity, the rate-limiting enzyme in GSH synthesis. Neurones, unlike astrocytes, were unable to increase GCL activity, upon exposure to OHPA. This observation may be one of the reasons why neurones, compared to astrocytes, are more susceptible to insults such as reactive nitrogen and oxygen species (Bolanos *et al.*, 1995; Iwata-Ichikawa *et al.*, 1999; Almeida *et al.*, 2001).

In future, OHPA has to be used carefully when investigating the mitochondrial GSH pool. The OHPA-mediated inhibition of complex II+III in neurones, astrocytes, and liver, means that it cannot be used to investigate the protection of mitochondrial respiratory chain by mitochondrial GSH. In neurones, the activities of complexes I and IV of the ETC, and CS, were affected following OHPA

treatment. Thus, it is difficult to ascertain whether these affects are due to the depletion of mitochondrial GSH, or the direct effect of OHPA, or one of its metabolites.

Chapter 5

The differential effect of nitric oxide on GSH metabolism in astrocytes and neurones

5.1. Introduction

The thiol group of glutathione (GSH) can readily react with reactive nitrogen species (RNS). While nitric oxide (NO) reacts slowly with GSH (Gaston, 1999), the oxidation and reduction products of NO (*e.g.,* NO^+, NO^-, and $ONOO^-$ (peroxynitrite)) readily react with GSH via several pathways (Singh *et al.*, 1996; Quijano *et al.*, 1997; Hughes, 1999). The intracellular concentration of GSH has been implicated in dictating cellular susceptibility to RNS (Bolanos *et al.*, 1995,1996; Barker *et al.*, 1996). Inhibition of succinate cytochrome c reductase (complex II+III) and cytochrome c oxidase (complex IV) following RNS exposure was suggested to be less in neurones cocultured with astrocytes, which contain twice the amount of GSH, compared to neurones cultured alone (Bolanos *et al.*, 1996). Furthermore, loss of complex I activity in astrocytes exposed to $ONOO^-$ only occurred when cellular GSH had previously been depleted by 95% (Barker *et al.*, 1996).

In Parkinson's disease (PD), a 40% loss of complex I activity, a 40% depletion in GSH, and evidence of increased NO production, has been reported in the substantia nigra of PD brains at post-mortem (Riederer *et al.*, 1989; Schapira *et al.*, 1990; Sian *et al.*, 1994a; Hunot *et al.*, 1996). The mechanism by which GSH is depleted in PD is unknown. The activity of γ-glutamyltranspeptidase (γ-GT), an ectoenzyme that cleaves GSH (Meister & Anderson, 1983; Ikeda *et al.*, 1995), is reported to be increased in PD brains (Sian *et al.*, 1994b). However, other enzymes involved in GSH metabolism, such as glutamate-cysteine ligase (GCL), the rate limiting enzyme in GSH synthesis (Meister & Anderson, 1983; Huang *et al.*, 1993a), GSH peroxidase, and GSH transferase have been reported to be unaffected in PD brains (Sian *et al.*, 1994b). A similar loss of GSH has been reported at post-mortem in incidental Lewy body disease brains (thought to be presymptomatic Parkinson's disease; Dexter *et al.*, 1994). The depletion of GSH precedes the loss of complex I activity, and the accumulation of iron (Dexter *et al.*, 1994), suggesting that GSH loss is an early event in PD. Increased NADPH diaphorase activity, a putative marker for NO synthase, is observed in glial cells in post-mortem PD brains (Hunot *et al.*, 1996). Furthermore, the 1-methyl-4-phenyl-1,2,3,6-tetrahydropyridine (MPTP) model of PD in mice is associated with a

significant upregulation of inducible NO synthase in the substantia nigra (Liberatore *et al.,* 1999). In addition, mice lacking inducible NO synthase were more resistant to MPTP associated dopaminergic neurodegeneration (Liberatore *et al.*, 1999).

The loss of complex I activity and GSH depletion in PD cannot only be occurring in dopaminergic neurones, since they have been estimated to account for only 2% of the total cells present in the substantia nigra (Jenner & Olanow, 1998). Therefore, since activated glia are reported in PD, this chapter has investigated the effect of NO on GSH metabolism in both astrocytes and neurones. The consequences of this on ETC function and cell viability have also been investigated.

The nitric oxide donor (Z)-1-[2-(2-aminoethyl)-N-(2-ammonioethyl)amino] diazen-1-ium-1,2-diolate (DETA-NO) was used to investigate the effects of nitric oxide on GSH metabolism. DETA-NO, when resuspended in aqueous solution, releases NO at a constant rate (**reaction 5.1**) with a half-life of at least 24 hours (Keefer *et al.*, 1996).

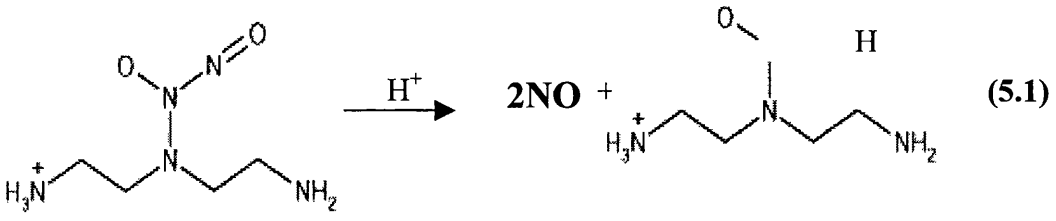

(5.1)

5.2. Methods

5.2.1. Cell culture

Primary astrocytes and neurones were cultured as described in section 2.2 and treated with 0.5 mM DETA-NO (in astrocyte or neurone medium (section 2.2.1)) on day 14 and day 6 in culture respectively for the period indicated.

5.2.2. GSH Quantitation

Cellular GSH levels in cultured astrocyte and neurone homogenates were analysed by reverse-phase HPLC as described in section 2.6.

5.2.3. Measurement of GSH release from astrocytes

GSH efflux from astrocytes was measured as previously described (Dringen *et al.*, 1997; Stone *et al.*, 1999). Astrocytes ($1x10^6$ cells/well) were treated with 0.5 mM DETA-NO for 24 hours, the media removed, and the cells washed twice in Hank's balanced salt solution (HBSS). Cells were than incubated in 1 ml of minimal medium (44 mM $NaHCO_3$, 110 mM NaCl, 1.8 mM $CaCl_2$, 5.4 mM $MgSO_4$, 0.92 mM NaH_2PO_4, 5 mM glucose, adjusted with CO_2 to pH 7.4 as described by Dringen *et al* (1997)) for the period indicated. One volume of minimal medium was then mixed with one volume of 15 mM orthophosphoric acid, and the GSH concentration in the minimal medium determined by reverse-phase HPLC as described in section 2.6.

5.2.4. Determination of GCL activity

GCL activity was measured in NO-treated astrocyte and neurone homogenates as described in section 3.2.

5.2.5. Spectrophotometric enzyme assays

Complexes I, II+III and IV of the ETC, and citrate synthase (CS) were assayed in cultured astrocyte and neurone homogenates as described in sections 2.4.1. – 2.4.4.

γ-GT was assayed in astrocytes (scraped into HBSS) as described in section 2.4.7.

Lactate dehydrogenase release from cultured astrocytes and neurones was measured as described in section 2.4.6.

5.2.6. Protein determination

Sample protein concentration was determined using the Lowry method as described in section 2.5.

5.2.7. Measurement of NO generated by DETA-NO

The steady state concentration of NO generated by 0.5 mM DETA-NO in astrocyte and neurone media at 37 °C was measured using an ISO NO electrode (WPI, Florida, USA; Brown et al., 1995). The NO electrode was calibrated by the addition of anaerobic NO saturated water (contains 2 mM NO at 20 °C; Brown et al., 1995).

5.2.8. Measurement of oxygen consumption in astrocytes

Oxygen consumption in astrocytes was measured in astrocytes as previously described by Brown *et al* (1995). Astrocytes (~$4x10^6$ cells) were removed from the flasks with trypsin (section 2.2.2.1) and resuspended in 1 ml respiration buffer (134 mM NaCl, 20 mM glucose, 20 mM HEPES, 5.3 mM KCL, 4.1 mM $NaHCO_3$, 2 mM $CaCl_2$, 0.4 mM KH_2PO_4, 0.3 mM Na_2HPO_4, pH 7.4). 250 µl of cells were then placed in a Clark-type oxygen electrode chamber (Yellow Springs Instrument Company, Ohio, USA). The chamber was maintained at 37 °C and contained a magnetic stirrer moving at 80 rpm. Oxygen consumption was measured for at least 5 minutes, and was measured on a chart recorder (Kompensograph X-T C1011, Siemens, Bracknell, UK). The oxygen electrode was calibrated against air saturated respiration buffer (100%) and respiration buffer containing sodium dithionate (0% oxygen).

5.2.9. RNA extraction

Astrocytes (~ $4x10^6$ cells) were treated with 0.5 mM DETA-NO on day 14 in culture for the period indicated, and removed from the flask with trypsin (section 2.2.2.1). Total cellular RNA was then extracted from astrocytes using the method described by Chomczynski & Sacchi (1987). Astrocytes were mixed with 600µl guanidinium reagent (4M guanidinium thiocyanate, 25 mM sodium citrate; pH 7.0, 0.5% (vol/vol) sarcosyl, 0.1 mM 2-mercaptoethanol), and the suspension mixed with 60 µl 2M sodium acetate (pH 4), 660 µl phenol (equilibriated with one volume 0.5 M Tris, pH 8) and 132 µl chloroform:isoamyl alcohol mixture (49:1 vol/vol). Following vigorous shaking for 1 minute, and incubation on ice for 15 minutes, the sample was centrifuged at 10000 x g for 45 minutes at 4 °C. The upper aqueous phase (~ 500 µl) containing the RNA was placed in a fresh tube and mixed with 1 ml isopropanol, and incubated at –20 °C for 30 minutes to precipitate the RNA. RNA was pelleted by centrifugation at 10000 x g for 15 minutes. The pellet was then resuspended in 180 µl water (containing 0.1% (vol/vol) diethylpyrocarbonate (DEPC)) and 20 µl 2M sodium acetate (pH 4). One volume of isopropanol was then added, mixed well, and RNA precipitated at – 20 °C for 30 minutes. RNA was pelleted by centrifugation at 10000 x g for 20 minutes. The pellet was then washed twice (centrifugation at 10000 x g for 5 minutes) with 500 µl 70% ethanol. Finally, the RNA pellet was dried in a vacuum pump for 10 minutes, and the RNA resuspended in 20 µl DEPC-water.

The quality and concentration of the isolated RNA was determined by spectrophotometry. In a quartz cuvette, 2 µl of RNA was mixed with 498 µl DEPC-water, and the absorbance measured at 260 and 280 nm. A 260/280 ratio of greater than 1.6 was considered to be good quality RNA. The extinction coefficient of RNA at 260 nm is approximately $10x10^3$ $M^{-1}cm^{-1}$.

2 µg of RNA was also mixed with RNA loading buffer (0.003% vol/vol bromophenol blue, 9 mM EDTA, 177 mM formaldehyde, 4% vol/vol glycerol, 6.2% vol/vol formamide, 1.25X MOPS (25 mM 3-[N-morpholino]propanesulfonic acid, 6.2 mM sodium acetate, 1 mM EDTA,

0.05mg/ml ethidium bromide; pH 7.0) and separated on a 0.8% (wt/vol) agarose gel (made in 1X TAE buffer (40 mM Tris, 1mM EDTA, 0.001% vol/vol glacial acetic acid; pH 8)) at 80 volts (running buffer: 1X TAE buffer) to check that the RNA was not digested (**Figure 5.1**).

5.2.10. Northern Blot

5.2.10.1. Electrophoresis

Extracted RNA (20 μg) was mixed with 1X MOPS, 50% (vol/vol) formamide, 15% (vol/vol) formaldehyde, and 1X RNA loading buffer, and heated at 65°C for 10 minutes to denature the RNA. The samples were then placed on ice for 5 minutes and then loaded onto a 1% (wt/vol) agarose gel (made in 1X MOPS, 6% formaldehyde; 24 x 20 cm). RNA was separated at 40V (running buffer: 1X MOPS) for 5½ hours (note that the gel was protected from light at all times).

5.2.10.2. RNA transference

The apparatus used to transfer RNA from the gel to the membrane is shown in **Figure 5.2**. The 3MM Whatman paper (Maidstone, UK) salt bridge (soaked in 10X SSC (1.5 M NaCl, 0.54 M sodium citrate)) was placed on an inverted electrophoresis tray and any air bubbles removed. Two pieces of 3MM Whatman paper, cut to the same size as the gel and soaked in 10X SSC, were placed on top of the salt bridge. The gel was then placed upside down (*i.e.,* bottom of wells facing up) on these two pieces of 3MM Whatman paper. The RNA membrane (GeneScreen Plus, NEN Life Science, Boston, USA) was cut to the size of the gel and soaked in 10X SSC, and placed on top of the gel (air bubbles were removed by rolling a pipette over the membrane). Two more pieces of 3MM Whatman paper cut to the same size as the gel, and soaked in 10X SSC, were then placed on top of the membrane. The apparatus was then placed in a tray containing 200 ml 10X SSC. Finally, paper towels (~ 10cm in height) and a weight (~ 1 kg) were placed on top of the stack containing the gel and membrane. RNA was allowed to transfer from the gel to the membrane for approximately 16 hours.

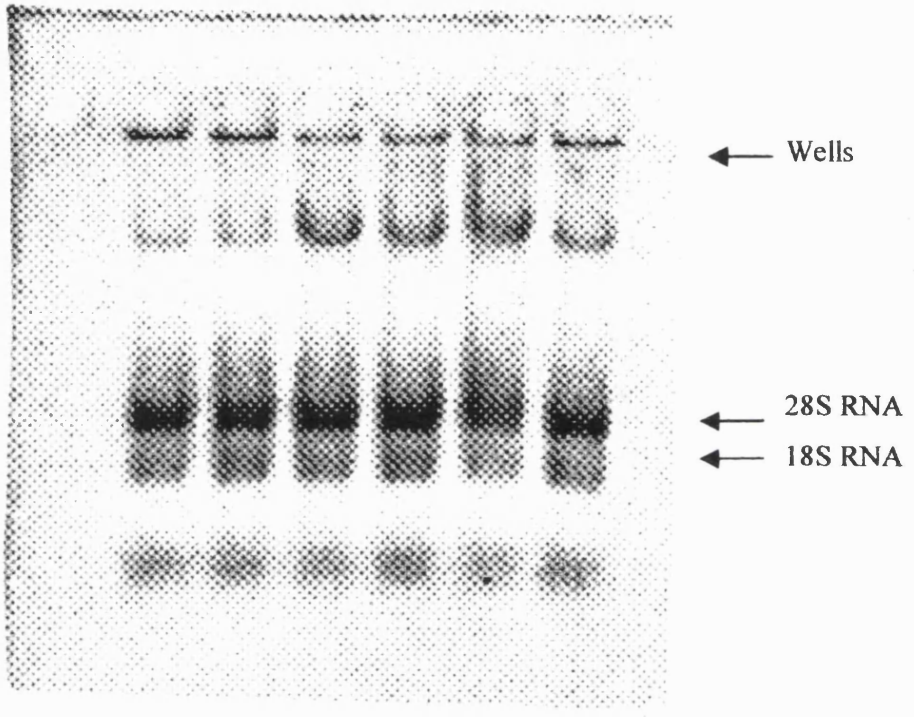

Figure 5.1. Electrophoresis of isolated astrocyte RNA

RNA was extracted from astrocytes, and separated on a 0.8% (wt/vol) agarose gel to check that the RNA was not digested. Both the 18S and 28S ribosomal RNA is intact, indicating that the RNA is not digested.

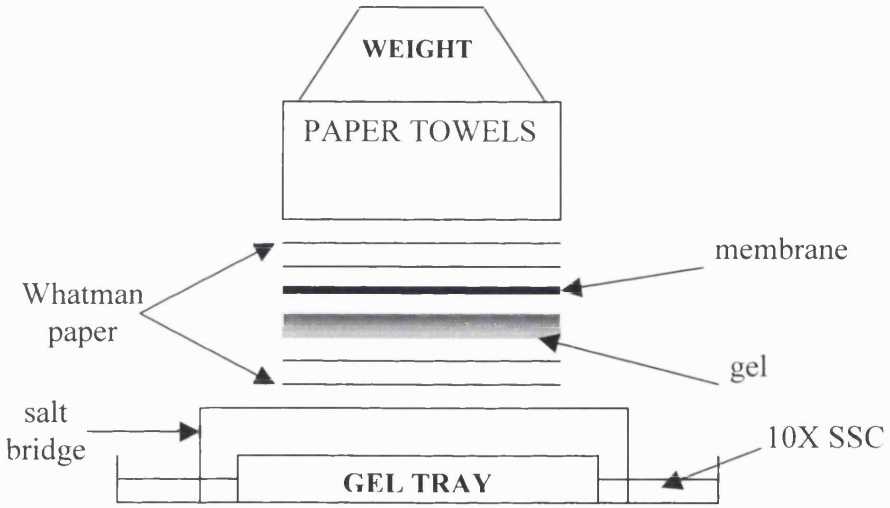

Figure 5.2. Northern blot apparatus

Following transference, all the paper was removed, and the membrane (RNA side face up) washed in 2X SSC (0.3 M NaCl, 0.11 M sodium citrate). The RNA was then fixed to the membrane by Ultraviolet light (approximately 20 seconds).

5.2.10.3. Labelling of GCL and cyclophilin probes

The rat cDNA fragments of both the catalytic and regulatory subunits of GCL (GCL_h and GCL_l respectively) were prepared by Dr. Juan Bolanos (Universidad de Salamanca, Spain). The 1.1 kb GCL_h and 0.9 kb GCL_l cDNA fragments were derived from their mRNA sequences (EMBL accession numbers J05181 and S65555, respectively) by RT-PCR from 1 μg of rat brain total RNA with the following sense and antisense primers respectively: 5'-CCG GAA TTC GCC ATG GGG CTG CTG-3' (5' position 24) and 5'-TGC CAG AAG GTG ATC GAT GCC TT-3' (3' position 1117) for GCL_h; and 5'-CGC GGA TCC CCT CGG GCG GCA GCT-3' (5' position 24) and 5'-CGC GGA TCC TAA ATA CAA GGC CCC TGA G-3' (3' position 905) for GCL_l. These fragments were subcloned into bluescript pKS vector plasmids. The 0.7 kb cDNA fragment of the rat cyclophilin gene was generously donated by Dr. Dionisio Martín-Zanca (Universidad de Salamanca, Spain). The northern blot was probed with cyclophilin to control for the amount of total RNA loaded in each lane.

Approximately 25 ng of the cDNA fragments were labeled using a Boëhringer-Mannheim random-primed labeling kit. DNA (10 μl) was mixed with 2 μl of [α-^{32}P]dCTP (20 μCi; 3,000 Ci/mmol), 3 μl of a mixture of dATP, dGTP and dTTP (0.5 mM each), 2 μl of hexanucleotide mix, and 1 μl (2 units) of Klenow enzyme (DNA polymerase I) for 30 min at 37 °C. The ^{32}P-labeled cDNA was then mixed with 60 μl TE buffer (10 mM Tris, 0.1 mM EDTA, pH 8), and the probe mixture spun through a sepharose column (1 ml, equilibrated with 1 ml TE; Sigma Chemicals) at 5000 rpm for 1 minute.

5.2.10.4. Hybridisation of GCL probes

The RNA membrane was soaked in 2X SSC for 10 minutes, and then transferred to a hybridisation tube containing 10 ml of prehybridisation solution (1% (vol/vol) SDS, 1M NaCl, 10% (vol/vol) Dextran sulphate), and incubated at 60°C for 10 minutes. The labelled GCL_l probe was then added to the hybridisation tube, and the membrane incubated for a further 18 hours at 60°C. Following hybridisation, the membrane was washed once with 2X SCC plus 0.1% (vol/vol) SDS for 5 minutes at 60°C, twice with 2X SCC plus 0.1% (vol/vol) SDS for 30 minutes at 60°C, and once with 0.1X SCC (0.15 M NaCl, 0.05 M sodium citrate) for 60 minutes at room temperature. The membrane was then exposed to Kodak XAR-5 film for 2-3 days at -70 °C. Autoradiograms were scanned, and the density of the GCL_h , GCL_l , and cyclophilin mRNA bands were quantified using image-analyzer software (NIH Image, National Institutes of Health, Bethesda, MD, U.S.A.). The density of the $GCL_{h\ or\ l}$ mRNA bands were expressed as a ratio against cyclophilin mRNA band density. The $GCL_{h\ or\ l}$/cyclophilin mRNA ratio at 0 h was arbitrarily given a value of 1, and the $GCL_{h\ or\ l}$/cyclophilin mRNA ratios at 9 and 24 hours compared to this.

5.3. Experimental protocols

The effect of DETA-NO on GSH metabolism and ETC

Astrocytes and neurones were treated with 0.5 mM DETA-NO for 6 to 24 hours, and the effect of NO-treatment on cellular GSH levels and GCL activity was determined. GCL mRNA levels, GSH efflux, and the activity of γ-GT was also assayed in astrocytes exposed to NO. The activities of the complexes of the ETC were also assayed in both astrocytes and neurones following exposure to DETA-NO.

5.4. Results

5.4.1. Determination of NO concentration generated by DETA-NO

DETA-NO (0.5 mM) in either astrocyte or neuronal medium generated a steady state NO concentration of 0.93 ± 0.07 μM (n=3) at 37°C. This NO concentration was observed within 30 minutes of DETA-NO being prepared in cell culture media, and was constant for at least 24 hours.

5.4.2. The effect of DETA-NO on cellular GSH levels

Cellular GSH levels were determined in astrocytes exposed to 0.5 mM DETA-NO for 6, 9, 18, and 24 hours (**Figure 5.3**). GSH levels were approximately doubled in astrocytes treated with DETA-NO for 18 and 24 hours. Astrocytes treated with 0.5 mM decomposed DETA-NO (left to decompose until NO release was undetectable) had no effect on GSH levels suggesting the effect was due to NO exposure rather than the donor molecule. Note that GSH levels in control astrocytes 9 hours after incubation with fresh media were significantly higher than the GSH levels prior to the change of media (con 0; **Figure 5.3**). Exposure of astrocytes to DETA-NO for 24 hours had no significant effect on viability (control, 5.0 ± 1.2; NO-treated, 6.5 ± 1.1 % LDH released into media (n=5)).

In order to ascertain whether brief exposure to NO is sufficient to elevate GSH levels, astrocytes were also treated with 0.5 mM DETA-NO for either 1 or 4 hours, the cells washed twice with HBSS, and then incubated for a further 23 or 21 hours in astrocyte media respectively, to see if GSH levels were still elevated after 24 hours. No increase in cellular GSH levels was observed for either treatment (control 24hr; 18.9 ± 2.1; NO 1hr + 23hr, 17.2 ± 2.4; NO 4hr + 20hr, 18.7 ± 0.9 (n=3 independent cell preparations)). This suggests that for GSH levels to be elevated in astrocytes, a prolonged exposure to NO (*i.e.*, greater than 4 hours) is necessary.

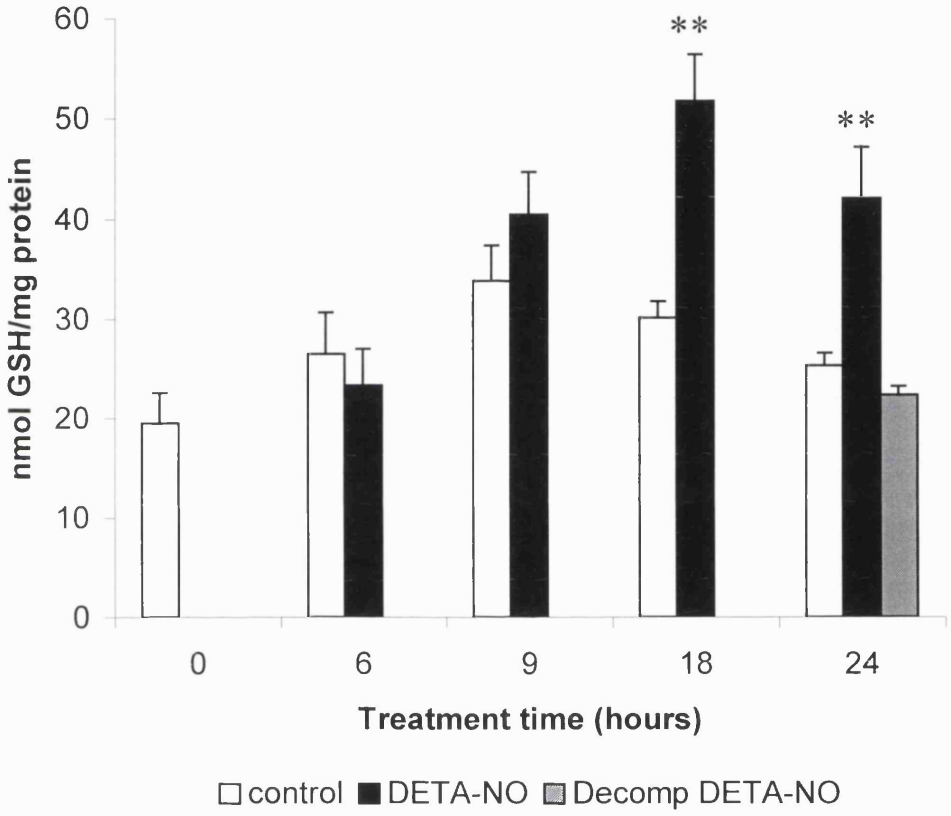

Figure 5.3. Cellular GSH levels in astrocytes treated with DETA-NO

Astrocytes were treated with 0.5mM DETA-NO for 6 to 24 hours, and cellular GSH levels determined. GSH levels were significantly elevated in astrocytes treated with DETA-NO for 18 and 24 hours. Values are mean ± SEM (n=4–9 independent cell preparations). Data were statistically evaluated by the Student's t-test. ** $p < 0.01$ compared with time matched controls.

Treatment of neurones with 0.5 mM DETA-NO for 24 hours resulted in extensive neuronal death (**Figure 5.4.**). This was not apparent (determined by measuring %LDH released by cells) following 9 hours of exposure to NO (control, 5.0 ± 2.4; NO-treated, 7.5 ± 2.3% (n=4)). However after 18 hours, a significant increase in LDH release was observed (control, 4.9 ± 1.7; NO-treated, 12.2 ± 2.3% (n=4). $p < 0.05$). GSH concentrations in neurones were unaltered after 6 and 9 hours of exposure to NO, but were decreased by 45% in surviving cells following 18 hours of exposure (**Figure 5.5**). Neurones were also exposed to 0.25 mM, 0.1 mM, and 0.05 mM DETA-NO for 18 hours to determine whether neurones increased GSH levels when exposed to lower NO concentrations (*e.g.,* 0.05 mM DETA-NO generated a steady state NO concentration of ~100 nM). LDH release and GSH levels were unchanged in neurones treated with these lower concentrations of DETA-NO. Neuronal media, unlike astrocyte media, contains 25 mM KCl. However, GSH levels were still significantly elevated in astrocytes exposed to 0.5 mM DETA-NO when grown in neuronal media (control, 20.0 ± 0.2; NO-treated, 31.5 ± 0.8 nmol GSH/mg protein, $p < 0.05$), suggesting that the presence of KCl in the media does not prevent elevation of GSH levels.

Cysteine has been reported to be the rate-limiting substrate for GSH synthesis (Kranich *et al.*, 1996; Dringen *et al.*, 1999a). Therefore, perhaps the amount of cysteine in neuronal media is limiting (*e.g.,* due to autooxidation of cysteine in neuronal media), and thus may cause the depletion of GSH levels upon exposure to NO. Neurones were therefore incubated in the absence or presence of 0.5 mM DETA-NO for 16 hours. The neuronal media of both control and NO-exposed neurones was then supplemented with 350 μM cysteine, a concentration that has previously been shown to be non-toxic to neurones and to elevate GSH levels within 1 hour in cysteine-starved neurones (Kranich *et al.*, 1996; Dringen *et al.*, 1999), and the neurones incubated for a further 2 hours. GSH levels in neurones exposed to NO were still significantly depleted, compared to control neurones (control + cysteine, 11.5 ± 0.6; NO-treated, 8.2 ± 0.6 nmol GSH/mg protein, $p < 0.01$). This may suggest that the cysteine concentration in neuronal media was not limiting GSH levels in neurones.

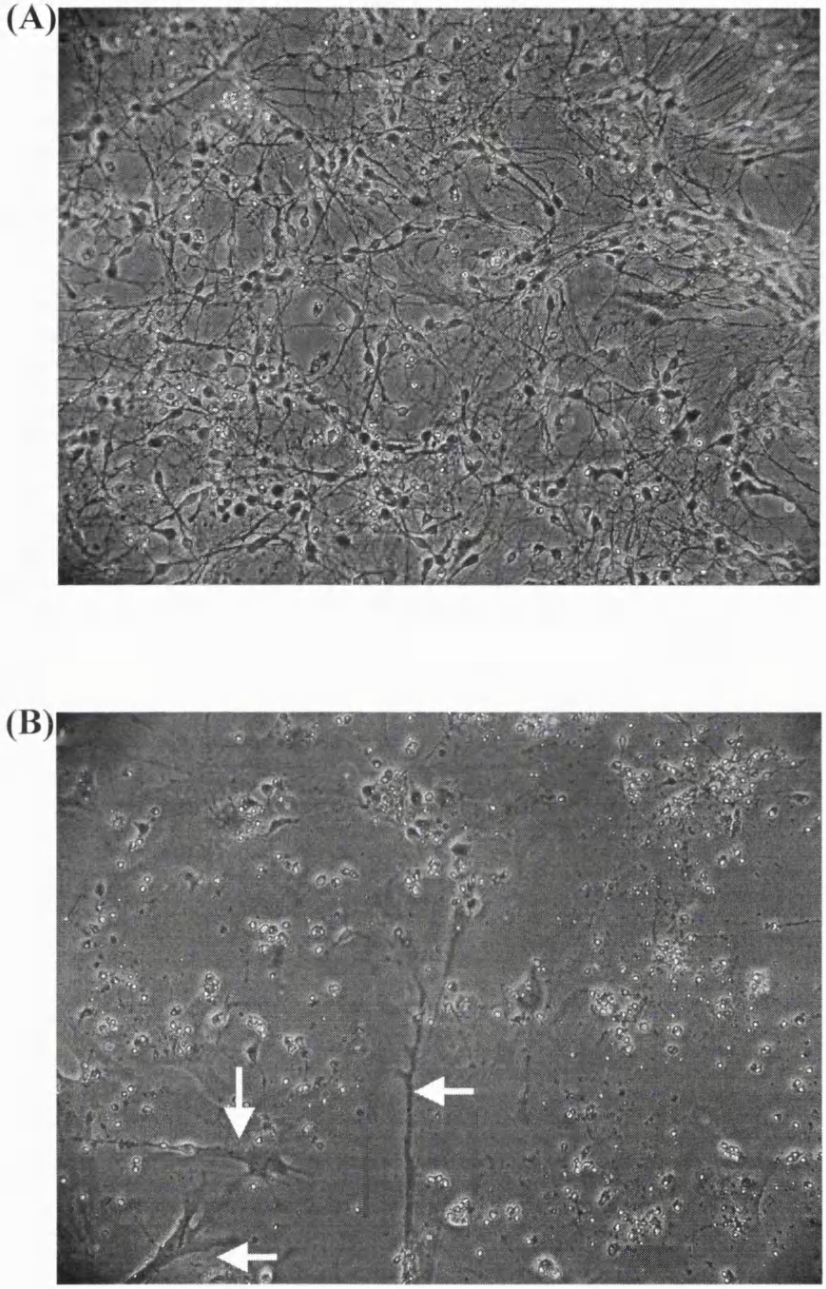

Figure 5.4. Neurones treated with 0.5 mM DETA-NO for 24 hours

Neurones treated in the absence (A) or presence (B) of 0.5 mM DETA-NO. Extensive neuronal death was observed in NO-treated neurones. Arrows point to surviving astrocytes. Neurones were viewed at 10X magnification.

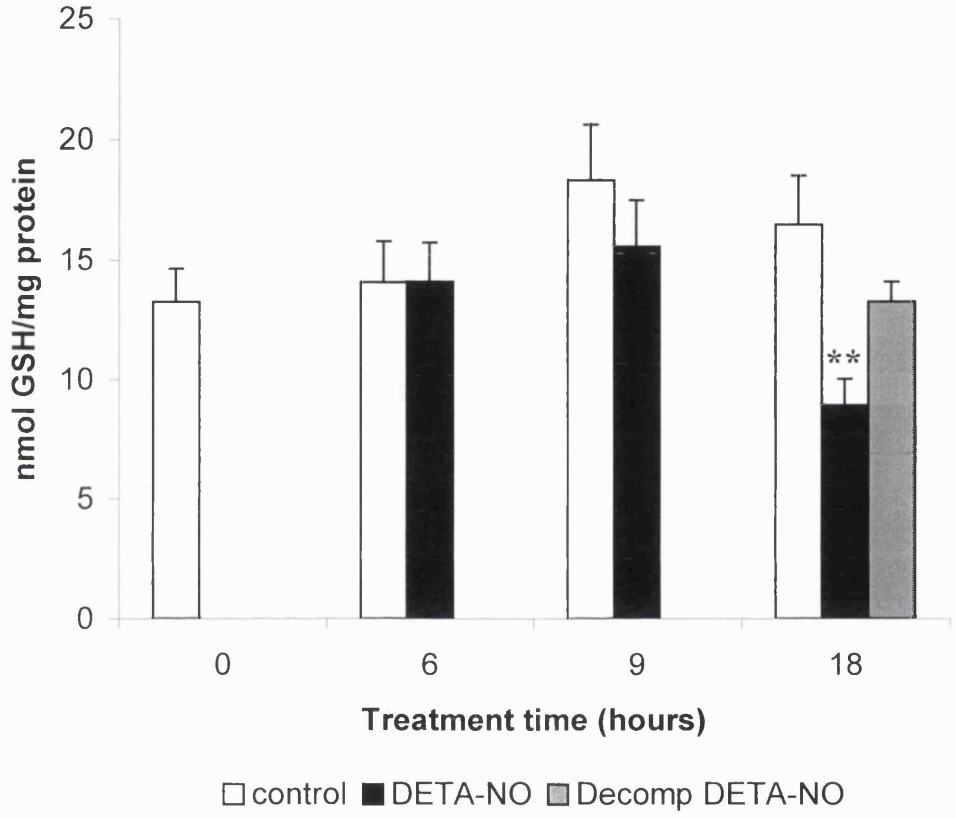

Figure 5.5. The effect of DETA-NO on GSH levels in neurones

Neurones were treated with 0.5mM DETA-NO for 6 to 18 hours, and cellular GSH levels determined. GSH levels were significantly depleted in neurones treated with DETA-NO for 18 hours. Values are mean ± SEM (n=4–9 independent cell preparations). Data were statistically evaluated by the Student's t-test. ** $p < 0.01$ compared with time matched controls.

5.4.3. GCL activity in astrocytes and neurones following exposure to DETA-NO

The activity of GCL, the rate limiting enzyme in GSH synthesis, was assayed in astrocytes and neurones exposed to DETA-NO, to determine whether an alteration in the rate of GSH synthesis may account for the elevation and depletion of GSH in astrocytes and neurones respectively. GCL activity was significantly increased in astrocytes exposed to DETA-NO for 9, 18, and 24 hours (**Figure 5.6A**). No change in GCL activity was observed in neurones treated with DETA-NO at any time point (**Figure 5.6B**). Furthermore, neuronal GCL activity was unchanged following incubation with 0.05, 0.1, 0.25 mM DETA-NO for 18 hours.

The increase in cellular GSH levels observed in control astrocytes 9 hours after change of media (see above) was concomitant with a significant increase in GCL activity in control astrocytes 9 hours after change of media ($p < 0.01$ compared to con 0). GCL activity in neurones was also higher in neurones 9 hours after change of media, although this was not significant.

5.4.4. Northern blot of astrocytes exposed to DETA-NO

RNA was isolated from astrocytes treated with DETA-NO to determine whether the increase in GCL activity observed could be due to increased expression of one, or both, GCL genes. The northern blot shows that the amount of mRNA coding for both GCL_h and GCL_l was increased in astrocytes exposed to DETA-NO (**Figure 5.7**). GCL_h mRNA levels were increased 1.6-fold following exposure to

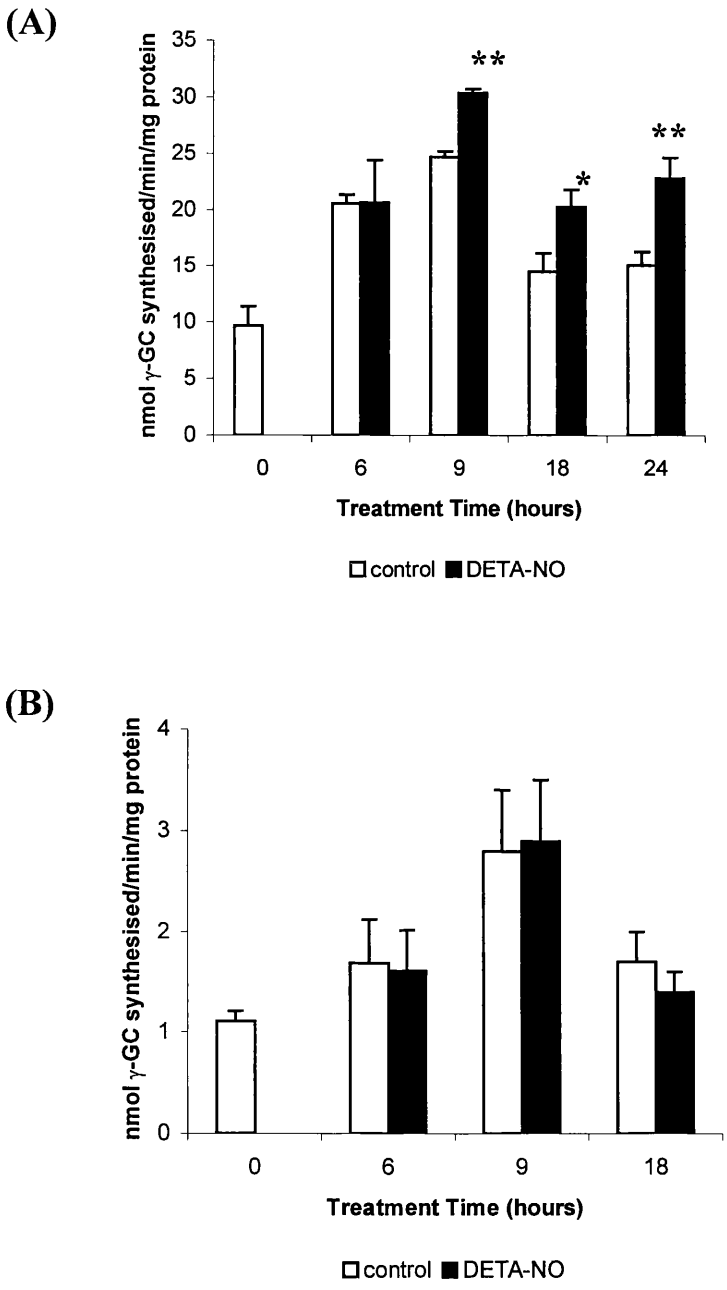

Figure 5.6. The effect of DETA-NO exposure on GCL activity in astrocytes and neurones

Astrocytes (A) and neurones (B) were treated with 0.5 mM DETA-NO for the period indicated, and GCL activity assayed. GCL activity was significantly elevated in astrocytes exposed to DETA-NO for 9, 18 and 24 hours. Values are mean ± SEM (n=4-7 independent cell preparations). Statistical significance was determined by the Student's t-test. * $p < 0.05$, ** $p < 0.01$ compared with time matched controls.

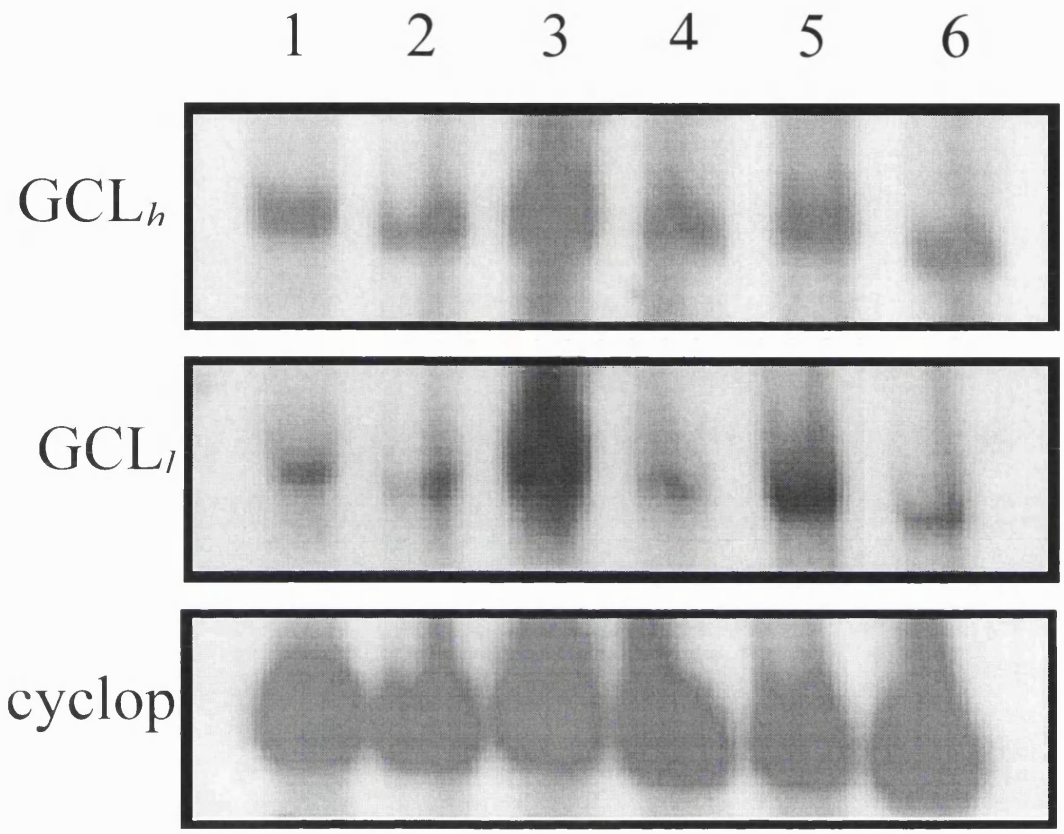

Figure 5.7. Northern blot of GCL_h and GCL_l mRNA in astrocytes exposed to DETA-NO

Total RNA was extracted from astrocytes (1) prior to change of media (0 hours); (2) control astrocytes, 9 hours; (3) astrocytes exposed to 0.5 mM DETA-NO for 9 hours; (4) control astrocytes, 24 hours; (5) astrocytes exposed to 0.5 mM DETA-NO for 24 hours; (6) astrocytes exposed to 0.5 mM decomposed DETA-NO for 24 hours. GCL_h mRNA levels were elevated following 9 hours of exposure to DETA-NO, while GCL_l mRNA levels were increased following 9 and 24 hours of DETA-NO exposure. Cyclophilin (cyclop) was probed to determine the relative amount of RNA loaded into every well.

DETA-NO for 9 hours, but returned to control levels following 24 hours of DETA-NO exposure **(Table 5.1)**. GCL_l mRNA levels were increased 2-fold following exposure to DETA-NO for both 9 and 24 hours. Exposure to decomposed DETA-NO had no effect on mRNA levels, and cyclophilin mRNA levels were similar in all samples.

5.4.5. The effect of cyanide on cellular GSH levels

NO is a competitive inhibitor of complex IV (Wainio, 1955), with 0.5 mM DETA-NO estimated to inhibit astrocyte oxygen consumption by 93-100% (Personal communication from Dr Jake Jacobson, Department of Molecular Pathogenesis, Division of Neurochemistry, Institute of Neurology, UCL, London, UK). Therefore, astrocytes were treated with cyanide (KCN), another inhibitor of complex IV (Scheffler, 1999), to see if this also elevated GSH levels. Treatment with 1 mM KCN almost completely abolished oxygen consumption in the astrocytes (control, 47.1 nmol O/min/mg protein; 1 mM KCN, 1.08 nmol O/min/mg protein). However, following 24-hour exposure, no increase in cellular GSH levels was observed (control, 25.7 ± 3.4; KCN, 26.2 ± 2.3 nmol GSH/mg protein (n=3 independent cell preparations)). No increase in cell death (determined by % LDH release) occurred following cyanide treatment of astrocytes (control, 3.3 ± 1.7; KCN, 3.4 ± 1.1 % LDH release (n=3 independent cell preparations)).

5.4.6. The effect of DETA-NO on the ETC in astrocytes and neurones

Given the proposed role of GSH in protecting the ETC from RNS, the activities of the ETC complexes were assayed in both astrocytes and neurones following exposure to DETA-NO. Astrocytes were exposed to 0.5 mM DETA-NO for 6, 9, 18 and 24 hours (**Table 5.2**). A significant 44% loss of complex IV activity was observed in astrocytes treated with DETA-NO for 18 hours, while a significant 23% loss of complex II+III activity was observed following 24-hour exposure.

Treatment	Relative mRNA levels	
	GCL_h	GCL_l
Control 0 hours	1.0	1.0
Control 9 hours	1.0	1.0
DETA-NO 9 hours	1.5	1.9
Control 24 hours	1.0	0.8
DETA-NO 24 hours	1.1	1.6
DecompDETA-NO 24 hours	1.0	1.0

Table 5.1. Relative mRNA amounts of GCL_h and GCL_l

The intensity of GCL_h and GCL_l mRNA bands were measured using NIH Image software and expressed as a ratio against cyclophilin mRNA intensity. The GCL_h and GCL_l ratios with cyclophilin at 0 hours was arbitrarily set at 1 and all ratios at 9 and 24 hours compared to this.

Hours	Treatment	ETC COMPLEX ACTIVITY			
		I	II+III	IV	CS
		nmol/min/mg	nmol/min/mg	k/min/mg	nmol/min/mg
6	control	30.4 ± 3.2	9.3 ± 1.0	1.7 ± 0.3	80.0 ± 14.6
	DETA-NO	30.8 ± 4.4	6.8 ± 1.0	1.6 ± 0.2	90.7 ± 9.5
9	control	34.8 ± 7.9	8.0 ± 0.9	1.4 ± 0.2	105.6 ± 11.7
	DETA-NO	31.8 ± 4.0	7.6 ± 0.9	1.4 ± 0.2	102.6 ± 8.1
18	control	31.3 ± 3.6	8.6 ± 1.1	1.6 ± 0.2	105.5 ± 7.1
	DETA-NO	32.8 ± 8.8	8.2 ± 1.3	0.9 ± 0.2*	117.8 ± 10.1
24	control	26.9 ± 2.9	9.7 ± 0.6	1.6 ± 0.2	119.0 ± 8.7
	DETA-NO	25.4 ± 4.6	7.5 ± 0.6*	1.2 ± 0.2*	123.0 ± 6.7

Table 5.2. The effect of DETA-NO on the ETC in astrocytes

Astrocytes ($1x10^6$ cells/well) were treated with 0.5 mM DETA-NO for the period indicated, and the ETC complexes assayed in cellular homogenates. A significant loss of Complex II+III activity was observed following 24-hour DETA-NO exposure, compared to the time matched control. Complex IV activity was significantly lower following exposure to DETA-NO for 18 and 24 hours. Data are mean ± SEM (n=4-8 independent cell preparations). Statistical significance was determined by the Student's t-test. * $p < 0.05$ compared to time matched control.

A significant loss in neuronal complex II+III (38%) and IV (33%) activity was observed following just 6 hours of exposure to DETA-NO in (**Table 5.3**). Following 18 hours of DETA-NO exposure, a greater loss in complex II+III and IV activity was observed (52% and 64% respectively). Furthermore, a significant 31% loss of complex I activity and a 25% loss of CS was observed following exposure to DETA-NO for 18 hours. When neuronal complex activity is expressed against citrate synthase activity, significant inhibition of complex II+III (control, 0.29 ± 0.01; NO-treated, 0.23 ± 0.01 (n=6) $p < 0.05$) and IV activity (control, 0.11 ± 0; NO-treated, 0.08 ± 0.01 (n=6) $p < 0.05$) persists, while significant loss of complex I activity is not observed.

5.4.7. GSH efflux from astrocytes treated with DETA-NO

Cultured astrocytes can release GSH (Yudkoff *et al.*, 1990; Dringen *et al.*, 1997; Stone *et al.*, 1999), with approximately 10% of intracellular GSH released per hour (Sagara *et al.*, 1996). Since GSH levels are approximately doubled in astrocytes treated with DETA-NO for 24 hours (**Figure 5.3**), the rate of GSH efflux from these cells was measured. The rate of GSH efflux from astrocytes treated with 0.5 mM DETA-NO for 24 hours was approximately double that of control astrocytes (**Figure 5.8A**). Intracellular GSH levels remained constant in control cells for 4 hours during the course of the GSH release experiments. GSH levels were also maintained in DETA-NO treated cells for the first two hours, but began to fall at 4 hours during the course of the GSH release experiment (**Figure 5.8B**). Since the minimal medium used in the GSH release studies does not contain cystine or cysteine, the release and recycling of GSH by γ-GT in these astrocytes might not supply enough cysteine to maintain the greater rate of GSH synthesis in these NO-exposed astrocytes.

The LDH released by both control and DETA-NO treated astrocytes was similar (control 1 hrs, 0.4 ± 0; DETA-NO 1 hr, 1.0 ± 0.4; control 2 hrs, 0.5 ± 0.1; DETA-NO 2 hrs, 0.5 ± 0.1 % LDH release). This observation suggests that the increased rate of GSH efflux observed from DETA-NO exposed astrocytes is due to controlled release, rather than cell death or increased membrane permeability.

		ETC COMPLEX ACTIVITY			
Hours	**Treatment**	**I** nmol/min/mg	**II+III** nmol/min/mg	**IV** k/min/mg	**CS** nmol/min/mg
6	control	16.2 ± 1.8	13.0 ± 1.6	2.1 ± 0.1	160.5 ± 15.1
	DETA-NO	16.0 ± 1.7	8.1 ± 0.9*	1.4 ± 0.2*	147.9 ± 6.8
9	control	16.3 ± 1.6	11.8 ± 1.4	2.0 ± 0.2	154.9 ± 7.2
	DETA-NO	14.9 ± 2.0	7.2 ± 1.0*	1.3 ± 0.2*	139.0 ± 10.2
18	control	14.7 ± 1.1	14.9 ± 1.2	2.2 ± 0.2	184.7 ± 10.9
	DETA-NO	10.1 ± 1.4*	7.2 ± 0.4**	0.8 ± 0.2**	137.1 ± 10.4*

Table 5.3. The effect of DETA-NO on the ETC in neurones

Neurones ($2.5x10^6$ cells/well) were treated with 0.5 mM DETA-NO for the period indicated, and the ETC complexes assayed in cellular homogenates. A significant loss of both complex II+III and IV activity was observed following 6 hours of DETA-NO exposure. A significant loss of complex I activity of the ETC, and CS activity, was observed following 18-hour DETA-NO exposure. Data are mean ± SEM (n=5-7 independent cell preparations). Statistical significance was determined by the Student's t-test. * $p < 0.05$; ** $p < 0.1$ compared to time match control.

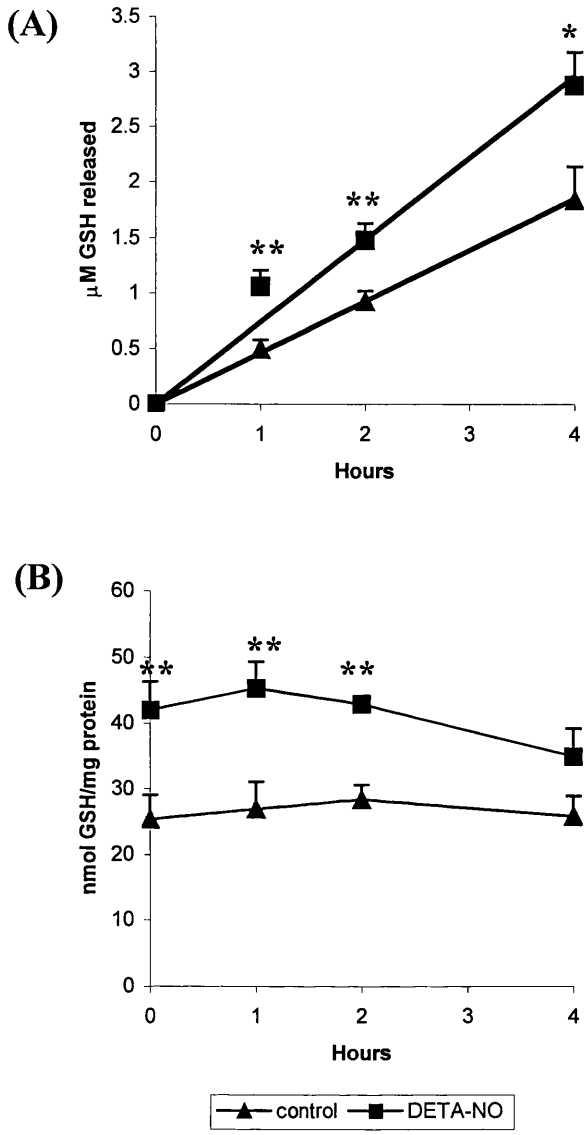

Figure 5.8. The effect of DETA-NO on GSH efflux

Astrocytes ($1x10^6$ cells/well) were treated with 0.5 mM DETA-NO for 24 hours. Cells were then washed in HBSS, and incubated in 1 ml minimal media for 1, 2, or 4 hours. The amount of GSH released into the media was measured by HPLC (A). Intracellular GSH levels were also measured during the period of release (B). The rate of GSH efflux is greater in astrocytes treated with DETA-NO, while intracellular GSH levels were maintained. Values are mean ± SEM (n=3-6 independent cell preparations). Statistical significance between and DETA-NO and time matched controls was determined by the Student's t-test. * $p< 0.05$, ** $p < 0.01$ compared to time matched control.

Acivicin (α-amino-3-chloro-4, 5-dihydro-5-isoxazoleacetic acid) is an inhibitor of γ-GT (Stole *et al.*, 1994), an ectoenzyme that metabolises extracellular GSH (Meister & Anderson, 1983; Dringen *et al.*, 1997). GSH efflux from astrocytes exposed to 0.5 mM DETA-NO for 24 hours was measured in the presence of 100 μM acivicin (previously shown to inhibit γ-GT activity by 100% (Dringen *et al.*, 1997)). The increase in extracellular GSH concentration due to the presence of acivicin, was greater in DETA-NO exposed astrocytes, compared to control cells, after 2 and 4 hours (**Table 5.4**). These results may suggest that the metabolism of GSH by γ-GT was greater in astrocytes exposed to DETA-NO. Consequently, γ-GT activity was determined in astrocytes exposed to DETA-NO.

5.4.8. The effect of DETA-NO on γ-GT activity

γ-GT activity was measured in astrocytes treated with DETA-NO for 1, 9, 18, and 24 hours (**Figure 5.9**). An increase in γ-GT activity was observed following incubation with DETA-NO for 18 and 24 hours. Decomposed DETA-NO had no effect on γ-GT activity (11.3 ± 0.9 nmol/min/mg protein (n=4 independent cultures)).

5.5. Discussion

When compared to astrocytes, the data presented here suggests that neurones are more susceptible, as judged by mitochondrial respiratory chain enzyme activities and LDH release, to NO exposure. This data is in accordance with previous studies (Bolanos *et al.*, 1995; Almeida *et al.*, 2001). This study also shows that astrocytes, but not neurones, increased cellular GSH levels upon exposure to NO. Following prolonged exposure to NO, GSH in astrocytes was approximately doubled, while GSH was depleted by up to 45% in neurones. The increased GSH levels in astrocytes could be attributed to the increase in GCL activity observed following exposure to NO. We also observed increased mRNA levels for both GCL_h (catalytic) and GCL_l (modifier) subunits in NO-treated astrocytes. This suggests that the increase in GCL activity observed in NO-treated astrocytes is

	GSH release (μM)					
Time (hr)	**1**		**2**		**4**	
	Control	DETA-NO	Control	DETA-NO	Control	DETA-NO
- acivicin	0.6 ± 0.0	1.2 ± 0.1	1.1 ± 0.1	1.7 ± 0.1	2.0 ± 0.2	3.1 ± 0.2
+ acivicin	0.8 ± 0.0	1.5 ± 0.3	1.3 ± 0.2	2.3 ± 0.4	2.5 ± 0.3	4.2 ± 0.4
△ GSH (%)	**129**	**121**	**123**	**138**	**125**	**136**

Table 5.4. The effect of acivicin on extracellular GSH concentration

Astrocytes ($1x10^6$ cells/well) were treated with 0.5 mM DETA-NO for 24 hours, washed twice, and GSH released into minimal medium in the absence (-) or presence (+) of 100μM acivicin was measured after 1, 2 or 4 hours. Values are mean ± SEM (n=3-5 independent cell preparations). △ GSH denotes the percentage increase of GSH present in minimal media in the presence of acivicin.

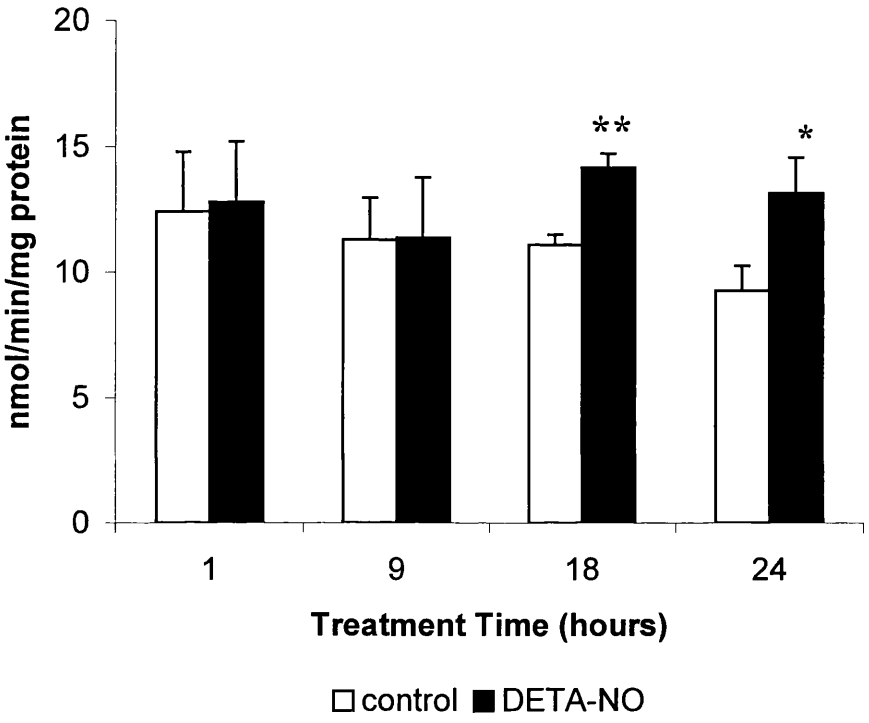

Figure 5.9. The effect of DETA-NO on astrocyte γ-GT activity

Astrocytes ($1x10^6$ cells/well) were incubated with 0.5 mM DETA-NO for the period indicated, scraped into HBSS, and γ-GT activity measured. γ-GT activity was significantly increased following exposure to DETA-NO for 18 and 24 hours (Values are mean ± SEM (n=4-9 independent cell preparations). Statistical significance was determined by the Student's t-test. * $p< 0.05$, ** $p < 0.01$ compared to time matched control.

due to increased expression of the enzyme. GCL activity was not increased in neurones upon exposure to NO.

The activity of GCL in untreated astrocytes was approximately 9-fold greater than in neurones supporting previous findings (Makar *et al.*, 1994). The lower GCL activity in untreated neurones, compared to astrocytes, may contribute to the lower basal concentration of GSH in these cells. Furthermore, the low GCL activity in neurones could mean that, upon acute exposure to NO (*e.g.,* 18 hours), the rate of GSH depletion may be greater than the rate of de novo GSH synthesis, resulting in a net loss of GSH. Since no inhibition of GCL activity was observed in neurones treated with NO, the low neuronal GCL activity, and the inability of neurones to increase GCL activity upon exposure to NO, could contribute towards the greater susceptibility of neurones to oxidative stress. The competitive inhibition of the mitochondrial respiration chain by NO may also contribute towards lower neuronal GSH levels. Astrocytes, unlike neurones, may invoke a glycolytic response upon exposure to NO, thus maintaining ATP synthesis (Bolanos *et al.*, 1994; Almeida *et al.*, 2001). Therefore upon NO exposure, the lower neuronal ATP levels may limit GSH synthesis since it is a substrate for both GCL and GSH synthetase. GSH levels were still depleted when neuronal condition media was supplemented with 350 μM cysteine suggesting that the depletion of GSH in neurones exposed to NO is not due to a lack of cysteine in the media.

A variety of chemical and physical treatments (e.g. metals, oxidants, GSH depletion) have been shown to induce transcription of either, or both, the GCL_h and GCL_l genes in endothelial, muscle and astrocyte cells (Iwata-Ichikawa *et al.*, 1999; Reviewed by Soltaninassab *et al.*, 2000 and Wild & Mulcahy, 2000;). Our results in astrocytes support those of Iwata-Ichikawa et al. (1999) who showed that astrocytes, but not neurones, are capable of increasing expression of GCL mRNA when exposed to hydrogen peroxide or 6-hydroxydopamine. The results in the present study also suggest that astrocytes are similar to both smooth muscle and endothelial cells which induce expression of both the GCL_h and GCL_l genes following exposure to NO (Moellering *et al.*, 1998; 1999).

The reason why astrocytes, but not neurones, can increase GCL activity upon exposure to NO or OHPA is unknown. The greater damage to the ETC and cell death observed in neurones exposed to either 0.5 mM NO or OHPA, compared to astrocytes, could be argued to be a reason why neurones are unable to increase GCL activity (*e.g.,* lack of ATP to increase expression). However, neurones incubated with 10-fold less NO, resulting in apparently no cell death, were still unable to increase GCL activity or GSH levels.

Cloning of the 5' flanking regions of both GCL genes has identified putative antioxidant response elements (also referred to as electrophile response element, EpRE; Mulcahy & Gipp, 1995; Moinova & Mulcahy, 1998). The binding of the transcription factor Nrf2 to EpREs, which can increase the transcription of both GCL genes in HepG2 cells, is thought to redox sensitive (Zipper & Mulcahy, 2000; Sekhar *et al.*, 2002). Therefore, prolonged exposure to NO (*e.g.,* greater than 4 hours) may induce the oxidation of transcription factors such as Nrf2, prompting increased transcription of the GCL genes. Recently, Murphy *et al* (2001) showed that induction of EpRE-mediated gene expression is largely restricted to astrocytes, and therefore could explain why astrocytes, but not neurones, exhibit increased GCL activity and GSH levels upon exposure to NO.

Incubation of astrocytes with cyanide did not result in elevated GSH levels, suggesting that inhibition of the respiratory chain at complex IV by NO, which may result in increased production of superoxide and hydrogen peroxide by the ETC (Boveris & Chance 1973), is probably not the 'trigger'. NO is also known to activate guanylate cyclase, which increases the levels of the secondary messenger cyclic-GMP (Garthwaite *et al.*, 1988; Agullo & Garcia, 1992). Therefore a cyclic-GMP-dependent signaling pathway may increase GCL expression in astrocytes. Indeed, the activation of guanylate cyclase by a variety of treatments (*e.g.,* glutamate, dopamine) has been shown to differ between astrocytes and neurones (Agullo & Garcia, 1992). Astrocytes could be incubated with an inhibitor of guanylate cyclase during NO exposure to see if this prevents the increase in GCL activity and GSH levels. However, Moellering *et al* (1999) have reported that the

induction of GCL expression and activity observed in bovine aortic endothelial cells following exposure to NO was guanylate cyclase-independent.

Post-translational modification of GCL cannot be ruled out as being a contributing factor for the increase in GCL activity upon NO exposure in astrocytes. A significant increase in GCL activity was observed in control astrocytes, 9 hours after change of media. However, the amount of GCL_h and GCL_l mRNA was the same at 9 hours, as it was prior to feeding (con 0). This suggests that posttranslational modification of GCL may increase enzyme activity following a change of media. Dephosphorylation of GCL has been reported to increase enzyme activity (Sun *et al.*, 1996). Western blot analysis with anti-phosphotyrosine, serine, or threonine antibodies could be used to determine whether a change in the phosphorylation state of GCL occurs following a change of media.

The observed increased rate of GSH efflux and activity of γ-GT by astrocytes exposed to NO for a short period could have important implications for neuroprotection *in vivo*. Cysteine is the rate-limiting substrate for GSH synthesis, with both astrocyte and neuronal GSH concentration determined by the availability of cysteine or cystine in the culture medium (Kranich *et al.*, 1996, 1998; Dringen *et al.*, 1999a). Astrocytes are thought to prefer cystine as the precursor for GSH synthesis (Kranich *et al.*, 1996, 1998), while neurones rely on cysteine for *de novo* GSH synthesis (Sagara *et al.*, 1993; Dringen *et al.*, 1999a). The preferred cysteine precursor for neuronal GSH synthesis appears to be cysteinylglycine (Dringen *et al.*, 1999a), which is generated by the metabolism of extracellular GSH by γ-GT (Meister & Anderson, 1983). Neurones co-cultured with astrocytes approximately double their GSH concentration (Bolanos *et al.*, 1996; Dringen *et al.*, 1999a). This increase in neuronal GSH concentration is abolished if astrocytes are incubated in the presence of acivicin, an inhibitor of γ-GT (Dringen *et al.*, 1999a). Therefore, the increased release of GSH from astrocytes, coupled with the increased rate of GSH metabolism to cysteinylglycine by γ-GT in astrocytes exposed to NO, could result in increased trafficking of GSH precursors to neurones. This in turn may elevate neuronal GSH levels, thus giving

greater protection against acute NO exposure (*e.g.,* 24 hour exposure; **Figure 5.10**). Indeed, neurones co-cultured with NO-generating astrocytes have an increased GSH concentration, and appear more resistant to oxidative stress compared to neurones cultured alone (Bolanos *et al.*, 1996; Stewart *et al.*, 1998a).

It should be noted that increased γ-GT activity, and evidence for increased NO synthase activity, has been found in the substantia nigra of PD brains (Sian *et al*, 1994b; Hunot *et al.*, 1996). The increased activity of γ-GT in PD maybe induced by exposure to NO, and could be a mechanism to increase the availability of GSH precursors in an attempt to protect neuronal cells from NO-mediated damage. Since an increase in γ-GT activity was observed in astrocytes following 18 and 24 hours of exposure to NO, this increase is likely to be due to an increase in γ-GT expression, rather than a posttranslational modification. A northern and/or western blot of astrocytes exposed to NO is required to confirm this. An increase in γ-GT mRNA, protein, and activity, has previously been reported in lung epithelial cells exposed to hydrogen peroxide (Kugelman *et al.*, 1994).

Throughout this study, only the effect of NO generated by a nitric oxide donor has been investigated on astrocytes and neurones. However, the steady state NO concentration of 1 μM generated by DETA-NO was comparable to that produced by astrocytes following activation by lipopolysaccharide and interferon-γ (Brown *et al.*, 1995). Micromolar concentrations of NO have also been reported following ischaemic insults (Murphy, 1999). The NO concentration used in this study therefore probably relates to pathological conditions. Basal NO concentrations of approximately 0.5 nM have been reported in both rat cortex and rat striatal brain slices (Cherian *et al.*, 2000; Griffiths *et al.*, 2002a). Incubation of astrocytes with a range of DETA-NO concentrations should indicate the minimal and maximal concentrations of NO that can elevate GSH levels in astrocytes.

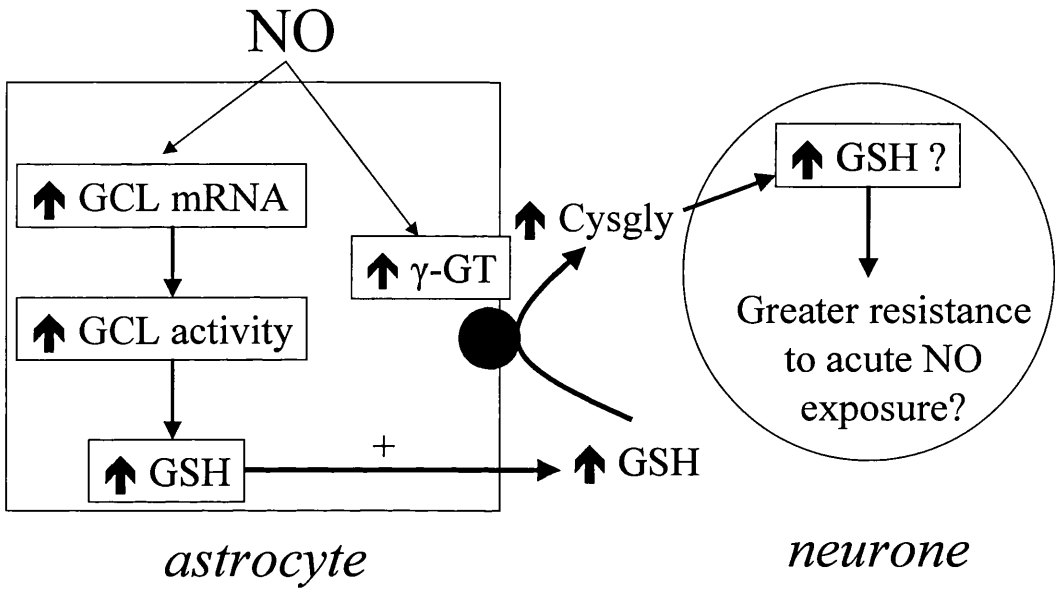

Figure 5.10. The proposed mechanism of protection of neurones by astrocytes following acute exposure to NO.

The increased release of GSH from astrocytes exposed to NO, coupled to the increased activity of γ-GT, may increase the extracellular concentration of CysGly. This putative increase in CysGly may be shuttled neurones in coculture or *in vivo*, and possibly elevate GSH levels. This may give greater protection to the neurones from exposure to NO.

5.6. Conclusion

Astrocytes increase cellular GCL activity upon acute exposure to NO, possibly due to increased expression of both GCL genes, resulting in an increased cellular GSH concentration. This may help to protect astrocytes from NO-mediated damage (*e.g.,* damage to the mitochondrial respiratory chain). Neurones in culture on their own are unable to increase GCL activity upon exposure to stress, and are therefore more susceptible to the effects of exposure to NO. However, the increased intracellular GSH concentration, rate of GSH release, and γ-GT activity in astrocytes exposed to NO may help protect neurones in coculture, and possibly *in vivo*, by supplying more GSH precursors, and thus elevating neuronal GSH levels.

Chapter 6

GSH metabolism in neurones cocultured with astrocytes

6.1. Introduction

Neurones grown in culture have been reported to have less GSH than astrocytes (see section 5.4; Sagara *et al*, 1993; Bolanos *et al.*, 1995; Dringen *et al.*, 1999a). It has been proposed that the availability of cysteine or cysteine precursors in culture media may in part determine neuronal GSH levels. Neurones, unlike astrocytes, are unable to use cystine as a precursor for GSH synthesis, and rely on cysteine or cysteine containing molecules when cultured *in vitro* (Sagara *et al.*, 1993; Kranich *et al.*, 1996; Dringen *et al.*, 1999a). The availability of glutamate and glycine, the remaining two components of GSH, do not appear to limit neuronal GSH synthesis (Dringen *et al.*, 1999a). Astrocytes on the other hand appear to prefer cystine rather than cysteine as a precursor for GSH synthesis when cultured *in vitro* (Kranich *et al.*, 1996, 1998).

When neurones are grown in coculture with astrocytes, neuronal GSH levels are approximately double that of neurones cultured alone (Sagara *et al*, 1993; Bolanos *et al.*, 1996; Dringen *et al.*, 1999a). It has been suggested that this elevation in neuronal GSH levels is due to the utilisation of GSH released from astrocytes (Sagara *et al*, 1993; Dringen *et al.*, 1999a; Wang & Cynader, 2000). GSH is released from astrocytes by an unidentified transport system (Yudkoff *et al.*, 1990, Sagara *et al.*, 1996, Stone *et al.*, 1999). The multi resistance drug protein 1 (MRP 1) transporter has been shown to transport GSH out of liver and kidney cells (Paulusma *et al.*, 1999), and is expressed in astrocytes (Hirrlinger *et al.*, 2001). To date, astrocytic MRP1 has been shown to transport GSSG out of astrocytes (Hirrlinger *et al.*, 2001), but no studies on GSH efflux from astrocytes have been published.

Wang and Cynader (2000) have proposed that the GSH released by astrocytes is used to reduce cystine to cysteine, which can then be utilisised by neurones for GSH synthesis (**Figure 1.7, route 1**). Alternatively Dringen *et al* (1999a) have postulated that the GSH released by astrocytes is metabolised by the astrocytic ectoenzyme γ-glutamyltranspeptidase (γ-GT) generating the dipeptide cysteinylglycine (CysGly; Meister & Anderson, 1983; Stole *et al.*, 1994; Dringen *et al.*, 1997a). The CysGly generated by γ-GT can then be used as a precursor for

neuronal GSH synthesis (**Figure 1.7, route 2**; Dringen *et al.*, 1999a, 2001). CysGly is thought to be a precursor for neuronal GSH synthesis since neuronal GSH levels are doubled within 4 hours when incubated with CysGly (Dringen et al., 1999a). Furthermore, inhibition of astrocytic γ-GT prevents the elevation of neuronal GSH levels when cocultured with astrocytes (Dringen *et al.*, 1999a). Aminopeptidase N (EC 3.4.11.2), an ectopeptidase localised on the outer leaflet of neuronal plasma membranes, has been reported to hydrolyse CysGly, and the cysteine and glycine taken up by neurones for *de novo* GSH synthesis (Dringen *et al.*, 2001). The observation that incubation of neurones with cysteine and glycine elevated neuronal GSH levels to a similar extent as CysGly (Dringen *et al.*, 1999a, 2001), and the lack of the peptide transporter PepT2 in neurones (Dringen *et al.*, 2001), which has been shown to transport CysGly into astrocytes (Dringen *et al.*, 1998), supports the hypothesis that CysGly is hydrolysed outside the cell, rather than taken up whole by neurones.

Neurones cultured alone, compared to astrocytes, appear to be more susceptible to oxidising species (*e.g.*, NO, peroxynitrite, hydrogen peroxide; see section 5.4; Bolanos *et al.*, 1995; Iwata-Ichikawa *et al.*, 1999; Almeida *et al.*, 2001). The greater cellular GSH concentration in astrocytes has been postulated to contribute towards the greater resistance of astrocytes to such insults (Bolanos *et al.*, 1995). Coculture experiments in which neurones have been incubated with astrocytes generating NO (referred to as activated astrocytes) further support this hypothesis (Bolanos *et al.*, 1996). Incubation of astrocytes with lipopolysaccharide (LPS) and the cytokine interferon-γ (IFN-γ) increases the expression of inducible NO synthase (Simmons & Murphy, 1992; Bolanos *et al.*, 1994; Brown *et al.*, 1995). Incubation of astrocytes with LPS and IFN-γ for 18-24 hours increases astrocytic NOS activity by 96-fold, generating a steady state NO concentration of approximately 1 μM (Bolanos *et al.*, 1994; Brown *et al.*, 1995). When neurones were cocultured with activated astrocytes, neuronal GSH levels were approximately doubled compared to untreated neurones cultured alone (Bolanos *et al.*, 1996). The complexes of the ETC were also observed to be less susceptible to NO-exposure, compared to neurones cultured alone exposed to a NO donor (Bolanos *et al.*, 1996; Stewart *et al.*, 1998a). Bolanos *et al* (1996) suggested that

the lower amount of ETC dysfunction in neurones cocultured with activated astrocytes was due to the greater GSH concentration present in these cells.

The aim of this chapter was to investigate further the mechanism by which GSH levels are elevated in neurones cocultured with astrocytes. Neurones were cocultured with astrocytes to determine whether the release of GSH by astrocytes was sufficient to increase neuronal GSH levels, or whether neuronal GCL activity was also increased. Astrocytes depleted of GSH by incubation with L-buthionine-S,R-sulfoximine (L-BSO), an inhibitor of glutamate-cysteine ligase (GCL), were also cocultured with neurones. In theory these astrocytes should release very little GSH, and therefore GSH levels in neurones cocultured with these cells should not be increased. The ETC complex activities in neurones cocultured with activated astrocytes were compared with neurones cocultured with activated astrocytes depleted of GSH. This experimental paradigm should indicate whether the increased neuronal GSH levels render the ETC more resistant to oxidative stress as previously suggested (Bolanos *et al.*, 1996; Stewart *et al*, 1998a).

6.2. Methods

6.2.1. Astrocyte and neurone primary culture

Astrocytes and neurones were isolated from Wistar rats and cultured as described in section 2.2.

6.2.2. Neurone- astrocyte coculture

The astrocyte-neurone coculture model used in the following experiments was previously described by Bolanos *et* al (1996), and is shown in **Figure 6.1**. Astrocytes were removed from flasks on day 13 by trypsin (section 2.2.2.1), and $1x10^6$ astrocytes (in 1 ml astrocyte media (section 2.2.1)) were seeded onto the membrane of a Costar transwell insert (Corning Inc., New York, USA). The membrane has a growth surface of 4.5 cm^2, is made of polycarbonate, and is

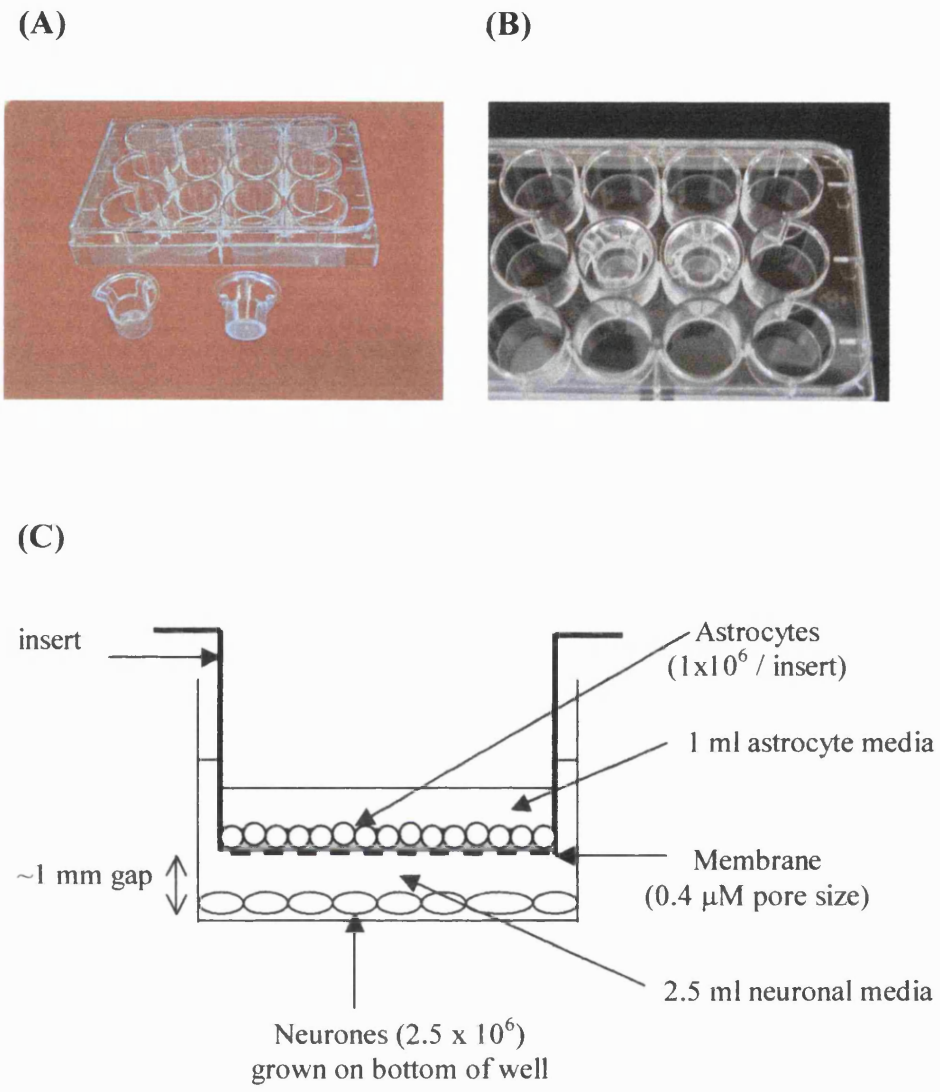

Figure 6.1. Neurone -Astrocyte coculture apparatus

(A) Picture of two inserts next to a 12-well plate. The insert on the right is placed on its side to show the membrane at the bottom of the insert. (B) Two inserts placed in a 12 well-plate. (C) A schematic diagram of the neurone-astrocyte coculture apparatus for 6-well plates.

permeable to molecules, ions, and macromolecules < 0.4 μm in size. The insert was then placed in the well of a six well plate (9.6 cm^2 area; Corning Inc.) containing 2.5 ml of astrocyte media and incubated for 24 hours to allow the astrocytes to attach to the membrane. Astrocytes were than induced to synthesise NO by incubating with 1 ml astrocyte media containing 1 μg/ml LPS (Sigma Chemicals) and 100 units/ml recombinant rat IFN-γ (CN Biosciences, Nottingham, UK) for 24 hours as previously described (Bolanos *et al*, 1994). Following 24 hours of incubation, the media was removed, and the astrocytes washed twice with HBSS. The insert was then placed in a well (9.6 cm^2 area; Corning, Inc) containing 2.5 x 10^6 neurones (day 6 *in vitro*). The neurones and astrocytes were then incubated together for 24 hours (initially 1 ml astrocyte media in insert; 2.5 ml neurone media in well). The inserts were then removed, and the neurones harvested from the well with trypsin (section 2.2.2.1), resupended in 500 μl isolation medium (section 2.2.4), and frozen at –70°C.

6.2.4. The Greiss and nitrate reductase assay

The Greiss assay coupled to nitrate reductase measures the amount of nitrite (NO_2^-) and nitrate (NO_3^-) in cell culture media, and is used as an indication of iNOS activity (Green *et al.*, 1982). Astrocytes were seeded into 6-well plates ($1x10^6$ cells/well) and incubated with 1 ml phenol red free minimal essential media supplemented with 2 mM glutamine and either 1 μg/ml LPS and 100 units/ml recombinant rat IFN-γ, or 1 μg/ml LPS, 100 units/ml recombinant rat IFN-γ, and 0.5 mM L-BSO for 24 hours. The media was then removed from the cells and stored at –70 °C until required.

1 ml of nitrate reductase (EC 1.7.1.3; 1U/ml; Boehringer-Mannheim) was mixed with 1.2 ml of 1mM NADPH. 30 μl of this mixture was then mixed with 50 μl of sample and 10 μl of 50 μM FAD in the well of a 96-well plate (Corning, Inc), and incubated at 37 °C for 15 minutes. 20 μl of a mixture containing 500 U/ml lactate dehydrogenase (LDH; Boehringer-Mannheim) and 0.5M pyruvate (Na^+ salt) was then added to each sample well and incubated at 37 °C for 5 minutes. 100μl of Greiss reagent (0.05% (vol/vol) naphthalethylenediaminedihydrochloride and

0.5% (vol/vol) sulphanilamide) was then added to each well and incubated at room temperature for 10 minutes. The reaction of NO_2^- with the Greiss reagent was assayed by measuring absorbance at 540 nm on a spectrophotometric plate reader (Spectramax Plus, Molecular Devices, Berkshire, UK). Absorbance was converted to concentration using a calibration curve of NO_2^- standards (0-100 μM) made up in phenol red free minimal essential medium. NO_3^- standards (0-100 μm) were also incubated with nitrate reductase *et cetera* as above, to make sure that conversion of NO_3^- to NO_2^- was greater than 95%.

6.2.3. Determination of GSH levels

Cellular GSH levels in astrocytes and neurones were determined by reverse-phase HPLC and electrochemical detection as described in section 2.6.

6.2.4. Measurement of GCL activity in neurones

GCL activity was measured in neuronal homogenates following coculture with astrocytes by reverse-phase HPLC and electrochemical detection as described in section 3.2.

6.2.5. Measurement of GSH release by astrocytes

The release of GSH by 1 x 10^6 astrocytes into 1 ml of minimal medium (section 5.2.3) following treatment for 24 or 48 hours was determined as previously described (section 5.2.3).

6.2.6. Spectrophotometric enzyme assays

The activities of complexes I-IV of the ETC and CS were measured in neurones following coculture as previously described (section 2.4.1-2.4.4).

LDH release by astrocytes and neurones was determined as previously described (section 2.4.6).

6.2.7. Protein determination

Sample protein concentration was determined using the Lowry method as described in section 2.5.

6.3. Experimental protocols

Determination of neuronal GSH levels, GCL activity, and ETC complex activity following coculture with astrocytes.

Neurones were cocultured with untreated astrocytes, astrocytes activated to generate NO by LPS and IFN-γ, astrocytes depleted of GSH by L-BSO, and activated astrocytes depleted of GSH, to determine the effect on (a) neuronal GSH levels (b) neuronal GCL activity, and (c) neuronal ETC complex activity.

6.4. Results

6.4.1. GSH release from activated astrocytes treated with L-BSO

Prior to culturing neurones with activated astrocytes depleted of GSH, intracellular GSH levels and GSH release from activated astrocytes depleted of GSH were determined. Astrocytes ($1x10^6$ cells/well) were incubated with LPS (1 μg/ml), IFN-γ (100 units/ml), and 0.5 mM L-BSO for 24 hours. The astrocytes were then washed twice with HBSS, and both intracellular GSH levels, and GSH released into minimal media after 1 hour were determined (**Figure 6.2**). In the coculture paradigm, this is the point at which the activated astrocytes depleted of glutathione would be transferred to the neurone-containing wells (section 6.2.2). In a sister well, astrocytes following incubation with LPS, IFN-γ, and L-BSO for 24 hours were washed twice with HBSS, and incubated for a further 24 hours in astrocyte media (without LPS, IFN-γ, L-BSO), to determine intracellular GSH

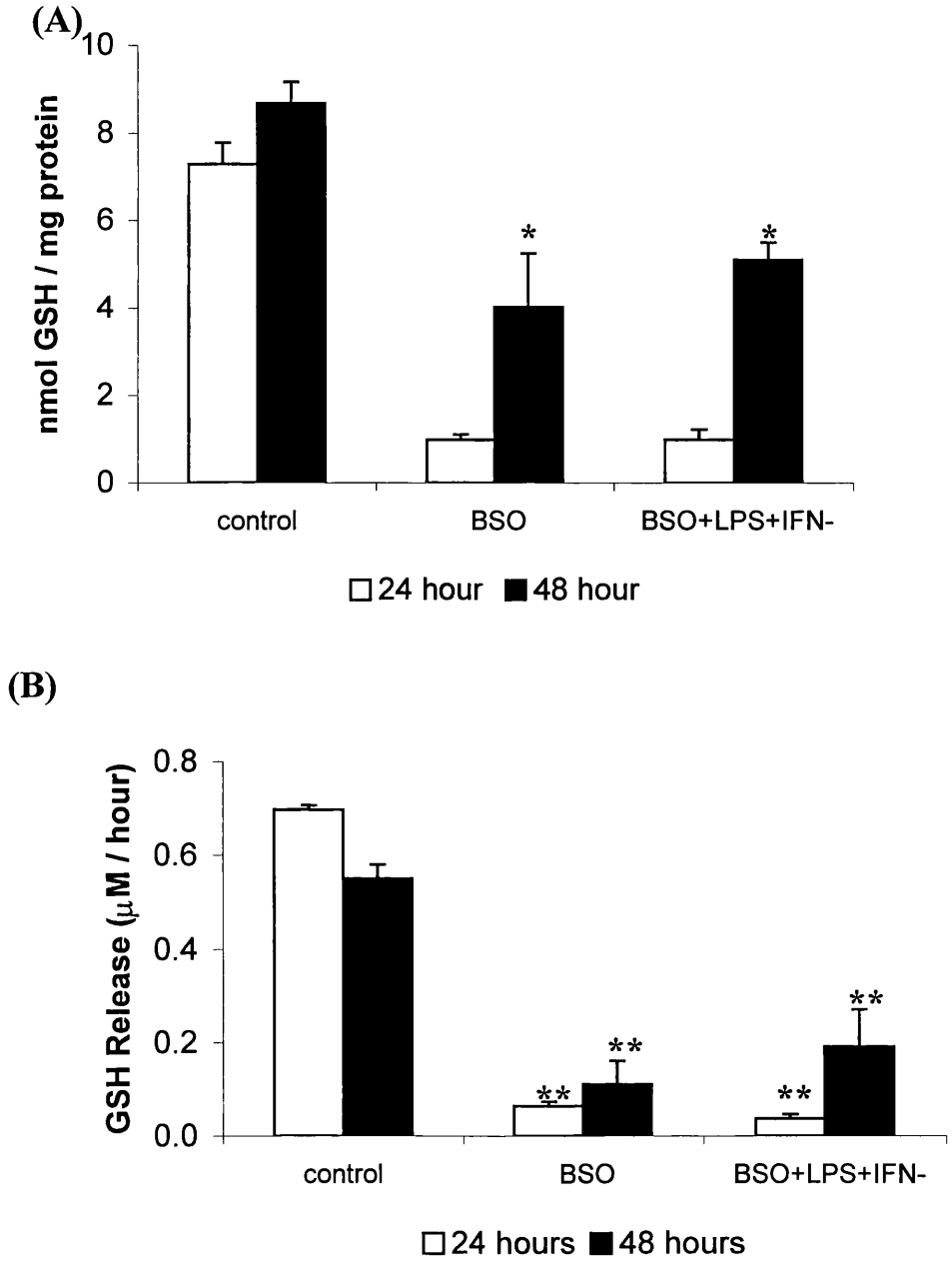

Figure 6.2. Intracellular GSH levels and GSH release from astrocytes treated with L-BSO

Astrocytes were treated with 0.5 mM L-BSO or LPS (1 μg/ml), IFN-γ (100 units/ml), and 0.5 mM L-BSO for 24 hours, the cells washed twice in HBSS, and incubated for a further 24 hours in astrocyte media. Intracellular GSH levels (A) and GSH released into 1 ml of minimal media in 1 hour (B) was determined at 24 hours and 48 hours after start of incubation. Values are mean ± SEM (n=3 independent cell preparations). Statistical significance was determined by one-way ANOVA followed by least significant difference test compared to time matched control. * $p < 0.05$; ** $p < 0.01$

levels and GSH release after 48 hours (equivalent to end of 24 hour incubation of activated astrocytes with neurones; **Figure 6.2**). Intracellular GSH was depleted by 87% in activated astrocytes treated with L-BSO after 24 hours (**Figure 6.2A**). The amount of GSH released into minimal media after 1 hour by these GSH depleted astrocytes was 94% lower than untreated astrocytes (**Figure 6.2B**). The depletion of intracellular GSH and release of GSH was similar in astrocytes treated with 0.5mM L-BSO alone (**Figure 6.2A,B**). Intracellular GSH levels and GSH release were higher in activated astrocytes 24 hours after the removal of L-BSO, but were still significantly lower compared to untreated astrocytes (**Figure 6.2A,B**). It should be noted that the GSH levels in untreated astrocytes (8.7 ± 0.5 nmol GSH/mg protein) were lower than in previous chapters. Variability of GSH levels in both animals and cell culture have been noted between experiments (Bolanos *et al.*, 1994,1995; Cock *et al.*, 2002), and could be the reason for the change in GSH levels noted here (see section 6.5).

The depletion of GSH appeared to have no effect on the activation of astrocytes by LPS and IFN-γ. NO_3^- and NO_2^- levels in culture media were similar for both activated astrocytes and activated astrocytes depleted of GSH (43.5 ± 2.5 and 50.8 ± 3.7 nmol NO_2^- + NO_3^- /million cells respectively (n=3 independent cell preparations)), and were significantly greater compared to control cells (26.4 ± 0.3 nmol NO_2^- + NO_3^- /million cells (n=3 independent cell preparations)). Cell viability, as measured by LDH release, was also unaffected by activation and GSH depletion (control, 13.9 ± 3.4; LPS + IFN-γ + L-BSO, 22.2 ± 4.7 % LDH release (n=4 independent cell preparations)). In conclusion, astrocytes can be simultaneously activated and depleted of GSH with no apparent affect on the induction of NOS activity or cell viability. The amount of GSH released by these astrocytes was considerably lower than from untreated astrocytes during the 24-hour period that they were cocultured with neurones.

6.4.2. Neurone-astrocyte coculture

Neurones were cocultured with either astrocytes depleted of GSH, or activated astrocytes depleted of GSH, to determine whether the diminished release of GSH

by these astrocytes had any effect on neuronal GSH levels and the ETC, compared to neurones cocultured with either untreated or activated astrocytes.

6.4.2.1. GSH metabolism in neurones cocultured with astrocytes

Astrocytes ($1x10^6$ cells/insert) were incubated with: LPS (1 μg/ml) and IFN-γ (100 units/ml); 0.5 mM L-BSO; or LPS (1 μg/ml), IFN-γ (100 units/ml), and 0.5 mM L-BSO for 24 hours. The astrocytes were then cocultured with neurones ($2.5x10^6$ cells/well) for 24 hours, the inserts removed, and neuronal GSH levels and GCL activity determined in neuronal homogenates. Neuronal GSH levels and GCL activities were also determined in untreated neurones cultured alone, or treated with 100 μM CysGly, for 24 hours.

Neuronal GSH levels were significantly greater in neurones cocultured with untreated or activated astrocytes, compared to neurones cultured alone (**Figure 6.3**), as previously described (Sagara *et al.*, 1993; Bolanos *et al.*, 1996; Dringen *et al.*, 1999a). GSH levels were not elevated in neurones cocultured with either GSH depleted astrocytes, or activated astrocytes depleted of GSH, and were significantly lower compared to neurones cocultured with untreated or activated astrocytes (**Figure 6.3**). GSH levels were unaffected in neurones treated with 100 μM CysGly.

Neuronal GCL activity was also determined in neurones cocultured with astrocytes. GCL activity in neurones cocultured with either untreated astrocytes or activated astrocytes was no greater than in neurones cultured alone, or with 100 μM CysGly (**Figure 6.4**). However, GCL activity was increased 2.2 fold in neurones cocultured with either GSH depleted astrocytes, or activated astrocytes depleted of GSH, compared to neurones cocultured with untreated or activated astrocytes (**Figure 6.4**).

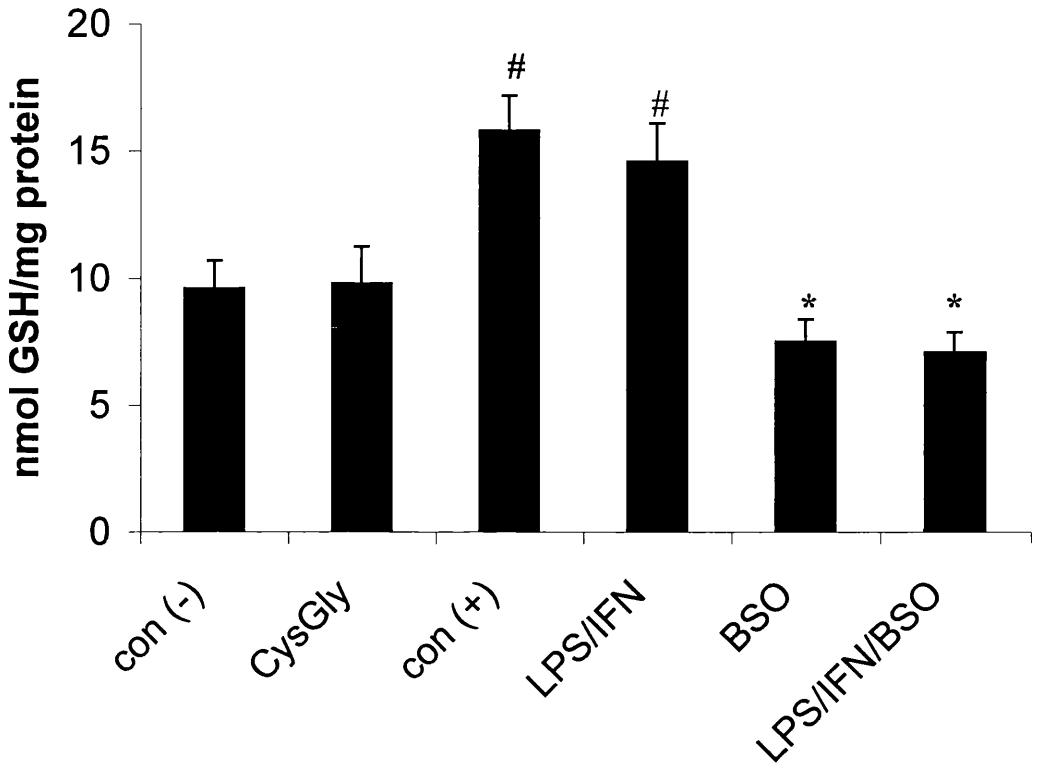

Figure 6.3. GSH levels in neurones cocultured with astrocytes

Neurones were incubated with neuronal media (con (-)), 100 μM CysGly, untreated astrocytes (con (+)), activated astrocytes (LPS/IFN), GSH depleted astrocytes (BSO), or activated astrocytes depleted of GSH (LPS/IFN/BSO), for 24 hours and GSH levels determined in neuronal homogenates. GSH levels were significantly elevated in neurones cocultured with either untreated or activated astrocytes, compared to neurones cultured alone. GSH levels in neurones cultured with GSH depleted astrocytes, or activated astrocytes depleted of GSH, were significantly lower than in neurones incubated with untreated or activated astrocytes. Values are mean ± SEM (n=4-7 independent cell preparations). Statistical significance was determined by one-way ANOVA followed by least significant difference test. # $p < 0.05$ compared to con (-); * $p < 0.05$ compared to con (+) and LPS/IFN.

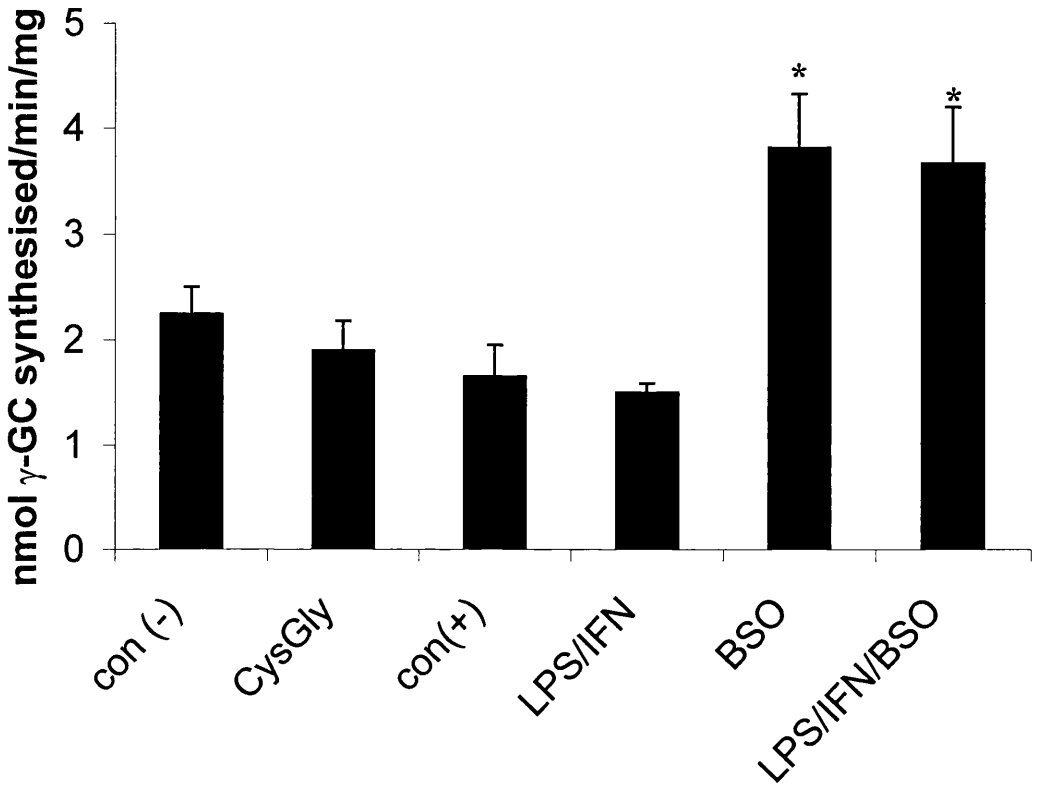

Figure 6.4. GCL activity in neurones cocultured with astrocytes

Neurones were incubated with neuronal media (con (-)), 100 μM CysGly, untreated astrocytes (con (+)), activated astrocytes (LPS/IFN), GSH depleted astrocytes (BSO), or activated astrocytes depleted of GSH (LPS/IFN/BSO), for 24 hours and GCL activity determined in neuronal homogenates. GCL activity was significantly elevated in neurones cultured with GSH depleted astrocytes, or activated astrocytes depleted of GSH in neurones compared to neurones cocultured with untreated or activated astrocytes, or neurones cultured alone. Values are mean ± SEM (n=4 independent cell preparations). Statistical significance was determined by one-way ANOVA followed by least significant difference test. * $p < 0.05$ compared to con (+) or con (-).

TREATMENT	ETC COMPLEX ACTIVITY			
	I	II+II	IV	CS
	nmol/min/mg	nmol/min/mg	k/min/mg	nmol/min/mg
con (+)	14.5 ± 2.0	15.2 ± 0.7	2.0 ± 0.0	196.9 ± 19.2
LPS/IFN	15.6 ± 3.3	12.8 ± 1.4	1.8 ± 0.1	190.7 ± 21.2
BSO	15.7 ± 2.1	13.1 ± 2.3	1.9 ± 0.3	227.1 ± 28.1
LPS/IFN/BSO	19.2 ± 1.3	10.8 ± 0.4*	1.5 ± 0.1* #	188.3 ± 26.6

Table 6.1. ETC complex activity in neurones cocultured with astrocytes

Neurones were incubated with untreated astrocytes (con (+)), activated astrocytes (LPS/IFN), GSH depleted astrocytes (BSO), or activated astrocytes depleted of GSH (LPS/IFN/BSO) for 24 hours, and ETC complex activity determined in neuronal homogenates. Complex II+III was significantly lower in neurones cocultured with activated astrocytes depleted of GSH compared to neurones cocultured with untreated astrocytes, while complex IV activity was significantly lower in neurones cocultured with activated astrocytes depleted of GSH compared to neurones cocultured with untreated or activated astrocytes. Values are mean ± SEM (n=4-6 independent cell preparations). Statistical significance was determined by one-way ANOVA followed by a least significant difference test. * $p < 0.05$ compared to con (+); # $p < 0.05$ compared to LPS/IFN.

6.4.2.2. ETC complex activities in neurones cocultured with astrocytes

The ETC complex activities were determined in neuronal homogenates cocultured with astrocytes (**Table 6.1**). A significant 29% loss of Complex II+III activity was observed in neurones cocultured with activated astrocytes depleted of GSH, compared to neurones cocultured with untreated astrocytes. Complex IV activity was significantly reduced by 24% and 17% in neurones cocultured with activated astrocytes depleted of GSH, compared to neurones cocultured with untreated or activated astrocytes respectively. No loss of complex I or citrate synthase activity was observed following incubation with activated astrocytes depleted of GSH.

No increase in LDH activity was observed in neurones cocultured with activated astrocytes (4.2 ± 1.1 %LDH release), GSH depleted astrocytes (4.0 ± 2.2 %LDH release), or activated astrocytes depleted of GSH (4.4 ± 1.5 %LDH release), compared to neurones cultured with untreated astrocytes (2.2 ± 0.4 %LDH release; n=4 independent cell preparations).

6.5. Discussion

The increased GSH levels observed in neurones cocultured with untreated or activated astrocytes, compared to neurones cultured alone, are consistent with previous studies (Sagara *et al.*, 1993; Bolanos *et al.*, 1996; Dringen *et al.*, 1999a). The results in this study suggest that the elevation of GSH levels in cocultured neurones is dependent on GSH release by astrocytes, since GSH levels were not elevated in neurones when they were cocultured with GSH depleted astrocytes that released very little GSH. The elevation of GSH levels in cocultured neurones was not concomitant with an increase in neuronal GCL activity, indicating that the release of GSH by astrocytes alone maybe sufficient to increase neuronal GSH levels. The lack of GSH released by astrocytes will significantly lower the amount of CysGly available to neurones, and may explain why neurones cannot increase GSH levels under these conditions. Dringen *et al* (1999a) have reported than inhibition of γ-GT, the ectoenzyme that metabolises GSH to CysGly, abolishes the elevation of neuronal GSH levels when cocultured with astrocytes, further supporting the hypothesis that CysGly is necessary for elevated neuronal GSH

levels. However, it should be noted that incubation of neurones with 100 μM CysGly for 24 hours in this chapter did not result in an increase in neuronal GSH levels. An explanation for this maybe that an increase in neuronal GSH levels may occur at an earlier time point, and that by 24 hours, all the CysGly has been exhausted (*i.e.,* taken up by neurones, oxidised to CysGly disulphide), and GSH levels have returned to basal levels. GSH levels in neurones need to be determined at earlier time points to see if this is the case. Neuronal GSH levels have been reported to double following incubation with 100 μM CysGly for 4 hours (Dringen *et al.*, 1999a).

The present results do not indicate whether the supply of cysteine to neurones in coculture is due to the reduction of cystine by GSH released from astrocytes (**Figure 1.7, route 1;** Wang & Cynader *et al.*, 2000), or metabolism of extracellular GSH by γ-GT to supply CysGly (**Figure 1.7, route 2**; Dringen *et al.*, 1999a). However, it should be noted that the experiments investigating the conversion of cystine to cysteine by extracellular GSH were performed in culture media containing 33 mM glucose (Wang & Cynader, 2000), which is far greater than the physiological concentration of approximately 5 mM. Furthermore, the rate of GSH release from these cultured rat cortical astrocytes was at least 5-fold lower than reported by others (Sagara *et al.*, 1996; Dringen *et al.*, 1997a; Stone *et al.*, 1999). The observed loss of cystine from the cell culture media by Wang & Cynader (2000) could be accounted for by astrocytic uptake, rather than conversion to cysteine, while the increased cysteine levels could be due to hydrolysis of CysGly. No experiments were performed in the presence of acivicin, an inhibitor of γ-GT, to see if this had any effect on extracellular GSH and cysteine levels.

GCL activity in neurones was unchanged when incubated with 100 μM CysGly, or cocultured with either untreated or activated astrocytes. However, neuronal GCL activity was increased by more than 2-fold when cocultured with either GSH depleted astrocytes or activated astrocytes depleted of GSH. Since GCL activity was increased by a similar amount in both cases, it would suggest that this observation is a result of incubation with astrocytes depleted of GSH, rather than

exposure to NO. Indeed, the previous chapter of this thesis (chapter 5) has indicated that neurones exposed to the NO donor DETA-NO do not increase GCL activity.

The results also suggest that the elevation in GCL activity maybe due to a signal released from the GSH depleted astrocytes, rather than just a response to a lack of GSH or GSH precursors (*e.g.,* CysGly), since GCL activity in neurones cultured alone, which in theory are exposed to very little GSH or CysGly, had similar GCL activity to that of neurones cocultured with untreated astrocytes or activated astrocytes. It is unclear whether the increased GCL activity observed in neurones cocultured with GSH depleted astrocytes is due to increased expression of the enzyme or a posttranslational modification of the enzyme. Determination of GCL activity at earlier time points (*e.g.,* 1 hour) and measurement of GCL mRNA levels at several time points may indicate the probable reason for the increase in enzyme activity.

Astrocytes release a variety of signalling molecules such as cytokines (*e.g.,* interleukin 1β), tumour necrosis factor (TNF), and neurotrophins (*e.g.,* brain derived neurotrophic factor (BDNF), glial derived neurotrophic factor (GDNF); Mollace *et al.*, 1998; McNaught & Jenner, 2000b). Interleukin 1β, TNF, and certain neurotrophic factors (e.g., nerve growth factor) have been reported to increase expression of GCL (Pan & Perez-Polo, 1993; Ikegami *et al.*, 2000; Soltaninassab *et al.*, 2000). Therefore, the depletion of GSH in astrocytes may prevent or induce the release of a particular signalling molecule. Indeed, astrocytes depleted of GSH have been reported to lower the release of BDNF and GDNF (McNaught & Jenner, 2000b). Furthermore, neurones incubated in astrocyte-conditioned media, but not neuronal media, are able to increase GSH levels and GCL expression upon exposure to hydrogen peroxide (Iwata-Ichikawa *et al.*, 1999).

Alternatively, the depletion of GSH in astrocytes may increase the amount of reactive oxygen species within the cell, which may be released, and act as a signal to increase GCL activity in the cocultured neurones.

Although GCL activity is increased in neurones cocultured with astrocytes depleted of GSH, no increase in neuronal GSH levels was observed. This in part can be explained by the lack of GSH released by astrocytes. However, it also may suggest that the amount of cysteine (or cysteine containing molecules) available to neurones in cell culture neuronal media maybe limiting the amount of *de novo* neuronal GSH synthesis. This could be due to low concentrations of cysteine following 24 hours of uptake by neurones and astrocytes. Supplementation of neuronal media with cysteine or CysGly following coculture for 24 hours with GSH depleted astrocytes, or a change of media at this point, followed by incubation for a short period (*i.e.,* 4 hours) prior to determination of GSH levels, may indicate whether a lack of cysteine in neuronal medium is preventing an elevation of GSH levels in neurones with increased GCL activity.

Previous experiments have suggested that the greater GSH levels in neurones cocultured with activated astrocytes resulted in the ETC being less susceptible to reactive nitrogen species, compared to neurones cultured alone exposed to the NO donor S-nitroso-N-acetylpenicillamine (Bolanos *et al.*, 1996; Stewart *et al.*, 1998a). The results from this chapter showed that complexes I, II+III and IV were unaffected in neurones cocultured with activated astrocytes. These results are similar to those reported by Bolanos *et al* (1996), but differ from those of Stewart *et al* (1998a). A 38% and 30% loss of complex II+III and IV activity was reported following exposure to activated astrocytes for 24 hours (Stewart *et al.*, 1998a). However, the astrocytes were activated with 500 units/ml IFN-γ, compared to 100 units/ml used in this chapter and Bolanos *et al* (1996). Therefore, the astrocytes used by Stewart *et al* (1998a) may have greater NOS activity, and consequently the cocultured neurones exposed to a greater concentration of NO.

When neurones were exposed to activated astrocytes depleted of GSH in this chapter, a significant 29% and 25% loss of complex II+III and IV activities respectively were observed, compared to neurones cocultured with untreated astrocytes. The activity of complex IV, but not complex II+III, in neurones cocultured with activated astrocytes depleted of GSH was also significantly lower than in neurones cocultured with activated astrocytes, which have almost twice the amount of GSH. This result supports the hypothesis that greater cellular GSH

levels protect the ETC from oxidative stress (Bolanos *et al.*, 1995; Barker *et al.*, 1996). However, the damage to the ETC in these cells, compared to neurones cocultured with activated astrocytes, was perhaps less than expected. Activated astrocytes have been shown to generate a steady state NO concentration of approximately 1 μM (Brown *et al.*, 1995) and is similar to that generated by 0.5 mM DETA-NO in the previous chapter. However the damage to neurones exposed to DETA-NO was much greater than in neurones cocultured with activated astrocytes depleted of GSH in this chapter. Perhaps other cellular antioxidant systems that may protect the ETC, in addition to the observed increase in GCL activity, could have been up regulated in these neurones. Mice over expressing CuZnSOD or Bcl-2 have been reported to prevent the loss in activity of complexes I, II and IV in the brain following GSH depletion by L-BSO (Merad-Saidoune *et al.*, 1999). Dopaminergic neurones that are induced to increase tetrahydrobiopterin levels, which can act as an antioxidant (Heales *et al.*, 1988), also prevent the toxicity associated with depletion of GSH (Nakamura *et al.*, 2000b).

As noted in the results, intracellular GSH levels were lower in both untreated astrocytes and neurones cultured alone, compared to previous chapters. These differences could be due variations between batches of animals. Variation between the batches of D- and L-valine minimal essential media or foetal bovine serum may also have affected the cells (*e.g.,* the availability of substrates or growth factors). In the case of astrocytes, variation in media may have affected the rate of proliferation during the two weeks of culture. Decreased GSH levels have been associated with high cell density in hepatocytes (Lu & Ge, 1992), or a decrease in the proliferation rate of colon adenocarcinoma cells (Kirlin *et al.*, 1999).

6.6. Conclusion

Neurones in coculture require astrocytes to release GSH in order to elevate neuronal GSH levels. GCL activity was similar in either neurones cultured alone, or cocultured with untreated or activated astrocytes, implying that the supply of

GSH/CysGly by astrocytes is sufficient to increase neuronal GSH levels in coculture. Interestingly, despite GSH levels not being elevated in neurones cocultured with astrocytes depleted of GSH, GCL activity was increased in these neurones. The results suggest that the increased neuronal GCL activity is due to a signal released from astrocytes (*e.g.,* neurotrophins, cytokines, reactive oxygen species) rather than exposure to NO, or a lack of GSH precursors supplied by astrocytes.

An increase in γ-GT activity has previously been reported in the substantia nigra of PD brains at post-mortem (Sian *et al.*, 1994b). This phenomenon has been postulated to be a protective mechanism by cells to increase the supply of GSH precursors to surviving neurones and glia. The release of signals from GSH depleted astrocytes that increase GCL activity in surviving neurones, in tandem with increased γ-GT activity, could maintain or increase GSH levels in these surviving neurones, and therefore give them greater protection. The depletion of GSH in the substantia nigra is thought to be an early event in the pathogenesis of the Parkinson's disease (PD; Dexter *et al.*, 1994). The isolation of the putative signal that induces GCL activity in neurones could lead to treatments that prevent the loss of GSH in PD, and perhaps progression of the disease.

Chapter 7

General Discussion and Conclusions

Several studies have indicated that neurones cultured alone are more susceptible to NO, peroxynitrite, and hydrogen peroxide exposure, compared to astrocytes (Bolanos *et al.*, 1995; Ben-Yoseph *et al.*, 1996; Iwata-Ichikawa *et al.*, 1999; Almeida *et al.*, 2001). The results from this thesis have also indicated that neurones cultured alone are much more susceptible to the effects of the proposed mitochondrial GSH depleting agent OHPA, and reactive nitrogen species (RNS), as measured by damage to the mitochondrial electron transport chain (ETC) and cell viability.

A reason for this differential susceptibility to RNS and OHPA may be that astrocytes, unlike neurones cultured alone, can modulate the activity of some of the components involved in GSH metabolism. Exposure to both RNS and OHPA increased the activity of astrocytic glutamate-cysteine ligase (GCL; **Table 4.6; Figure 5.6**), and therefore cellular GSH levels (**Figures 4.5, 5.3**). The increased GCL activity in astrocytes exposed to NO, and possibly OHPA, was due to the increased expression of both GCL genes (**Figure 5.7**). The increased GSH levels in these cells may well contribute to the greater resistance of the ETC in astrocytes to oxidative stress (**Tables 4.7, 5.2, 5.3**).

Previously, cultured rat astrocytes have also been postulated to protect themselves from oxidative stress by increasing the activity of the pentose phosphate pathway (PPP) and glycolysis (Ben-Yoseph *et al.*, 1996; Garcia-Nogales *et al.*, 1999; Almeida *et al.*, 2001). The PPP synthesises NADPH, which is the cofactor required by GSH reductase to reduce GSSG back to GSH, and therefore maintain the high GSH:GSSG ratio. Astrocytes activated with LPS to produce NO, or exposed to hydrogen peroxide, increased the activity of the PPP (Ben-Yoseph *et al.*, 1996; Garcia-Nogales *et al.*, 1999), probably by inducing transcription of the rate limiting enzyme glucose-6-dehydrogenase (Garcia-Nogales *et al.*, 1999). This resulted in the maintenance of GSH levels following 60 hours of incubation with LPS (Garcia-Nogales *et al.*, 1999), and increased resistance to the toxicity of hydrogen peroxide (Ben-Yoseph *et al.*, 1996). Neurones can also increase the activity of the PPP upon exposure to hydrogen peroxide, although only a fraction compared to astrocytes (Ben-Yoseph *et al.*, 1996). Consequently, the neurones were much more susceptible to hydrogen peroxide mediated cell death.

Astrocytes unlike neurones also appear to be able to increase glycolysis upon exposure to reactive nitrogen species (Bolanos *et al.*, 1994; Almeida *et al.*, 2001). The increase in astrocytic glycolysis results in the maintenance of ATP levels (Almeida *et al.*, 2001), and therefore probably a variety of biological processes such as perhaps the synthesis of GSH.

Astrocytes exposed to NO also increased the rate of GSH efflux (**Figure 5.8A**) and the activity of γ-glutamyltranspeptidase (γ-GT; **Figure 5.9**). The increased activity of GCL and γ-GT, and the increased rate of GSH release observed in astrocytes, maybe a co-ordinated response to oxidative stress. Multidrug resistance protein 1 (MRP1), the transporter that has been implicated in GSH release (Paulusma *et al.*, 1999; Hirrlinger *et al.*, 2001), and GCL_h mRNA levels are increased in tandem in hepatoma and colorectal cancer cell lines exposed to either NO or superoxide (Yamane *et al.*, 1998; Ikegami *et al.*, 2000), while increased GCL and γ-GT mRNA levels have been reported in lung epithelial cells exposed to superoxide and hydrogen peroxide (Liu *et al.*, 1996). The increased extracellular concentration of GSH, coupled with increased γ-GT activity should generate an increased amount of CysGly, which can be taken up by astrocytes for *de novo* GSH synthesis (**Figure 7.1;** Dringen *et al*, 1997b, 1998). Indeed, the elevation of GSH levels observed in rat lung epithelial and bovine aortic endothelial cells following exposure to superoxide and NO is abolished when γ-GT is inhibited by acivicin (Kugelman *et al.*, 1994; Moellering *et al.*, 1999). This proposed coordinated response by astrocytes might also be important in protecting neurones from oxidative stress *in vivo* and coculture (see below).

As opposed to neurones cultured alone, GSH metabolism can be increased in neurones when cocultured with astrocytes. Neuronal GSH levels can be elevated when cocultured with astrocytes (**Figure 6.3**; Sagara *et al.*, 1993; Bolanos *et al.*, 1996; Dringen *et al.*, 1999a), and has been suggested to be a possible reason why neurones cocultured with astrocytes are much less susceptible to ETC dysfunction and cell death following exposure to reactive nitrogen or oxygen species (Langeveld *et al.*, 1995; Bolanos *et al.*, 1996; Desagher *et al.*, 1996; Iwata-Ichikawa *et al.*, 1999). Indeed, this thesis has shown that the activity of complex

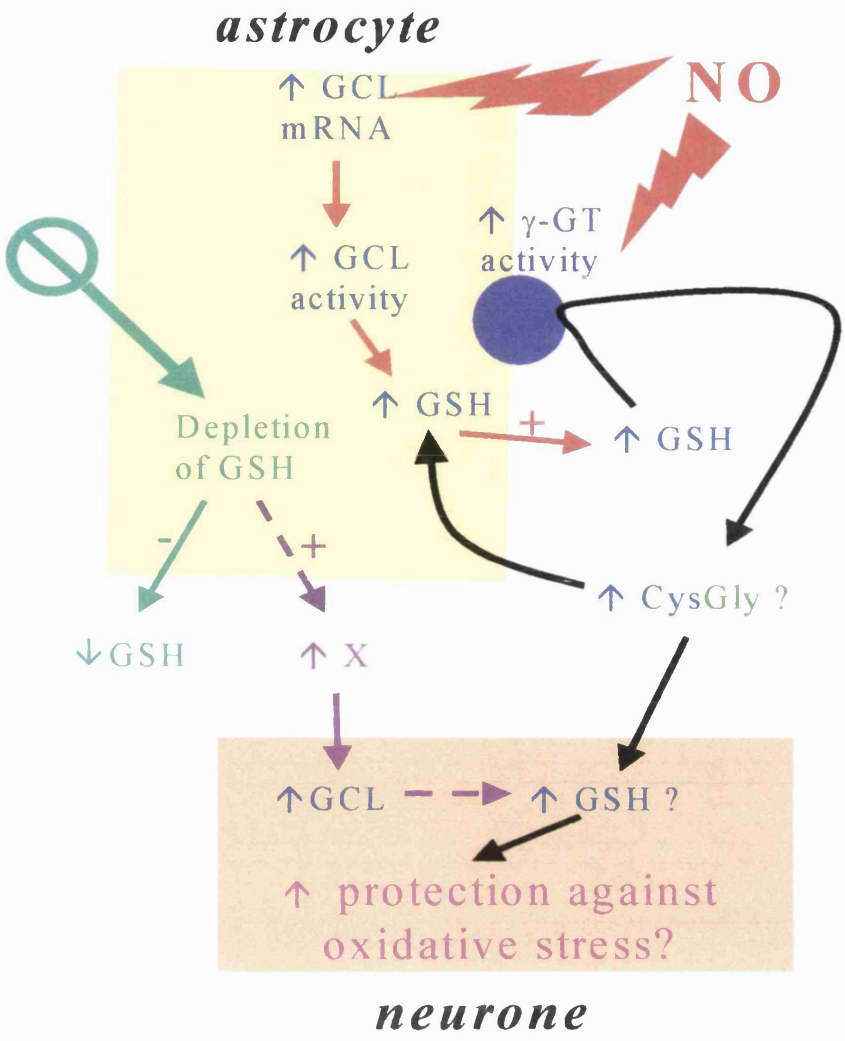

Figure 7.1. Postulated scheme of GSH metabolism in astrocytes and neurones upon oxidative stress

Astrocytes exposed to NO increase intracellular GSH levels, the rate of GSH efflux and the activity of γ-GT. The increased rate of GSH efflux and γ-GT activity may possibly increase the supply of CysGly. CysGly could be taken up by astrocytes to help maintain the increased GSH levels, or shuttled to neurones, thereby increasing neuronal GSH levels. This may give extra protection to neurones at time of oxidative stress. Conversely, depletion of GSH in astrocytes (green arrow) results in a decrease in GSH efflux, and possibly the release of a factor (X), which increases GCL activity in neurones, and depending on substrate availability, GSH levels.

IV was significantly lower in neurones cocultured with activated astrocytes that released very little GSH, compared to neurones cocultured with activated astrocytes (**Table 6.1**). The latter neurones contained approximately twice the amount of GSH as the neurones cocultured with the activated astrocytes depleted of GSH (**Figure 6.3**). Neurones cocultured with either astrocytes that release very little GSH (**Figure 6.3**), or astrocytes incubated with acivicin to inhibit γ-GT (Dringen *et al.*, 1999a), have GSH levels comparable to neurones cultured alone. Therefore, these results suggest that the supply of CysGly by astrocytes is necessary for *de novo* neuronal GSH synthesis (**Figure 7.1**). Furthermore, the results from this study also indicate that the increase in neuronal GSH levels upon coculture is due to the supply of precursors only, and not also due to a concomitant increase in neuronal GCL activity (**Figure 6.4**).

Therefore the availability of CysGly to neurones upon oxidative stress in coculture, and possibly *in vivo*, could be vital in dictating neuronal susceptibility to attack. The increased GSH efflux and γ-GT activity observed in astrocytes upon exposure to NO (discussed above), may also increase the supply of CysGly to neurones in coculture, and possibly *in vivo*, and therefore provide extra protection at times of nitrosative stress (**Figure 7.1**). Interestingly, GCL activity was increased in neurones cocultured with astrocytes that released very little GSH, compared to neurones cocultured with untreated astrocytes (**Figure 6.4**). Since GCL activity was also greater in the former neurones than in neurones cultured alone, this suggests that the signal to increase enzyme activity is not due to a lack of GSH or CysGly in the media, but maybe a messenger released by astrocytes (*e.g.,* neurotrophins, cytokines) at times of GSH depletion (**Figure 7.1**). Therefore, if the adjacent astrocytes *in vivo* are no longer providing CysGly to neurones, astrocytes may induce GCL activity in these neurones so that they may maintain GSH levels using other sources of cysteine within the brain. Increased GSH levels and transcription of GCL mRNA have also been reported in neurones cultured in astrocyte-conditioned media upon exposure to hydrogen peroxide (Iwata-Ichikawa *et al.*, 1999). Neither induction of GCL expression, nor an increase in GSH levels, were observed in neurones cultured in neuronal medium upon exposure to hydrogen peroxide, or in neurones cultured in astrocyte-

conditioned media in the absence of hydrogen peroxide (Iwata-Ichikawa *et al.*, 1999). This would suggest that molecules in astrocyte-conditioned media other than GSH or CysGly could stimulate transcription of GCL in neurones when they are exposed to oxidative stress, but not under basal conditions.

The induction of protective mechanisms upon oxidative stress in both cultured astrocytes and neurones have all been reported following acute incubations (*i.e.*, 72 hours or less). It is unclear for how long the induction of these putative protective pathways can be maintained. For example, the increased expression of GCL in astrocytes upon exposure to NO, and the increased synthesis of GSH, will require increased amounts of ATP at a time when the function of the mitochondrial ETC is impaired by NO. Indeed, the levels of GCL_h and GCL_l mRNA are greater following 9 hours of exposure to NO, compared to 24 hours, which may suggest that the cells are unable to maintain increased expression of GCL indefinitely. Failure of these mechanisms during chronic exposure to oxidative stress, which may occur during the pathogenesis of neurological disorders such as Parkinson's disease, may result in the loss of the putative protection provided by astrocytes to neurones, and consequently lead to neurodegeneration.

In conclusion, the work presented in this thesis has shown that astrocytes, but not neurones cultured alone, can increase the rate of GSH metabolism upon exposure to reactive nitrogen species and OHPA, and may contribute to the greater resistance of this cell type to oxidative stress. The supply of GSH precursors by astrocytes can also increase neuronal GSH levels in coculture. Should the supply of neuronal GSH precursors by astrocytes be perturbed, neuronal GCL activity can also be increased.

Suggested Future Work

Future experiments could investigate the molecular mechanisms by which astrocytes modulate neuronal GSH metabolism when in coculture. Experiments to date have shown that astrocytes exposed to NO can increase the release of GSH, and also the activity of γ-GT. Northern and western blot analysis of astrocytes treated with NO will possibly indicate whether these two events are due to increased transcription of the multidrug resistance-1 protein and γ–GT activity. In theory, the combination of increased GSH efflux and γ-GT activity should result in an increased extracellular concentration of CysGly. This hypothesis should be investigated. Although CysGly is electrochemically active, the HPLC conditions used to detect GSH and γ-GC cannot be used, since other molecules interfere with the CysGly peak. Either the electrochemical potentials used to detect CysGly will have to be changed, or the thiol group will be derivitised by monobromobimane, and the fluorescence detected following separation by HPLC (Liu *et al.*, 1998; Noctor & Foyer, 1998). If extracellular CysGly levels are increased, the utilisation of CysGly in the neurone-astrocyte coculture system in the presence of DETA-NO should also be investigated. Is the vast majority of CysGly recycled by astrocytes in order to maintain the high GSH levels observed during exposure to NO, or do the increased levels of CysGly also result in an elevation of neuronal GSH levels, compared to neurones cocultured with astrocytes in the absence of DETA-NO?

The increased activity of GCL in neurones cocultured with GSH-depleted astrocytes should also be investigated. Despite the increase in GCL activity, GSH levels were not elevated, compared to neurones cultured alone which had 2-fold lower GCL activity. A lack of substrates in culture media has been postulated to be a reason. Therefore, neurones could be incubated with CysGly for a short period of time (*e.g.*, 4 hours) to see if neuronal GSH levels were elevated. Northern and western blot analysis of these neurones may also indicate whether the increase in GCL activity is due to an increase in expression. The identity of the putative signal released by astrocytes should also be investigated. Initially astrocyte conditioned-media containing the putative molecule could be fractionated by centrifugal filters with differing molecular mass cut-offs (*e.g.*, 1, 3,

10 kDa) prior to incubation with neurones, to estimate the size of the molecule that increases GCL activity. Immunoprecipitation of particular molecules (*e.g.,* nerve growth factor) from astrocyte conditioned-media prior to incubation with neurones may also identify the molecule that increases GCL activity. Alternatively, neuronal media could be supplemented with a variety of prospective molecules to determine which molecule can increase GCL activity. The use of agonists and antagonists of neuronal receptors (*e.g.,* the Trk family of neurotrophin receptors; neurotransmitter receptors) may also help to identify molecules that increase neuronal GCL activity.

Should this putative molecule released from GSH-depleted astrocytes be identified, it may be useful in the diagnosis and treatment of Parkinson's disease (PD). The depletion of GSH has been postulated to be an early event in PD and precedes the onset of symptoms (Dexter *et al.*, 1994). Therefore, the detection of this molecule in cerebrospinal fluid could be used as an early diagnostic marker for the onset of the disease. Furthermore, administration of this molecule, in combination with cysteine-containing molecules that can cross the blood brain barrier (*e.g.,* N-acetylcysteine, monoethyl GSH), to patients with PD may help them to maintain or replenish the GSH levels in the surviving cells, and therefore possibly preventing/slowing down the progression of the disease.

REFERENCES

Abrahams J.P., Leslie A.G.W., Lutter R. and Walker J.E. (1994) Structure at 2.8 Å resolution of F_1-ATPase from bovine heart mitochondria. Nature 370, 621-628

Ackrell B.A.C. (2000) Progress in understanding structure-function relationships in respiratory chain complex II. FEBS Lett. 466, 1-5

Alderton W.K., Cooper C.E., and Knowles R.G. (2001) Nitric oxide synthases: structure, function and inhibition. Biochem. J. 357, 593-615

Almeida A., Allen K.L., Bates T.E. and Clark J.B. (1995) Effect of reperfusion following cerebral ischaemia on the activity of the mitochondrial respiratory chain in the gerbil brain. J. Neurochem. 65, 1698-1703

Allen K.L., Almeida A., Bates T.E. and Clark J.B. (1995) Changes of respiratory chain activity in mitochondrial and synaptosomal fractions isolated from the gerbil brain after graded ischaemia. J. Neurochem. 64, 2222-2229.

Allen J.W., Shanker G. and Aschner M. (2001) Methylmercury inhibits the in vitro uptake of the glutathione precursor, cystine, in astrocytes, but not in neurons. Brain Res. 894, 131-140

Almeida A. & Medina J.M. (1998) A rapid method for the isolation of metabolically active mitochondria from rat neurones and astrocytes in primary culture. Brain. Res. Protocols. 2, 209-214

Almeida A., Heales S.J.R., Bolanos J.P. and Medina J.M. (1998) Glutamate neurotoxicity is associated with nitric oxide-mediated mitochondrial dysfunction and glutathione depletion. Brain Res. 790, 209-216

Anderson S., Bankier A.T., Barrell B.G., de Bruijn M.H., Coulson A.R., Drouin J., Eperon I.C., Nierlich D.P., Roe B.A., Sanger F., Schreier P.H., Smith A.J.,

Staden R. and Young I.G. (1981) Sequence and organization of the human mitochondrial genome. Nature. 290, 457-465

Anderson J.K., Mo Q., Hom D.G., Lee F.Y., Harnish P., Hamill R.W. and McNeill T.H. (1996) Effect of buthionine sulfoximine, a synthesis inhibitor of the antioxidant glutathione, on the murine nigrostriatal neurons. J. Neurochem. 67, 2164-2171

Anderson M.F. and Sims N.R. (2002) The effects of focal ischemia and reperfusion on the glutathione content of mitochondria from rat brain subregions. J. Neurochem. 81, 541-549

Arroyo A., Navarro F., Gomez-Diaz C., Crane F.L., Alcain F.J., Navas P. and Villalba J.M. (2000) Interactions between ascorbyl free radical and coenzyme Q at the plasma membrane. J. Bioenerg. Biomembr. 32, 199-210

Baader S.L. and Schilling K. (1996) Glutamate receptors mediate dynamic regulation of nitric oxide synthase expression in cerebellar granule cells. J. Neurosci. 16, 1440-1449

Bagasra O., Michaels F.H., Zheng Y.M., Bobroski L.E., Spitsin S.V., Fu Z.F., Tawadros R., Koprowski H. (1995) Activation of the inducible form of nitric oxide synthase in the brains of patients with multiple sclerosis. Proc. Natl. Acad. Sci. U S A. 92, 12041-12045

Balijepalli S., Annepu J., Boyd M.R. and Ravindranath V. (1999) Effect of thiol modification on brain mitochondrial complex I activity. Neurosci. Lett. 272, 203-206

Barker J.E., Bolanos J.P., Land J.M., Clark J.B. and Heales S.J.R. (1996) Glutathione protects astrocytes from peroxynitrite mediated mitochondrial damage: Implications for neuronal/astrocytic trafficking and neurodegeneration. Dev. Neurosci. 18, 391-396

Bates T.E., Heales S.J., Davies S.E., Boakye P. and Clark J.B. (1994) Effects of 1-methyl-4-phenylpyridinium on isolated rat brain mitochondria: evidence for a primary involvement of energy depletion. J. Neurochem. 63, 640-648

Bates T.E., Loesch A., Burnstock G. and Clark J.B. (1995) Immunocytochemical evidence for a mitochondrially located nitric oxide synthase in brain and liver. Biochem. Biophys. Res. Commun. 213, 896-900

Beal M.F., Ferrante R.J., Browne S.E., Matthews R.T., Kowall N.W. and Brown R.H. Jr. (1997) Increased 3-nitrotyrosine in both sporadic and familial amyotrophic lateral sclerosis. Ann. Neurol. 42, 644-654

Beal M.F. (2002) Oxidatively modified proteins in aging and disease. Free Radic. Biol. Med. 32, 797-803

Beckman J.S. and Crow J.P. (1993) Pathological implications of nitric oxide, superoxide and peroxynitrite formation. Biochem. Soc. Trans. 21, 330-334

Beckman J.S., Carson M., Smith C.D. and Koppenol W.H. (1993) ALS, SOD and peroxynitrite. Nature. 364, 584

Beckman J.S. and Koppenol W.H. (1996) Nitric oxide, superoxide, and peroxynitrite: the good, the bad, and ugly. Am. J. Physiol. 271, C1424-C1437

Ben-Yoseph O., Boxer P.A. and Ross B.D. (1996) Assessment of the role of the glutathione and pentose phosphate pathways in the protection of primary cerebrocortical cultures from oxidative stress. J. Neurochem. 66, 2329-2337

Berman S.B. and Hastings T.G. (1999) Dopamine oxidation alters mitochondrial respiration and induces permeability transition in brain mitochondria: implications for Parkinson's disease. J. Neurochem. 73, 1127-1137

Betarbet R., Sherer T.B., Mackenzie G., Garcia-Osuna M., Panov A.V. and Greenamyre J.T. (2000) Chronic systemic pesticide exposure reproduces features of Parkinson's disease. Nat. Neuosci. 3, 1301-1306

Birago C., Marchei E., Pennino R. and Valvo L. (2001) Assay of γ-glutamylcysteine synthetase activity in *Plasmodium berghei* by liquid chromatography with electrochemical detection. J. Pharm. Biomed. Anal. 25, 759-765

Bo L., Dawson T.M., Wesselingh S., Mork S., Choi S., Kong P.A., Hanley D. and Trapp B.D. (1994)Induction of nitric oxide synthase in demyelinating regions of multiple sclerosis brains. Ann. Neurol. 36, 778-786

Bolanos J.P., Peuchen S., Heales S.J.R., Land J.M. and Clark J.B. (1994) Nitric oxide-mediated inhibition of the mitochondrial respiratory chain in cultured astrocytes. J. Neurochem. 63, 910-916

Bolanos J.P., Heales S.J.R., Land J.M. and Clark J.B. (1995) Effect of peroxynitrite on the mitochondrial respiratory chain: Differential susceptibility of neurones and astrocytes in primary culture. J. Neurochem. 64, 1965-1972

Bolanos J.P., Heales S.J.R., Peuchen S., Barker J.E., Land J.M. and Clark J.B. (1996) Nitric oxide-mediated mitochondrial damage: A potential neuroprotective role for glutathione. Free. Rad. Biol. Med. 7, 995-1001

Bolanos J.P., Almeida A., Stewart V., Peuchen S., Land J.M., Clark J.B. and Heales S.J.R. (1997) Nitric oxide-mediated mitochondrial damage in the brain: mechanisms and implications for neurodegenerative diseases. J. Neurochem. 68, 2227-2240

Borst P., Evers R., Kool M., Wijnholds J. (1999) The multidrug resistance protein family. Biochim. Biophys. Acta. 1461, 347-357

Borthwick G.M., Johnson M.A., Ince P.G., Shaw P.J. and Turnbull D.M. (1999) Mitochondrial enzyme activity in amyotrophic lateral sclerosis: implications for the role of mitochondria in neuronal cell death. Ann. Neurol. 46, 787-790

Boveris A. & Chance B. (1973) The mitochondrial generation of hydrogen peroxide. General properties and effect o fhyperbaric oxygen. Biochem. J. 134, 707-716

Boyer P.D. (1997) The ATP synthase: a splendid molecular machine. Ann. Rev. Biochem. 66, 717-749

Bredt D.S. and Snyder S.H. (1990) Isolation of nitric oxide synthetase, a calmodulin-requiring enzyme. Proc. Natl. Acad. Sci. U S A. 87, 682-685

Brigelius-Flohe R. (1999) Tissue-specific functions of individual glutathione peroxidases. Free Radic. Biol. Med. 27, 951-965

Brigelius-Flohe R. and Traber M.G. (1999) Vitamin E: function and metabolism. FASEB J. 13, 1145-1155

Brookes P.S., Salinas E.P., Darley-Usmar K., Eiserich J.P., Freeman B.A., Darley-Usmar V.M. and Anderson P.G. (2000) Concentration-dependent effects of nitric oxide on mitochondrial permeability transition and cytochrome c release. J. Biol. Chem. 275, 20474-20479

Brown G.C., Bolanos J.P., Heales S.J.R., and Clark J.B. (1995) Nitric oxide produced by activated astrocytes rapidly and reversibly inhibits cellular respiration. Neurosci. Lett. 193, 201-204

Browne S.E., Bowling A.C., MacGarvey U., Baik M.J., Berger S.C., Muqit M.M., Bird E.D., Beal M.F. (1997) Oxidative damage and metabolic dysfunction in Huntington's disease: selective vulnerability of the basal ganglia. Ann. Neurol. 41, 646-653

Buckley B.J. & Whorton A.R. (2000) Adaptive responses to peroxynitrate: increased glutathione levels and cystine uptake in vascular cells. Am. J. Physiol. Cell. Physiol. 279, p C1168-1176

Cai J., Huang Z. and Lu S.C. (1997) Differential regulation of γ-glutamylcysteine synthetase heavy and light subunit gene expression. Biochem J. 326, 167-172

Campbell E.B., Hayward M.L., and Griffith O.W. (1991) Analytical and preparative separation of the diastereoisomers of L-buthionine (SR)-sulfoximine, a potent inhibitor of glutathione biosynthesis. Anal. Biochem. 194, 267-277

Canevari L., Clark J.B. and Bates T.E. (1999) beta-Amyloid fragment 25-35 selectively decreases complex IV activity in isolated mitochondria. FEBS Lett. 457, 131-134

Cannella B. and Raine C.S. (1995) The adhesion molecule and cytokine profile of multiple sclerosis lesions. Ann. Neurol. 37, 424-35

Cardoso S.M., Pereira C. and Oliveira C.R. (1999) Mitochondrial function is differentially affected upon oxidative stress. Free. Rad. Biol. Med. 26, 3-13

Casley C.S., Canevari L., Land J.M., Clark J.B. and Sharpe M.A. (2002) Beta-amyloid inhibits integrated mitochondrial respiration and key enzyme activities. J. Neurochem. 80, 91-100

Cassarino D.S., Fall C.P., Swerdlow R.H., Smith T.S., Halvorsen E.M., Miller S.W., Parks J.P., Parker W.D. Jr. and Bennett J.P. Jr. (1997) Elevated reactive oxygen species and antioxidant enzyme activities in animal and cellular models of Parkinson's disease. Biochim. Biophys. Acta. 1362, 77-86

Chen Z. and Lash L.H. (1998) Evidence for mitochondrial uptake of glutathione by dicarboxylate and 2-oxoglutarate carriers. J. Pharm. Exp. Therap. 285, 608-618

Chen Z., Putt D.A., and Lash L.H. (2000) Enrichment and functional reconstitution of glutathione transport activity from rabbit kidney mitochondria: Further evidence for the role of the ducarboxylate and 2-oxo-glutarate carriers in mitochondrial glutathione transport. Arch. Biochem. Biophys. 373, 193-202

Chen D., Cao G., Hastings T., Feng Y., Pei W., O'Horo C. and Chen J. (2002) Age-dependent decline of DNA repair activity for oxidative lesions in rat brain mitochondria. J. Neurochem. 81, 1273-1284

Cheng K.C., Cahill D.S., Kasai H., Nishimura S. and Loeb L.A. (1992) 8-Hydroxyguanine, an abundant form of oxidative DNA damage, causes G-T and A-C substitutions. J. Biol. Chem. 267, 166-172

Cherian L., Goodman J.C., Robertson C.S. (2000) Brain nitric oxide changes after controlled cortical impact injury in rats. J. Neurophysiol. 83, 2171-2178

Chinopoulos C., Tretter L., and Adam-Vizi V. (1999) Depolarization of in situ mitochondria due to hydrogen peroxide-induced oxidative stress in nerve terminals: inhibition of alpha-ketoglutarate dehydrogenase. J. Neurochem. 73, 220-228

Cho Y. and Bannai S. (1990) Uptake of glutamate and cysteine in C-6 glioma cells and cultured astrocytes. J. Neurochem. 55, 2091-2097

Cholewinski A.J., Reid J.C., McDermott A.M. and Wilkin G.P. (1989) Purification of astroglial cell cultures from rat spinal cord – the use of D-valine to inhibit fibroblast growth. Neurochem. Int. 15, 365-369

Chomczynski P. and Sacchi N. (1987) Single-step method of RNA isolation by acid guanidinium thiocyanate-phenol-chloroform extraction. Anal. Biochem. 162, 156-159

Clementi E., Brown G.C., Feelisch M. and Moncada S. (1998) Persistent inhibition of cell respiration by nitric oxide: Crucial role of S-nitrosylation of

mitochondrial complex I and protective action of glutathione. Proc. Natl. Acad. Sci. USA. 95, 7631-7636

Cock H.R., Tong X., Hargreaves I.P., Heales S.J.R., Clark J.B., Patsalos P.N., Thom M., Groves M., Schapira A.H., Shorvon S.D., Walker M.C. (2002) Mitochondrial dysfunction associated with neuronal death following status epilepticus in rat. Epilepsy Res. 48, 157-168

Cohen G. and Kesler N. (1999) Monoamine oxidase and mitochondrial respiration. J. Neurochem. 73, 2310-2315

Costantini P., Chernyak B.V., Petronilli V. and Bernardi P. (1996) Modulation of the mitochondrial permeability transition pore by pyridine nucleotides and dithiol oxidation at two separate sites. J. Biol. Chem. 271, 6746-6751

Cotgreave I.A. and Gerdes R.G. (1998) Recent trends in glutathione biochemistry--glutathione-protein interactions: a molecular link between oxidative stress and cell proliferation? Biochem. Biophys. Res. Commun. 242, 1-9

Crofts A.R., Guergova-Kuras M., Huang L., Kuras R., Zhang Z. and Berry E.A. (1999) Mechanism of ubiquinol oxidation by the bc_1 complex: Role of the iron-sulphur protein and its mobility. Biochemistry 38, 15791-15806

Crompton M., Virji S., Doyle V., Johnson N. and Ward J.M. (1999) The mitochondrial permeability transition pore. Biochem. Soc. Symp. 66, 167-179

Croteau D.L., Rhys C.M., Hudson E.K., Dianov G.L., Hansford R.G. and Bohr V.A. (1997) An oxidative damage-specific endonuclease from rat liver mitochondria. J. Biol. Chem. 272, 27338-27344

Dahl N., Pigg M., Ristoff E., Gali R., Carlsson B., Mannervik B., Larsson A. and Board P. (1997) Missense mutations in the human glutathione synthetase gene result in severe metabolic acidosis, 5-oxoprolinuria, hemolytic anemia and neurological dysfunction. Hum. Mol. Genet. 6, 1147-1152

Dalton T.P., Dieter M.Z., Yang Y., Shertzer H.G. and Nebert D.W. (2000) Knockout of the mouse glutamate cysteine ligase catalytic subunit (Gclc) gene: embryonic lethal when homozygous, and proposed model for moderate glutathione deficiency when heterozygous. Biochem. Biophys. Res. Commun. 279, 324-329

Darbouy M., Chobert M.N., Lahuna O., Okamoto T., Bonvalet J.P., Farman N. and Laperche Y. (1991) Tissue-specific expression of multiple gamma-glutamyl transpeptidase mRNAs in rat epithelia. Am. J. Physiol. 261, C1130-1137

Davey G.P. and Clark J.B. (1996) threshold effects and control of oxidative phosphorylation in nonsynaptic rat brain mitochondria. J. Neurochem. 66, 1617-1624

Davey G.P., Peuchen S. and Clark J.B. (1998) Energy thresholds in brain mitochondria. J. Biol. Chem. 273, 12753-12757

Desagher S., Glowinski J. and Premont J. (1996) Astrocytes protect neurones from hydrogen peroxide toxicity. J. Neurosci. 16, 2553-2562

Desagher S. and Martinou J.C. (2000) Mitochondria as the central control point of apoptosis. Trends Cell. Biol. 10, 369-377

Dexter D.T., Sian J., Rose S., Hindmarsh J.G., Mann V.M., Cooper J.M., Wells F.R., Daniel S.C., Lees A.J., Schapira A.H.V. Jenner P. and Marsden C.D. (1994) Indices of oxidative stress and mitochondrial function in individuals with incidental Lewy body disease. Ann. Neurol. 35, 38-44

Dringen R. and Hamprecht B. (1997) Involvement of glutathione peroxidase and catalase in the disposal of exogenous hydrogen peroxide by cultured astroglial cells. Brain Res. 759, 67-75

Dringen R., Kranich O., and Hamprecht B. (1997a) The gamma-glutamyl transpeptidase inhibitor acivicin preserves glutathione released by astroglial cells in culture. Neurochem. Res. 22, 727-733

Dringen R., Kranich O., Loschmann P.A. and Hamprecht B. (1997b) Use of dipeptides for the synthesis of glutathione by astroglia-rich primary cultures. J. Neurochem. 69, 868-874

Dringen R., Hamprecht B. and Broer S. (1998) The peptide transporter PepT2 mediates the uptake of the glutathione precursor CysGly in astroglia rich primary cultures. J. Neurochem. 71, p 388-393

Dringen R., Pfeiffer B. and Hamprecht B. (1999a) Synthesis of the antioxidant glutathione in neurones: Supply by astrocytes of CysGly as precursor for neuronal glutathione. J. Neurosci. 19, 562-569

Dringen R., Kussmaul L., Gutterer J.M., Hirrlinger J. and Hamprecht B. (1999b) The glutathione system is less efficient in neurones than in astroglial cells. J. Neurochem. 72, 2523-2530

Dringen R., Gutterer J.M. and Hirrlinger J. (2000) Glutathione metabolism in the brain. Eur. J. Biochem. 267, 4912-4916

Dringen R., Gutterer J.M., Gros C., and Hirrlinger J. (2001) Aminopeptidase N mediates the utilization of the GSH precursor CysGly by cultured neurons. J. Neurosci. Res. 66, 1003-1008

Ellman G. L. (1959) Tissue sulfhydryl groups. Arch. Biochem. Biophys. 82, 70-77

Ehrhart J. and Zeevalk G.D. (2001) Hydrogen peroxide removal and glutathione mixed disulfide formation during metabolic inhibition in mesencephalic cultures. J. Neurochem. 77, 1496-1507

Endoh M., Maiese K., Wagner J. (1994) Expression of the inducible form of nitric oxide synthase by reactive astrocytes after transient global ischemia. Brain Res. 651, 92-100

Eskes R., Antonsson B., Osen-Sand A., Montessuit S., Richter C., Sadoul R., Mazzei G., Nichols A. and Martinou J.C. (1998) Bax-induced cytochrome C release from mitochondria is independent of the permeability transition pore but highly dependent on Mg^{2+} ions. J. Cell. Biol. 143, 217-224

Figlewicz D.A., Delattre O., Guellaen G., Krizus A., Thomas G., Zucman J. and Rouleau G.A. Mapping of human gamma-glutamyl transpeptidase genes on chromosome 22 and other human autosomes. Genomics 17, 299-305

Flohe L., Gunzler W.A. and Schock H.H. (1973) Glutathione peroxidase: a selenoenzyme. FEBS Lett. 32, 132-134

Fujita K., Yamauchi M., Shibayama K., Ando M., Honda M. and Nagata Y. (1996) Decreased cytochrome c oxidase activity but unchanged superoxide dismutase and glutathione peroxidase activities in the spinal cords of patients with amyotrophic lateral sclerosis. J. Neurosci. Res. 45, 276-281

Fukami W.H. and Williamsom J.R. (1971) Mechanism of inhibition of fatty acid oxidation by 4-pentenoic acid in rat liver mitochondria. J.Biol. Chem. 246, 1206-1212

Hayes D.J., Byrne E., Shoubridge E.A., Morgan-Hughes J.A., and Clark J.B. (1985) Experimentally induced defects of mitochondrial metabolism in rat skeletal muscle. Biological effects of the NADH: coenzyme Q reductase inhibitor diphenyleneiodonium. Biochem J. 229, 109-17.

Gali R.R. and Board P.G. (1995) Sequencing and expression of a cDNA for human glutathione synthetase. Biochem. J. 310, 353-358

Garcia-Nogales P., Almeida A., Fernandez E., Medina J.M. and Bolanos J.P. (1999) Induction of glucose-6-phosphate dehydrogenase by lipopolysaccharide contributes to preventing nitric oxide mediated glutathione depletion in cultured rat astrocytes. J. Neurochem. 72, 1750-1758

Garci-Ruiz C., Collel A., Morales A., Kaplowitz N. and Fernandez-Checa J.C. (1995) Role of oxidative stress generated from the mitochondrial electron transport chain and mitochondrial glutathione status in loss of mitochondrial function and activation of transcription factor nuclear factor-κB: Studies with isolated mitochondria and hepatocytes. Mol. Pharmacology. 48, 825-834

Gardner P.R., Nguyen D.D., and White C.W. (1994) Aconitase is a sensitive and critical target of oxygen poisoning in cultured mammalian cells and in rat lungs. Proc Natl. Acad. Sci. U S A 91,12248-12252

Gaston B. (1999) Nitric oxide and thiol groups. Biochim. Biophys. Acta 1411, 323-333

Gerlach M., Blum-Degen D., Lan J. and Riederer P. (1999) Nitric oxide in the pathogenesis of Parkinson's disease. Adv. Neurol. 80, 239-245

Gibbons C., Montgomery M.G., Leslie A.G.W and Walker J.E. (2000) The structure of the central stalk in bovine F_1-ATPase at 2.4 Å resolution. Nat. Struct. Biol. 7, 1055-1061

Gipp J.J., Bailey H.H. and Mulcahy R.T. (1995) Cloning and sequencing of the cDNA for the light subunit of human liver gamma-glutamylcysteine synthetase and relative mRNA levels for heavy and light subunits in human normal tissues. Biochem. Biophys. Res. Commun. 206, 584-589

Giulivi C., Poderoso J.J. and Boveris A. (1998) Production of nitric oxide by mitochondria. J. Biol. Chem. 273, 11038-11043

Gluck M., Ehrhart J., Jayatilleke E. and Zeevalk G.D. (2002) Inhibition of brain mitochondrial respiration by dopamine: involvement of H_2O_2 and hydroxyl radicals but not glutathione-protein-mixed disulfides. J. Neurochem. 82, 66-74

Grant C.M., MacIver F.H. and Dawes I.W. (1997) Glutathione synthetase is dispensable for growth under both normal and oxidative stress conditions in the yeast Saccharomyces cerevisiae due to an accumulation of the dipeptide gamma-glutamylcysteine. Mol. Biol. Cell. 8, 1699-1707

Grant C.M., Quinn K.A. and Dawes I.W. (1999) Differential protein S-thiolation of glyceraldehydes-3-phosphate dehydrogenase isoenzymes influences sensitivity to oxidative stress. Mol. Cell. Biol. 19, 2650-2656

Green L.C., Wagner D.A., Glogowski J., Skipper P.L., Wishnok J.S. and Tannenbaum S.R. (1982) Analysis of nitrate, nitrite, and [15N]nitrate in biological fluids. Anal. Biochem. 126, 131-138

Griffith O.W. and Meister A. (1979) Potent and specific inhibition of glutathione synthesis by buthionine sulfoximine (S-n-butyl homocysteine sulfoximine). J. Biol. Chem. 254, 7558-60.

Griffith O.W. (1982) Mechanism of action, metabolism, and toxicity of buthionine sulfoximine and its higher homologs, potent inhibitors of glutathione synthesis. J. Biol. Chem. 257, 13704-13712

Griffith O.W. (1999) Biologic and pharmacologic regulation of mammalian glutathione synthesis. Free Rad. Biol. Med. 27, 922-935

Griffiths C., Garthwaite G., Goodwin D.A., and Garthwaite J. (2002a) Dynamics of nitric oxide during simulated ischaemia-reperfusion in rat striatal slices measured using an intrinsic biosensor, soluble guanylyl cyclase. Eur. J. Neurosci. 15, 962-968

Griffiths H.R., Moller L., Bartosz G., Bast A., Bertoni-Freddari C., Collins A., Cooke M., Coolen S., Haenen G., Hoberg A.M., Loft S., Lunec J., Olinski R., Parry J., Pompella A., Poulsen H., Verhagen H. and Astley S.B. (2002b) Biomarkers. Mol. Aspects Med. 23, 101-208

Grigorieff N. (1999) Structure of the respiratory NADH:ubiquinone reductase (complex I). Curr. Opin. Struct. Biol. 9, 476-483

Grossman L.I. and Lomax M.I. (1997) Nuclear genes for cytochrome c oxidase. Biochim. Biophys. Acta. 1352, 174-192

Gu M., Gash M.T., Mann V.M., Javoy-Agid F., Cooper J.M. and Schapira A.H. (1996) Mitochondrial defect in Huntington's disease caudate nucleus. Ann. Neurol. 39, 385-389

Hagerhall C. (1997) Succinate:quinone oxidoreductases: Variations on a conserved theme. Biochim. Biochim. Biophys. Acta. 1320, 107-141

Halestrap A.P., Kerr P.M., Javadov S. and Woodfield K.Y. (1998) Elucidating the molecular mechanism of the permeability transition pore and its role in reperfusion injury of the heart. Biochim. Biophys. Acta. 1366, 79-94

Halestrap A.P., Doran E., Gillespie J.P. and O'Toole A. (2000) Mitochondria and cell death. Biochem. Soc. Trans. 28, 170-177

Halliwell B. and Gutteridge M.C. (1989) Free radicals in biology and medicine 2nd edition. Oxford University Press.

Ham A.J. and Liebler D.C. (1997) Antioxidant reactions of vitamin E in the perfused rat liver: product distribution and effect of dietary vitamin E supplementation. Arch. Biochem. Biophys. 339, 157-164

Han D., Williams E. and Cadenas E. (2001) Mitochondrial respiratory chain-dependent generation of superoxide anion and its release into the intermembrane space. Biochem J. 353, 411-416

Han J., Cheng F.C., Yang Z. and Dryhurst G. (1999) Inhibitors of mitochondrial respiration, iron (II), and hydroxyl radical evoke release and extracellular hydrolysis of glutathione in rat striatum and substantia nigra: potential implications to Parkinson's disease. J. Neurochem73, 1683-1695

Hanigan M.H. gamma-Glutamyl transpeptidase, a glutathionase: its expression and function in carcinogenesis. Chem. Biol. Interact. 111-112, 333-342

Hargreaves I.P., Lee P.J., and Briddon A. (2002) Homocysteine and cysteine – albumin binding in homocystinuria: assessment of cysteine status and implications for glutathione synthesis. Amino Acids 22, 109-118

Hashmi M., Graf S., Braun M. and Anders M.W. (1996) Enantioselective depletion of mitochondrial glutathione concentrations by (S)- and (R)-3-hydroxybutyrate dehydrogenase. Chem. Res. Toxicol. 9, 361-364

Heales S.J., Blair J.A., Meinschad C. and Ziegler I (1988) Inhibition of monocyte luminol-dependent chemiluminescence by tetrahydrobiopterin, and the free radical oxidation of tetrahydrobiopterin, dihydrobiopterin and dihydroneopterin. Cell. Biochem. Funct. 6, 191-195

Heales S.J.R., Davies S.E.C., Bates T.E. and Clark J.B. (1995) Depletion of brain glutathione is accompanied by impaired mitochondrial function and decreased N-acetyl aspartate concentration. Neurochemical Res. 20, 31-38

Heales S.J., Bolanos J.P. and Clark J.B. (1996a) Glutathione depletion is accompanied by increased neuronal nitric oxide synthase activity. Neurochem. Res. 21, 35-39

Heales S.J.R., Bolanos J.P., Brand M.P., Clark J.B. and Land J.M. (1996b) Mitochondrial damage: An important feature in a number of inborn errors of metabolism. J. Inherit. Dis. 19, 140-142

Hemmings S.J. and Storey K.B. (1999) Brain gamma-glutamyltranspeptidase: characteristics, development and thyroid hormone dependency of the enzyme in isolated microvessels and neuronal/glial cell plasma membranes. Mol. Cell. Biochem. 202, 119-130

Hensley K., Hall N., Subramaniam R., Cole P., Harris M., Aksenov M., Aksenova M., Gabbita S.P., Wu J.F., and Carney J.M. (1995) Brain regional correspondence between Alzheimer's disease histopathology and biomarkers of protein oxidation. J. Neurochem. 65, 2146-2156

Hirawake H., Taniwaki M., Tamira A., Amiro H., Tomitsuka E. and Kita K. (1999) Characterisation of the human SDHD gene encoding the small subunit of cytochrome b (cybS) in mitochondrial succinate-ubiquinone oxidoreductase. Biochim. Biophys. Acta. 1412, 295-300

Hirrlinger J., Konig J., Keppler D., Lindenau J., Schulz J.B. and Dringen R. (2001) The multidrug resistance protein MRP1 mediates the release of glutathione disulfide from rat astrocytes during oxidative stress. J. Neurochem. 76, 627-636

Huang CS., Chang L.S., Anderson M.E. and Meister A. (1993a) Catalytic and regulatory properties of the heavy subunit of rat kidney γ-glutamylcysteine synthetase. J. Biol. Chem. 268, 19675-19680

Huang CS., Chang L.S., Anderson M.E. and Meister A. (1993b) Amino acid sequence and function of the light subunit of rat kidney γ-glutamylcysteine synthetase. J. Biol. Chem. 268, 20578-20583

Huang C.S., He W., Meister A. and Anderson M.E. (1995) Amino acid sequence of rat kidney glutathione synthetase. Proc. Natl. Acad. Sci. U S A. 92, 1232-1236

Huang Z.A, Yang H., Chen C., Zeng Z. and Lu S.C. (2000) Inducers of gamma-glutamylcysteine synthetase and their effects on glutathione synthetase expression. Biochim. Biophys. Acta. 1493, 48-55

Hughes M.N. (1999) Relationships between nitric oxide, nitroxyl ion, nitrosonium cation and peroxynitrite. Biochim. Biophys. Acta 1411, 263-272

Hunot S., Boissiere F., Faucheux B., Brugg B., MouattPrigent A., Agid Y. and Hirsch E.C. (1996) Nitric oxide synthase and neuronal vulnerability in Parkinson's disease. Neuroscience. 72, 355-363

Huttemann M., Kadenbach B. and Grossman L.I. (2001) Mammalian subunit IV isoforms of cytochrome c oxidase. Gene 267, 111-123

Hwang C., Sinskey A.J., and Lodish H.F. (1992) Oxidised redox state of glutathione in the endoplasmic reticulum. Science. 257, 1496-1502

Ibi M., Sawada H., Kume T., Katsuki H., Kaneko S., Shimohama S., Akaike A. (1999) Depletion of intracellular glutathione increases susceptibility to nitric oxide in mesencephalic dopaminergic neurons. J. Neurochem 73, 1696-1703

Ikeda Y., Fujii J., Taniguchi N. and Meister A. (1995) Expression of an active glycosylated human gamma-glutamyltranspeptidase mutant that lacks a membrane anchor domain. Proc. Natl. Acad. Sci. U S A. 92, 126-130

Ikegami Y., Tatebe S., Lin-Lee Y.C., Xie Q.W., Ishikawa T., Kuo M.T. (2000) Induction of MRP1 and gamma-glutamylcysteine synthetase gene expression by interleukin 1beta is mediated by nitric oxide-related signalings in human colorectal cancer cells. J. Cell. Physiol. 185, 293-301

Iwata S., Ostermeier C., Ludwig B. and Michel H. (1995) Structure at 2.8 Å resolution of cytochrome c oxidase from Paracoccus denitrificans. Nature. 376, 660-669

Iwata S, Lee J.W., Okada K., Lee J.K., Iwata M., Rasmussen B., Link T.A., Ramaswamy S. and Jap B.K. (1995) Complete structure of the 11-subunit bovine mitochondrial cytochrome bc_1 complex. Science. 281, 64-71

Iwata-Ichikawa E., Kondo Y., Miyazaki I., Asanuma M. and Ogawa N. (1999) Glial cells protect neurones against oxidative stress via transcriptional upregulation of the glutathione synthesis. J. Neurochem. 72, 2334-2344

Jackson M.J., Papa S., Bolanos J., Bruckdorfer R., Carlsen H., Elliott R.M., Flier J., Griffiths H.R., Heales S., Holst B., Lorusso M., Lund E., Oivind Moskaug J., Moser U., Di Paola M., Cristina Polidori M., Signorile A., Stahl W., Vina-Ribes J. and Astley S.B. (2002) Antioxidants, reactive oxygen and nitrogen species, gene induction and mitochondrial function. Mol. Aspects Med. 23, 209-285

Jain A., Martensson J., Stole E., Auld P.A. and Meister A. (1991) Glutathione deficiency leads to mitochondrial damage in brain. Proc. Natl. Acad. Sci. 88, 1913-7

Jenner P. & Olanow C.W. (1998) Understanding cell death in Parkinson's disease. Ann. Neurol. 44, S72-S84

Jha N., Jurma O., Lalli G., Liu Y., Pettus E.H., Greenamyre J.T., Liu R., Forman H.J. and Andersen J.K. (2000) Glutathione depletion in PC12 cells results in selective inhibition of mitochondrial complex I activity: implications for Parkinson's disease. J. Biol. Chem. 275, 26096-26101

Johnson A.W., Land J.M., Thompson E.J., Bolanos J.P., Clark J.B. and Heales S.J. (1995) Evidence for increased nitric oxide production in multiple sclerosis. J. Neurol. Neurosurg. Psychiatry 58, 107

Jung C.H. and Thomas J.A. (1996) S-glutathiolated hepatocyte proteins and insulin disulfides as substrates for reduction by glutaredoxin, thioredoxin, protein disulfide isomerase, and glutathione. Arch. Biochem. Biophys. 335, 61-72

Kang Y., Viswanath V., Jha N., Qiao X., Mo J.Q. and Andersen J.K. (1999) Brain gamma-glutamyl cysteine synthetase (GCS) mRNA expression patterns correlate with regional-specific enzyme activities and glutathione levels. J. Neurosci. Res. 58, 436-441

Karrasch S. & Walker J.E. (1999) Novel features in the structure of bovine ATP synthase. J. Mol. Biol. 290, 379-384

Keefer L.K., Nims R.W., Davies K.M. and Wink D.A. (1996) NONOates (1-substituted biazen-1-ium-1,2-diolates) as nitric oxide donors: convenient nitric oxide dosage forms. Meth. Enzym. 268, 281-286

Kelly B.S., Antholine W.E. and Griffith O.W. (2002) *Escherichia coli* γ-glutamylcysteine synthetase. J. Biol. Chem. 277, 50-58

Kharatinov V.G., Bonaventura J., and Sharma V.S. (1996) Interactions of nitric oxide with heme proteins using UV-VIS spectroscopy (in Methods in nitric oxide research; Eds, Feelisch M. and Stamler J.S; Wiley Publishing) p 39-45

Kim H., Xia D., Yu C., Xia J., Kachurin A., Zhang L., Yu L. and Deisenhoffer J. (1998) Inhibitor binding changes domain mobility in the iron-sulphur protein of the mitochondrial bc1 complex from bovine heart. Proc . Natl. Acad. Sci. 95, 8026-8033

King T.E. (1967) Preparation of succinate cytochrome c reductase and the cytochtom bc1 particle, and the reconstitution of cytochrome c reductase. Methods Enzymol. 10, 216-225

Kirlin W.G., Cai J., Thompson S.A., Diaz D., Kavanagh T.J. and Jones D.P. (1999) Glutathione redox potential in response to differentiation and enzyme inducers. Free Radic. Biol. Med. 27, 1208-1218

Kish S.J., Bergeron C., Rajput A., Dozic S., Mastrogiacomo F., Chang L.J., Wilson J.M., DiStefano L.M. and Nobrega J.N. (1992) Brain cytochrome oxidase in Alzheimer's disease. J. Neurochem. 59, 776-779

Klatt P. and Lamas S. (2000) Regulation of protein function by S-glutathiolation in response to oxidative and nitrosative stress. Eur. J. Biochem. 267, 4928-4944

Klingenberg M. (1992) Structure-function of the ADP/ATP carrier. Biochem. Soc. Trans. 20, 547-550

Knowles R.G. and Moncada S. (1994) Nitric oxide synthases in mammals. Biochem. J. 298, 249-258

Kranich O., Hamprecht B., and Dringen R. (1996) Different preferences in the utilization of amino acids for glutathione synthesis in cultured neurons and astroglial cells derived from rat brain. Neurosci. Lett. 219, 211-214

Kranich O., Dringen R., Sandberg M. and Hamprecht B. (1998) Utilisation of cysteine and cysteine precursors for the synthesis of glutathione in astroglial cultures: Preference for cystine. Glia 22, 11-18

Kugelman A., Choy H.A., Liu R., Shi M.M., Gozal E., Forman H.J. (1994) gamma-Glutamyl transpeptidase is increased by oxidative stress in rat alveolar L2 epithelial cells. Am. J. Respir. Cell. Mol. Biol.11, 586-92.

Kwon N.S., Nathan C.F., Gilker C., Griffith O.W., Matthews D.E., and Stuehr D.J. (1990) L-citrulline production from L-arginine by macrophage nitric oxide synthase. The ureido oxygen derives from dioxygen. J. Biol. Chem. 265, 13442-13445

Lancaster C.R.D., Kroger A., Auer M. and Michel M. (1999) Structure of fumarate reductase from Wolinella succinogenes at 2.2 Å resolution. Nature 402, 377-385

Landi L., Fiorentini D., Galli M.C., Segura-Aguilar J. and Beyer R.E. (1997) DT-Diaphorase maintains the reduced state of ubiquinones in lipid vesicles thereby promoting their antioxidant function. Free Radic. Biol. Med. 22, 329-335

Langeveld C.H., Jongenelen C.A.M., Schepens E., Stoof J.C., Bast A., and Drukarch B. (1995) Cultured rat striatal and cortical astrocytes protect mesencephalic dopaminergic neurons against hydrogen peroxide toxicity independent of their effect on neuronal development. Neurosci. Letts. 192, 13-16

Lee G.Y., He D., Yu L. and Yu C. (1995) Identification of the ubiquinone-binding domain in QPs1 of succinate:ubiquinone reductase. J. Biol. Chem. 270, 6193-6198

Lee M., Hyun D.H., Marshall K.A., Ellerby L.M., Bredesen D.E., Jenner P. and Halliwell B. (2001) Effect of overexpression of BCL-2 on cellular oxidative damage, nitric oxide production, antioxidant defenses, and the proteasome. Free Radic. Biol. Med. 31, 1550-1559

Lemasters J.J., Nieminen A.L., Qian T., Trost L.C., Elmore S.P., Nishimura Y., Crowe R.A., Cascio W.E., Bradham C.A., Brenner D.A. and Herman B. (1998) The mitochondrial permeability transition in cell death: a common mechanism in necrosis, apoptosis and autophagy. Biochim. Biophys. Acta. 1366, 177-196

Leone A.M., Palmer R.M., Knowles R.G., Francis P.L., Ashton D.S., and Moncada S. (1991) Constitutive and inducible nitric oxide synthases incorporate molecular oxygen into both nitric oxide and citrulline. J. Biol. Chem. 266, 23790-23795

Li H. and Dryhurst G. (1997) Irreversible inhibition of mitochondrial complex I by 7-(2-aminoethyl)-3,4-dihydro-5-hydroxy-2H-1.4-benzothiazine-3-carboxylic acid (DHBT-1): a putative nigral endotoxin of relevance to Parkinson's disease. J. Neurochem. 69, 1530-1541

Liberatore G.T., Jackson-Lewis V., Vukosavic S., Mandir A.S., Vila M., McAuliffe W.G., Dawson V.L., Dawson T.M., Przedborski S. (1999) Inducible nitric oxide synthase stimulates dopaminergic neurodegeneration in the MPTP model of Parkinson disease. Nat. Med. 5, 1403-9

Liu R.M., Gao L., Choi J. and Forman H.J. (1998) γ-glutamylcysteine synthetase: mRNA stabilisation and independent subunit transcription by 4-hydroxyl-2-nonenal. Am. J. Physiol. 275, L861-869

Liu R. and Choi J. (2000) Age associated decline in γ-glutamylcysteine synthetase gene expression in rats. Free. Rad. Biol. Med. 28, 566-574

Liu R.M. (2002) Down-regulation of gamma-glutamylcysteine synthetase regulatory subunit gene expression in rat brain tissue during aging. J. Neurosci. Res. 68, 344-351

Loeffen J.L., Triepels R.H., van den Heuvel L.P., Schuelke M., Buskens C.A., Smeets R.J., Trijbels J.M. and Smeitink J.A. (1998) cDNA of eight nuclear encoded subunits of NADH:ubiquinone oxidoreductase: human complex I cDNA characterization completed. Biochem. Biophys. Res. Commun. 253, 415-422

Lovell M.A., Ehmann W.D., Butler S.M. and Markesbery W.R. (1995) Elevated thiobarbituric acid-reactive substances and antioxidant enzyme activity in the brain in Alzheimer's disease. Neurology 45, 1594-1601

Lowe P.N., Smith D., Stammers D.K., Riveros-Moreno V., Moncada S., Charles I., and Boyhan A. (1996) Identification of the domains of neuronal nitric oxide synthase by limited proteolysis. Biochem. J. 314, 55-62

Lowry O.H., Rosebrough N.J., Farr A.L. and Randall R.J. (1951) Protein measurement with the Folin phenol reagent. J. Biol. Chem. 193, 265-275

Lu S.C. and Ge J.L. (1992) Loss of suppression of GSH synthesis at low cell density in primary cultures of rat hepatocytes. Am. J. Physiol. 263, C1181-1189

Lu F., Selak M., O'Connor J., Croul S., Lorenzana C., Butunoi C. and Kalman B. (2000) Oxidative damage to mitochondrial DNA and activity of mitochondrial enzymes in chronic active lesions of multiple sclerosis. J. Neurol. Sci. 177, 95-103

Lu S.C. (2000) Regulation of glutathione synthesis. Curr. Top. Cell. Reg. 36, 95-116

Luo J-L., Huang C.S., Babaoglu K. and Anderson M.E. (2000) Novel kinetics of mammalian glutathione synthetase: characterisation of γ-glutamyl substrate cooperative binding. Biochem. Biophys. Res. Comm. 275, 577-581

Maher P. and Schubert D. (2000) Signaling by reactive oxygen species in the nervous system. Cell. Mol. Life Sci. 57, 1287-1305

Makar T.K., Nedergaard M., Preuss A., Gelbard A.S., Perumal A.S. and Cooper A.J.L. (1994) Vitamin E, ascorbate, glutathione, glutathione disulfide, and enzymes of glutathione metabolism in cultures of chick astrocytes and neurons: Evidence that astrocytes play an important role in antioxidative processes in the brain. J. Neurochem. 62, 45-53

Marcus D.L., Thomas C., Rodriguez C., Simberkoff K., Tsai J.S., Strafaci J.A. and Freedman M.L. (1998) Increased peroxidation and reduced antioxidant enzyme activity in Alzheimer's disease. Exp. Neurol. 150, 40-44

Marks A.R., McIntyre J.O., Duncan T.M., Erdjument-Bromage H., Tempst P., and Fleischer S. (1992) Molecular cloning and characterization of (R)-3-hydroxybutyrate dehydrogenase from human heart J. Biol. Chem. 267, 15459-1546

Mathews C.K. and van Holde K.E. (1990) Biochemistry 2nd Edition. Benjamin Cummings, San Francisco, USA.

Mayatepek E. (1999) 5-Oxoprolinuria in patients with and without defects in the gamma-glutamyl cycle. Eur. J. Pediatr. 158, 221-225

McBean G.J. and Flynn J. (2001) Molecular mechanisms of cystine transport. Biochem. Soc. Trans. 29, 717-722

McNaught K.S. and Jenner P. (2000a) Extracellular accumulation of nitric oxide, hydrogen peroxide, and glutamate in astrocytic cultures following glutathione depletion, complex I inhibition, and/or lipopolysaccharide-induced activation. Biochem. Pharmacol. 60, 979-988

McNaught K.S. and Jenner P. (2000b) Dysfunction of rat forebrain astrocytes in culture alters cytokine and neurotrophic factor release. Neurosci. Lett. 285, 61-65

Mecocci P., MacGarvey U., Kaufman A.E., Koontz D., Shoffner J.M., Wallace D.C. and Beal M.F. (1993) Oxidative damage to mitochondrial DNA shows marked age-dependent increases in human brain. Ann. Neurol. 34, 609-616

Mecocci P., Fano G., Fulle S., MacGarvey U., Shinobu L., Polidori M.C., Cherubini A., Vecchiet J., Senin U. and Beal M.F. (1999) Age-dependent increases in oxidative damage to DNA, lipids, and proteins in human skeletal muscle. Free Radic. Biol. Med. 26, 303-308

Meister A. & Anderson M.E. (1983) Glutathione. Ann. Rev. Biochem. 52, 711-760

Meister A. (1994) Glutathione-ascorbic acid antioxidant system in animals. J. Biol. Chem. 269, 9397-9400

Meredith M.J. and Reed D.J. (1982) Status of the mitochondrial pool of glutathione in the isolated hepatocyte. J. Biol. Chem. 257, 3747-3753

Michel H. (1998) The mechanism of proton pumping by cytochrome c oxidase. Proc. Natl. Acad. Sci. USA. 95, 12819-12824

Michel H., Behr J., Harrenga A. and Kannt A. (1998) Cytochrome c oxidase: Structure and spectroscopy. Ann. Rev. Biophys. Biomol. Struct. 27, 329-356

Mitchell P. (1961) Coupling of phosphorylation to electron and hydrogen transfer by a chemi-osmotic type of mechanism. Nature. 191, 144-148

Mitrovic B., Ignarro L.J., Montestruque S., Smoll A., Merrill J.E. (1994) Nitric oxide as a potential pathological mechanism in demyelination: its differential effects on primary glial cells in vitro. Neuroscience. 61, 575-585

Moellering D., McAndrew J., Patel R.P., Cornwell T., Lincoln T., Cao X., Messina J.L., Forman H.J., Jo H. and Darley-Usmar V.M. (1998) Nitric oxide dependent induction of glutathione synthesis through increased expression of γ-glutamylcysteine synthetase. Arch. Biochem. Biophys. 358, 74-82

Moellering D., McAndrew J., Patel R.P., Forman H.J., Mulcahy R.T., Jo H. and Darley-Usmar V.M. (1999) The induction of GSH synthesis by nanomolar concentrations of nitric oxide in epithelial cells: a role for γ-glutamylcysteine synthetase and γ-glutamyltranspeptidase. FEBS Lett. 448, 292-296

Mohr S., Hallak H., de Boitte A., Lapetina E.G., Brune B. (1999) Nitric oxide-induced S-glutathionylation and inactivation of glyceraldehyde-3-phosphate dehydrogenase. J. Biol. Chem. 274, 9427-9430

Mollace V., Colasanti M., Muscoli C., Lauro G.M., Iannone M., Rotiroti D., and Nistico G. (1998) The effect of nitric oxide on cytokine-induced release of PGE2 by human cultured astroglial cells. Br. J. Pharmacol. 124, 742-746

Montine T., Neely M., Quinn J., Beal M., Markesbery W., Roberts L. and Morrow J. (2002) Lipid peroxidation in aging brain and Alzheimer's disease. Free Radic. Biol. Med. 33, 620

Murphy M.P. (1999) Nitric oxide and cell death. Biochim. Biophys. Acta 1411, 401-14

Mutisya E.M., Bowling A.C. and Beal M.F. (1994) Cortical cytochrome oxidase activity is reduced in Alzheimer's disease. J. Neurochem. 63, 2179-2184

Nagley P. and Wei Y.H. (1998) Ageing and mammalian mitochondrial genetics. Trends. Genet. 14, 513-517

Nakamura K., Bindokas V.P., Marks J.D., Wright D.A., Frim D.M., Miller R.J. and Kang U.J. (2000a) The selective toxicity of 1-methyl-4-phenylpyridinium to dopaminergic neurons: the role of mitochondrial complex I and reactive oxygen species revisited. Mol. Pharmacol. 58, 271-278

Nakamura K., Wright D.A., Wiatr T., Kowlessur D., Milstien S., Lei X.G. and Kang U.J. (2000b) Preferential resistance of dopaminergic neurons to the toxicity of glutathione depletion is independent of cellular glutathione peroxidase and is mediated by tetrahydrobiopterin. J. Neurochem74, 2305-2314

Narita M., Shimizu S., Ito T., Chittenden T., Lutz R.J., Matsuda H. and Tsujimoto Y. (1998) Bax interacts with the permeability transition pore to induce permeability transition and cytochrome c release in isolated mitochondria. Proc. Natl. Acad. Sci. U S A. 95, 14681-14686

Nash B. and Tate S.S. (1984) In vitro translation and processing of rat kidney gamma-glutamyltranspeptidase. J. Biol. Chem. 259, 678-685

Nieminen A.L., Saylor A.K., Tesfai S.A., Herman B., Lemasters J.J. (1995) Contribution of the mitochondrial permeability transition to lethal injury after exposure of hepatocytes to t-butylhydroperoxide. Biochem. J. 307, 99-106

Nishimura J.S., Dodd E.A. and Meister A. (1964) Intermediate formation of dipeptide-phosphate anhydride in enzymatic tripeptide synthesis. J. Biol. Chem. 239, 2553-2558

Njalsson R., Norgren S., Larsson A., Huang C.S., Anderson M.E. and Luo J.L. (2001) Cooperative binding of gamma-glutamyl substrate to human glutathione synthetase. Biochem. Biophys. Res. Commun. 289, 80-84

Noctor G. and Foyer C.H. (1998) Simultaneous measurement of foliar glutathione, γ-glutamylcysteine, and amino acids by high-performance liquid chromatography: Comparison with two other assay methods for glutathione. Anal. Biochemistry. 264, 98-110

Noji H., Yasuda R., Yoshida M. and Kinosita Jnr K. (1997) Direct observation of the rotation of F_1-ATPase. Nature 386, 299-302

Ohnishi T. (1998) Iron-sulfur clusters / semiquinones in complex I. Biochim. Biophys. Acta. 1364, 186-206

Oppenheimer L., Wellner V.P., Griffith O.W. and Meister A. (1979) Glutathione synthetase: purification from rat kidney and mapping of the substrate binding site. J. Biol. Chem. 254, 5184-5190

Orlowski M. and Meister A. (1971) Partial reactions catalyzed by -glutamylcysteine synthetase and evidence for an activated glutamate intermediate. J. Biol. Chem. 246, 7095-7105

Oury T.D., Ho Y.S., Piantadosi C.A., and Crapo J.D. (1992) Extracellular superoxide dismutase, nitric oxide, and central nervous system O2 toxicity. Proc. Natl. Acad. Sci. U S A 89, 9715-9719

Pai E.F. and Schulz G.E. (1983) The catalytic mechanism of glutathione reductase as derived from X-ray diffraction analyses of reaction intermediates. J. Biol. Chem. 258, 1752-1757

Palmer R.M., Ferrige A.G. and Moncada S. (1987) Nitric oxide release accounts for the biological activity of endothelium-derived relaxing factor. Nature **327**, 524-526

Pan Z. and Perez-Polo R. (1993) Role of nerve growth factor in oxidant homeostasis: glutathione metabolism. J. Neurochem. 61, 1713-1721

Papa S., Scacco S., Sardanelli A.M., Vergari R., Papa F., Budde S., van den Heuvel L. and Smeitink J. (2001) Mutations in the NDUFS4 gene of complex I abolishes cAMP dependent activation of the complex in a child with fatal neurological syndrome. FEBS Lett. 489, 259-262

Paradies G., Petrosillo G., Pistolese M. and Ruggerio F.M. (2000) The effect of reactive oxygen species generated from the mitochondrial electron transport chain on the cytochrome c oxidase activity and on the cardiolipin content in bovine heart submitochondrial particles. FEBS Lett. 466, p 323-326

Park L.C., Zhang H., Sheu K.F., Calingasan N.Y., Kristal B.S., Lindsay J.G., and Gibson G.E. (1999) Metabolic impairment induces oxidative stress, compromises inflammatory responses, and inactivates a key mitochondrial enzyme in microglia. J. Neurochem. 72, 1948-1958

Patel R.P., McAndrew J., Sellak H., White C.R., Jo H., Freeman B.A., and Darley-Usmar V.M. (1999) Biological aspects of reactive nitrogen species. Biochim. Biophys. Acta. 1411, 385-400

Paulusma C.C., van Geer M.A., Evers R., Heijn M., Ottenhoff R., Borst P., Oude Elferink R.P. (1999) Canalicular multispecific organic anion transporter/multidrug resistance protein 2 mediates low-affinity transport of reduced glutathione. Biochem. J. 338, 393-401

Perry T.L., Yong V.W., Bergeron C., Hansen S. and Jones K. (1987) Amino acids, glutathione, and glutathione transferase activity in the brains of patients with Alzheimer's disease. Ann. Neurol. 21, 331-336

Pettus E.H., Betarbet R., Cottrell B., Wallace D.C., Madyastha V., Greenamyre J.T. (2000) Immunocytochemical characterization of the mitochondrially encoded ND1 subunit of complex I (NADH : ubiquinone oxidoreductase) in rat brain. J. Neurochem. 75, 383-392

Pineda-Molina E., Klatt P., Vazquez J., Marina A., Garcia de Lacoba M., Perez-Sala D., and Lamas S. Glutathionylation of the p50 subunit of NF-kappaB: a mechanism for redox-induced inhibition of DNA binding. Biochemistry 40, 14134-14142

Przedborski S., Donaldson D., Jakowec M., Kish S.J., Guttman M., Rosoklija G. and Hays A.P. (1996) Brain superoxide dismutase, catalase, and glutathione peroxidase activities in amyotrophic lateral sclerosis. Ann. Neurol. 39, 158-165

Quijano C., Alvarez B., Gatti R.M., Augusto O., and Radi R. (1997) Pathways of peroxynitrite oxidation of thiol groups. Biochem. J. 322, 167-173

Ragan C.I., Wilson M.T., Darley-Usmar V.M. and Lowe P.N. (1987) Subfractionation of mitochondria and isolation of the proteins of oxidative phosphorylation, in Mitochondria, a practical approach. (Darley-Usmar V.M., Rickwood D. and Wilson M.T., eds) 79-112. IRL Press, London.

Ramsay R.R. and Singer T.P. (1986) Energy-dependent uptake of N-methyl-4-phenylpyridinium, the neurotoxic metabolite of 1-methyl-4-phenyl-1,2,3,6-tetrahydropyridine, by mitochondria. J. Biol. Chem. 261, 7585-7587

Ramsay R.R., Krueger M.J., Youngster S.K., Gluck M.R., Casida J.E. and Singer T.P. (1991) Interaction of 1-methyl-4-phenylpyridinium ion (MPP+) and its analogs with the rotenone/piericidin binding site of NADH dehydrogenase. J. Neurochem. 56, 1184-1190

Reyes E. and Barela T.D. (1980) Isolation and purification of multiple forms of gamma-glutamyltranspeptidase from rat brain. Neurochem. Res. 5, 159-170

Rice M.E. (2000) Brain ascorbate. Trends Neurosci. 23, 209-216

Riederer P., Sofic E., Rausch W.D., Schmidt B., Reynolds G.P., Jellinger K., and Youdim M.B.H. (1989) Transition metals, ferritin, glutathione, and ascorbic acid in parkinsonian brains. J. Neurochem. 52, 515-520

Riistama S., Puustinen A., Verkhovsky M.I., Morgan J.E. and Wikstrom M. (2000) Binding of O_2 and its reduction are both retarded by replacement of valine 279 by isoleucine in cytochrome c oxidase from Paracoccus denitrificans. Biochemistry. 39, 6365-6372

Ristoff E. and Larsson A. (1998) Patients with genetic defects in the gamma-glutamyl cycle. Chem. Biol. Interact. 111-112, 113-21

Rosen D.R., Siddique T., Patterson D., Figlewicz D.A., Sapp P., Hentati A., Donaldson D., Goto J., O'Regan J.P. and Deng H.X. (1993) Mutations in Cu/Zn superoxide dismutase gene are associated with familial amyotrophic lateral sclerosis. Nature 362, p 59-62

Sagara J.I., Miura K. and Bannai S. (1993) Maintenance of neuronal glutathione by glial cells. J. Neurochem. 61, 1672-1676

Sagara J., Makino N. and Bannai S. (1996) Glutathione efflux from cultured astrocytes. J. Neurochem. 66, 1876-1881

Sakagami H., Satoh K., Ida Y., Hosaka M., Arakawa H. and Maeda M. (1998) Interaction between sodium ascorbate and dopamine. Free Radic. Biol. Med. 25, 1013-1020

Salvemini F., Franze A., Iervolino A., Filosa S., Salzano S. and Ursini M.V. (1999) Enhanced glutathione levels and oxidoresistance mediated by increased glucose-6-phosphate dehydrogenase expression. J. Biol. Chem. 274, 2750-2757

Sardanelli A.M., Technikova-Dobrova Z., Scacco S.C., Speranza F. and Papa S. (1995) Characterization of proteins phosphorylated by the cAMP-dependent protein kinase of bovine heart mitochondria. FEBS Lett. 377, 470-474

Sazanov L.A., Peak-Chew S.Y., Fearnley I.M. and Walker J.E. (2000) Resolution of the membrane domain of complex I into subcomplexes: Implications for the structural organisation of the enzyme. Biochemistry 39, 7229-7235

Scacco S., Vergari R., Scarpulla R.C., Technikova-Dobrova Z., Sardanelli A., Lambo R., Lorusso V. and Papa S. (2000) cAMP-dependent phosphorylation of the nuclear encoded 18-kDa (IP) subunit of respiratory complex I and activation of the complex in serum-starved mouse fibroblast cultures. J. Biol. Chem. 275, 17578-17582

Schapira A.H.V., Cooper J.M., Dexter D., Clark J.B., Jenner P., and Marsden C.D. (1990) Mitochondrial complex I deficiency in Parkinson's disease. J. Neurochem. 54, 823-827

Schapira A.H. (1999) Mitochondrial involvement in Parkinson's disease, Huntington's disease, hereditary spastic paraplegia and Friedreich's ataxia. Biochim. Biophys. Acta. 1410, 159-170

Scheffler I.E. (1999). Mitochondria. Wiley-Liss, New York.

Schopfer F., Riobo N., Carreras M.C., Alvarez B., Radi R., Boveris A., Cadenas E. and Poderoso J.J. (2000) Oxidation of ubiquinol by peroxynitrite: implications for protection of mitochondria against nitrosative damage. Biochem. J. 349, 35-42

Schuppe-Koistinen I., Gerdes R., Moldeus P. and Cotgreave I.A. (1994) Studies on the reversibility of protein S-thiolation in human endothelial cells. Arch. Biochem. Biophys. 315, 226-234

Schulz H. (1987) Inhibitors of fatty acid oxidation. Life Sci. 40, p 1443-1449

Schulz J.B., Lindenau J., Seyfried J. and Dichgans J. (2000) Glutathione, oxidative stress and neurodegeneration. Eur. J. Biochem. 267, 4904-4911

Seelig G.F. and Meister A. (1982) Cystamine-Sepharose. A probe for the active site of gamma-glutamylcysteine synthetase. J. Biol. Chem. 257, 5092-5096

Seelig G.F. and Meister A. (1984) γ-glutamylcysteine synthetase. J. Biol. Chem. 259, 3534-3538

Seelig G.F. and Meister A. (1985) Glutathione biosynthesis; γ-glutamylcysteine synthetase from rat kidney. Methods Enzymol. 113, 379-390

Sekhar K.R., Spitz D.R., Harris S., Nguyen T.T., Meredith M.J., Holt J.T., Guis D., Marnett L.J., Summar M.L., and Freeman M.L. (2002) Redox-sensitive interaction between KIAA0132 and Nrf2 mediates indomethacin-induced expression of gamma-glutamylcysteine synthetase. Free Radic. Biol. Med. 32, 650-662

Shan X., Jones D.P., Hashmi M. and Anders M.W. (1993) Selective depletion of mitochondrial glutathione concentrations by (R,S)-3-hydroxy-4-pentenoate potentiates oxidative cell death. Chem. Res. Toxicol. 6, 75-81

Sharpe M.A. and Cooper C.E. (1998) Interaction of peroxynitrite with mitochondrial cytochrome oxidase. Catalytic production of nitric oxide and irreversible inhibition of enzyme activity. J. Biol. Chem. 273, 30961-30972

Shenoy S.K., Yu L. and Yu C. (1999) Identification of quinone-binding and heme-ligating residues of the smallest membrane anchoring subunit (QPs3) of

bovine heart mitochondrial succinate:ubiquinone reductase. J. Biol. Chem. 274, 8717-8722

Sheta E.A., McMillan K., and Masters B.S. (1994) Evidence for a bidomain structure of constitutive cerebellar nitric oxide synthase. J. Biol. Chem. 269, 15147-15153

Shepherd J.A. and Garland P.B. (1969) Citrate synthase from rat liver. Methods Enzymol. 13, 11-19

Shimizu S., Narita M. and Tsujimoto Y. (1999) Bcl-2 family proteins regulate the release of apoptogenic cytochrome c by the mitochondrial channel VDAC. Nature 399, 483-7

Shine H.D. and Haber B. (1981) Immunocytochemical localization of gamma-glutamyl transpeptidase in the rat CNS. Brain Res. 217, 339-349

Sian J., Dexter D.T., Lees A.J., Daniel S., Ayid Y., Savoy-Agid F., Jenner P. and Marsden C.D. (1994a) Alterations in glutathione levels in Parkinson's disease and other neurodegenerative diseases affecting basal ganglia. Ann. Neurol. 36, 348-355

Sian J., Dexter D.T., Lees A.J., Daniel S., Jenner P. and Marsden C.D. (1994b) Glutathione-related enzymes in brain in Parkinson's disease. Ann. Neurol. 36, 356-361

Sies H. (1999) Glutathione and its role in cellular functions. Free Radic. Biol. Med. 27, 916-921

Simmons M.L., and Murphy S. (1992) Induction of nitric oxide synthase in glial cells. J. Neurochem. 59, 897-905

Sims N.R., Anderson M.F., Hobbs L.M., Kong J.Y., Phillips S., Powell J.A., Zaidan E. (2000) Impairment of brain mitochondrial function by hydrogen peroxide. Brain Res. Mol. Brain Res. 77, 176-184

Singh S.P., Wishnok J.S., Keshive M., Deen W.M. and Tannenbaum S.R. (1996) The chemistry of the S-nitrosoglutathione/glutathione system. Proc. Natl. Acad. Sci. U S A. 93, 14428-14433

Smith M.A., Richey Harris P.L., Sayre L.M., Beckman J.S. and Perry G. (1997) Widespread peroxynitrite-mediated damage in Alzheimer's disease. J. Neurosci. 17, 2653-2657

Snyder C.H., Gutierrez-Cirlos E.B. and Trumpower B.L. (2000) Evidence for a concerted mechanism of ubiquinol oxidation by the cytochrome bc_1 complex. J. Biol.Chem. 275, 13531-13541

Soltaninassab S.R., Sekhar K.R., Meredith M.J. and Freeman M.L. (2000) Multi-faceted regulation of γ-glutamylcysteine synthetase. J. Cell. Physiol. 182, 163-170

Sriram K., Shankar S.K., Boyd M. and Ravindranath V. (1998) Thiol oxidation and loss of mitochondrial complex I precedes excitatory amino acid mediated neurodegeneration. J. Neurosci. 18, 0287-10296

Stewart V.C., Land J.M., Clark J.B., and Heales S.J.R. (1998a) Pretreatment of astrocytes with interferon-alpha/beta prevents neuronal mitochondrial respiratory chain damage. J. Neurochem. 70, 432-434

Stewart V.C., Land J.M., Clark J.B. and Heales S.J. (1998b) Comparison of mitochondrial respiratory chain enzyme activities in rodent astrocytes and neurones and a human astrocytoma cell line. Neurosci. Lett. 247, 201-203

Stewart V.C., Sharpe M.A., Clark J.B. and Heales S.J.R (2000) Astrocyte-derived nitric oxide causes both reversible and irreversible damage to the neuronal mitochondrial respiratory chain. J. Neurochem. 75, 694-700

Stole E., Seddon A.P., Wellner D. and Meister A. (1990) Identification of a highly reactive threonine residue at the active site of gamma-glutamyl transpeptidase. Proc. Natl. Acad. Sci. U S A. 87, 1706-1709

Stole E., Smith T.K., Manning J.M., and Meister A. (1994) Interaction of gamma-glutamyl transpeptidase with acivicin. J. Biol. Chem. 269, 21435-21439

Stone R., Stewart V.C., Hurst R.D., Clark J.B., and Heales S.J.R. (1999) Astrocyte nitric oxide causes neuronal mitochondrial damage, but antioxidant release limits neuronal cell death. Ann. N. Y. Acad. Sci. 893, 400-403

Stuehr D.J, Cho H.J., Kwon N.S., Weise M.F., and Nathan C.F. (1991) Purification and characterization of the cytokine-induced macrophage nitric oxide synthase: an FAD- and FMN-containing flavoprotein.Proc. Natl. Acad. Sci. U S A. 88,7773-7777

Stuehr D.J. (1999) Mammalian nitric oxide synthases. Biochim. Biophys. Acta. 1411, 217-230

Sun W., Huang Z. and Lu S.C. (1996) Regulation of γ-glutamylcysteine synthetase by protein phosphorylation. Biochem. J. 320, 321-328

Susin S.A., Zamzami N., Castedo M., Hirsch T., Marchetti P., Macho A., Daugas E., Geuskens M. and Kroemer G. (1996) Bcl-2 inhibits the mitochondrial release of an apoptogenic protease. J. Exp. Med. 184, 1331-1341

Swerdlow R.H., Parks J.K., Cassarino D.S., Trimmer P.A., Miller S.W., Maguire D.J., Sheehan J.P., Maguire R.S., Pattee G., Juel V.C., Phillips L.H., Tuttle J.B., Bennett J.P. Jr, Davis R.E. and Parker W.D Jr. (1998) Mitochondria in sporadic amyotrophic lateral sclerosis. Exp. Neurol. 153, 135-142

Taanman J.W. (1999) The mitochondrial genome: structure, transcription, translation and replication. Biochim. Biophys. Acta. 1410, 103-123

Tabernero A., Bolanos J.P. and Medina J.M. (1993) Lipogenesis from lactate in rat neurones and astrocytes in primary culture. Biochem J. 294, 635-638

Tamura T., McMicken H.W., Smith C.V. and Hansen T.N. (1996) Mitochondrial targeting of glutathione reductase requires a leader sequence. Biochem. Biophys. Res. Commun. 222, 659-663

Tatoyan A. & Giulivi C. (1998) Purification and characterization of a nitric-oxide synthase from rat liver mitochondria. J. Biol. Chem. 273, 11044-11048

Tatton W.G. and Olanow C.W. (1999) Apoptosis in neurodegenerative diseases: the role of mitochondria. Biochim. Biophys. Acta. 1410, 195-213

Tian L., Shi M.M. and Forman H.J. (1997) Increased transcription of the regulatory subunit of γ-glutamylcysteine synthetase in rat lung epithelial L2 cells exposed to oxidative stress or glutathione depletion. Arch. Biochem. Biophys. 342, 126-133

Thompson S.A., White C.C., Krejsa C.M., Diaz D., Woods J.S., Eaton D.L., Kavanagh T.J. (1999) Induction of glutamate-cysteine ligase (gamma-glutamylcysteine synthetase) in the brains of adult female mice subchronically exposed to methylmercury. Toxicol. Lett. 110, 1-9

Tormo J.R and Estornell E. (2000) New evidence for the multiplicity of ubiquinone and inhibitor binding sites in the mitochondrial complex I. Arch. Biochem. Biophys. 381, 241-246

Ton C., Hwang D.M., Dempsey A.A. and Liew C.C. (1997) Identification and primary structure of five human NADH-ubiquinone oxidoreductase subunits. Biochem. Biophys. Res. Commun. 241, 589-594

Tsuchiya K., Mulcahy R.T., Reid L.L., Disteche C.M. and Kavanagh T.J. (1995) Mapping of the glutamate-cysteine ligase catalytic subunit gene (GLCLC) to

human chromosome 6p12 and mouse chromosome 9D-E and of theregulatory subunit gene (GLCLR) to human chromosome 1p21-p22 and mouse chromosome 3H1-3. Genomics. 30, 630-632

Tsukihara T., Aoyama H., Yamashita E., Tomizaki T., Yamagucji H., Shinzawa-Itoh K., Nakashima R. Yaona R. and Yoshikawa S. (1996) The whole structure of the 13-subunit oxidised cytochrome c oxidase at 2.8 Å. Science. 272, 1136-1144

Tsunoda S., Aggeler R., Yoshida M. and Capaldi R.A. (2001) Rotation of the c subunit oligomer in fully functional F_1F_0 ATP synthase. Proc. Natl. Acad. Sci 98, 898-902

Tu Z. and Anders M.W. (1998a) Expression and characterisation of human glutamate-cysteine ligase. Arch. Biochem. Biophys. 15, 247-254

Tu Z. and Anders M.W. (1998b) Identification of an important cysteine residue in human glutamate-cysteine ligase catalytic subunit by site directed mutagenesis. Biochem J. 336, 675-680

Vasquez O.L., Almeida A., and Bolanos J.P. (2001) Depletion of glutathione up-regulates mitochondrial complex I expression in glial cells. J. Neurochem. 76, 1593-1596

Vassault A. (1983) L-Lactate dehydrogenase. UV method with pyruvate and NADH, in Methods of Enzymatic Analysis, Vol. 3 (Bergmeyer J. and Grassl M., eds) 118-126. Verlag Chemie GmbH, Weinheim

Videira A. (1998) Complex I from the fungus Neurospora crassa. Biochim. Biophys. Acta. 1364, 89-100

Viner R.I., Williams T.D., Schoneich C. (1999) Peroxynitrite modification of protein thiols: oxidation, nitrosylation, and S-glutathiolation of functionally

important cysteine residue(s) in the sarcoplasmic reticulum Ca-ATPase. Biochemistry. 38, 12408-12415

Voehringer D.W., McConkey D.J., McDonnel T.J., Brisbay S., and Meyn R.E. (1998) Bcl-2 expression causes redistribution of glutathione to the nucleus. Proc. Natl. Acad. Sci. USA 95, 2956-2960

Voet D. and Voet J.G. (1990) Biochemistry. Wiley Publishing.

Wainio W.W. (1955) Reactions of cytochrome oxidase. J. Biol. Chem. 212, 723-733

Wang X.F. and Cynader C.S. (2000) Astrocytes provide cysteine to neurons by releasing glutathione. J. Neurochem. 74, 1434-1142

Wild A.C. and Mulcahy R.T. (2000) Regulation of gamma-glutamylcysteine synthetase subunit gene expression: insights into transcriptional control of antioxidant defenses. Free Radic. Res. 32, 281-301

Winters R.A., Zukowski J., Ercal N., Matthews R.H. and Spitz D.R. (1995) Analysis of glutathione, glutathione disulfide, cysteine, homocysteine, and other biological thiols by high-performance liquid chromatography following derivatization by n-(1-pyrenyl)maleimide. Anal Biochem. 227, 14-21

Wharton D.C. and Tzagoloff A. (1967) Cytochrome oxidase from beef heart mitochondria. Methods Enzymol. 10, 245-250

Wullner U., Seyfried J., Groscurth P., Beinroth S., Winter S., Gleichmann M., Heneka M., Loschmann A., Schulz J.B., Weller M. and Klockgether T. (1999) Glutathione depletion and neuronal cell death: the role of reactive oxygen intermediates and mitochondrial function. Brain. Res. 826, 53-62

Yamane Y., Furuichi M., Song R., Van N.T., Mulcahy R.T., Ishikawa T. and Kuo M.T. (1998) Expression of multidrug resistance protein/GS-X pump and gamma-

glutamylcysteine synthetase genes is regulated by oxidative stress. J. Biol. Chem. 273, 31075-31085

Yang J., Liu X., Bhalla K., Kim C.N., Ibrado A.M., Cai J., Peng T.I., Jones D.P., Wang X. (1997) Prevention of apoptosis by Bcl-2: release of cytochrome c from mitochondria blocked. Science. 275, 1129-1132

Yang H., Wang J., Ou X., Huang Z.Z., Lu S.C. (2001a) Cloning and analysis of the rat glutamate-cysteine ligase modifier subunit promoter. Biochem. Biophys. Res. Commun. 285, 476-482

Yang H., Wang J., Huang Z.Z., Ou X., Lu S.C. (2001b) Cloning and characterization of the 5'-flanking region of the rat glutamate-cysteine ligase catalytic subunit. Biochem. J. 357, 447-455

Yim M.B., Kang J.H., Yim H.S., Kwak H.S., Chock P.B., Stadtman E.R. (1996) A gain-of-function of an amyotrophic lateral sclerosis-associated Cu,Zn-superoxide dismutase mutant: An enhancement of free radical formation due to a decrease in Km for hydrogen peroxide. Proc. Natl. Acad. Sci. U S A. 93, 5709-5714

Yip B. and Rudolph F.B. (1976) The kinetic mechanism of rat kidney γ-glutamylcysteine synthetase. J. Biol. Chem. 251, 3563-3568

Yoshikawa S., Shinzawa-Itoh K. and Tsukihara T. (2000) X-ray structure and reaction mechanism of bovine heart cytochrome c oxidase. J. Inorg. Biochem. 82, p 1-7

Yudkoff M., Nissim I., and Hertz L. (1990) Precursors of glutamic acid nitrogen in primary neuronal cultures: studies with 15N glutamate. Neurochem. Res. 15, 1191-1196

Zaidan E., Nilsson M. and Sims N.R. (1999) Cyclosporin A-sensitive changes in mitochondrial glutathione are an early response to intrastriatal NMDA or forebrain ischaemia in rats. J. Neurochem. 73, 2214-2217

Zhang W.W., Churchill S. and Churchill P. (1989) Developmental regulation of D-beta-hydroxybutyrate dehydrogenase in rat liver and brain. FEBS Lett. 256, 71-74.

Zhang Y., Marcillat O., Giulivi C., Ernster L. and Davies K.J. (1990) The oxidative inactivation of mitochondrial electron transport chain components and ATPase. J. Biol. Chem. 265, 16330-16336

Zhang Z., Huang L., Schulmeister V.M., Chi Y., Kim K.K., Hunh L., Crofts A.R., Berry E.A. and Kim S. (1998) Electron transfer by domain movement in cytochrome bc_1. Nature 392, 677-684

Zhang Y., Dawson V.L. and Dawson T.M. (2000) Oxidative stress and genetics in the pathogenesis of Parkinson's disease. Neurobiol. Dis. 7, 240-250

Zipper L.M. and Mulcahy R.T. (2000) Inhibition of ERK and p38 MAP kinases inhibits binding of Nrf2 and induction of GCS genes. Biochem. Biophys. Res. Commun. 278, 484-492

Appendix 1

Publications

0.005% (w/v) trypsin (550 units). Cells were cultured in 80 cm^2 flasks in D-valine-based minimal essential medium supplemented with 10% fetal calf serum and 2 mM glutamine for 7 days (media changed every 3 days). D-Valine-based minimal essential medium inhibits the growth of fibroblasts, while allowing astrocytes to proliferate (25). The cells were then split and the media changed to minimal essential medium (L-valine substituted for D-valine) and supplemented as above. The astrocytes were then cultured for a further 7 days until confluent.

Determination of GCL Activity in Cultured Astrocytes

Astrocytes (14 days after isolation) were removed from flasks with trypsin and centrifuged at 500*g*. Cells were resuspended in isolation medium (320 mM sucrose, 10 mM Tris, 1 mM EDTA (K^+ salt), pH 7.4) and freeze/thawed in liquid nitrogen three times. Samples were centrifuged at 3000*g* for 5 min at 4°C to pellet cell debris. The supernatant was then centrifuged through a microcon centrifugal filter device with a 10-kDa molecular mass cutoff filter at 12,000*g* for 15 min at 4°C. Approximately 70% of the liquid was forced through the columns. No wash steps are necessary during the procedure. This step removes glycine, other amino acids, cofactors, and small molecules (e.g., GSH) from the cell extracts preventing (i) the conversion of γ-GC to GSH during the course of the assay (see reaction [b]) and (ii) GSH and other molecules interfering with the assay. An aliquot of retained protein (10–40 μg protein) was mixed with assay buffer (0.1 M Tris-HCl, 0.15 M KCl, 20 mM $MgCl_2$, 2 mM EDTA (K^+ salt), pH 8.2), 10 mM ATP, 10 mM L-cysteine, 40 mM L-glutamate, and 220 μM acivicin (total volume 100 μl) for 15 min at 37°C. Note that during optimization of the assay, higher concentrations of cysteine (≥20 mM) interfered with the assay. To assess the specificity of the assay, the samples were preincubated with 5 nM–5 mM L-buthionine-*SR*-sulfoximine (L-BSO), a specific inhibitor of GCL (26), and 10 mM ATP for 5 min at room temperature and then assayed as above in the presence of L-BSO. The reaction was stopped by the addition of 1 vol of 15 mM orthophosphoric acid and centrifugation at 14,000*g* for 5 min. The γ-GC in the supernatant was then separated by HPLC as described above.

γ-Glutamyltranspeptidase Assay

γ-Glutamyltranspeptidase activity was measured using a diagnostic kit purchased from Sigma Diagnostics. γ-Glutamyltranspeptidase catalyzes the formation of 5-amino-2-nitrobenzoate from γ-glutamyl-3-carboxy-4-nitroanilide at 37°C. Enzyme activity was followed at an absorbance of 405 nm.

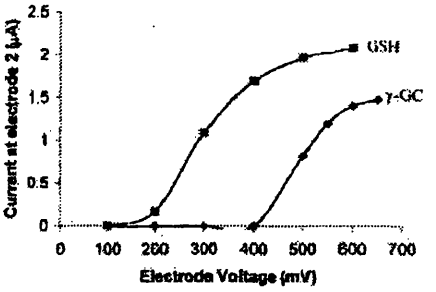

FIG. 1. Voltamogram of γ-GC. γ-GC and GSH standards (5 μM were separated by reverse-phase HPLC and detected electrochemically. Electrode 1 was set at 100 mV, while electrode 2 voltage was sequentially increased by 50-mV increments. Optimal γ-GC and GSH detection occurs when the voltage of the downstream electrode is +600 to +650 mV.

Protein Determination

Protein concentration of samples was determined by the method described by Lowry *et al.* (27).

Statistical Analysis

Data are expressed as means ± SEM where *n* = number of independent cell culture preparations. Linear regression was calculated using Microsoft Excel.

RESULTS

Chromatography and Electrochemical Detection of γ-GC

The thiol group of GSH can be detected electrochemically following HPLC separation using orthophosphoric acid as the mobile phase (21). We hypothesized that γ-GC should be amenable to the HPLC conditions used for GSH and should also be electrochemically active under such conditions. γ-GC standards (5 μM) were separated by reverse-phase HPLC and measured at various downstream electrode potentials to ascertain the optimal parameters for γ-GC detection (see Materials and Methods; Fig. 1). γ-GC was electrochemically active. The voltamogram revealed attainment of a plateau between +600 and +650 mV. However, when astrocyte samples were analyzed (see below), several extra peaks were detected at +650 mV compared to +600 mV, which obscured detection of γ-GC. Consequently a downstream electrode potential of +600 mV was chosen for optimal γ-GC detection. Detection of γ-GC was linear between 1 and 10 μM (correlation coefficient, 0.9984).

Electrochemical detection of both γ-GC and GSH occurred at a potential of +600 mV (Fig. 1). However the voltamogram of γ-GC was distinct from that of GSH. Furthermore, the signal generated by equimolar γ-GC was less than that for GSH. As the GSH and

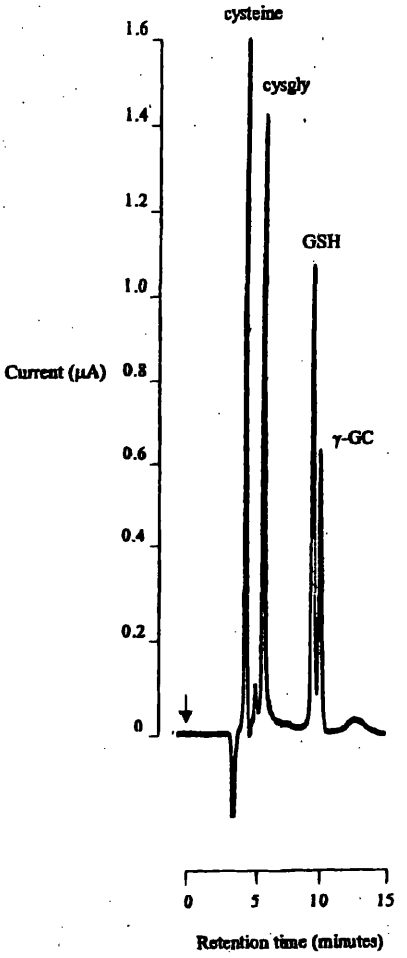

FIG. 2. Chromatogram of γ-GC, GSH, cysteine, and cysteinylglycine standards (2.5 μM). Arrow denotes injection of standards.

γ-GC were between 98 and 99% in the reduced form, this difference in signal is likely related to the difference in electrochemical properties of the two molecules under the chromatographic conditions employed. Separation of γ-GC and GSH standards by HPLC is shown in Fig. 2. The retention time of γ-GC was 11.4 min and was, under the conditions employed, 30 s longer than GSH (10.9 min). The results above indicate that γ-GC and GSH are distinguishable from each other when using reverse-phase HPLC with electrochemical detection.

GCL Activity in Cultured Astrocytes

The GCL assay described here has been developed using samples derived from rat primary astrocyte cultures. Following incubation of astrocyte cell extracts with the assay reaction mixture, γ-GC could clearly b detected (Fig. 3). GCL activity was calculated by mea suring the amount of γ-GC synthesized over a define period of time and related to the protein content of th sample assayed. The activity of GCL in astrocytes wa estimated to be 9.7 ± 1.7 nmol γ-GC synthesized min/mg protein (n = 9 independent cell culture prep arations). The method was reproducible; activity of a astrocyte homogenate assayed three times in separat reaction mixtures (e.g., different assay buffer, ATP was 6.1 ± 0.4 nmol/min/mg protein.

The GCL assay is linear with respect to both protei (10 to 40 μg of protein (Fig. 4a)) and time (0 to 20 mi (Fig. 4b)). Assaying of 5 μg of protein generated a smal γ-GC peak (≤0.2 μA); however, this was found to be a the limit of detection and is not advisable.

When the assay was performed in the presence o L-buthionine-(*SR*)-sulfoximine (5 mM) synthesis o γ-GC was totally abolished. Astrocyte samples were also incubated with a range of L-BSO concentrations (5

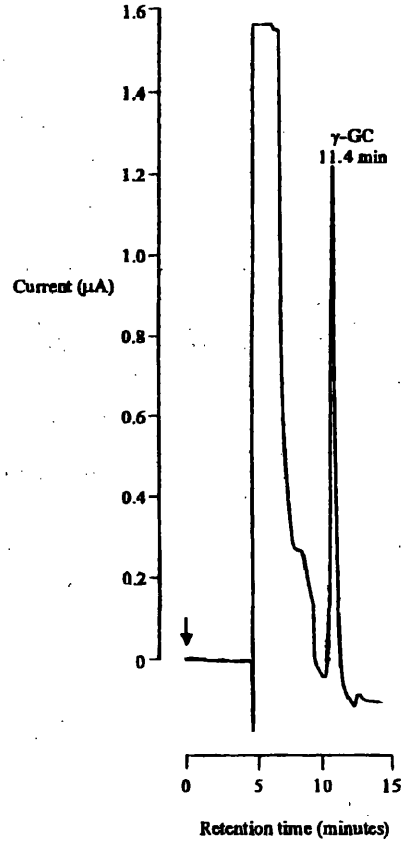

FIG. 3. GCL assay chromatogram. Astrocyte cell extracts were incubated as described in the text. Arrow denotes injection of sample.

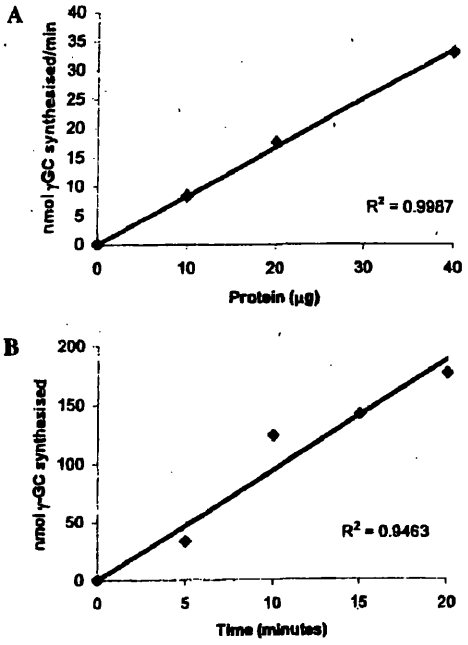

FIG. 4. GCL activity against protein (A) and time (B). Sample was assayed for 15 min when determining linearity against protein, and 15 μg of protein was assayed for each time point in plot B. Each point was assayed in triplicate (see text for details).

nM–500 μM) to obtain an inhibition curve (Fig. 5). The K_i of L-BSO was estimated to be approximately 100 μM. No γ-GC peak was observed following incubation of sample with just ATP alone (no cysteine or glutamate). Both cysteine and cysteinylglycine (derived from the enzymatic degradation of GSH by γ-glutamyltranspeptidase (γ-GT)) were found to have a shorter retention time than γ-GC (Fig. 2) and did not interfere with the γ-GC peak. The electrode potentials used in this assay do not detect cystine or GSSG (oxidized glutathione). It should be noted that a residual GSH peak is occasionally observed following sample preparation. The amount of residual GSH was estimated to be 0.91 ± 0.1 μM (n = 7). This should not affect the assay, as the K_i of GCL for GSH is 8.2 mM (7). A 97–100% (n = 3) recovery of γ-GC standard was obtained when samples were spiked, indicating that there was little loss of product following acid extraction and precipitation of protein prior to loading on to the HPLC column. Spiking also indicated that there was no metabolism of γ-GC by enzymes in the cell extract such as γ-GT and γ-glutamylcyclotransferase of the γ-glutamyl cycle (5). Note that γ-GT activity in the astrocyte samples (measured spectrophotometrically) was completely abolished within 1 min when treated with the acivicin concentration used in the GCL assay.

DISCUSSION

In the present study we have reported that γ-GC i electrochemically active. This has enabled us to de velop a GCL assay based on the electrochemical dete tion of γ-GC synthesized in the assay. Separation c synthesized γ-GC is achieved by reverse-phase HPLC This assay appears specific as γ-GC synthesis was tc tally abolished in the presence of L-buthionine-(*SR*) sulfoximine. This rapid, convenient, and sensitive as say allows GCL activity to be measured in culture cells such as astrocytes. Furthermore, the electrochem ical conditions used, once established, result in highl reproducible results.

This assay estimated that GCL activity in culture rat astrocytes was 9.7 ± 1.7 nmol γ-GC synthesized min/mg protein. The activity of GCL in chick astrocyte has been reported to be 2.8 ± 0.5 nmol γ-GC synthe sized/min/mg protein (22). However, wide ranges o GSH levels have been reported in astrocytes. Indeed variability of GSH levels in both animals and primar cell cultures has been observed between batches (28- 30). Furthermore, GCL activity has also been shown t be sensitive to low levels of stress (4, 11). In view o potential variability, we recommend that for each cel culture preparation, linearity of the assay against pro tein, time, and L-BSO sensitivity should be deter mined.

Chick GCL activity was estimated by measurin the activity of a coupled enzyme, γ-glutamylcyclo transferase (31) (reaction [c], route 2). The couple enzyme assay measures the production of ^{14}C-la beled 5-oxo-proline from labeled glutamate in the pres ence of aminobutyrate (instead of cysteine) and ar excess of γ-glutamylcyclotransferase. Unfortunatel γ-glutamylcyclotransferase is not commercially avail able and is therefore less convenient than the assa

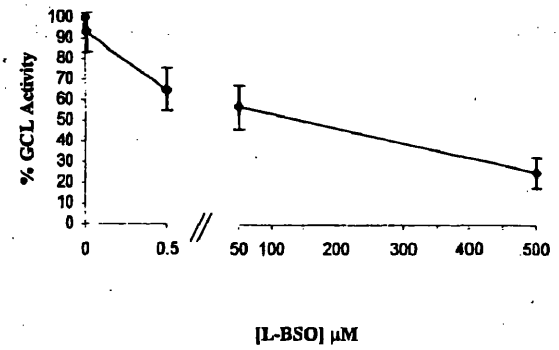

FIG. 5. L-BSO inhibition curve. Sample (15 μg) was preincubate with L-BSO (0–500 μM) and 10 mM ATP for 5 min at room temper ature. GCL activity was then assayed in the presence of L-BSO Three independent cell culture preparations were assayed.

described here and also prevented us from making a direct comparison.

$$\text{L-Cys} + \text{L-Glu} \xrightarrow{GCL} \gamma\text{-GC} \xrightarrow{2} \text{5-oxoproline} + \text{L-Cys}$$
$$\downarrow 1$$
$$\text{GSH}$$

[c]

The L-BSO inhibition curve in Fig. 5 estimates that the K_i of GCL for L-BSO is approximately 100 μM. This compares favorably with previous inhibition studies of mammalian GCL. Cloned human GCL shows a 50% loss of activity when preincubated with 50 μM L-BSO for 5 min (32). GCL activity in this case was measured by the widely used spectrophotometric method described by Seelig and Meister (16).

Increased transcription of either one or both subunits of GCL has been reported following a variety of stimuli (e.g., oxidative stress, GSH depleting agents, transition metals (4, 10, 12, 13)). This assay will complement such expression studies by determining whether changes in transcription results in altered enzyme activity in the cytosol. Furthermore, loss of GSH has also been reported in ageing and several diseases such as Parkinson's disease (14, 15). This method will be useful in ascertaining whether alterations in GCL activity are associated with such disorders.

ACKNOWLEDGMENTS

We are grateful to the Brain Research Trust (UK) for supporting this work and to Dr. Juan Bolanos (University of Salamanca, Spain) and Dr. Ralf Dringen (University of Tubingen, Germany) for their helpful discussions.

REFERENCES

1. Bolanos, J. P., Heales, S. J. R., Land, J. M., and Clark, J. B. (1995) Effect of peroxynitrite on the mitochondrial respiratory chain: Differential susceptibility of neurones and astrocytes in primary culture. *J. Neurochem.* **64**, 1965–1972.
2. Barker, J. E., Bolanos, J. P., Land, J. M., Clark, J. B., and Heales, S. J. R. (1996) Glutathione protects astrocytes from peroxynitrite mediated mitochondrial damage: Implications for neuronal/astrocytic trafficking and neurodegeneration. *Dev. Neurosci.* **18**, 391–396.
3. Dringen, R., Pfeiffer, B., and Hamprecht, B. (1999) Synthesis of the antioxidant glutathione in neurones: Supply by astrocytes of CysGly as precursor for neuronal glutathione. *J. Neurosci.* **19**, 562–569.
4. Lu, S. C. (2000) Regulation of glutathione synthesis. *Curr. Top. Cell. Regul.* **36**, 95–116.
5. Meister, A., and Anderson, M. E. (1983) Glutathione. *Annu. Rev. Biochem.* **52**, 711–760.
6. Yip, B., and Rudolph, F. B. (1976) The kinetic mechanism of rat kidney γ-glutamylcysteine synthetase. *J. Biol. Chem.* **251**, 3563–3568.
7. Huang, C. S., Chang, L. S., Anderson, M. E., and Meister, A. (1993) Catalytic and regulatory properties of the heavy subunit of rat kidney γ-glutamylcysteine synthetase. *J. Biol. Chem.* **268** 19675–19680.
8. Tu, Z., and Anders, M. W. (1998) Expression and characterisation of human glutamate-cysteine ligase. *Arch. Biochem. Biophys.* **15**, 247–254.
9. Buckley, B. J., and Whorton, A. R. (2000) Adaptive response to peroxynitrite: Increased glutathione levels and cystine uptake in vascular cells. *Am. J. Physiol. Cell. Physiol.* **279**, C1168–C1176.
10. Iwata-Ichikawa, E., Kondo, Y., Miyazaki, I., Asanuma, M., and Ogawa, N. (1999) Glial cells protect neurones against oxidative stress via transcriptional upregulation of the glutathione synthesis. *J. Neurochem.* **72**, 2334–2344.
11. Moellering, D., McAndrew, J., Patel, R. P., Forman, H. J. Mulcahy, R. T., Jo, H., and Darley-Usmar, V. M. (1999) The induction of GSH synthesis by nanomolar concentrations of nitric oxide in epithelial cells: A role for γ-glutamylcysteine synthetase and γ-glutamyltranspeptidase. *FEBS Lett.* **448**, 292–296.
12. Moellering, D., McAndrew, J., Patel, R. P., Cornwell, T., Lincoln T., Cao, X., Messina, J. L., Forman, H. J., Jo, H., and Darley-Usmar, V. M. (1998) Nitric oxide dependent induction of glutathione synthesis through increased expression of γ-glutamylcysteine synthetase. *Arch. Biochem. Biophys.* **358**, 74–82.
13. Cai, J., Huang, Z., and Lu, S. C. (1997) Differential regulation of γ-glutamylcysteine synthetase heavy and light subunit gene expression. *Biochem. J.* **326**, 167–172.
14. Sian, J., Dexter, D. T., Lees, A. J., Daniel, S., Ayid, Y., Savoy-Agid, F., Jenner, P., and Marsden, C. D. (1994) Alterations in glutathione levels in Parkinson's disease and other neurodegenerative diseases affecting basal ganglia. *Ann. Neurol.* **36**, 348–355.
15. Schulz, J. B., Lindenau, J., Seyfried, J., and Dichgans, J. (2000) Glutathione, oxidative stress and neurodegeneration. *Eur. J. Biochem.* **267**, 4904–4911.
16. Seelig, G. F., and Meister, A. (1984) γ-Glutamylcysteine synthetase. *J. Biol. Chem.* **259**, 3534–3538.
17. Birago, C., Marchei, E., Pennino, R., and Valvo, L. (2001) Assay of γ-glutamylcysteine synthetase activity in *Plasmodium berghei* by liquid chromatography with electrochemical detection. *J. Pharm. Biomed. Anal.* **25**, 759–765.
18. Noctor, G., and Foyer, C. H. (1998) Simultaneous measurement of foliar glutathione, γ-glutamylcysteine, and amino acids by high-performance liquid chromatography: Comparison with two other assay methods for glutathione. *Anal. Biochem.* **264**, 98–110.
19. Liu, R. M., Gao, L., Choi, J., and Forman, H. J. (1998) γ-Glutamylcysteine synthetase: mRNA stabilisation and independent subunit transcription by 4-hydroxyl-2-nonenal. *Am. J. Physiol.* **275**, L861–L869.
20. Winters, R. A., Zukowski, J., Ercal, N., Matthews, R. H., and Spitz, D. R. (1995) Analysis of glutathione, glutathione disulfide, cysteine, homocysteine, and other biological thiols by high-performance liquid chromatography following derivatization by *n*-(1-pyrenyl)maleimide. *Anal. Biochem.* **227**, 14–21.
21. Riederer, P., Sofic, E., Rausch, W. D., Schmidt, B., Reynolds, G. P., Jellinger, K., and Youdim, M. B. H. (1989) Transition metals, ferritin, glutathione, and ascorbic acid in parkinsonian brains. *J. Neurochem.* **52**, 515–520.
22. Makar, T. K., Nedergaard, M., Preuss, A., Gelbard, A. S., Perumal, A. S., and Cooper, A. J. L. (1994) Vitamin E, ascorbate, glutathione, glutathione disulfide, and enzymes of glutathione metabolism in cultures of chick astrocytes and neurons: Evi-

dence that astrocytes play an important role in antioxidative processes in the brain. *J. Neurochem.* **62**, 45–53.

23. Ellman, G. L. (1959) Tissue sulfhydryl groups. *Arch. Biochem. Biophys.* **82**, 70–77.
24. Tabernero, A., Bolanos, J. P., and Medina, J. M. (1993) Lipogenesis from lactate in rat neurones and astrocytes in primary culture. *Biochem. J.* **294**, 635–638.
25. Cholewinski, A. J., Reid, J. C., McDermott, A. M., and Wilkin, G. P. (1989) Purification of astroglial cell cultures from rat spinal cord—The use of D-valine to inhibit fibroblast growth. *Neurochem. Int.* **15**, 365–369.
26. Griffith, O. W., and Meister, A. (1979) Potent and specific inhibition of glutathione synthesis by buthionine sulfoximine (*S-n*-butyl homocysteine sulfoximine). *J. Biol. Chem.* **254**, 7558–7560.
27. Lowry, O. H., Rosebrough, N. J., Farr, A. L., and Randall, R. J. (1951) Protein measurement with the Folin phenol reagent. *J. Biol. Chem.* **193**, 265–275.
28. Cock, H. R., Tong, X., Hargreaves, I. P., *et al.* (in press) Mitochondrial dysfunction associated with neuronal death following status epilepticus in rat. *Epilepsy Res.*
29. Bolanos, J. P., Peuchen, S., Heales, S. J. R., Land, J. M., and Clark, J. B. (1994) Nitric oxide-mediated inhibition of the mitochondrial respiratory chain in cultured astrocytes. *J. Neurochem.* **63**, 910–916.
30. Bolanos, J. P., Heales, S. J. R., Land, J. M., and Clark, J. B. (1995) Effect of peroxynitrate on the mitochondrial respiratory chain: Differential susceptibility of neurones and astrocytes in primary culture. *J. Neurochem.* **64**, 1965–1972.
31. Seelig, G. F., and Meister, A. (1985) Glutathione biosynthesis; γ-glutamylcysteine synthetase from rat kidney. *Methods Enzymol.* **113**, 379–390.
32. Y. Kelly, B. S., Antholine, W. E., and Griffith, O. W. (2002) *Escherichia coli* γ-glutamylcysteine synthetase. *J. Biol. Chem.* **277**, 50–58.

Journal of Neurochemistry, 2002, 83, 984–991

Preservation of extracellular glutathione by an astrocyte derived factor with properties comparable to extracellular superoxide dismutase

Victoria C. Stewart,* Rebecca Stone,* Matthew E. Gegg,* Martyn A. Sharpe,* Roger D. Hurst,† John B. Clark* and Simon J. R. Heales*,‡

**Department of Molecular Pathogenesis, Division of Neurochemistry, UCL, Institute of Neurology, London, UK*

†Faculty of Applied Sciences, University of West of England, Bristol, UK

‡Department of Clinical Biochemistry, Neurometabolic Unit, National Hospital for Neurology and Neurosurgery, London, UK

Abstract

Cultured rat and human astrocytes and rat neurones were shown to release reduced glutathione (GSH). In addition, GSH oxidation was retarded by the concomitant release of a factor from the cells. One possibility is that this factor is extracellular superoxide dismutase (SOD). In support of this, the factor was found to bind heparin, have a molecular mass estimated to be between 50 and 100 kDa, and CuZn-type SOD protein and cyanide sensitive enzyme activity were demonstrated in the cell-conditioned medium. In addition, supplementation of native medium with exogenous CuZn-type SOD suppressed GSH oxidation. We propose that preservation of released GSH is essential to allow for maximal up-regulation of GSH metabolism in neurones. Furthermore, cytokine stimulation of astrocytes increased release of the extracellular SOD, and enhanced stability of GSH. This may be a protective strategy occurring *in vivo* under conditions of oxidative stress, and suggests that SOD mimetics may be of therapeutic use.

Keywords: antioxidants, brain, cell culture, neuroprotective factor, oxidative stress.

J. Neurochem. (2002) 83, 984–991.

Within the brain, reduced glutathione (GSH) availability appears to play a key role with regards to dictating cellular susceptibility to oxidative stress (Heales *et al.* 1995; Barker *et al.* 1996). Furthermore, there is evidence that in neurodegenerative disorders such as Parkinson's disease, loss of brain GSH may be an early event in the sequence of events that lead to disruption of cellular metabolism, possibly at the level of the mitochondrion, and ultimately neuronal cell death (Schapira *et al.* 1990; Jenner *et al.* 1992).

When co-cultured with astrocytes, the neuronal intracellular GSH concentration is reported to significantly increase due to the release of GSH and GSH precursors from the astrocytes. (Bolanos *et al.* 1996; Dringen *et al.* 1999). Furthermore, glial cells have been reported to lead to an increased expression of neuronal γ-glutamylcysteine synthetase (Iwata-Ichikawa *et al.* 1999). Such studies suggest that metabolic interactions occur between astrocytes and neurones leading to an up-regulation of neuronal intracellular GSH status, and thus provide an explanation for the apparent diminished sensitivity of neurones towards oxidative stress under co-culture conditions (Stewart *et al.* 1998).

The release of GSH, by astrocytes, has been reported and is suggested to play an important role in maintaining and enhancing neuronal GSH status (Yudkoff *et al.* 1990; Sagara *et al.* 1996; Dringen *et al.* 1999; Wang and Cynader 2000). Whilst the exact mechanism whereby GSH is released from astrocytes is not known, efflux is reported to be carrier mediated and ion independent (Sagara *et al.* 1996). Recently, under conditions of oxidative stress, the multidrug transporter protein, MRP 1, has been shown to be responsible for the

Received June 26, 2002; revised manuscript received August 29, 2002; accepted September 9, 2002.

Address correspondence and reprint requests to Dr Simon J. R. Heales, Division of Neurochemistry, Institute of Neurology, Queen Square, London WC1N 3BG, UK. E-mail: sheales@ion.ucl.ac.uk

Abbreviations used: EcSOD, extracellular superoxide dismutase; FBS, fetal bovine serum; GR, glutathione reductase; HA, human astrocytoma; IFN, interferon; LPS, lipopolysaccharide; MEM, minimal essential medium; PBS, phosphate-buffered saline; SOD, superoxide dismutase.

efflux of oxidized glutathione (GSSG) from astrocytes (Hirrlinger *et al.* 2001). Whether, MRP 1, under normal conditions, is responsible for GSH release remains to be demonstrated.

A number of mechanisms have been proposed whereby released GSH is utilized by neurones. Thus, Dringen *et al.* (1999) have proposed that the ectoenzyme γ-glutamyltranspeptidase utilizes GSH to generate cysteinyl-glycine which is utilized by neurones as the precursor for GSH synthesis whilst Wang and Cynader (2000) suggest that GSH is used to reduce cystine to cysteine which is then used for neuronal GSH synthesis. Whether one or both of these mechanisms predominate *in vivo* is not yet clear. However, they both require the released GSH to remain in the reduced state.

Extracellular fluid and cell culture medium can be a potential source of oxidizing species, e.g. glucose can autooxidize to yield superoxide ($O_2^{\cdot-}$) (Wolff and Dean 1987). GSH will react favourably with $O_2^{\cdot-}$ to yield, via a series of reactions, GSSG and further $O_2^{\cdot-}$ (Winterbourn and Metodiewa 1995). Thus, unless $O_2^{\cdot-}$ is removed from the system, an autocatalytic degradation of GSH will ensue.

Superoxide dismutase (SOD) has been demonstrated in extracellular fluids (Marklund 1982). Although this enzyme contains Cu and Zn, it is distinct from CuZn SOD (type I) (Marklund 1982) and is known as extracellular SOD (EcSOD, type III). EcSOD is produced by a number of cell types including glia (Marklund 1990). Thus, it is possible that EcSOD and other 'guardian' molecules are also released by glial cells in order to protect GSH from oxidation, i.e. in order to maximize availability for up-regulation of neuronal GSH status.

In this study, we have further characterized the release of GSH from astrocytes and neurones, and additionally demonstrated that GSH oxidation is retarded in cell-conditioned medium. Evidence is provided to suggest that protection is afforded, at least in part, by a CuZn-type SOD.

Materials and methods

Materials

Cell culture reagents and plastics were purchased from Life Technologies (Renfrewshire, UK). Interferon-γ (IFN-γ) (rat, recombinant) was from CN Biosciences (Nottingham, UK). CuZnSOD ELISA kit was obtained from Bender MedSystems (Vienna, Austria). Centricon centrifugal filter devices were obtained from Millipore (Watford, UK). Heparin-sepharose PD-10 affinity columns were provided by Amersham Pharmacia Biotech (Uppsala, Sweden). All other chemicals were purchased from Sigma Chemical Co. (Poole, UK).

Cell culture

Primary cortical rat astrocytes were prepared from neonatal Wistar rats (1–2 days old) as previously described (Stewart *et al.* 2000). Astrocytes were cultured for 7 days in D-valine-based minimal essential medium (MEM), supplemented with 10% (v/v) fetal bovine serum (FBS) and 2 mM glutamine, followed by 7 days in L-valine-based MEM. Primary forebrain neuronal cultures were prepared from fetal Wistar rats (day 17 gestation) as described by Almeida *et al.* (2001). Cells were plated at a density of 2.5×10^5 cells/cm^2 in Dulbecco's modified Eagle's medium (DMEM) supplemented with 10% FBS onto six-well plates previously coated with polyornithine (0.01%). Forty-eight hours after plating, the medium was replaced with DMEM supplemented with 5% horse serum and 2 mM glutamine. Cytosine arabinofuranoside (10 μM) was added to prevent non-neuronal proliferation. Under these culture conditions, immunocytochemistry using neurofilament antibody confirmed the neuronal cell population to be > 85% neuronal and astrocyte cultures showed 90–95% immunopositivity against glial fibrillary acidic protein (Tabernero *et al.* 1993). The human astrocytoma cell line 1321 N1 was provided by the European Collection of Animal Cell Cultures (ECACC No: 8603042), and cultured in DMEM containing 10% FBS and 2 mM glutamine. All cells were incubated at 37°C in a humidified atmosphere containing 5% CO_2 and 95% O_2.

Neurons were used at days 10 *in vitro*. Confluent monolayers of human astrocytoma cells were trypsinized and seeded onto six-well plates at a density of 1.1×10^5 cells/cm^2. Similarly, at day 13 *in vitro*, primary rat astrocytes were seeded onto six-well plates at a density of 1.1×10^5 cells/cm^2. Some rat astrocyte wells were stimulated with IFN-γ (100 U/mL) + LPS (1 μg/mL) or IFN-γ (500 U/mL) + LPS (1 μg/mL) for up to 72 h, with medium containing fresh IFN-γ + LPS replenished every 24 h to ensure optimal stimulation. Prior to starting experiments using minimal medium, cell culture medium was removed and the cells washed three times with phosphate-buffered saline (PBS) to remove all trace of serum-containing medium and/IFN-γ + LPS.

As a measure of cell viability, lactate dehydrogenase (LDH; EC 1.1.1.27) activity was determined as described by Vassault (1983). Release of LDH was used as an index of cell death (Koh and Choi 1987). In this study, none of the treatments caused any increase in LDH leakage compared with controls.

Preparation of conditioned medium

Medium was removed and replaced with minimal medium (44 mM $NaHCO_3$, 110 mM NaCl, 1.8 mM $CaCl_2$, 5.4 mM KCl, 0.8 mM $MgSO_4$, 0.92 mM NaH_2PO_4, 5 mM glucose, adjusted to pH 7.4 with CO_2) (Dringen *et al.* 1997). Minimal medium was then incubated with primary rat astrocytes (density; 1×10^6 cells/mL), human astrocytoma cells (density; 1×10^6 cells/mL) or primary rat neurones (density; 2.5×10^6 cells/mL) for 4 h.

GSH efflux

For the measurement of GSH efflux, the cell culture medium was replaced by minimal medium ($t = 0$ h) as described above. At set time points (0.25–4 h), the experiment was terminated by removal of the medium. This was frozen immediately, by immersion in liquid nitrogen, and stored at −80°C for GSH analysis.

GSH stability experiments

GSH was added (final concentration; 5 or 20 μM) to minimal medium or conditioned minimal medium and incubated at 37°C in a humidified atmosphere containing 5% CO_2 and 95% O_2. At set time

points (up to 5 h), the GSH concentration was determined by HPLC. For those studies utilizing conditioned medium, the GSH concentration arising from cellular GSH efflux was determined and subtracted from the final determined GSH concentration. In some experiments with conditioned media, the CuZn-type SOD inhibitors sodium cyanide (15 mM) or sodium azide (15 mM) were added 45 min prior to addition of exogenous GSH (20 μM). In other experiments, bovine CuZnSOD (0–30 μg/mL; reconstituted in cell culture medium from lyophilized powder) was added to native unconditioned minimal medium and the stability of exogenous GSH (20 μM) was then monitored over a 5-h period. GSSG (5 or 20 μM) was also added to astrocyte conditioned medium and GSH formation monitored for up to 5 h. Furthermore, in view of the possibility that GSSG conversion to GSH can only occur in the presence of cells, GSSG (5 or 20 μM) was also added to the minimal medium bathing the astrocytes. GSH formation was again monitored for up to 5 h.

Conditioned medium was also centrifuged through filters with varying molecular mass cut-offs (10–100 kDa nominal molecular mass limit) in accordance with the manufacturers (Centricon Centrifugal Devices, Millipore, Watford, UK) instructions. The stability of exogenous GSH (20 μM) was then determined in the filtered media.

GSH analysis

GSH was analysed using reverse phase HPLC coupled to an electrochemical detector according to the method of Riederer *et al.* (1989). For GSH analysis, samples were thawed and mixed 1 : 1 with 15 mM orthophosphoric acid. Following mixing and centrifugation (15 000 *g*, 5 min), 20 μL of supernatant was injected onto the HPLC column.

In order to determine whether any oxidized glutathione (GSSG) was present in the cell culture medium, glutathione reductase (EC 1.6.4.2; bovine intestinal mucosa) (1 U) and 80 μM NADPH were added to some of the collected media. Following an incubation for 10 min at 37°C, 15 mM orthophosphoric acid was added (1 : 1) and the sample treated as for GSH determination. Under such conditions the total glutathione concentration is determined.

SOD activity assay

Native minimal medium and conditioned medium were centrifuged through a filter with a nominal molecular mass limit of 10 kDa. Any retained material was resuspended in phosphate buffer (50 mM, pH 7.8) and SOD activity determined as described previously (Hargreaves *et al.* 1999). Protein concentration was determined by the method of Lowry *et al.* (1951).

CuZnSOD ELISA

An ELISA was used for the quantitative detection of CuZnSOD in cell culture media and cell homogenates. This ELISA showed no detectable cross-reactivity for MnSOD according to the manufacturer (Bender MedSystems). The detection limit of the assay was 0.07 ng/mL.

Heparin affinity columns

In order to differentiate between CuZnSOD and EcSOD, samples of conditioned medium were concentrated using the Centricon devices and then applied to a heparin-sepharose affinity column. EcSOD has an affinity for heparin, whereas CuZnSOD does not. Following the affinity chromatography, fractions were assayed for CuZnSOD using the ELISA.

Statistical analysis

Results are expressed as mean ± SEM values for the number of independent cell culture preparations indicated. Statistical significance for the comparison of two groups was evaluated using Student's *t*-test. Multiple comparisons were made by one-way ANOVA followed by the least significant difference multiple range test. In all cases, $p < 0.05$ was considered significant.

Results

Rat astrocytes, human astrocytoma cells and rat neurones all release GSH (Fig. 1). The rat neurones released approximately 25-fold less GSH after 4 h than rat astrocytes. Furthermore, the rodent astrocytes released almost 40% more GSH than the human astrocytoma cells. GSH release was linear over the time period of the study, e.g. with rat astrocytes at 0.25 h the extracellular GSH concentration was 0.29 ± 0.05 μM increasing to 2.6 ± 0.28 μM at 4 h. During this time course, the percentage of total glutathione present in the reduced form, i.e. as GSH, increased (Table 1). Under all the conditions employed, there was no significant release, by any of the cell types, of LDH into the extracellular medium (data not shown).

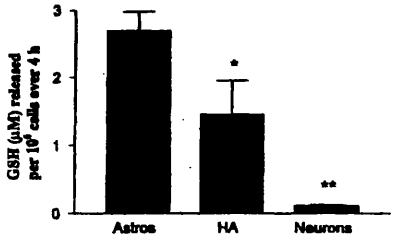

Fig. 1 Comparison of the levels of GSH released per million cells over 4 h by rat astrocytes (astros), human astrocytoma cells (HA) and rat neurones (neurones). Data are expressed as μM (mean ± SEM, $n = 4$). *$p < 0.05$ when compared with rat astrocytes; **$p < 0.05$ when compared with rat and human astrocytes.

Table 1 Proportion of total glutathione released by astrocytes present in the reduced form (GSH)

Time (h)	% of total glutathione as GSH
0.25	39 ± 2.5
2.00	59.6 ± 6.0
4.00	67.0 ± 5.1

Data are expressed as mean ± SEM ($n = 3$).

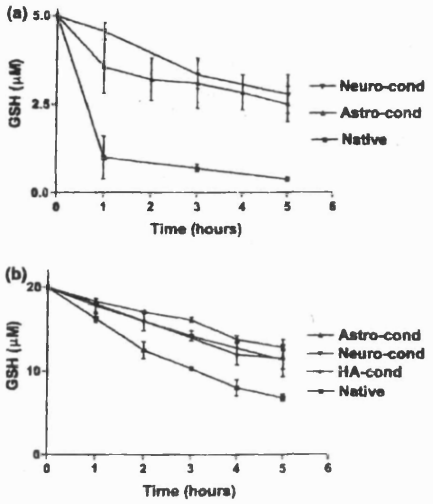

Fig. 2 (a) Stability of 5 μM GSH over 5 h in native unconditioned medium (native) and medium previously conditioned for 4 h by rat astrocytes (astro-cond) or rat neurones (neuro-cond). Data are expressed as mean ± SEM, $n = 4$. At all time points (1–5 h), levels of GSH was significantly greater in cell-conditioned media than in native medium ($p < 0.05$). (b) Stability of 20 μM GSH over 5 h in native unconditioned medium (native) and medium previously conditioned for 4 h by rat astrocytes (astro-cond), rat neurones (Neuro-cond) or human astrocytoma cells (HA-cond). Data are expressed as mean ± SEM, $n = 4$. At all time points (1–5 h), levels of GSH was significantly greater in cell-conditioned media than in native medium ($p < 0.05$).

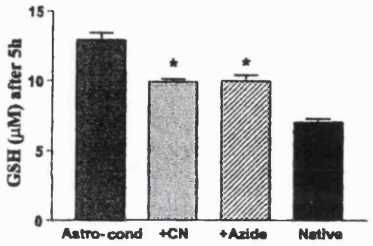

Fig. 3 Concentration of GSH remaining in the presence or absence of CuZn-type SOD inhibitors in rat astrocyte-conditioned medium. The initial GSH concentration was 20 μM. Astrocyte-conditioned medium was preincubated with 15 mM sodium cyanide (+ CN) or sodium azide (+ azide) for 45 min prior to the addition of 20 μM GSH. In parallel incubations, 20 μM GSH was added to astrocyte-conditioned medium alone (astro-cond) or native unconditioned medium (native). Data are expressed as μM GSH remaining after 5 h (mean ± SEM, $n = 3$). *$p < 0.05$ compared with level in astrocyte-conditioned medium alone.

Addition of exogenous GSH (5 μM) to native unconditioned minimal medium revealed that the GSH very rapidly disappeared from the medium (Fig. 2a). In contrast, both rat astrocyte- and neurone-conditioned medium significantly retarded the rate of loss of GSH (Fig. 2a). In view of the rapid decay of 5 μM GSH from the native medium, and in order to allow for more accurate quantification in subsequent experiments, a higher GSH concentration (20 μM) was utilized. Using this concentration, the three types of cell-conditioned medium suppressed GSH oxidation (Fig. 2b). In all cases, the loss of GSH could be accounted for by a corresponding increase in GSSG, i.e. after 5 h incubation and subsequent treatment with glutathione reductase the GSH concentration was found to be 21 ± 0.6 μM. Furthermore, addition of GSSG to the conditioned media did not lead to GSH formation (data not shown). Similarly addition of GSSG to culture medium in the presence of astrocytes did not lead to GSH formation (data not shown).

Addition of the CuZn-type SOD inhibitors sodium cyanide or sodium azide (15 mM) to the astrocyte-conditioned medium resulted in a partial loss of the ability to protect GSH (Fig. 3), suggesting the presence of CuZn-type SODs in the conditioned medium. Supplementation of native (i.e. unconditioned) minimal medium with reconstituted bovine CuZnSOD at the level of 15 and 30 μg/mL also conveyed protection towards GSH. However, no protection was afforded with a lower amount of SOD. Thus, in the absence of any exogenous SOD, only 34 ± 3% of the original 20 μM GSH could be accounted for after 5 h incubation in native medium. In contrast, in the presence of 15 and 30 μg/mL SOD, 43 ± 0.6% and 62 ± 0.6% of the initial GSH concentration could be accounted for, respectively.

Centrifugation of astrocyte-conditioned medium through filters with molecular mass cut-offs of between 10 and 50 kDa resulted in a loss of ability to protect exogenous GSH from oxidation (Fig. 4). This suggests that the factor responsible for protecting the GSH against oxidation has a molecular mass greater than 50 kDa. Using the 100 kDa cut-off filters, GSH stability was comparable to unfiltered conditioned medium (Fig. 4).

Assessment of CuZn-type SOD (cyanide-sensitive) activity in the resuspended material retained by the 10 kDa filter revealed detectable activity (2.4 ± 0.2 units/mg protein). No SOD activity could be detected in native cell culture medium treated in an identical manner. Furthermore, resuspension of this material in native minimal medium resulted in the medium behaving as conditioned medium, i.e. GSH oxidation was suppressed (data not shown).

CuZnSOD detection by ELISA showed that while both cell types released CuZnSOD, astrocytes released approximately eight times higher levels than neurones (astrocytes: 1.48 ± 0.24; neurones: 0.19 ± 0.05 ng/mL after 4 h incubation.). In view of the possibility that the CuZnSOD ELISA may not cross-react with EcSOD (also a CuZn-type SOD),

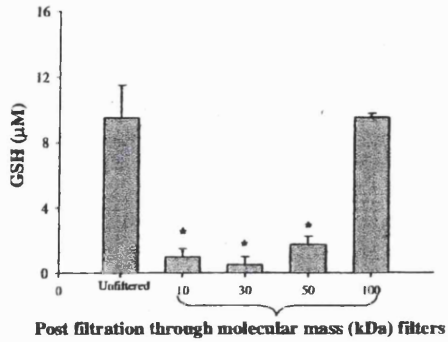

Fig. 4 Concentration of GSH remaining after 5 h incubation of 20 μM GSH with rat astrocyte-conditioned medium (unfiltered) and conditioned medium that had previously been filtered through filters of varying molecular mass cut-offs. $^*p < 0.05$ compared with unfiltered conditioned medium (mean ± SEM, $n = 3$–5).

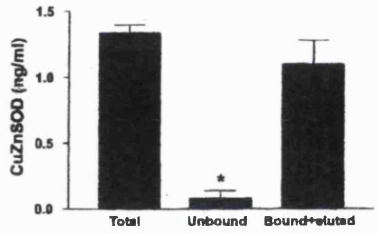

Fig. 5 Effect of heparin affinity chromatography on levels of CuZn-type SOD detected in astrocyte-conditioned medium. Levels of CuZn-type SOD were assayed in astrocyte-conditioned medium (total), the fraction which did not bind to the heparin column (unbound), and the bound fraction following elution (bound + eluted). Results are expressed as ng/mL (mean ± SEM, $n = 4$). $^*p < 0.05$ compared with total (i.e. astrocyte-conditioned medium).

fractions of astrocyte-conditioned medium were subjected to affinity chromatography using a heparin-sepharose column and then analysed using the ELISA. Using this procedure, fractions of astrocyte-conditioned medium remaining unbound when passed through the affinity column, contained only approximately 6% of the level of CuZnSOD detected in the original fraction (Fig. 5). In contrast, upon elution of the bound fraction, CuZnSOD levels comparable to that of the original fraction were detected (Fig. 5). These results suggest that the astrocyte-conditioned medium contains CuZn-type SOD with heparin affinity, e.g. EcSOD.

Cytokines have been reported to up-regulate EcSOD expression (Marklund 1992; Stralin and Marklund 2000). Consequently, the effect of IFN-γ + LPS exposure on the levels of both intracellular and released CuZn-type SOD was

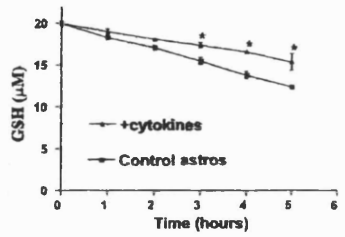

Fig. 6 Stability of 20 μM GSH over 5 h in rat astrocyte-conditioned medium. Conditioned medium was prepared from either unstimulated astrocytes (control astros) or from astrocytes previously treated from 24 h with IFN-γ (100 U/mL) + LPS (1 μg/mL) (+ cytokines). Data expressed as mean ± SEM, $n = 4$. $^*p < 0.05$ when compared with conditioned medium prepared from control unstimulated rat astrocytes.

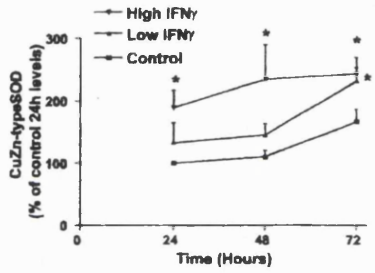

Fig. 7 Stimulation with cytokines for up to 72 h increased the levels of CuZn-type SOD released into medium over 4 h. Astrocytes were unstimulated (control) or incubated with IFN-γ (100 U/mL) + LPS (1 μg/mL) (low IFN-γ), or IFN-γ (500 U/mL) + LPS (1 μg/mL) (high IFN-γ) for 24 h, 48 h or 72 h prior to determination of CuZnSOD release. Results expressed as a percentage relative to the level released by control astrocytes at 24 h (Mean ± SEM, $n = 4$). $^*p < 0.05$ compared with control.

also investigated. Minimal medium conditioned by astrocytes for 4 h was prepared following exposure of astrocytes to IFN-γ (100 U/mL) + LPS (1 μg/mL) for 24 h. Conditioned medium produced by astrocytes previously exposed to cytokines resulted in enhanced levels of GSH stability (Fig. 6). Exposure of astrocytes to either (i) low IFN-γ [IFN-γ (100 U/mL) + LPS (1 μg/mL)] or (ii) high IFN-γ [IFN-γ (500 U/mL) + LPS (1 μg/mL)] did not alter the level of CuZn-type SOD in cell homogenates (data not shown). However this exposure did increase the level of CuZn-type SOD released (Fig. 7).

Discussion

In this study, we have demonstrated that both rat and human astroglia and rat neuronal cells are capable of releasing GSH

via a process that is not simply due to a loss of plasma membrane integrity, i.e there was no evidence of extracellular LDH accumulation in any of the experiments performed. GSH has been shown to be unstable in cell culture medium (Long and Halliwell 2001). In view of the susceptibility of GSH to oxidation in native minimal medium, we were surprized to note that over 65% of the total glutathione released, after 4 h, was present in the reduced form. Consequently, GSH oxidation in conditioned medium was monitored. The degradation of GSH in conditioned medium was clearly suppressed. Furthermore, comparable results were obtained with media conditioned either by neurones, or by the rodent or human astroglial cells. The rate of decay of 5 μM GSH, in native medium appeared to be considerably greater than for 20 μM GSH. A likely explanation for this difference is that the ratio of oxidant(s) in the medium, e.g. $O_2^{\cdot-}$, to GSH will be greater at lower GSH concentrations.

One explanation for the above findings is that conditioned medium contains a factor capable of reducing any generated GSSG back to GSH, e.g. glutathione reductase. However, neither conditioned medium nor media in the presence of astrocytes was able to reduce GSSG to GSH. Another possibility for our findings is that a factor is released by the astrocytes that removes oxidizing species, e.g. EcSOD. EcSOD is released from glial cells and a number of potential roles for this enzyme have been proposed, e.g. it is suggested to be involved in prolonging the lifespan of nitric oxide (Oury *et al.* 1992), and decreasing the production of peroxynitrite (Huie and Padmaja 1993). However, to our knowledge, protection of released GSH has not been considered.

EcSOD displays a strong sequence homology to CuZn-SOD, and is itself a CuZn-type SOD (Hjalmarsson *et al.* 1987). Until recently the only SOD isozyme thought to be secreted by glia and fibroblasts was EcSOD, but CuZnSOD has also been found to be secreted by some human cell lines (Mondola *et al.* 1996, 1998). Cyanide and azide are inhibitors of EcSOD and CuZnSOD, but not the manganese containing isoform of SOD (Marklund 1982). These agents diminished the stability of GSH in conditioned medium, suggesting the functional presence of EcSOD and/or CuZnSOD. This was further supported by the determination of cyanide sensitive SOD activity in conditioned medium. Supplementation of native medium with exogenous CuZnSOD also limited GSH oxidation. Whilst this latter observation suggests that, if present, CuZn-type SOD can protect GSH in the extracellular environment, it is clear that relatively large amounts of SOD had to be added to convey protection towards GSH. In view of this, it is possible that bovine CuZnSOD is less potent at retarding GSH oxidation than the cellular factor released and/or lyophilization and reconstitution of SOD leads to a loss of activity.

The molecular mass of the factor present in conditioned medium can, from the use of the molecular mass filters, be estimated to be between 50 and 100 kDa. Rat astrocyte conditioned medium was used for these experiments and the reported molecular mass of rodent EcSOD is between 85 and 97 kDa (Willems *et al.* 1993). In contrast, CuZnSOD is estimated to be approximately 33 kDa (McCord and Fridovich 1969).

Using a CuZnSOD ELISA, SOD was detected in the astrocyte-conditioned medium, confirming that this cell type can release SOD. CuZnSOD and EcSOD are often described as immunologically distinct (Marklund 1982). Therefore, we were concerned that the CuZnSOD ELISA used may not cross-react with EcSOD. In contrast to type-I SOD, EcSOD has a high heparin affinity (Karlsson and Marklund 1987) and so conditioned medium was subjected to affinity chromatography through a heparin-sepharose column. Fractions that did not bind to the heparin affinity column had very low levels of CuZn-type SOD according to the ELISA employed. In contrast, CuZn-type SOD levels comparable to that of the original conditioned medium fraction, were detected in fractions that had been bound and then eluted from the heparin affinity column. These results suggest that the astrocyte-conditioned medium contains a CuZn-type SOD with heparin affinity, e.g. EcSOD. Therefore, it appears that the CuZnSOD ELISA used can, under the conditions employed, detect both CuZn forms of SOD.

We have previously demonstrated in co-culture that astrocytes provide neurones with GSH precursors, thereby up-regulating intracellular neuronal GSH levels (Bolanos *et al.* 1996). In view of the generation of reactive nitrogen species, we were initially surprized to find that IFN-γ/LPS-treated astrocytes also up-regulate neuronal GSH to a similar level (Bolanos *et al.* 1996). Consequently, we postulated that there maybe a mechanism whereby stimulated astrocytes can further protect extracellular GSH from reactive nitrogen species. This appears to be the case as, in the current study, IFN-γ + LPS-treated astrocytes produced conditioned medium with a superior ability to diminish GSH degradation. EcSOD is reported to be up-regulated by cytokines, including IFN-γ, whereas CuZnSOD is unaffected (Marklund 1992; Stralin and Marklund 2000). As cytosolic type-I SOD would account for the majority of cellular CuZn-type SOD, this would explain why the intracellular levels of CuZn-type SOD was not affected by cytokine treatment. In contrast, the level of CuZn-type SOD released was significantly elevated by cytokine exposure over 72 h. Thus, under such conditions of nitrosative stress, GSH stability may be maximized by the further increase in SOD availability in the extracellular environment.

The cultured neuronal preparations utilized in this study also appear to be capable of releasing GSH and a CuZn-type SOD. However, the amount of GSH and SOD

released by these cells is markedly less than that seen with the astrocyte preparations. Despite this difference, the neuronal conditioned medium, in terms of potency, appears comparable to that of astrocytes when considering the protective effect towards added GSH. Such a finding could suggest that the amount released by neurones is sufficient to retard GSH autoxidation and that astrocytes have a reserve that could become increasingly important under certain conditions such as oxidative/nitrosative stress. Alternatively, it is also possible that other unidentified factors are released by the neurones that also convey protection towards GSH.

In view of the cyanide/azide sensitivity of this protective factor, estimated molecular mass, heparin affinity column results, demonstrable SOD activity in conditioned medium and cytokine sensitivity, our data suggest that astrocytes, and possibly neurones, release a factor that has properties comparable to EcSOD.

In summary, we propose that astrocytes release GSH, to both provide extracellular protection and precursors for neuronal GSH synthesis. However, GSH is susceptible to oxidation. To prevent this, astrocytes, and possibly neurones, appear to release protective factors that may include extracellular SOD, which enhances GSH stability. Under conditions of oxidative stress, the level of SOD released by astrocytes is increased, thereby enhancing GSH stability and optimizing GSH available in the extracellular environment. Recently CuZn SOD has been reported to display thiol oxidase activity (Winterbourn *et al.* 2002). However, under the conditions employed in our study CuZn SOD does not appear to be enhancing GSH oxidation. In support of this finding, it should be noted that whilst CuZn SOD displays high oxidase activity for cysteine and cysteamine the rate is much lower with GSH (Winterbourn *et al.* 2002).

The potential role for EcSOD in the neurodegenerative process is further illustrated by the finding that mice lacking EcSOD are more sensitive to hyperoxia and that overexpression of this enzyme leads to an increased resistance of hippocampal neurones to ischaemic damage (Carlsson *et al.* 1995; Sheng *et al.* 2000). Thus, during conditions of chronic oxidative stress e.g. Alzheimer's disease, Parkinson's disease, there may be a therapeutic window of opportunity for treatment with SOD mimetics. Therefore, by strengthening the GSH-SOD system during the initial phase of neurodegenerative disease, it may be possible to limit the oxidative/nitrosative damage associated with these diseases.

Acknowledgements

We are grateful to the Brain Research Trust, the Hospital Savings Association and the Worshipful Company of Pewterers' for supporting our work.

References

Almeida A., Almeida J., Bolanos J. P. and Moncada S. (2001) Different responses of astrocytes and neurons to nitric oxide: the role of glycolytically generated ATP in astrocyte protection. *Proc. Natl Acad. Sci. USA* **98**, 15294–15299.

Barker J. E., Bolanos J. P., Land J. M., Clark J. B. and Heales S. J. R. (1996) Glutathione protects astrocytes from peroxynitrite-mediated mitochondrial damage. Implications for neuronal/astrocytic trafficking and neurodegeneration. *Dev. Neurosci.* **18**, 391–396.

Bolanos J. P., Heales S. J. R., Peuchen S., Barker J. E., Land J. M. and Clark J. B. (1996) Nitric oxide-mediated mitochondrial damage: a potential neuroprotective role for glutathione. *Free Rad. Biol. Med.* **21**, 995–1001.

Carlsson L. M., Jonsson J., Edlund T. and Marklund S. L. (1995) Mice lacking extracellular superoxide dismutase are more sensitive to hyperoxia. *Proc. Natl Acad. Sci. USA* **92**, 6264–6268.

Dringen R., Kranick O. and Hamprecht B. (1997) The γ-glutamyltranspeptidase inhibitor acivicin preserves glutathione released by astroglial cells in culture. *Neurochem. Res.* **22**, 727–733.

Dringen R., Pfeiffer B. and Hamprecht B. (1999) Synthesis of the antioxidant glutathione in neurones: supply by astrocytes of cysgly as precursor for neuronal glutathione. *J. Neurosci.* **19**, 562–569.

Hargreaves I. P., Heales S. J. R. and Land J. M. (1999) Mitochondrial respiratory chain defects are not accompanied by an increase in the activities of lactate dehydrogenase or manganese superoxide dismutase in paediatric skeletal muscle biopsies. *J. Inher. Metab. Dis.* **22**, 925–931.

Heales S. J. R., Davies S. E. C., Bates T. E. and Clark J. B. (1995) Depletion of brain glutathione is accompanied by impaired mitochondrial function and decreased *N*-acetylaspartate concentration. *Neurochem. Res.* **20**, 31–38.

Hirrlinger J., Konig J., Keppler D., Lindenau J., Schulz J. B. and Dringen R. (2001) The multidrug resistance protein MRP1 mediates the release of glutathione disulfide from rat astrocytes during oxidative stress. *J. Neurochem.* **76**, 627–636.

Hjalmarsson K., Marklund S. L., Engstrom A. and Edlund T. (1987) Isolation and sequence of complimentary DNA encoding human extracellular superoxide dismutase. *Proc. Natl Acad. Sci. USA* **84**, 6340–6344.

Huie R. E. and Padmaja S. (1993) The reaction of NO with superoxide. *Free Rad. Res. Commun.* **18**, 195–199.

Iwata-Ichikawa E., Kondon Y., Miyazaki I., Asamuma M. and Ogawa N. (1999) Glial cells protect neurones against oxidative stress via transcriptional up-regulation of the glutathione synthesis. *J. Neurochem.* **72**, 2334–2344.

Jenner P., Dexter D., Sian J., Schapira A. H. V. and Marsden C. D. (1992) Oxidative stress as a cause of nigral cell death in Parkinson's disease and incidental Lewy body disease. *Ann. Neurol.* **32**, S82–S87.

Karlsson K. and Marklund S. L. (1987) Heparin-induced release of extracellular superoxide dismutase to human blood plasma. *Biochem. J.* **242**, 55–59.

Koh J. Y. and Choi D. W. (1987) Quantitative measurement of glutamate mediated cortical neuron injury in cell culture by lactate dehydrogenase efflux assay. *Neurosci. Methods* **20**, 83–90.

Long L. H. and Halliwell B. (2001) Oxidation and generation of hydrogen peroxide by thiol compounds in commonly used cell culture media. *Biochem. Biophys. Res. Commun.* **286**, 991–994.

Lowry O. H., Rosebrough N. J., Farr A. L. and Randall R. J. (1951) Protein measurement with the Folin phenol reagent. *J. Biol. Chem.* **193**, 265–275.

Marklund S. L. (1982) Human copper-containing superoxide dismutase of high molecular weight. *Proc. Natl Acad. Sci. USA* **79**, 7634–7638.

Marklund S. L. (1990) Expression of extracellular superoxide dismutase by human cell lines. *Biochem. J.* **266**, 213–219.

Marklund S. L. (1992) Regulation by cytokines of extracellular superoxide dismutase and other superoxide dismutase isoenzymes in fibroblasts. *J. Biol. Chem.* **267**, 6696–6701.

McCord J. M. and Fridovich I. (1969) Superoxide dismutase. *J. Biol. Chem.* **244**, 6049–6055.

Mondola P., Annella T., Santillo M. and Santangelo F. (1996) Evidence for secretion of cytosolic CuZn superoxide dismutase content by HEPG2 cells and human fibroblasto. *Int. J. Biochem. Cell. Biol.* **28**, 677–681.

Mondola P., Annella T., Seru R., Santangelo F., Iossa S., Gioielli A. and Santillo M. (1998) Secretion and increase of intracellular CuZn superoxide dismutase content in human neuroblastoma SK-N-BE cells subjected to oxidative stress. *Brain Res. Bull.* **45**, 517–520.

Oury T. D., Ho Y. S., Piantadosi C. A. and Crapo J. D. (1992) Extracellular superoxide dismutase, nitric oxide and central nervous system O_2 toxicity. *Proc. Natl Acad. Sci. USA* **89**, 9715–9719.

Riederer P., Sofic E., Rausch W., Schmidt B., Reynolds G. P., Jellinger K. and Youdim M. B. H. (1989) Transition metals, ferritin, glutathione and ascorbic acid in Parkinsonian brains. *J. Neurochem.* **52**, 512–520.

Sagara J., Makino N. and Bannai S. (1996) Glutathione efflux from cultured astrocytes. *J. Neurochem.* **66**, 1876–1881.

Schapira A. H. V., Cooper J. M., Dexter D., Clark J. B., Jenner P. and Marsden C. D. (1990) Mitochondrial complex I deficiency in Parkinson's disease. *J. Neurochem.* **54**, 823–827.

Sheng H., Kudo M., Mackensen B., Pearlstein R. D., Crapo J. D. and Warner D. S. (2000) Mice overexpressing extracellular superoxide dismutase have increased resistance to global cerebral ischemia. *Exp. Neurol.* **163**, 392–398.

Stewart V. C., Land J. M., Clark J. B. and Heales S. J. R. (1998) Pretreatment of astrocytes with interferon-α/β prevents neuronal mitochondrial respiratory chain damage. *J. Neurochem.* **70**, 432–434.

Stewart V. C., Sharpe M. A., Clark J. B. and Heales S. J. R. (2000) Astrocyte-derived nitric oxide causes both reversible and irreversible damage to the neuronal mitochondrial respiratory chain. *J. Neurochem.* **75**, 694–700.

Stralin P. and Marklund S. L. (2000) Multiple cytokines regulate the expression of extracellular superoxide dismutase in human vascular smooth muscle cells. *Atherosclerosis* **151**, 433–441.

Tabernero A., Bolanos J. P. and Medina J. M. (1993) Lipogenesis from lactate in rat neurons and astrocytes in primary culture. *Biochem. J.* **294**, 657–661.

Vassault A. (1983) Lactate dehydrogenase. UV method with pyruvate and NADH, in *Methods of Enzymatic Analysis*, Vol. 3 (Bergmeyer J. and Grassl M., eds), pp. 118–126. Verlag Chemie GmbH, Weinheim.

Wang X. F. and Cynader M. S. (2000) Astrocytes provide cysteine to neurones by releasing glutathione. *J. Neurochem.* **74**, 1434–1442.

Willems J., Zwijsen A., Slegers H., Nicolai S., Bettadapura J., Raymackers J. and Scarcez T. (1993) Purification and sequence of rat extracellular superoxide dismutase secreted by C6 glioma. *J. Biol. Chem.* **268**, 24614–24621.

Winterbourn C. C. and Metodiewa D. (1995) Reaction of superoxide with glutathione and other thiols. *Methods Enzymol.* **251**, 81–86.

Winterbourn C. C., Peskin A. V. and Parsons-Mair H. N. (2002) Thiol oxidase activity of copper, zinc superoxide dismutase. *J. Biol. Chem.* **277**, 1906–1911.

Wolff S. P. and Dean R. T. (1987) Glucose autooxidation and protein modification. *Biochem. J.* **245**, 243–250.

Yudkoff M., Pleasure D., Cregar L., Lin Z., Nissim I., Stern J. and Nissim I. (1990) Glutathione turnover in cultured astrocytes: studies with [^{15}N]glutamate. *J. Neurochem.* **55**, 137–145.

OXIDATIVE PHOSPHORYLATION: STRUCTURE, FUNCTION, AND INTERMEDIARY METABOLISM

Simon J. R. Heales,[1] Matthew E. Gegg, and John B. Clark

Departments of Neurochemistry
and Clinical Biochemistry (Neurometabolic Unit)
Institute of Neurology and National Hospital
Queen Square, London, WC1N 3BG, United Kingdom

I. Historical Background

Although Kölliker had described granules in striated muscle in the middle nineteenth century, it was not until the turn of the twentieth Century that the name *mitochondrion* came into use. Altman, in his "Die Elementar Organismen und ihre Beziehungen zu den Zellen" (Leipzig, 1890), spoke of primitive self-replicating bodies or bioblasts that he stained specifically and referred to as "elementary particles." However, it was the cytologist Benda who in 1898 coined the name *mitochondrion* from the Greek for thread (*mitos*) and grain (*chondros*) from his studies on the thread-like granules he observed in sperm and ova. Two years later Michaelis, using a variety of dyestuffs including Janus Green, demonstrated that these granules had oxidoreduction activities.

Au: Please add ref. list: Leipzig 1890, Nash 1965, and Clark *et al.*, 1977. Also please add refs. for Kölliker; Altman; Benda; Warburg; Wieland; Krebs; Keilin & Hartree; Meenes; Kennedy; Hogeboom; Polade & Sjöstand; Boyer; Chance; Green; Mitchell; Slater; Williams if at all possible or necessary.

[1]To whom correspondence should be addressed.

0074-7742/02 $35.00

We then enter what can only be described as the golden era of the German school in which the likes of Warburg, Wieland, and more later Krebs studied the respiration and metabolism of various cellular preparations. Warburg in 1913 described oxygen respiratory granules in liver cells and Wieland in 1932 published on the mechanism of oxidation. These studies were complemented by those of Keilin and Hartree, on cytochromes during the same period. However, the importance of these phenomena both in terms of their cellular localization to the mitochondria and their relevance to cellular energetics and ATP production were largely unappreciated until the late 1930s. In the same way, it is interesting to note that Meeves in 1918 suggested that mitochondria have hereditary characteristics, a suggestion which was largely ignored until the controversies of the mid-1960s (Lehninger, 1965).

The advent of the electron microscope and the high-speed refrigerated centrifuge during the 1940s and 1950s allowed a quantum leap in our understanding of both the structure and function of mitochondria. The development of the technique of differential centrifugation by Claude and others in the 1940s allowed the isolation of relatively pure preparations of mitochondria, permitting detailed studies of the main metabolic activities of these organelles in the early 1950's by Kennedy, Lehninger, Hogeboom, and others. This was complemented by the high-resolution electron micrograph (EM) studies by Palade and Sjöstrand, thus providing the basis for a firm and a detailed understanding of the structure and function of mitochondria.

Au: EM spelledout correctly?

Following on from this period, the next two decades or more were taken up with the sometimes heated controversies relating to the mechanism of the process of oxidative phosphorylation. Contributors to this were many but include Boyer, Chance, Green, Mitchell, Slater, and Williams, resulting in a consensus at this time that although basically chemiosmotic in nature nevertheless has aspects drawn from the other so-called chemical and conformational theories. The mid-1960s also brought a renewal of the controversy of whether mitochondria contained DNA. The work of Roodyn, Wilkie, and Work (Roodyn and Wilkie, 1968) was central to this, providing the evidence that this was not due to bacterial contamination, and Nass concluded in 1965 that "DNA is an integral part of most and probably all mitochondria." This also provided support for the concept that the mitochondrion has evolved from a symbiotic bacterium and had its own capability of coding for and synthesizing its own proteins. This was of course proved beyond doubt, when in the 1980s the complete sequence of mitochondrial DNA (mtDNA) was sequenced by the laboratories of Sanger and Attardi (see previous chapter). This coincided with a growing recognition of mitochondrial diseases, pioneered by the work of Clark, Morgan-Hughes, Land (1977), and

Au: It is unclear to what you are refering to with "Sanger & Attardi (see previous chapter)" I cannot find these authors in this volume, and chap 1 (your previous chapter in this volume) cites a few Attardi refs. but no Sanger. Please clarify meaning here.

others in which the biochemical defects at the level of the mitochondrial electron transport chain had been described in certain neuromuscular disorders.

In the 21st century we are now grappling with relating the clinical phenotype with genotype in these diseases, together with attempting to understand the mechanisms whereby mitochondrial dysfunction is caused, e.g., oxidative stress and how this relates to cell death (apoptosis/necrosis) in neurodegenerative disease.

II. The Mitochondrial Electron Transport Chain

Each human cell contains hundreds of mitochondria that are approximately 1 μ in length. The shape of these organelles varies from spherical to rod-like, and on occasion, they appear to form a network. Each mitochondrion has a double membrane structure, i.e., the outer mitochondrial membrane surrounds the inner membrane. This inner membrane is invaginated and forms cristae (Scheffler, 1999) The space between the two membranes is known as the intermembrane space while the inner membrane encloses that matrix where a number of metabolic processes occur, e.g., the tricarboxylic acid (TCA) cycle, heme synthesis, part of the urea cycle and fatty acid oxidation.

The inner mitochondria membrane is the site of the electron transport chain (ETC) and is where the process of oxidative phosphorylation occurs that facilitates ATP synthesis. The ETC is composed of more than 80 polypeptides components that are grouped together into four enzymatic complexes (Fig. 1). The polypeptides that constitute complex I (NADH: ubiquinone oxidoreductase), III (ubiquinol cytochrome c reductase), and IV (cytochrome c oxidase) are coded for by both nuclear and mitochondrial DNA. In contrast, complex II (succinate:ubiquinone oxidoreductase) is coded exclusively by the nuclear genome. In general terms, transfer of reducing equivalents from NADH or $FADH_2$ (generated, e.g., from carbohydrate or fatty acid metabolism, see below) to molecular oxygen is coupled to the pumping of protons across the inner mitochondrial membrane, i.e, from the matrix into the intermembrane space. This transport of protons generates an electrochemical gradient that has two components: (a) a pH gradient resulting in a pH difference (ΔpH) across the inner membrane of approximately 1.4, and (b) a membrane potential ($\Delta\psi$), due to charge separation, of about 150 mV. The resulting proton motive force is then dissipated, when there is a need to synthesise ATP, i.e, when the cellular ADP concentration increases. Dissipation of this gradient through the membrane

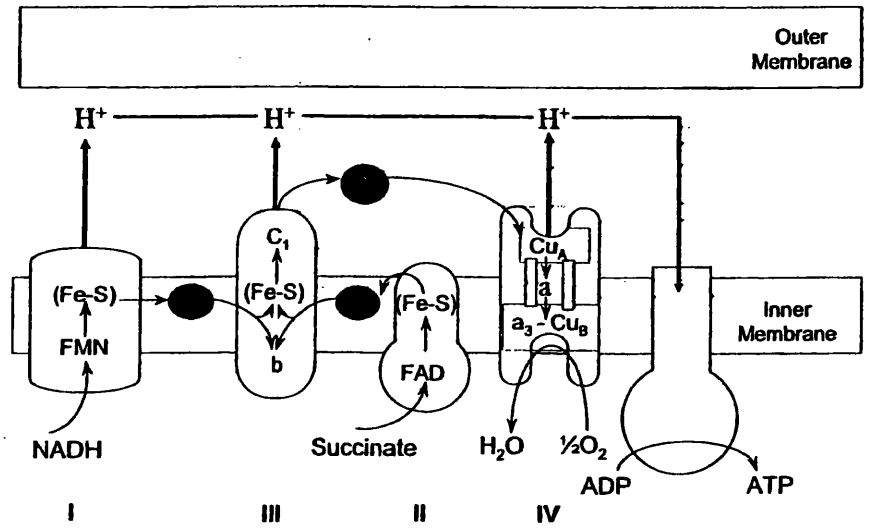

FIG. 1. Schematic of the mitochondrial ETC. Details of this system can be found in the text. C and Q represent the mobile electron carriers, cytochrome c and ubiquinone, respectively.

sector of the ATP synthase leads to the phsophorylation of ADP (Mitchell, 1961).

The rate of ATP synthesis, by the above system, is under tight control and is regulated via ADP. The cellular concentration of ADP is approximately 0.14 mmol/L, which is about 10-fold lower than that of ATP. Thus, a small decrease in ATP concentration, due to an increase in metabolic demand, is accompanied by a relatively large percentage increase in cellular ADP. Regulation of this system by ADP is known as respiratory control and ensures that oxidative phophorylation occurs only when there is a need to replenish ATP.

In view of the key role the ETC plays in energy metabolism, damage to one or more of the respiratory chain complexes could lead to an impairment of cellular ATP formation. However, each of the complexes of the ETC appears to exert varying degrees of control over respiration. Furthermore, *in vitro,* studies suggest that substantial loss of activity of an individual complex may be required before ATP synthesis is compromised. However, the degree of control a particular complex exerts over respiration may differ between cell types. Within the brain, mitochondria appear to be heterogeneous. Thus, complex I, of nonsynaptic mitochondria, has to be inhibited by approximately 70% before inhibition of ATP synthesis occurs. However, for synaptic mitochondria, impairment of ATP synthesis occurs when complex I is inhibited by 25% (Davey *et al.*, 1997).

A. Complex I

NADH:ubiquinone oxidoreductase (complex I; EC 1.6.5.3) is the first and largest enzyme in the electron transport chain. Complex I catalyzes the transfer of two electrons from NADH to ubiquinone. These are transferred through the enzyme by bound prosthetic groups. This transfer is coupled to the translocation of four to five protons from the matrix, across the inner membrane, to the intermembrane space.

The three-dimensional structures of complex I from *Escherichia coli, N. crassa,* and bovine heart have been determined by electron microscopy (Guenebaut *et al.,* 1997; Grigorieff, 1998; Guenebaut *et al.,* 1998). All the structures show a characteristic L shape, with one arm embedded in the membrane and the other projecting into the matrix (Fig. 2). The matrix domain has a globular structure, and it is connected to the elongated membrane domain by a narrow stalk. A constriction in the membrane domain is present in both the *N. crassa* and bovine enzymes.

Au: Please spell out genus name at 1st mention.

Bovine complex I has 43 different subunits with a molecular mass of approximately 900 kDa. The molecular masses of the matrix domain, including the stalk, and the membrane domain were determined as 520 and 370 kDa, respectively (Grigorieff, 1999).

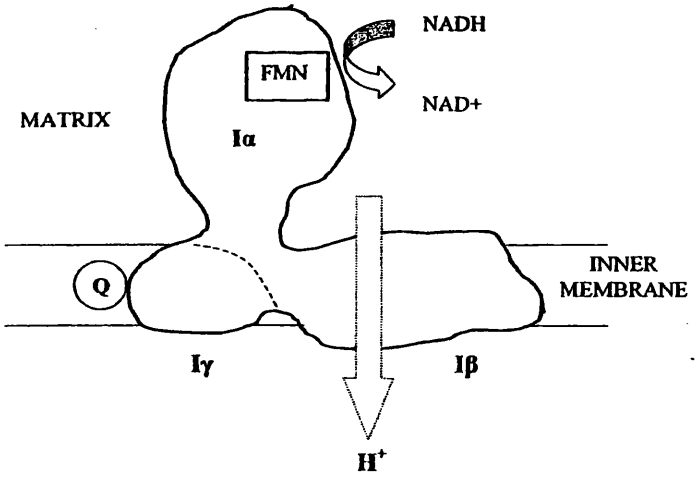

FIG. 2. Structure of complex I. Characteristic L-shaped structure of complex I. The NADH oxidation occurs in the peripheral matrix domain, while subunits in the membrane domain are thought to be responsible for proton pumping. Treatment of complex I with detergent yields the subcomplexes Iα and I β. Harsher treatment divides the membrane domain into Iβ and Iγ (denoted by dashed line). Transfer of electrons to ubiquinone (Q) is thought to be mediated by subunits located in Iγ.

Complex I has one noncovalently bound flavin mononucleotide molecule (FMN) and at least six iron–sulfur clusters and two ubiquinone binding sites. Only four or five iron–sulfur clusters have been resolved and characterized by electron paramagnetc resonance spectroscopy. The location of the remaining iron–sulfur clusters (Ohnishi, 1998) and the ubiquinone binding sites (Tormo and Estornall, 2000) is still highly contentious. Consequently, the mechanism of electron transfer, and how this is coupled to proton transfer, remains unresolved.

In the absence of crystal structures and genetic approaches, treatment of bovine complex I with the chaotrope, percholate, and the detergent, N,N-dimethyldodecylamine N-oxide, have contributed to the understanding of both the location, organization, and properties of the 43 subunits. Treatment of the bovine enzyme with percholate releases three fractions, a water-soluble fragment known as the flavoprotein (FP) fraction, the iron–sulfur protein, and a hydrophobic complex. The FP fraction retains the ability to transfer electrons from NADH to ferricyanide, and it consists of three subunits, the 51-, 24-, and 10-kDa subunits. The 51-kDa subunit is the site for binding of both NADH and the primary electron acceptor, FMN. The 51- and 24-kDa subunits also both contain iron–sulfur clusters. The nondenaturing detergent N,N-dimethyldodecylamine N-oxide dissociates complex I differently, yielding two subcomplexes termed Iα and Iβ. The Iα retains the biochemical activity of the complex and primarily contains the soluble peptides that reside in the matrix domain. The membrane domain with no biochemical activity is therefore the Iβ complex.

Complex I from *E. coli* and other bacteria are made up of at least 14 polypeptides and are all present as homologues in both *N. crassa* and mammalian mitochondria. These proteins are considered to be the "minimal" subunits required for electron transfer and proton translocation. Seven bovine homologues from the bovine Iα fraction are found in *E. coli*: 75, 51, 49, 30, 24, TYKY, and PSST. The polypeptides in Iα that are not minimal subunits have been termed as "accessory" proteins, although the majority of subunits have yet to be assigned a particular function. Many of the polypeptides have no relation to other proteins. The 18-kDa subunit contains a cAMP-dependent kinase phosphorylation site motif (Sardanelli *et al.*, 1995). Phosphorylation of this subunit activates complex I, and it is proposed to be an additional mechanism whereby overall respiratory chain activity is regulated (Papa *et al.*, 2001). Subunit SDAP is an acyl-carrier protein and may be involved in lipid biosynthesis and/or repair.

The stalk between the matrix and membrane domains has a diameter of 30 Å and is postulated to be part of the electron transfer pathway linking

the NADH binding domain in the matrix to the ubiquinone binding sites of the membrane domain. The iron–sulfur cluster N2 is considered to play an important role in complex I. It has the highest reduction potential of all the clusters in complex I and it is one electron reduction/oxidation is coupled to the binding and release of one proton. This cluster has been located to the stalk region. Both PSST and TYKY have been advocated to be the subunit that binds N2 (Ohnishi *et al.*, 1998). The two candidates are both amphipathic and in direct interaction with the membrane domain. The N2 cluster transfers electrons to ubiquinone; the distance between N2 and one of the ubiquinone binding sites is only 8–11 Å. The N2 cluster is most likely located inside the membrane. Au: Semicolon correct?

Seven subunits of mammalian complex I are coded for by mitochondrial DNA: ND 1, 2, 3, 4, 4L, 5, and 6. They are all located in the membrane domain and constitute the remaining seven minimal subunits found in bacterial complex I. The ND subunits are similar to bacterial cation/H^+ antiporters, and they are thought responsible for proton translocation. The constriction of the membrane arm divides the domain into one-third and two-thirds portions. Relatively harsh N,N-dimethyldodecylamine N-oxide treatment produces, in addition to subcomplexes Iα and Iβ, the small subcomplex known as Iγ (Fig. 2). The smaller Iγ fraction contains subunits from the smaller part of the membrane arm, while Iβ constitutes the larger part of the arm (Sazanov *et al.*, 2000). The ND1, 2, 3, 4L, and the nuclear-encoded KFY1, are found in Iγ, while ND4 and ND5 and 11 nuclear subunits reside in Iβ. The ND6 could not be located. ND1 and ND2 form a subcomplex within Iγ. The ND1 binds rotenone and ubiquinone, and it is probably intimately involved with ubiquinone binding and reduction. The location of ND1 in Iγ locates the subunit close to the redox centers of Iα and the stalk. At least two functional and spatially distinct ubiquinone reaction centers are thought to exist in complex I. A wide inhibitor binding domain between the two ubiquinone reaction centers has been proposed (Tormo and Estornell, 2000).

Experiments in *N. crassa* have indicated that the matrix and membrane domains undergo independent assembly (Videira, 1998). Whether this phenomena is analogous to mammals is uncertain. In fungi, the nuclear- and mitochondrial-coded genes are exclusive to the matrix and membrane domains respectively. This is not the case in mammalian mitochondria. Frame shift mutations in ND4 and ND6 (in human and mouse) results in defective assembly of the mitochondrial-encoded subunits with loss of complex I activity. However, NADH:ferricyanide oxidoreductase activity is unaffected, indicating that the flavoprotein fragment is present (Bai and Attardi, 1998).

B. Complex II

The flavoprotein succinate:ubiquinone oxidoreductase (complex II; EC 1.3.5.1) oxidizes succinate to fumarate, transferring the electrons to ubiquinone. Complex II is the only enzyme that serves as a direct link between the citric acid cycle (succinate dehydrogenase) and the electron transport chain. The enzyme is both structurally and catalytically closely related to the fumarate reductases. Fumarate reductases are synthesized in anaerobic organisms that utilize fumerate as the terminal electron acceptor. The elucidation of complex II structure and function has been achieved using both the mammalian enzyme and prokaryotic fumarate reductases (reviewed in Ackrell, 2000, and Hagerhall, 1997).

Bovine complex II is comprised of a hydrophilic domain that projects into the matrix and a hydrophobic membrane anchor (Fig. 3). The hydrophilic domain contains a flavoprotein subunit (70 kDa) intimately associated with an iron–sulfur subunit (30 kDa). This domain functions as a succinate dehydrogenase in the presence of an artificial electron acceptor such as ferricyanide, but does not interact directly with ubiquinone. The anchor domain contains the two polypeptides QPs-1 and QPs-3 (15 and 13 kDa, respectively). The anchor domain needs to be present for the reduction of ubiquinone to occur. Ubisemiquinone has been detected bound to intact or reconstituted complex II formed from QPs and succinate dehydrogenase, but not succinate dehydrogenase alone. The primary sequences of both the

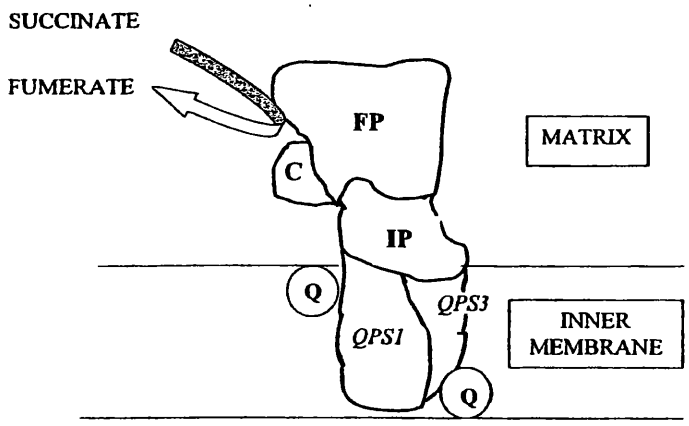

FIG. 3. Structure of mammalian complex II. The matrix domain responsible for catalytic activity contains the flavoprotein (FP), the capping domain (C), and the iron-sulfur protein (IP). The matrix domain is attached to the membrane by QPS-1 and QPS-3. The membrane spanning domain contains the ubiquinone binding sites (Q).

flavoprotein and the iron–sulfur subunits are highly homologous between species, while the anchor domain illustrates greater diversity. Unlike the other complexes in the electron transport chain, the four polypeptides of mammalian complex II are all coded for by nuclear genes (Hirawake *et al.*, 1999).

The flavoprotein subunit polypeptide is folded into four domains [a large flavin adenine dinucleotide (FAD) binding domain, a mobile capping domain, a helical domain, and a C-terminal consisting of an antiparallel β-sheet] and contains the dicarboxylate binding site (Hagerhall, 1997; Lancaster *et al.*, 1999; Ackrell, 2000). The FAD binding domain has a Rossmann-type fold and is very similar to other FAD binding domains such as thioredoxin reductase. The FAD prosthetic group is covalently bound to the protein by a histidine residue (several H-bonds further hold the FAD in place). Flavin adenine dinucleotide is the primary electron acceptor in complex II. To aid electron transfer, the dicarboxylate binding site is predominantly formed by the FAD isoalloxazine ring (Lancaster *et al.*, 1999).

The iron–sulfur subunit has an N-terminal "plant ferredoxin" domain and a C-terminal "bacterial ferredoxin" domain, and binds three iron–sulfur centers. The N-terminal domain contains the [2Fe–2S] iron–sulfur center, while the [4Fe–4S] and [3Fe–4S] iron–sulfur centers are located in the C-terminal. Three groups of highly conserved cysteine residues serve as ligands to the centers. X-ray crystallography has indicated that the [2Fe–2S] iron–sulfur center is closest to the FAD moiety (12.3 Å in *W. succinogenes* and *E. coli* (Ackrell, 2000)). The [4Fe–4S] center connects the [2Fe–2S] center with the [3Fe–4S] center. Electrons are passed singly from the [3Fe–4S] center to ubiquinone forming semiubiquinone before becoming fully reduced and exchanging with the ubiquinone pool in the membrane. The [3Fe–4S] center also appears to have an important structural role. Purified flavoprotein + iron–sulfur protein fractions can only rebind to the anchor domain when the [3Fe–4S] center is intact (Hagerhall, 1997). The cysteine residues that ligate this center are within segments that are in contact with the anchor domain (Lancaster *et al.*, 1999).

The structure of the anchor domain varies greatly between species. The anchors are classified into four types, and differ in topology, number of polypeptides, and cytochrome b content (Hagerhall, 1997; Hirawake *et al.*, 1999). Mammalian complex II consists of two membrane subunits, QPs-1 and QPs-3, and one cytochrome b prosthetic group. Each subunit has three helices that span the membrane (Yu *et al.*, 1992; Hagerhall and Hederstedt, 1996).

Structural, EPR, and inhibitor studies indicate that there are probably two ubiquinone binding sites in the mammalian membrane anchor, with

both polypeptides providing a site each (Lee *et al.*, 1995; Shenoy *et al.*, 1999). The QPs-1 site is located close to the negative (matrix) side of the membrane. This site appears to be bordered by both the iron–sulfur and anchor domains, and it is close to both the [3Fe–4S] center and the b-type heme. The QPs-3 site is located on the positive side of the membrane.

Isolated QPs contains 27 nmol of cytochrome b/mg of protein. The function of the heme in complex II is still unknown. Studies of *B. subtilis* and *E. coli* succinate:ubiquinone oxidoreductase have implicated the heme in playing an important role in the assembly of the enzyme. Absence of heme leads to the synthesis of apocytochrome, and to the accumulation of both the flavoprotein and iron–sulfur domains in the cytoplasm (Hagerhall *et al.*, 1997). The ligand for the b-type heme in complex II has been identified as being a bishistidine. Expression of both polypeptide anchors in *E. coli* is necessary for heme insertion and enzyme activity, indicating that one ligand is provided from each polypeptide (Shenoy *et al.*, 1999). The core of the membrane anchor in mammalian complex II is proposed to be a four-helix antiparallel bundle (two helices each from QPs-1 and QPs-3) with the heme group oriented approximately perpendicular to the membrane plane (Hagerhall and Hederstedt, 1996).

au: Please spell out genus at 1st mention

Au: Hager-hall et al 97 not in Ref. list. Please add there or delete from text.

C. Complex III

Ubiquinol:cytochrome c reductase (complex III; EC 1.10.2.2) is also known, because of the two cytochromes found within it, as the bc_1 complex. This component of the ETC transfers electrons from reduced ubiquinone (ubiquinol) to cytochrome c. This electron transfer is coupled to proton pumping from the matrix to the inner membrane space, contributing to the proton gradient required for ATP synthesis.

The structure of complex III in a variety of mammalian species has been elucidated (Iwata *et al.*, 1998; Kim *et al.*, 1998; Zhang *et al.*, 1998). The protein exists as a homodimer with each monomer consisting of 11 different subunits with a total molecular mass of approximately 240 kDa (see Table I). The two monomers of the complex have a twofold axis of symmetry in the plane of the membrane (Fig. 4). Chicken complex III is 150 Å in length, spanning the membrane, and projecting into both the intermembrane space and matrix by 31 and 79 Å respectively (Zhang *et al.*, 1998).

Functionally, the most important subunits in complex III are cytochrome b (containing both a low and high potential b-type heme, b_L and b_H), cytochrome c (containing one c_1-type heme), and the Rieske protein (bound to a [2Fe–2S] iron–sulfur center). This observation is supported by the fact that in purple bacteria, the complex is comprised of just three or four subunits containing the redox centers above. The functions of the eight

TABLE I
SUBUNITS OF BOVINE HEART COMPLEX III

Subunit	Prosthetic group	Location	M_r(kDa)
1. Core 1		Matrix	49.1
2. Core 2		Matrix	46.5
3. Cytochrome b	Hemes b_H, b_L	Membrane	42.6
4. Cytochrome c_1	Heme c_1	Membrane and intermembrane space	27.3
5. Rieske protein	[2Fe–2S]	Membrane and intermembrane space	21.6 21.6
6. 13.4 K		Matrix	13.3
7. Q binding		Membrane	9.6
8. c_1 hinge		Intermembrane space	9.2
9. Presequence of Rieske protein		Matrix	8
10. c_1 associated		Membrane	7.2
11. 6.4 K		Membrane	6.4

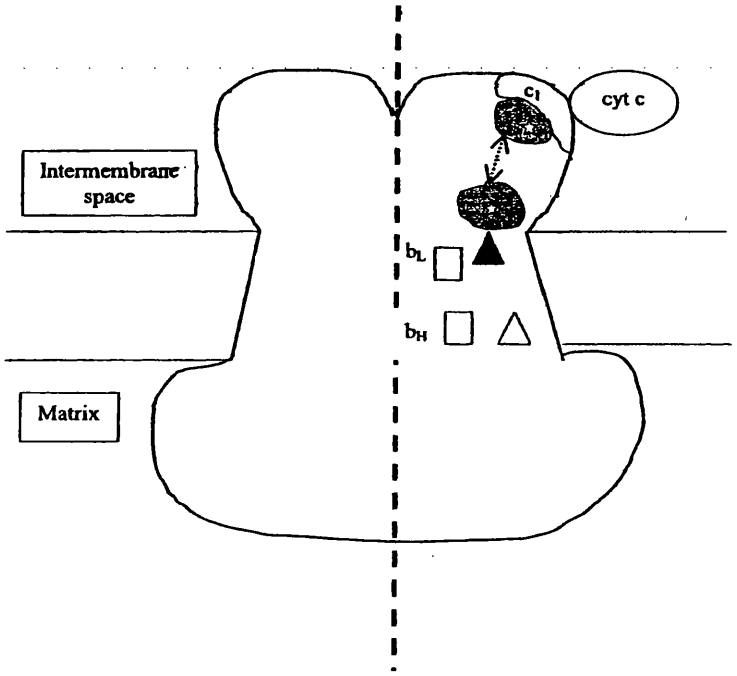

FIG. 4. Structure of complex III. Complex III exists as a dimer with the monomers related by a twofold axis in the plane of the paper (dashed line). The intermembrane domain of the Rieske protein (shaded grey with a star denoting the Fe–S center) is mobile. The domain can be close to the transmembrane domain, which is also the location of the two ubiquinone binding sites, Q_o (black triangle) and Q_i (white triangle), and the high (b_H) and low potential (b_L) b-type hemes (white squares). In the other conformation, the Reiske protein is located close to cytochrome c_1 and soluble cytochrome c.

additional polypeptides present in mammalian complex III are still largely unknown. Genetic studies in yeast have indicated that, with the exception of subunit 6, mutations inserted into subunits containing no prosthetic groups are respiration deficient. Therefore these polypeptides are still necessary for complex III activity.

The intermembrane side of bc_1 contains the functional domains of cytochrome c_1 (including the heme), the Rieske iron–sulfur protein and subunit 8. The transmembrane domain is comprised of 13 transmembrane helices, one each from cytochrome c_1, the Rieske protein, and subunits 7, 10, and 11 and eight from cytochrome b. Cytochrome b also has four horizontal helices on the intermembrane side. The intermembrane domains of cytochrome c_1, the iron–sulfur protein and subunit 8 are positioned on top of these helices (Iwata *et al.*, 1998). Hemes b_H and b_L are close to the matrix and intermembrane sides, respectively, and are in the middle of a four-helix bundle. More than half of the molecular mass of the complex is located in the matrix domain. The two large core proteins, subunits 1 and 2, subunit 6 and subunit 9, reside in this domain. These subunits are thought to have more of a structural role, with subunit 2 implicated in the stabilization of the dimer. Subunits 1 and 2 have homology with the two subunits of mitochondrial matrix processing peptidase. Evidence for the possible protease activity of subunits 1 and 2 is provided by the location of subunit 9. Subunit 9 is the presequence of the nuclear-encoded Rieske protein. In mammals, subunit 9 is cleaved from the iron sulfur protein following import into the mitochondria and resides between subunits 1 and 2 (Iwata *et al.*, 1998; Scheffler, 1999).

The mechanism by which electrons are transferred through complex III has been termed the Q cycle. Complex III has two ubiquinone sites, Q_o and Q_i, that are located near the membrane surface facing the intermembrane space and matrix, respectively. Electron transfer from ubiquinol bound at the Q_o site is bifurcated. One electron is sequentially transferred to the Rieske iron–sulfur protein, cytochrome c_1 and finally to soluble cytochrome c. The oxidation of ubiquinol by the Rieske protein results in the release of two protons into the intermembrane space and the generation of ubisemiquinone at the Q_o site. The electron from semiubiquinone bound at Q_o is transferred consecutively to heme b_L, b_H, and finally to ubiquinone bound at the Q_i site, thus forming semiubiquinone. The sequential oxidation of a second ubiquinol at Q_o will reduce semiubiquinone to ubiquinol at the Q_i site. The two protons required for this are taken up from the matrix. Ubiquinol is then free to bind to Q_o, thus completing the cycle (Crofts *et al.*, 1999; Snyder *et al.*, 2000).

The X-ray crystal structures of complex III from chicken, cow, and rabbit in the absence and the presence of inhibitors of quinone oxidation have

shown that the extrinsic domain of the Rieske iron–sulfur protein assumes one of two conformations (Zhang *et al.*, 1998). Crystals in the presence of stigmatellin, a Q_o site inhibitor, shows the extrinsic domain of the iron sulfur center close to the heme groups of cytochrome b and the Q_o site. Histidine 161, a ligand for the iron–sulfur center, is in an H-bond distance of the Q_o site (Zhang *et al.*, 1998). This is termed the *proximal conformation*. However, crystals in the native form show the extrinsic domain of the iron–sulfur center is close to the electron acceptor, the heme of cytochrome c_1 (distal conformation). The relative position of the iron–sulfur center in chicken crystals in the presence of inhibitor is 16 Å from that of the native structure. When the Rieske protein is in the distal conformation (close to cytochrome c_1), the distance from the [2Fe–2S] center to the expected center of the substrate (in this case stigmatellin, ubiquinol *in vivo*) is approximately 22 Å. Rapid electron transfer is possible over this distance given a proper protein matrix. However, when the Rieske protein is in the distal conformation, the iron–sulfur center is separated from the Q_o site by a cleft, which is likely to be aqueous (Crofts *et al.*, 1999). Given the differing conformations observed, and the inherent physical obstacles preventing efficient electron transfer between donor and acceptor sites, it has been suggested that the reaction mechanism of complex III involves movement of the extrinsic domain of the Rieske iron–sulfur protein. Both the transmembrane helix and matrix side are unaltered in the presence of stigmatellin. The coil consisting of residues 68–73 is stretched in the presence of stigmatellin, implying that this region is responsible for the movement of the extrinsic domain (Zhang *et al.*, 1998).

Au: Histidine correct?

In the proximal conformation, the Q_o binding pocket is buried between the [2Fe–2S] center and the heme of cyt b_L. The binding pocket is bifurcated, with a lobe to both cyt b_L and the iron–sulfur protein docking interface. The Q_i site is thought to either bind the inhibitor antimycin or at least overlap with the inhibitor's binding site (Kim *et al.*, 1998). X-ray crystals indicate that antimycin is bound in a cavity surrounded by heme b_H, three transmembrane helices and the amphipathic surface helix of cytochrome b (Zhang *et al.*, 1998).

The same face of the iron–sulfur protein interacts with both the Q_o site and cyt c_1. A loop present in cytochrome c and c_2 is absent in cyt c_1, exposing heme propionates to the surface. This is within the electron transfer distance of the iron–sulfur center in the distal conformation, and it could be the route by which cyt c_1 is reduced (Zhang *et al.*, 1998). Reduction of cytochrome c by c_1 is thought to require subunit 8, also termed the "hinge protein". The protein has eight glutamate residues at the N-terminal that may form part of the cytochrome c docking site together with helix $\alpha 1$ of cytochrome c_1 (Iwata *et al.*, 1998).

D. Complex IV

Cytochrome c oxidase (complex IV; EC 1.9.3.1) is the terminus for electron transfer in the respiratory chain. The enzyme couples the reduction of oxygen to water, using electrons from cytochrome c, to the pumping of protons from the matrix.

Cytochrome c oxidase has the distinction of being the first complex of the ETC to be crystallised. Crystallization of bovine heart complex IV by Tsukihara *et al.* (1996) revealed that the mammalian enzyme has 13 different subunits. Biochemical and spectroscopic analysis had previously alluded to the presence of two cytochromes (hemes a and a3) and two copper sites. Crystallization of the complex not only pinpointed their location but also revealed the location of two additional metal centers (one magnesium, one zinc), two cholates, and eight phospholipids (five phosphatidyl ethanolamine and three phosphatidyl glycerols) associated with it. The protein exists in the inner membrane as a dimer with each monomer having a molecular mass of 204 kDa (211 kDa including constituents). Viewed from the cytosolic side, the monomers face each other around a twofold axis of symmetry. The surface of each monomer facing the other is concave, forming a large opening between them (Fig. 5b). The X-ray structure failed to reveal any association between the phospholipid, cardiolipin, and complex IV. Cardiolipin is essential for complex IV activity and Tsukihara *et al.* (1996) suggest that there is space for two cardiolipin molecules within the intermonomer space.

Subunits I–III are mitochondrially encoded and form the core of the protein. Subunit I binds heme a and heme a_3 and also forms the Cu_B redox center, while subunit II binds the Cu_A center. Elucidation of the bacterial cytochrome c oxidase in *Paracoccis dentrificans* (Iwata *et al.*, 1995; Michel *et al.*, 1998) illustrates that the protein contains only four subunits, the core of which, subunits I–III, are virtually identical at an atomic level to their mammalian counterpart. Only subunits I and II are required for a functionally active protein. This suggests that subunits I–III form the functional core of the protein. Viewed perpendicularly to the membrane, the core of cytochrome c oxidase looks like a trapezoid with an extension on the smaller side (Fig. 5a). The trapezoid forms the transmembrane domain, while the extension is a globular domain of subunit II that projects into the intermembrane space.

Subunit I is a membranous protein with 12 transmembrane helices. Viewed from the intermembrane side, the helices are arranged in an anticlockwise fashion into three semicircles, each containing four helices bundles. This arrangement forms a "whirlpool" conformation (Tsukihara *et al.*, 1996) with a threefold axis of symmetry. This structure forms three pores,

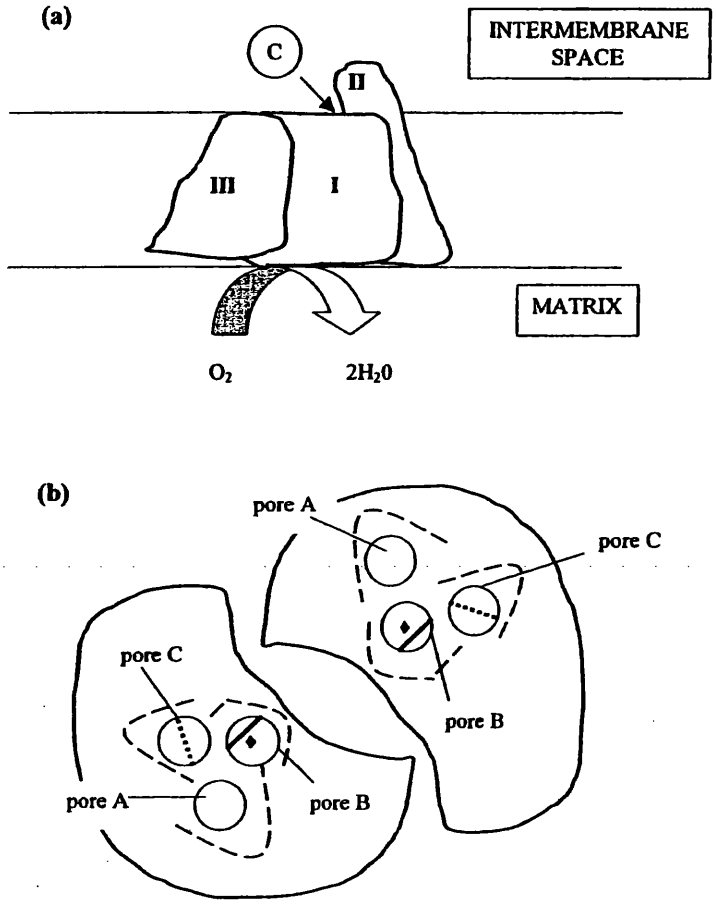

FIG. 5. Schematic representation of complex IV. The trapezoid topology of subunits I–III perpendicular to the membrane plane is shown in (a). Cytochrome c binds at the corner formed by subunits I and II on the intermembrane side. The complex IV dimer as a cross section at the membrane surface when viewed from the cytosolic side is shown in (b). The three 4 helices bundles of subunit I, which form pores A, B, and C (open circles), are shown as dashed curves. Heme in pore C is represented by a dashed diagonal line. The heme a_3–Cu_B center in pore B is denoted by a diagonal line (a3) and a diamond (Cu).

A, B and C (Fig. 5b). Subunit I contains the two hemes, heme a is located in pore C, while heme a_3 is found in pore B. Heme a_3, together with the copper atom Cu_B, forms the binuclear site involved in the reduction of oxygen to water. Both hemes are arranged perpendicularly to the membrane plane. Pore A is mainly filled with conserved aromatic residues. The helices of subunit I are not completely perpendicular to the membrane

surface, with the helices sloping toward convergence on the intermembrane side.

Subunits II and III associate with subunit I without any direct contact between each other. Subunit II has two transmembrane helices that interact with subunit I and an extramembranous globular domain in the intermembrane space. The globular domain has a ten-stranded β-barrel and sits upon part of the intermembrane face of subunit I (Tsukihara *et al.*, 1996). This domain also contains the Cu_A site (comprised of two copper atoms) and is only 7 Å from the surface of the protein. The Cu_A site is the primary electron acceptor from cytochrome c. The corner formed by the extramembrane domain of subunit II and the flat cytosolic surface of subunit I is thought to be the most likely cytochrome c binding site (Fig. 5a, Michel *et al.*, 1998). This region contains ten exposed acidic residues that could bind the lysine residues at the heme edge of cytochrome c. The electrons are then transferred to heme a and then finally on to the heme a_3–Cu_b binuclear site for the reduction of oxygen. The two heme edges are only 4.5 Å apart in subunit I. A hydrophilic cleft between subunits I and II proceeds from the binuclear site to the intermembrane surface of the enzyme and is thought to be a water channel. The channel has highly conserved hydrophilic residues and the magnesium binding site.

Subunit III is almost entirely housed within the membrane and consists of seven transmembrane helices. These helices are divided into two bundles (helices I–II and III–VII) by a V-shaped cleft. In the mitochondria, the cleft contains two phosphatidylethaolamine and one phosphatidylglycerol molecule. The V-shaped cleft has been proposed to be the oxygen channel. The channel starts at the center of the lipid bilayer, where oxygen solubility is greater than in the aqueous phase, above a tightly bound lipid molecule, and leads directly to the binuclear site in subunit I. The mechanisms of proton transfer to the oxygen reduction site and proton pumping are still highly contentious (Michel, 1998; Michel *et al.*, 1998; Riistama *et al.*, 2000; Yoshikawa *et al.*, 2000). Putative pathways for the transfer of protons in a protein moiety via a network of hydrogen bonds have been identified. Coupled proton pumping may occur either via a direct conformational change at the binuclear site or a structural change distant from the active site.

The remaining ten subunits of mitochondrial cytochrome c oxidase are nuclear encoded. The function of these subunits is still largely unknown. They may play a role in insulation, regulation stabilization, or assembly. No cytochrome c oxidase activity is observed in yeast in the absence of either subunit IV, VI, VII, or VIIa. In mammals, the nuclear-encoded subunits IV, VIa, VIIa, and VIII exist as two tissue-specific isoforms (Grossman and Lomax, 1997; Huttemann *et al.*, 2001). The isoforms vary in the N-terminus of the protein (termed heart and liver type), and they are coded for by separate genes. The heart-type isoforms are expressed in heart and skeletal

muscle, while the liver-type isoform appears to be ubiquitously expressed. In humans, only the liver-type isoform of VIII is present in all tissues. These isoforms may provide a method by which cytochrome c oxidase can be differentially regulated depending on the tissue's requirements.

Seven subunits each possess one transmembrane helix, forming an irregular cluster surrounding the metal sites. The packing of the transmembrane subunits with one another is thought to aid the stability of the enzyme and increase the solubility of the core subunits within the membrane. Many areas of the core remain uncovered, especially on the cytosolic side. The remaining three subunits have extramembrane domains. Subunits Va and Vb are located on the matrix side, while VIb, which binds zinc, is on the cytosolic side.

E. Complex V

The ATP synthase (F_1F_0-ATP synthase) uses the proton motive force generated across the inner mitochondrial membrane by electron transfer through the ETC to drive ATP synthesis. Bovine heart ATP synthase is comprised of 16 different subunits and is divided into three domains (Abrahams *et al.*, 1994). The matrix globular domain, F1, containing the catalytic site is linked to the intrinsic membrane domain, F_0, by a central stalk (Fig. 6a) (Abrahams *et al.*, 1994; Karrasch and Walker, 1999). Proton flux through F_0 is coupled to ATP synthesis in the F_1 domain by rotation of the central stalk.

Au: No subscript one, correct?

The F_1 catalytic domain is a flattened sphere 80 Å high and 100 Å in diameter, and contains three α subunits and three β subunits [$(\alpha\beta)_3$]. The subunits are arranged alternately like segments of an orange about the central stalk that contains the γ, δ, and ε subunits (Fig. 6a) (Gibbons *et al.*, 2000). The α and β subunits are homologous (20% identical), and have a very similar fold. Both subunits bind nucleotides, however, only the β subunits show catalytic activity. The nucleotide binding sites are located at the interfaces between the α and β subunits. The catalytic sites are predominantly in the β subunits with some residues from the α-subunits contributing. The structures of the three β-subunit catalytic sites are always different and cycle through "open," "loose," and "tight" states (Fig. 6b). This cycle is known as the "binding-change mechanism," and was originally proposed by Paul Boyer and colleagues (1997). When the catalytic site is in the tight state, there is a high affinity for ADP and inorganic phosphate resulting in ATP forming spontaneously. The open state has very low affinity for substrate/product, while the loose state binds substrate reversibly. Release of ATP from the open state depends on binding of ADP and P_i to the loose state (Boyer, 1997), indicating cooperative binding between sites.

Structural, biochemical, and spectroscopic studies have suggested that the γ subunit of the stalk rotates, coupling the proton motive force at the

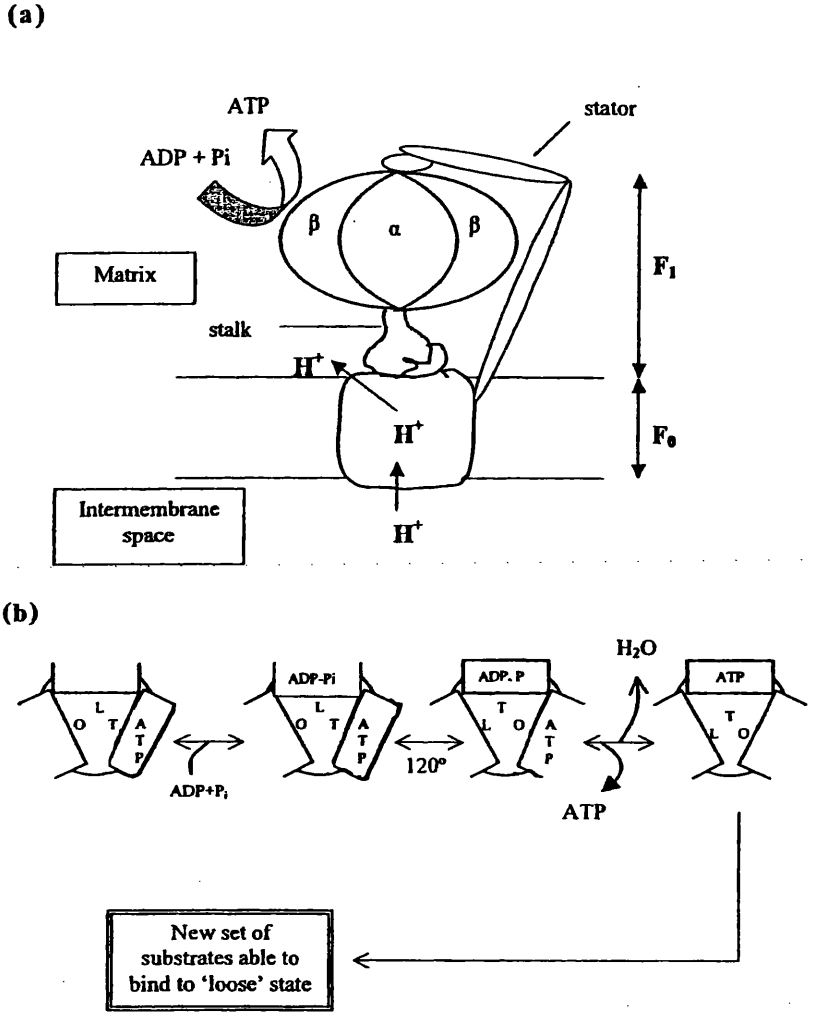

FIG. 6. Structure and mechanism of action of ATP synthase (complex V). A representation of the proposed structure of ATP synthase is shown in (a). The stalk rotates in an anticlockwise direction when viewed from the membrane. The $(\alpha\beta)_3$ domain is prevented from rotating by the stator. The stalk rotation occurs in 120° steps, this movement results in the three β subunits cycling through the three states proposed by the binding-change mechanism (b). In the absence of an input of energy (rotation of the stalk), the tight state (T) is occupied by ATP and the loose state (L) is able to bind ADP and P_i. A 120° rotation of the stalk changes the conformations of the β subunits, trapping bound ADP and P_i in the tight state and allowing ATP to escape from the open state (O). A second ATP is formed in the tight state and a new set of substates (ADP and P_i) is free to bind to the β subunit currently in loose state. And so the cycle repeats.

membrane to ATP synthesis over 100 Å away. The C-terminal of the γ subunit is a 90 Å α-helix and fits into the central cavity formed by the $(\alpha\beta)_3$ domain. The C-terminal emerges to form a dimple, 15 Å below the top of the hexameric domain. The lower half of the helix forms an asymmetric antiparallel coiled coil leading into a single α-helix at the N-terminal. This helix extends 47 Å below the $(\alpha\beta)_3$ domain and forms part of the stalk domain between the F_1 and F_0 domains (Abrahams *et al.*, 1994; Gibbons *et al.*, 2000). Reversible disulfide crosslinks between a mixture of radioactive and unlabeled β subunits and the γ subunit confirmed that the γ subunit can bind each β subunit freely, regardless of which state it is in. Furthermore, the $(\alpha\beta)_3$ domain loses most of its catalytic activity and shows little cooperative binding of nucleotides when the γ subunit is disassociated. Several specific polar interactions and hydrophobic loops between the $(\alpha\beta)_3$ domain and γ subunit have also been observed. Attachment of a fluorescent actin filament to the γ subunit showed directly that the γ subunit rotates counterclockwise in ATP synthase when viewed from the F_0 domain (Noji *et al.*, 1997). Neither the δ or ε subunits (the two remaining components of the stalk) are necessary for rotation. The γ subunit rotates in 120° steps with a frequency of 100–200 Hz. This rotation changes the nucleotide binding affinities of each β subunit, cycling them through the open, loose, and tight states (Fig. 5b). This is because each β subunit is sequentially exposed to a different surface of the γ subunit as it rotates. For example, in the open state, the position of the γ subunit, relative to the β-subunit, prevents the β subunit from adopting a nucleotide binding formation.

Crystallization of the F_1 domain bound to the inhibitor dicyclohexylcarbodiimide resolved the structure of the stalk. A hitherto unseen Rossmann fold toward the bottom of the γ subunit at the base of the stalk (adjacent to the F_0 domain) was identified. The δ and ε subunits interact extensively with this fold, forming a foot (Gibbons *et al.*, 2000). This foot interacts with the c ring of the F_o domain. Electron microscopy of bovine ATP synthase also has revealed a peripheral stalk connecting the $(\alpha\beta)_3$ domain to a collar (possibly the foot) at the top of the F_o domain (Karrasch and Walker, 1999). This is postulated to be a stator, preventing the $(\alpha\beta)_3$ domain from following the rotation of the γ subunit. Subunits b, d, F_6 and oligomycin-sensitivity-conferring protein (OSCP) of the F_o domain have been proposed to be part of this peripheral stalk. The peripheral stalk (stator) in bacterial ATP synthases is comprised of just two b subunits from F_0 and the bacterial homologue of OSCP. The two copies of the b subunit extend to the top of F_1 where they interact with the OSCP homologue that is associated with the F_1 domain.

The F_0 domain spans the membrane and is the site of proton translocation required to drive ATP synthesis. Unfortunately, no high-resolution crystal structures are available for this domain. The F_0 domain of bovine

heart ATP synthase contains 9 different subunits, a, b, c, d, e, f, g, A6L, and F_6. Subunits a, b, d, and F6 are present in the complex with one copy each. In bacteria, two copies of b are observed. One of the subunits present in eukaryoate, but absent in bacterial ATP synthase, probably substitutes for the second copy of b required in the stator. The stoichiometry of subunit c is unclear, 9–12 copies have been suggested to form a ring.

Subunit a in conjunction with the ring of c subunits is thought to provide the pathway for proton translocation. Subunit a is believed to act as a proton inlet channel. At the interface between the a and c subunits, a proton that has passed through subunit a, is thought to bind to Asp61 of the c subunit. The c-subunit ring of *E. coli* ATP synthase has been shown to rotate (Tsunoda *et al.*, 2001). Therefore, upon protonation, the c-subunit site leaves the interface with the a subunit and rotates into the lipid phase. The c subunit rotates nearly 360°, releasing the proton to the outlet channel in subunit a as it reenters the subunit a–subunit c interface. The presence of one mutant c subunit blocks proton translocation, indicating that there is cooperativity between the c subunits. The inhibition of ATP synthase exerted by dicyclohexylcarbodiimide is achieved by a unique reaction with Asp61. If the mammalian ATP synthase has 12 c subunits, one full turn of the rotor will yield three ATP molecules (four protons translocated per ATP).

The γ, δ, and ε subunits of the central stalk are intimately attached to the ring of c subunits. The rotation of the stalk conferred to it by the movement of the c ring provides a mechanism by which proton translocation across the membrane is coupled to ATP synthesis in the matrix over 100 Å away.

F. ADP–ATP Translocator

ATP generated in the mitochondrial matrix is transported to the cytosol via the ATP–ADP translocator. For every ATP molecule exported, an ADP molecule from the cytosol is imported. The exchange of ATP for ADP is driven by the membrane potential since ATP has one more negative charge than ADP.

The ATP–ADP translocator is an integral protein with six transmembrane helices and a molecular mass of 32 kDa. Dimerization of the translocator subunits is thought to form the channel through which ATP and ADP are transported (Klingenberg, 1992; Scheffler, 1999). It is estimated that the translocator accounts for up to 15% of the total protein content of mitochondria.

The use of two specific ATP–ADP translocator inhibitors, atractyloside and bongkrekic acid, have shed light on the mechanism of translocation. Atractyloside only binds to the cytoplasmic side of the translocator since it is unable to cross the inner membrane, while bongkrekic acid can enter

the mitochondria and binds exclusively to the matrix side. The presence of inhibitors prevents the binding of both ATP and ADP. However, both inhibitors cannot bind at the same time, despite occupying opposite sides of the translocator. This indicates that the ATP–ADP translocator is only open for one substrate at a time (e.g., ATP on the matrix side). The postulated transition between the two conformational states (open on the matrix side to open on the cytosolic side) results in the translocation of the substrate across the membrane (Scheffler, 1999). Studies have suggested that the ATP–ADP translocator is one of the components of the mitochondrial permeability transition pore. Formation of this pore is postulated to be a factor in the initiation of apoptosis (Tatton and Olanow, 1999).

III. Intermediary Metabolism

Reducing equivalents, for utilization by the ETC, are generated via a number of integrated metabolic pathways. Below are brief descriptions of the predominant metabolic pathways, located to mitochondria, that are responsible for NADH and $FADH_2$ generation. Details of other metabolic pathways that occur within mitochondria but are not directly related to energy transduction, e.g., heme synthesis and the urea cycle, are not covered, but can be found elsewhere (e.g., Scheffler, 1999).

A. Pyruvate Dehydrogenase

Cytosolic pyruvate, under aerobic conditions, is metabolized further by the TCA cycle. The transport of pyruvate into mitochondria is via the monocarboxylate translocator, and entry of pyruvate into the TCA cycle (see below) is regulated by pyruvate dehydrogenase (PDH). This enzyme complex catalyzes the conversion of pyruvate to acetyl CoA and NADH. The PDH complex consists of 132 subunits and is composed of three main enzymes: (a) pyruvate decarboxylase (E_1) which is a tetramer, encoded by two genes on the X chromosome and composed of 2α and 2β subunits; (b) a transacetylase (E_2) of 52 kDA, which exists as a monomer with lipoic acid; and (c) dihydrolipoyl dehydrogenase (E_3), a 55-kDA dimer that also functions in the branched chain ketoacid dehyrogenases and the α-ketoglutarate dehydrogenase complex. A lipoic acid containing moiety known as the "X" protein is also present in the complex and is believed to have an acyl transfer function (Patel and Roche, 1990). As PDH catalyzes a key regulatory step of aerobic glucose oxidation, activity is tightly regulated. The mechanism for this regulation is phosphorylation (inactive) and dephosphorylation

Au: Fig 7 cited correctly? if not, please cite appropriately.

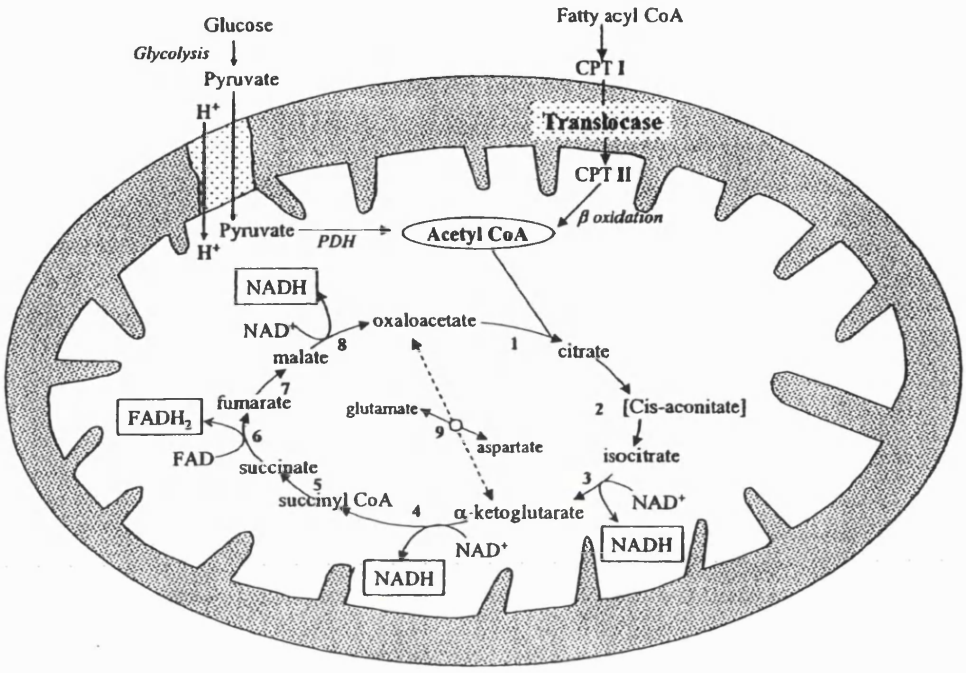

FIG. 7. Integration of energy metabolism within the mitochondria. Acetyl CoA, generated via PDH and fatty acid β oxidation, is metabolized by TCA (Kreb's cycle). Reducing equivalents (NADH and $FADH_2$) generated by this cycle, PDH activity, and β oxidation are oxidized by the electron transport chain resulting in the generation of ATP synthesis. The enzymes of the TCA cycle are as follows: (1) citrate synthase, (2) aconitase, (3) isocitrate dehydrogenase, (4) α-ketoglutarate dehydrogenase, (5) succinyl-CoA synthase, (6) succinate dehydrogenase, (7) fumarase, (8) malate dehydrogenase. The splitting of the cycle into "mini cycles" is depicted by the dotted line and requires aspartate amino transferase, 9.

(active) of PDH by a kinase and a phosphatase, respectively (Linn *et al.*, 1969; Scheffler, 1999). (See Fig. 7.)

B. THE TCA CYCLE

The TCA cycle, also known as the Kreb's cycle or the citric acid cycle, was elucidated in 1937. A major function of this cycle is generation of reduced NADH and $FADH_2$ that can be utilized by the ETC for ATP synthesis. This cycle of eight enzyme catalyzed reactions is located to the mitochondrial matrix and links a number of metabolic pathways that generate acetyl CoA (Fig. 8). Furthermore, intermediates generated in the cycle are utilized in

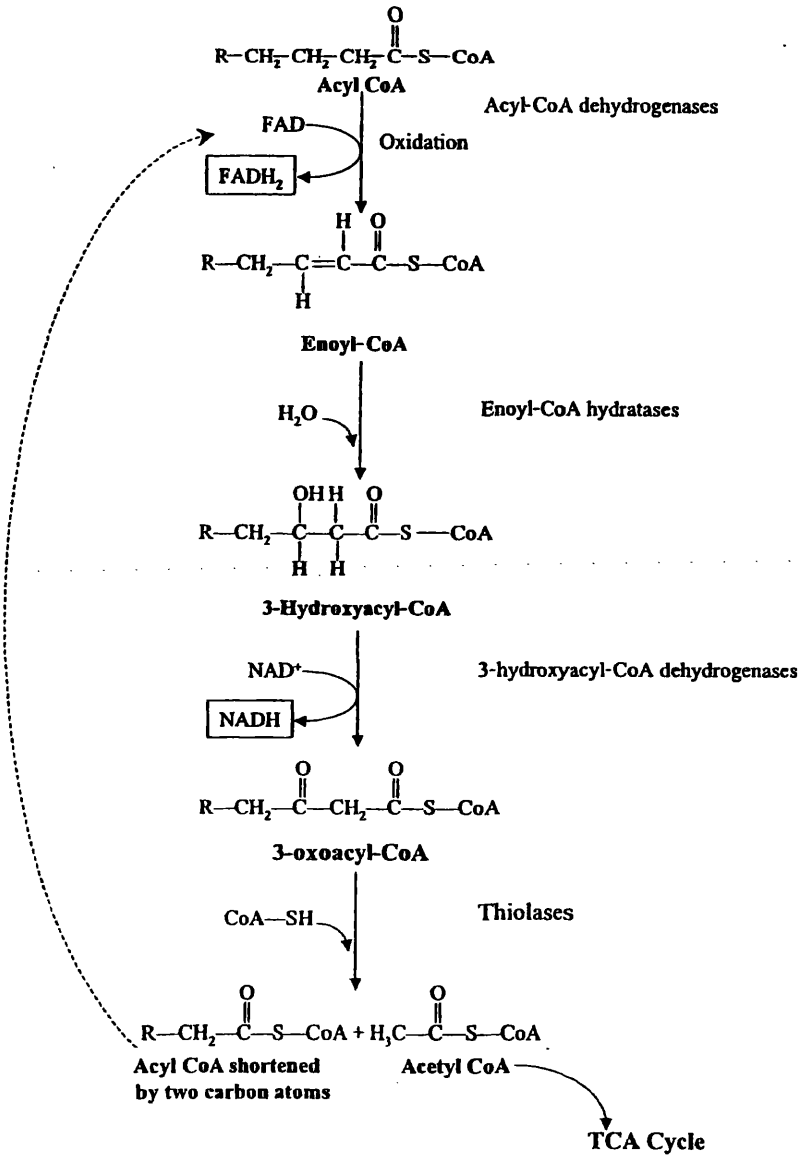

FIG. 8. Mitochondrial β oxidation of fatty acids.

a number of anaplerotic pathways. The enzymes of the TCA cycle are all encoded by nuclear genes and are constitutively expressed. Further details relating to the cycle and disorders affecting this pathway can be found in Rustin *et al.* (1997) and Scheffler (1999).

Metabolically related enzymes of the cycle appear to be associated together within the matrix in order to allow for substrate channeling (Robinson and Srere, 1985). Regulation of the cycle occurs at the level of citrate synthase, isocitrate dehydrogenase, and α-ketoglutyrate dehydrogenase. Thus, alterations in the NADH:NAD^+ ratio, the energy charge, and calcium can act to regulate the TCA cycle.

Functional splitting of the TCA cycle into complementary "mini Krebs cycles" has been proposed (Yudkoff *et al.*, 1994). It is suggested that two independent segments of the cycle exist, i.e., from α-ketoglutarate to oxaloacetate and from oxaloacetate to α-ketoglutarate. For these two cycles to function, aspartate amino transferase needs to be present (Fig. 8). The finding of normal respiration rates in cells derived form patients with TCA cycle defects is suggested to arise as a result of an upregulation of the minicycle with the full complement of enzymes (Rustin *et al.*, 1997).

C. Mitochondrial Fatty Acid Oxidation

Fatty acids are a major energy source, particularly during periods of fasting. While most tissues exhibit an ability to oxidize fatty acids, this process appears particularly important in muscle where approximately 70% of energy demands, under resting conditions, are met by fatty acid oxidation (Di Donato, 1997).

Fatty acids, depending on carbon chain length and degree of unsaturation, can be oxidized, via a number of reactions (α, β, or ω oxidation), which utilize enzyme systems found within peroxisomes and mitochondria. However, we focus here only upon the mitochondrial β oxidation of saturated straight chain fatty acids. Further details relating to peroxisomal fatty acid metabolism, oxidation branch chain, and unsaturated fatty acids can be found in Moser (1997) and Wanders *et al.* (1999).

Following liberation from adipose tissue, fatty acids are transported to tissues bound primarily to albumin. The cellular uptake and transport of fatty acids from the cell membrane to the mitochondrion is poorly understood, but may involve specific membrane transporters and cytosolic binding proteins. The initial step in the process of harnessing energy from fatty acids is the generation of an acyl-CoA thioester from free coenzyme A and the corresponding free fatty acid. For long chain fatty acids (greater than 12 carbons)

this reaction is catalyzed by a long-chain acyl-CoA synthetase located on the outer mitochondrial membrane (Roe and Coates, 1995).

The series of reactions that are involved in fatty acid β oxidation are catalyzed by group of enzymes located on the matrix side of the inner mitochondrial membrane and within the mitochondrial matrix. However, the inner mitochondrial membrane is not permeable to long-chain (>12 carbon units) fatty acyl-CoA esters. In order to traverse this membrane, a transport system involving carnitine has evolved (Brivet *et al.*, 1999).

1. *Carnitine Transport of Long Chain Fatty Acids*

Carnitine palmitoyl transferase I (CPT I), found on the outer mitochondrial membrane, transfers the fatty acyl moiety from acyl CoA to carnitine, leading to the formation of an acyl carnitine. This acyl carnitine is then "shuttled," by the carnitine–acylcarnitine translocase, across the inner mitochondrial membrane, in exchange for free carnitine. Carnitine palmitoyl transferase II (CPT II) then transfers the acyl group back to CoA and the liberation of free carnitine. The regenerated fatty acyl CoA can then enter the β-oxidation spiral.

CPT I and CPT II have different mitochondrial locations, are distinct proteins, and display different biochemical properties, e.g., CPT I, in contrast to CPT II, can be inhibited by malonyl CoA. Furthermore, CPT I exists as tissue-specific isoforms, i.e, liver and muscle type that are encoded by genes that are located on chromosomes 11 and 22, respectively. The two isoforms are of similar size (liver: 773 amino acids, 88.1 kDa; Muscle: 772 amino acids, 88.2 kDa), but they differ in their kinetic properties. Tissue-specific isoforms of CPT II have not been reported. This enzyme is encoded on chromosome 1, and a 658 amino acid proenzyme is synthesized that is imported into the mitochondrion. Following import, a 25 amino acid leader sequence is removed. The active protein has an approximate molecular weight of 71 kDa. Further details relating to the carnitine transport system can be found in Brivet *et al.* (1999).

The gene for the carnitine–acylcarnitine translocase has been assigned to chromosome 3, and encodes for a protein comprising of 301 amino acids. In common with other mitochondrial carrier proteins, the translocase contains a three-fold repeat sequence of approximately 100 amino acids. Furthermore, there are six transmembrane α-helices that are connected by hydrophilic loops (Indiveri *et al.*, 1997).

2. *β-Oxidation of Fatty Acids*

The complete oxidation of unsaturated fatty acyl-CoA molecules to acetyl CoA is achieved by a series of four enzyme reactions, i.e., dehydrogenation

(oxidation), hydration, further dehydrogenation (oxidation), and thiolysis (Fig. 8).

The initial step of β oxidation is catalyzed by a group of enzymes known as the acyl-CoA dehydrogenases. At least four enzymes have been identified that catalyze essentially the same reaction but display specificity toward acyl-CoA molecules of differing carbon chain lengths. These enzymes, referred to as the short-chain (SCAD), medium-chain (MCAD), long-chain (LCAD), and very long-chain (VLCAD) acyl-CoA dehydrogenases, insert a double bond between the α and β carbons of the acyl-CoA molecule. An enoyl-CoA molecule is the product of this reaction, and the electrons removed from the acyl CoA are donated to an electron transfer flavoprotein (ETF). This ETF is then oxidized by ETF dehydrogenase, leading to formation of ubiquinol, which is oxidized by the ETC (Wanders *et al.*, 1999).

The true role of LCAD in the oxidation of fatty acids, *in vivo*, is not clear. Studies, *in vitro*, suggest considerable overlap in specificity for LCAD and VLCAD. Furthermore, cell culture studies suggest that VLCAD is exclusively required for palmitate (C16) oxidation. Current data now suggest that the major role of LCAD is in the oxidation of branched chain fatty acids and it is proposed that LCAD be renamed as long-branch chain acyl-CoA dehydrogenase (Wanders *et al.*, 1998).

Considerable data are available relating to SCAD, MCAD, and LCAD. The active forms of these enzymes are to be found in the mitochondrial matrix and are each composed of four identical subunits that bind FAD. These enzyme subunits are synthesized in the cytosol as precursor proteins that contain leader sequences that direct them to the mitochondrion. Following mitochondrial import, the enzyme subunits are processed into the active enzymes, i.e., leader sequences are removed followed by tetramerization and incorporation of FAD. VLCAD is bound, in contrast to the other acyl CoA dehyrogenases, to the inner mitochondrial membrane and is ideally situated to receive long-chain substrates that have been transported by the carnitine system (Wanders *et al.*, 1999).

The second step in fatty acid β oxidation is hydration of enoyl CoA to form 3-hydroxyacyl CoA. Current evidence suggests that there are at least two mitochondrial enzymes that catalyze this reaction. Short-chain enoyl CoA hydratase, also known as crotonase, is found in the mitochondrial matrix and is active, with decreasing efficiency, on enoyl-CoA molecules of chain length between 4 and 16 carbon units. Crotonase is comprised of six identical subunits that are synthesized in the cytosol as precursors containing mitochondrial targeting signals. Following transport into the mitochondria assembly of the hexamer can occur. The long-chain enoyl CoA hydratase is part of the membrane-bound mitochondrial trifunctional protein (see below) (Wanders *et al.*, 1999).

The next step in β oxidation is a dehydrogenation reaction catalyzed by the 3-hydroxyacyl CoA dehydrogenases. At least two enzymes have been identified that have specificity for short- and long-chain hydroxyacyl CoA molecules. The NADH generated by these enzymes is utilized by the ETC for ATP synthesis. Short-chain hydroxyacyl-CoA dehydrogenase (SCHAD) is a dimer comprised of identical subunits (33 kDa). Precursor proteins are synthesized in the cytosol and are transported into the mitochondrial matrix where assembly of the active enzyme occurs. The SCHAD appears to have a broad specificity, i.e., is capable of oxidising hydroxyacyl CoA molecules of between 4 and 16 carbon units. However, maximal activity is toward substrates having between 4 and 10 carbon units. Long-chain hydroxyacyl-CoA dehydrogenase (LCHAD) is membrane bound and is a constituent of the mitochondrial trifunctional protein (see below). The enzyme has broad substrate specificity and displays maximal activity toward hydroxylacyl-CoA molecules having between 12 and 16 carbons (Wanders *et al.*, 1999).

The final stage in mitochondrial β oxidation is thiolytic cleavage. In this step, the 3-oxoacyl CoA generated by SCHAD or LCHAD is split into acetyl-CoA and a shortened acyl-CoA ester that can reenter the β oxidation spiral. The acetyl CoA generated at this stage can then be metabolized further by the TCA cycle. Two mitochondrial thiolases have been identified that are involved in β oxidation; a general (medium-chain) thiolase and a thiolase associated with the mitochondrial trifunctional protein (see below). The general thiolase is active toward 3-oxoacyl CoA molecules, located in the mitochondrial matrix, a homotetramer, and it is active toward 3-oxoacyl CoA molecules with between 4 and 12 carbons (Wanders *et al.*, 1999).

The mitochondrial trifunctional protein (MTP), as the name suggests, displays enoyl-CoA hydratase, 3-hydroxyacyl-CoA dehydrogenase, and thiolase activity. This inner mitochondrial membrane complex has an approximate molecular weight of 460 kDA, and is an heteroctomer comprised of four α and four β subunits. The α subunits are associated with enoyl-CoA hydratase and 3-hydroxyacyl-CoA dehydrogenase activity, while the β units contain the thiolase (Uchida *et al.*, 1992).

D. Ketone Body Metabolism

Plasma levels of the ketone bodies, acetoacetate and 3-hydroxybutyrate, significantly rise during periods of starvation as a result of accelerated catabolism of fatty acids (Girard *et al.*, 1992). Under such conditions, entry of acetyl CoA into the TCA cycle is limited as oxaloacetate is also being used for gluconeogenesis. Three mitochondrially located enzymes are involved in

the formation of acetoacetate. Thus, in the presence of acetoacetyl-CoA thiolase, two molecule of acetyl CoA are utilized to form acetoacetyl CoA. A third molecule of acetyl CoA is then utilized to form 3-hydroxy-3-methylglutaryl CoA (HMG CoA) a reaction catalyzed by HMG-CoA synthase. The HMG CoA so formed is then further metabolized by a HMG-CoA lyase to form acetoacetate and acetyl CoA. In the presence of NADH, the acetoacetate is reduced to 3-hydroxybutyrate by 3-hydroxybutyrate dehydrogenase. The liver is traditionally considered to be a major site of ketogenesis, while brain muscle and heart are referred to as nonketogenic. However, studies have provided evidence to suggest that the brain may have the full complement of enzymes required for ketone body production (Cullingford *et al.*, 1998).

During periods of starvation, ketone bodies become an increasingly important metabolic fuel for the brain. Acetoacetate and 3-hydroxybutyrate, generated by the liver, readily cross the blood–brain barrier and are subsequently metabolized. 3-Hydroxybutyrate dehydrogenase, located on the inner mitochondrial membrane, forms acetoacetate and NADH from 3-hydroxybutyrate. In the presence of 3-ketoacyl-CoA transferase, CoA is transferred from succinyl CoA to acetoacetate, thereby forming succinate and acetoacetyl CoA. Finally, in the presence of free CoA and acetoacetyl-CoA thiolase, two molecules of acetyl CoA are formed. This acetyl CoA can then be oxidized via the TCA cycle (Mitchell *et al.*, 1995).

IV. Concluding Remarks

Optimal mitochondrial function, as discussed above, is clearly essential for cell survival. In view of this critical role, it is perhaps not surprising that inherited deficiencies affecting mitochondrial metabolism are often associated with a striking clinical picture. Furthermore, there is an increasing body to evidence to suggest that mitochondrial dysfunction occurs in a number of neurodegenerative disorders. Subsequent chapters in this book consider potential mechanisms and the metabolic consequences of impaired mitochondrial function.

References

Au: Please check original? all that contain genus & species names as well as in vitro, in vivo, etc., to see if any should appear as italic in this reference list.

Abrahams, J. P., Leslie, A. G. W., Lutter, R., and Walker, J. E. (1994). Structure at 2.8 Å resolution of F_1-ATPase from bovine heart mitochondria. *Nature* **370**, 621–628.

Ackrell, B. A. C. (2000). Progress in understanding structure-function relationships in respiratory chain complex II. *FEBS Lett.* **466**, 1–5.

Bai, Y, and Attardi, G. (1998). The mtDNA-encoded ND6 subunit of mitochondrial NADH dehydrogenase is essential for the assembly of the membrane arm and the respiratory function of the enzyme. *EMBO J.* **17**, 4848–4858.

Boyer, P. D. (1997). The ATP synthase: A splendid molecular machine. *Ann. Rev. Biochem.* **66**, 717–749.

Brivet, M., Boutron, A., Slama, A., Costa, C., Thuillier, L., Demaugre, F., Rabier, D., Saudubray, J. M., and Bonnefont, J. P. (1999). Defects in activation and transport of fatty acids. *J. Inher. Metab. Dis.* **22**, 428–441.

Crofts, A. R., Guergova-Kuras, M., Huang, L., Kuras, R., Zhang, Z., and Berry, E. A. (1999). Mechanism of ubiquinol oxidation by the bc_1 complex: Role of the iron-sulfur protein and its mobility. *Biochemistry* **38**, 15791–15806.

Cullingford, T. E., Dolphin, C. T., Bhakoo, K. K., Peuchen, S., Canevari, L., and Clark, J. B. (1998). Molecular cloning of rat mitochondrial 3-hydroxy-3-methylglutaryl CoA lyase and detection of the corresponding mRNA and of those encoding the remaining enzymes comprising the ketogenic 3-hydroxy-3-methylglutaryl CoA cycle in central nervous system of suckling rat. *Biochem. J.* **329**, 373–381.

Davey, G. P., Canevari, L., and Clark, J. B. (1997). Threshold effects in synaptosomal and non-synaptic mitochondria from hippocampal CA1 and paramedian neocortex brain regions. *J. Neurochem.* **69**, 2564–2570.

Di Donato, S. (1997). Diseases associated with defects of beta oxidation. *In* "The Molecular and Genetic Basis of Neurological Disease" (R. N. Rosenburg, S. B. Prusiner, S. DiMauro, and R. L. Barchi, eds.), pp. 273–314. Butterworth-Heinemann, Boston.

Gibbons, C., Montgomery, M. G., Leslie, A. G. W., and Walker, J. E. (2000). The structure of the central stalk in bovine F_1-ATPase at 2.4 Å resolution. *Nat. Struct. Biol.* **7**, 1055–1061.

Girard, J., Ferre, P., Pegorier, J. P., and Duee, P. H. (1992). Adpatations of glucose and fatty acid metabolism during perinatal period and suckling weaning transition. *Phys. Rev.* **72**, 507–562.

Grigorieff, N. (1998). Three-dimensional structure of bovine NADH:ubiquinone oxidoreductase (complex I) at 22 Å in ice. *J. Mol. Biol.* **277**, 1033–1046.

Grigorieff, N. (1999). Structure of the respiratory NADH:ubiquinone reductase (complex I). *Curr. Opin. Struct. Biol.* **9**, 476–483.

Grossman, L. I., and Lomax, M. I. (1997). Nuclear genes for cytochrome c oxidase. *Biochim. Biophys. Acta* **1352**, 174–192.

Guenebaut, V., Vincentelli, R., Mills, D., Weiss, H., and Leonard, K. (1997). Three-dimensional structure of NADH-dehydrogenase from Neurospora crassa by electron microscopy and conical tilt reconstruction. *J. Mol. Biol.* **265**, 409–418.

Guenebaut, V., Schlitt, A., Weiss, H., Leonard, K., and Friedrich, T. (1998). Consistent structure between bacterial and mitochondrial NADH:ubiquinone oxidoreductase (complex I). *J. Mol. Biol.* **276**, 105–112.

Hagerhall, C. (1997). Succinate:quinone oxidoreductases: Variations on a conserved theme. *Biochim. Biophys. Acta* **1320**, 107–141.

Hagerhall, C., and Hederstedt, L. (1996). A structural model for the membrane-integral domain of succinate:ubiquinone oxidoreductases. *FEBS Lett.* **389**, 25–31.

Hirawake, H., Taniwaki, M., Tamura, A., Amino, H., Tomitsuka, E., and Kita, K. (1999). Characterisation of the human SDHD gene encoding the small subunit of cytochrome b (cybS) in mitochondrial succinate-ubiquinone oxidoreductase. *Biochim. Biophys. Acta* **1412**, 295–300.

Huttemann, M., Kadenbach, B., and Grossman, L. I. (2001). Mammalian subunit IV isoforms of cytochrome c oxidase. *Gene* **267**, 111–123.

Indiveri, C., Iacobazzi, V., Giangregorio, N., and Palmieri, F. (1997). The mitochondrial carnitine carrier protein: cDNA cloning, primary structure and comparison with other mitochondrial transport proteins. *Biochem. J.* **321,** 713–719.

Iwata, S., Ostermeier, C., Ludwig, B., and Michel, H. (1995). Structure at 2.8 Å resolution of cytochrome c oxidase from Paracoccus denitrificans. *Nature* **376,** 660–669.

Iwata, S., Lee, J. W., Okada, K., Lee, J. K., Iwata, M., Rasmussen, B., Link, T. A., Ramaswamy, S., and Jap, B. K. (1998). Complete strucure of the 11-subunit bovine mitochondrial cytochrome bc_1 complex. *Science* **281,** 64–71.

Karrasch, S., and Walker, J. E. (1999). Novel features in the structure of bovine ATP synthase. *J. Mol. Biol.* **290,** 379–384.

Kim, H., Xia, D., Yu, C., Xia, J., Kachurn, A. M., Zhang, L., Yu, L., and Deisenhoffer, J. (1998). Inhibitor binding changes domain mobility in the iron-sulfur protein of the mitochondrial bc1 complex from bovine heart. *Proc. Natl. Acad. Sci.* **95,** 8026–8033.

Klingenberg, M. (1992). Structure-function of the ADP/ATP carrier. *Biochem. Soc. Trans.* **20,** 547–550.

Lancaster, C. R. D., Kroger, A., and Michel, H. (1999). Structure of fumarate reductase from Wolinella succinogenes at 2.2 Å resolution. *Nature* **402,** 377–385.

Lehninger, A. L. (1965). "The Mitochondrion: Molecular Basis of Structure and Function." W. A. Benjamin, New York.

Lee, G. Y., He, D., and Yu, C. (1995). Identification of the ubiquinone-binding domain in QPs1 of succinate:ubiquinone reductase. *J. Biol. Chem.* **270,** 6193–6198.

Linn, T. C., Petit, F. H., and Reed, L. J. (1969). α-Keto acid dehydrogenase complexes, X. Regulation of the activity of pyruvate dehydrogenase complex from beef kidney mitochondria by phosphorylation and dephosphorylation. *Proc. Natl. Acad. Sci. USA* **62,** 234–241.

Michel, H. (1998). The mechanism of proton pumping by cytochrome c oxidase. *Proc. Natl. Acad. Sci.* **95,** 12819–12824.

Michel, H., Behr, J., Harrenga, A., and Kannt, A. (1998). Cytochrome c oxidase: Structure and spectroscopy. *Ann. Rev. Biophys. Biomol. Struct.* **27,** 329–356.

Mitchel, G. A., Kassovskabratinova, S., Boukaftane, Y., Robert, M. F., Wang, S. P., Ashmarina, L., Lambert, M., Lapierre, P., and Poitier, E. (1995). Medical aspects of ketone body metabolism. *Clin. Invest. Med.* **18,** 193–216.

Mitchell, P. (1961). Coupling of phosphorylation to electron and hydrogen tranfer by a chemiosmotic type of mechanism. *Nature* **191,** 144–148.

Morgan-Hughes, J., Darvenzia, P., Kahn, S. H., Landon, D. M., Sherratt, R. M., Land, J. M., and Clark, J. B. (1977). A mitochondrial myopathy characterised by a deficiency in reducible cytochrome b. *Brain* **100,** 617–640.

Moser, H. W. (1997). Peroxisomal disorders. *In* "The Molecular and Genetic Basis of Neurological Disease" (R. N. Rosenburg, S. B. Prusiner, S. DiMauro, and R. L. Barchi, eds.), pp. 273–314. Butterworth-Heinemann, Boston.

Noji, H., Yasuda, R., Yoshida, M., and Kinosita, K., Jr. (1997). Direct observation of the rotation of F_1-ATPase. *Nature* **386,** 299–302.

Ohnishi, T. (1998). Iron-sulfur clusters/semiquinones in complex I. *Biochim. Biophys. Acta* **1364,** 186–206.

Papa, S., Scacco, S., Sardanella, A. M., Vergari, R., Papa, F., Buddle, S., Van den Heuvel, L., and Smeitink, J. (2001). Mutations in the NDUFS4 gene of complex I abolishes cAMP dependent activation of the complex in a child with fatal neurological syndrome. *FEBS Lett.* **489,** 259–262.

Patel, M.S., and Roche, T. E. (1990). Molecular biology and biochemistry of pyruvate dehydrogenase complexes. *FASEB J.* **4,** 3224–3223.

Au: Morgan-Hughes et al 77, and Patel + Roche 90, both not cited in text. Please cite or delete from Ref. list.

Riistama, S., Puustinen, A., Verkhovsky, M. I., Morgan, J. E., and Wikstrom, M. (2000). Binding of O_2 and its reduction are both retarded by replacement of valine 279 by isoleucine in cytochrome c oxidase from Paracoccus denitrificans. *Biochemistry* **39**, 6365–6372.

Robinson, J. B., and Srere, P. A. (1985). Organisation of Krebs tricarboxylic acid cycle enzymes in mitochondria. *J. Biol. Chem.* **260**, 800–805.

Roodyn, D. B., and Wilkie, D. (1968). "The Biogenesis of mitochondria." Methuen, London.

Roe, C. R., and Coates, P. M. (1995). Mitochondrial fatty acid oxidation disorders. *In* "The Metabolic and Molecular Basis of Inherited Disease" (C. R. Scriver, A. L. Beaudet, W. S. Sly, and D. Valle, eds.), pp. 1501–1535. McGraw-Hill, New York.

Rustin, P., Bourgeron, T., Parfait, B., Chretein, D., Munnich, A., and Rotig, A. (1997). Inborn errors of the Krebs cycle: A group of unusual mitochondrial diseases in human. *Biochim. Biophys. Acta* **1361**, 185–197.

Au: Should this be plural?

Sardanelli, A. M., Technikova-Dobrova, Z., Scacco, S. C., Speranza, F., and Papa, S. (1995). Characterization of proteins phosphorylated by the cAMP-dependent protein kinase of bovine heart mitochondria. *FEBS Lett.* **377**, 470–474.

Sazanov, L. A., Peak-Chew, S. W., Fearnley, I. M., and Walker, J. E. (2000). Resolution of the membrane domain of complex I into subcomplexes: Implications for the structural organisation of the enzyme. *Biochemistry* **39**, 7229–7235.

Scheffler, I. E. (1999). "Mitochondria." Wiley-Liss, New York.

Shenoy, S. K., Yu, L., and Yu, C. (1999). Identification of quinone-binding and heme-ligating residues of the smallest membrane anchoring subunit (QPs3) of bovine heart mitochondrial succinate:ubiquinone reductase. *J. Biol. Chem.* **274**, 8717–8722.

Snyder, C. H., Gutierrez-Cirlos, E. B., and Trumpower, B. L. (2000). Evidence for a concerted mechanism of ubiquinol oxidation by the cytochrome bc_1 complex. *J. Biol. Chem.* **275**, 13535–13541.

Tatton, W. G., and Olanow, C. W. (1999). Apoptosis in neurodegenerative diseases: The role of mitochondria. *Biochim. Biophys. Acta* **1410**, 195–213.

Tormo, J. R., and Estornell, E. (2000). New evidence for the multiplicity of ubiquinone and inhibitor binding sites in the mitochondrial complex I. *Arch. Biochem. Biophys.* **381**, 241–246.

Tsukihara, T., Aoyama, H., Yamashita, E., Tomizaki, T., Yamaguchi, H., Shinzawa-Itoh, K., Nakashima, R., Yaono, R., and Yoshikawa, S. (1996). The whole structure of the 13-subunit oxidised cytochrome c oxidase at 2.8 Å. *Science* **272**, 1136–1144.

Tsunoda, S., Aggeler, R., Yoshida, M., and Capaldi, R. A. (2001). Rotation of the c subunit oligomer in fully functional F_1F_0 ATP synthase. *Proc. Natl. Acad. Sci. USA* **98**, 898–902.

Au: Ok to add USA?

Uchida, Y., Izai, K., Orii, T., and Hashimoto, T. (1992). Novel fatty acid beta oxidation enzymes in rat live mitochondria. II. Purification and properties of enoyl-coenzyme A (CoA) hydratase/3-hydroxyacyl CoA dehydrogenase/3-ketoacyl-CoA thiolase trifunctional protein. *J. Biol. Chem.* **267**, 1034–1041.

Videira, A. (1998). Complex I from the fungus Neurospora crassa. *Biochim. Biophys. Acta* **1364**, 89–100.

Wanders, R. J., Denis, S., Ruiter, J. P., Ijlst, L., and Dacremont, G. (1998). 2,6-Dimethylheptanoyl CoA is a specific substrate for long chain acyl CoA dehydrogenase (LCAD): Evidence for a major role of LCAD in branched chain fatty acid oxidation. *Biochim. Biophys. Acta* **1393**, 35–40.

Wanders, R. J. A., Vreken, P., Den Boer, M. E. J., Wijburg, F. A., Van Gennip, A. H., and Ijlst, L. (1999). Disorders of mitochondrial fatty acyl CoA β-oxidation. *J. Inher. Metab. Dis.* **22**, 442–487.

Yoshikawa, S., Shinzawa-Itoh, K., and Tsukihara, T. (2000). X-ray structure and reaction mechanism of bovine heart cytochrome c oxidase. *J. Inorg. Biochem.* **82**, 1–7.

Yu, L., Wei, Y., Usui, S., and Yu, C. (1992). Cytochrome b_{560} (QPs1) of mitochondrial succinate-ubiquinone reductase. *J. Biol. Chem.* **267**, 24508–24515.

Yudkoff, M., Nelson, D., Daikhin, Y., and Erecinska, M. (1994). Tricarboxylic acid cycle in rat brain. Fluxes and interactions with aspartate aminotransferase and malate aspartate shuttle. *J. Biol. Chem.* **269**, 27414–27420.

Zhang, Z., Huang, L., Shulmeister, V. M., Chi, Y., Kim, K. K., Hung, L., Crofts, A. R., Berry, E. A., and Kim, S. (1998). Electron transfer by domain movement in cytochrome bc_1. *Nature* **392**, 677–684.